The role of the transcription elongation factor SPT4-SPT5 in plant growth and development

DISSERTATION

ZUR ERLANGUNG DES DOKTORGRADES
DER NATURWISSENSCHAFTEN (DR. RER. NAT.)
DER FAKULTÄT FÜR BIOLOGIE UND VORKLINISCHE MEDIZIN
DER UNIVERSITÄT REGENSBURG

vorgelegt von

Julius Dürr

aus Nürtingen

im Oktober 2013

Das Promotionsgesuch wurde eingereicht am: 08.10.2013

Die Arbeit wurde angeleitet von: Prof. Dr. Klaus D. Grasser

Unterschrift:

Julius Dürr

Table of contents

List of figures

List of tables

Abbreviations

A. thaliana	*Arabidopsis thaliana*
A. tumefaciens	*Agrobacterium tumefaciens*
aa	Amino acid
AB	Antibody
AB	Antibody
amiRNA	Artificial micro RNA
ARF	Auxin response factor
At	*Arabidopsis thaliana*
Aux/IAA	AUXIN/INDOLE-ACETIC ACID
AUX1/LAX1	AUXIN1/LIKE AUXIN1
AuxRE	Auxin responsive element
C. elegans	*Caenorhabditis elegans*
CBC	Cap-binding complex
CBP	Cap-binding protein
CCR4-NOT	Carbon catabolite repression 4-Negative on TATA
Cdh1	Chromodomain helicase DNA-binding 1
Cdk	Cyclin-dependent kinase
cDNA	complementary DNA
ChIP	Chromatin immunoprecipitation
Col-0	Columbia-0
CPSF	Cleavage and polyadenylation factor
CstF	Cleavage stimulatory factor
CTD	C-terminal domain
CTR	C-terminal repeat domain
D. melanogaster	*Drosophila melanogaster*
DAF	Days after fertilsation
DAS	Days after stratification
Dm	*Drosophila melanogaster*
DNA	Deoxynucleic acid
DOG1	DELAY OF GERMINATION 1
DRB	5,6-dichloro-1-β-D-ribofuranosyl-1H-benzimidazole
DSIF	DRB-sensitivity inducing factor
DW	Dry weight
E. coli	*Escherichia coli*
e. g.	For example, latin: *exempli gratia*
EEC	Early elongation complex
EJC	Exon junction complex
ELL	Lysine-rich in leukaemia
ET	Ethylene
FACT	Facilitates chromatin transcription
Fcp1	TFIIF-associated CTD-phosphatase

FLC	Flowering locus C
FT	Flowering locus T
FW	Fresh weight
GABI KAT	German plant genomics research program-Kölner Arabidopsis T-DNA lines
GFP	Green fluorescent protein
GH3	GRETCHEN HAGEN 3
Glu	Glutamate
GO	Gene ontology
GST	Glutathione S-Transferase
GTF	General transcription factor
GUS	β-glucuronidase
HAT	Histone acetyltransferase
HMT	Histone methyltransferase
Hs	*Homo sapiens*
HUB1	HISTONE MONOUBIQUITINATION1
i. e.	That is, latin: *id est*
IAA	Indole-3-acetic acid
ITC	Initially transcribing complex
JA	Jasmonic acid
KOW	Kyprides, Ouzounis, Woese
LB	Left border
LD	Long day
L*er*	*Landsberg erecta*
MDR	MULTI DRUG RESISTANT
MED14	Mediator complex subunit 14
miRNA	MicroRNA
mRNA	Messenger RNA
MS	Murashige-Skoog
N. benthamiana	*Nicotiana benthamiana*
NASC	Nottingham Arabidopsis Stock Centre
ncRNA	Non-coding RNA
NELF	Negative elogantion factor
NGN	NusG N-terminal domain
NLS	Nuclear localisation signal
NRPB	Nuclear RNA polymerase II
Os	*Oryza sativa*
PAS	Poly (A) signal
PGP	P-Glycoprotein
PIC	Pre-initiation complex
PIN	PIN-FORMED
PR	Pathogenesis-related
Pt	*Populus trichocarpa*
P-TEFb	Positive transcription elongation factor b
qRT-PCR	Quantitative reverse transcription-polymerase chain reaction

RB	Right border
RdDM	RNA-directed DNA methylation
RNA	Ribonucleic acid
RNAi	RNA interference
RNAP	RNA Polymerase
RNP	Ribonucleoprotein
rRNA	Ribosomal RNA
S. cerevisiae	*Saccharomyces cerevisiae*
SA	Salicylic acid
SAIL	Syngenta Arabidopsis Insertion Library
Sc	*Saccharomyces cerevisiae*
SCF	Skp1-Cullin-F-box
SD	Short day
Ser	Serine
Set1 and 2	Su(var)3-9, Enhancer-of-zeste Trithorax 1 and 2
SIGnAL	Salk Institute Genomic Analysis Laboratory
snRNA	Small nuclear RNA
SPT5	Suppressor of Ty
SPT5L	SPT5-like
SSRP1	Structure specific recognition protein 1
swp	*struwwelpeter*
SYD	SPLAYED
TBP	TATA box-binding protein
T-DNA	Transfer DNA
TEF	Transcription elongation factor
TF	Transcription factor
TFII#	General transcription factor necessary for RNAPII mediated transcription
Thr	Threonine
TIR	TRANSPORT INHIBITOR RESISTANT 1
TREX	transcription/export
tRNA	Transfer RNA
UTR	Untranslated region
Vv	*Vitis vinifera*
XVE	LexA (X), VP16 (V) and estrogen receptor (E)
Zm	*Zea mays*

CHAPTER 1

INTRODUCTION

1. Introduction

1.1 Initiation of transcription

Three multisubunit RNA Polymerases (RNAP) are transcribing the eukaryotic genome, namely RNAP I, RNAPII, and RNAPIII (Vannini and Cramer, 2012). The three polymerases transcribe different classes of RNA. RNAP I transcribes the 25S, 18S, and 5.8S rRNA precursor. RNAPII transcribes the messenger RNA (mRNA) most non-coding RNAs (ncRNAs), small nuclear RNAs (snRNAs), small nucleolar RNAs (snoRNAs), and microRNAs (miRNAs). The third RNA polymerase, RNAPIII is important for transcription of short untranslated RNAs (tRNA and 5S rRNA) (Grummt, 2003; Dieci et al., 2007; Egloff and Murphy, 2008). RNAP I, II and III contain 14, 12, and 17 subunits, respectively. Five of these subunits are identical for all three polymerases. All three RNA Polymerases share a subset of associated factors like the TATA box-binding protein (TBP), and the general transcription factors (GTF) TFIIB, TFIIE, and TFIIF or proteins structurally and functionally related to parts of these factors (Cormack and Struhl, 1992; Vannini and Cramer, 2012). In plants two additional, plant specific RNA polymerases, RNAP IV and RNAP V, were identified (Pontier et al., 2005). RNAP IV and RNAP V are both involved in the small interfering RNA (siRNA)-mediated RNA-directed DNA methylation pathway (RdDM) (Herr et al., 2005; Onodera et al., 2005). Since the focus of this thesis is on transcript elongation factors that modulate the processivity of elongation by RNAPII, only transcription by RNAPII will be described in detail.

1.2 Transcription by RNA Polymerase II

Transcription by RNA Polymerase II can be divided into a number of distinct steps (Figure 1). First, RNAPII is recruited to the promoter, and then the general transcription factors bind RNAPII and initiate transcription (pre-initiation complex assembly, open complex formation, and initiation). These early events have been shown to be the main target of regulation of transcription. After initiation, promoter clearance takes place and structural changes in the RNAPII complex lead to productive mRNA elongation (Thoma, 1991). Subsequent efficient elongation requires that RNAPII does not pause or stall because of unusual DNA structures or

proteins bound to DNA (Svejstrup, 2002, 2003). During transcript elongation, RNA processing takes place. Processes like capping and splicing, as well as the termination and polyadenylation factors are recruited all co-transcriptionally and most of the processing events even take place co-transcriptionally (Proudfoot et al., 2002; Pandit et al., 2008; Moore and Proudfoot, 2009). Finally, transcription is terminated and RNAPII is recycled for a new round of the transcription cycle (Sims et al., 2004; Shandilya and Roberts, 2012).

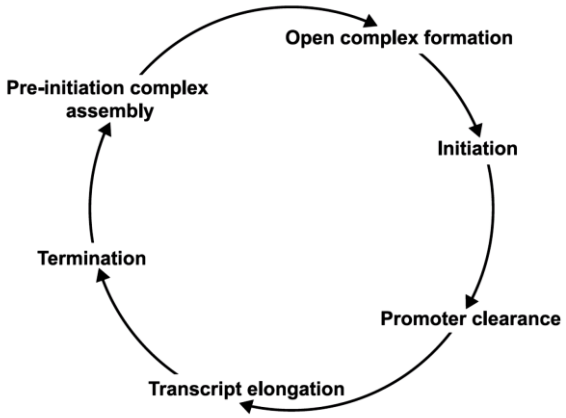

Figure 1. Transcription cycle. The different steps in the transcription cycle are shown starting with the pre-initiation complex assembly (Svejstrup, 2004).

1.2.1 Initiation of transcription

The initiation of transcription is of particular interest because of the tight regulation. Transcriptional activators and repressors exert their effects at this early stage of transcription. Transcription starts with the sequence specific binding of activators to enhancer elements and the recruitment of general transcription factors and the RNAPII to the target gene promoters (Thomas and Chiang, 2006). Each gene can be categorised on the basis of the presence of certain core promoter elements (Juven-Gershon et al., 2008). The presence or absence of a TATA box is used for classification as TATA-containing or TATA-less promoters (Mathis and Chambon, 1981; Baumann et al., 2010). The 5'-TATAA-3' sequence is recognised by the TBP and several associated factors forming the transcription factor TFIID. The binding of TBP is tightly regulated by transcriptional activators and negative factors (Cang et al., 1999; Kuras and Struhl, 1999). The TATA box containing promoter can also be recognised by the SAGA co-activator complex instead of TFIID (Basehoar et al., 2004). The SAGA complex is a histone acetyltransferase and deubiquitinase, it

interacts with transcriptional activators and the general transcription machinery (Koutelou et al., 2010). TFIID and similar complexes also recognise promoter sequences lacking the canonical TATA sequence (Baumann et al., 2010). The RNAPII binds to the promoter sequence together with the general transcription factors forming the huge pre-initiation complex (PIC). The transcription factor TFIIB is involved in DNA recruitment, unwinding of the DNA and determines the directionality of transcription by the recognition of promoter flanking sequences (Littlefield et al., 1999; Bushnell et al., 2004; Kostrewa et al., 2009). In a next step the Mediator complex and TFIIH are recruited to the PIC (Figure 2). The PIC undergoes a series of rearrangements and a stable elongation complex is formed when the nascent RNA grows to a length of about 25 residues. A mayor step is the transformation from the closed to the open status with the unwound DNA forming the “transcription bubble” (Liu et al., 2013). The Mediator complex transduces signals from sequence-specific transcriptional regulators to the general transcription machinery. The association of Mediator with RNAPII, and its function in transcription, depends on the RNAPII C-terminal domain (CTD). The Mediator complex binds to an non-phosphorylated CTD just after recruitment of RNAPII (Myers et al., 1998). The Mediator complex also stimulates the CTD kinase activity of TFIIH (Sogaard and Svejstrup, 2007). TFIIH controls the ATP-dependent transition from the closed to the open complex by phosphorylation of the RNAPII CTD (Laine and Egly, 2006).

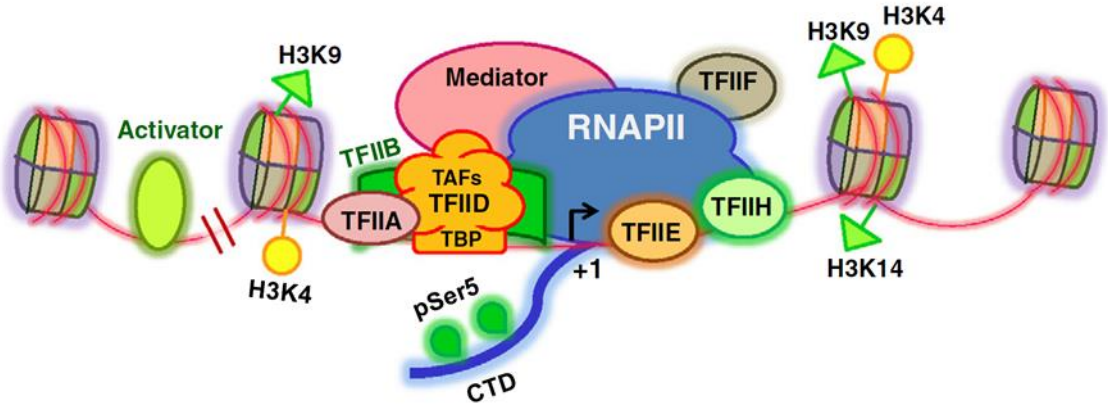

Figure 2. Formation of the pre-initiation complex. Activators bind to its enhancer sequence for recruitment of general transcription factors (GTFs). GTFs recognize and bind to the core promoter elements. TFIID containing TBP binds the TATA box and TFIIB, together with other GTFs, facilitates the recruitment of hypo-phosphorylated RNA polymerase II to assemble the pre-initiation complex (PIC). Activators mediate the recruitment of histone modifying enzymes, as well as ATP-driven nucleosome remodellers. The CTD repeat of RNAPII is hyper-phosphorylated at Ser5. The nucleosomes flanking the promoter regions are methylated at H3K4 and acetylated at H3K9/14, which are marks for active transcription (Shandilya and Roberts, 2012).

The formation of the PIC does not guarantee productive transcription: transcripts of less than 5 nt are unstable, resulting in a high frequency of abortive initiation. At about 10 nt, promoter escape is favoured over abortive initiation, and at about 25 nt productive transcription elongation starts (Saunders et al., 2006). Gene specific activators mediate the recruitment of histone modifying enzymes to chromatin, which in concert with chromatin remodelling factors reorganise the chromatin architecture. Histone acetylates and methylases add acetyl- (H3K9, H3K14 and H4K16) and methyl-groups ($H3K4me^2$ and $H3K4me^3$) to histones of promoter-proximal nucleosomes (Li et al., 2007a). These histone modifications hallmark an open permissive chromatin competent for transcription (Ansari et al., 2009). Chromatin remodellers recognise these modifications and render the chromatin accessible for transcription to begin (Clapier and Cairns, 2009). One of these chromatin remodellers is the facilitates chromatin transcription (FACT) complex, structure specific recognition protein 1 (SSRP1) and suppressor of Ty 16 (Spt16) (Brewster et al., 2001). FACT is a histone chaperone and stimulates RNAPII transcription (Belotserkovskaya et al., 2003). FACT destabilises nucleosomes by removing the histone H2A/H2B dimer and thereby assists the passage of RNAPII through chromatin. Interestingly, FACT also restores nucleosome structure behind the elongating RNA polymerase (Mason and Struhl, 2003; Reinberg and Sims, 2006; Formosa, 2008).

1.2.2 Transcription elongation

Productively elongating RNAPII can transcribe a whole gene in a highly processive manner without dissociating from the template DNA or releasing the nascent RNA. To acquire these properties, initiating RNAPII must undergo structural changes as described in the following chapter.

1.2.2.1 Promoter clearance

Promoter escape or promoter clearance describes the earliest of these steps where the RNAPII breaks its contact with the promoter and promoter-associated factors. Promoter clearance depends on interaction of the RNAPII with the nascent RNA and sequences in the template DNA and is regulated by intrinsic factors (Dvir, 2002). Promoter clearance starts by forming the initially transcribing complex (ITC) and is completed when the nascent RNA associates stably with the transcription complex and the early elongation complex (EEC) is formed (Figure 3). During early

transcription, the ITC undergoes abortive initiation, which is reduced with the addition of the fourth nucleotide (Holstege et al., 1997). The rate-limiting step of promoter clearance occurs after the addition of the eighth nucleotide, and coincides with the transition to the EEC and a sudden collapse of the transcription bubble (Holstege et al., 1997; Hieb et al., 2006). The EEC remains unstable and has a tendency to undergo transcript slippage and backtracking until the nascent RNA has reached a length of 25 nt (Pal and Luse, 2003). Backtracking by only a few nucleotides leads to transcriptional pausing that can be overcome by RNAPII itself. More extensive backtracking causes transcriptional arrest, which is irreversible (Shilatifard et al., 2003). Arrested EEC are converted to active EEC by the transcription factor TFIIS, which stimulates the intrinsic RNA cleavage activity of RNAPII (Fish and Kane, 2002; Cramer, 2004). TFIIS binds to the RNAPII and extends from the polymerase surface via a pore to the internal active site of the enzyme and thereby activates the intrinsic cleavage site of RNAPII (Cramer, 2004). Moreover, TFIIS induces structural changes in RNAPII and facilitates realignment of the RNA in the active site for catalysis of new nucleotides to the nascent RNA (Kettenberger et al., 2003). The activity of TFIIS is also necessary for, efficient release of RNAPII from promoter-proximal pause sites (Adelman et al., 2005 Schwer and Shuman 2011).

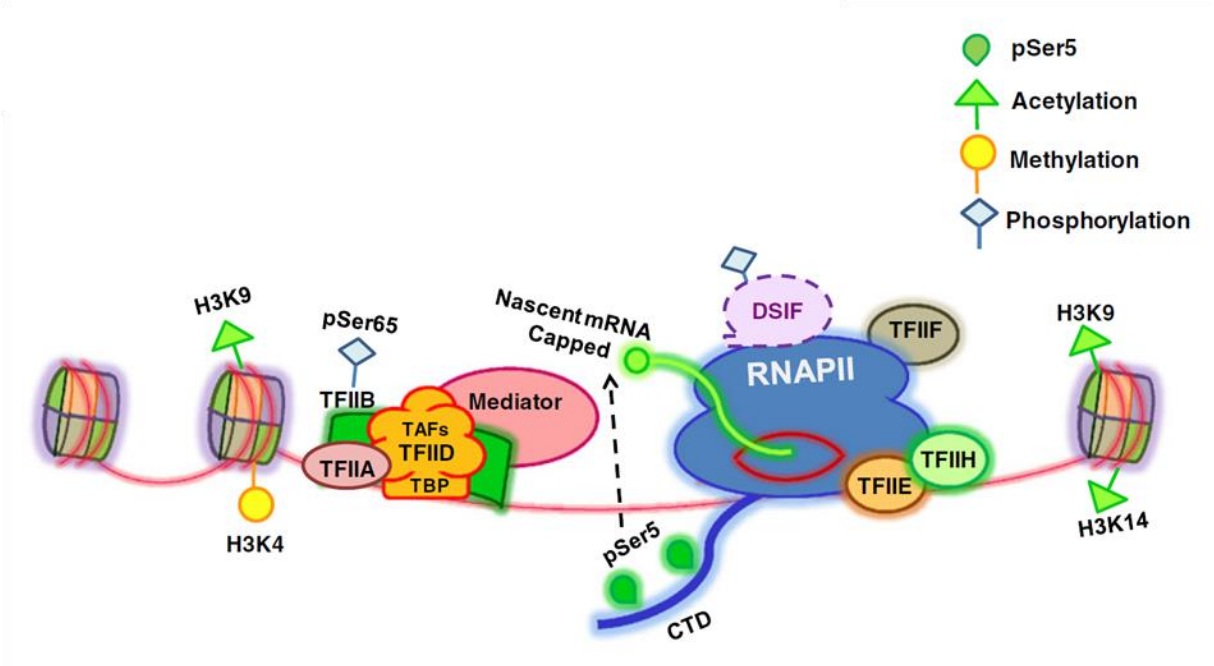

Figure 3. Active transcription initiation. Active initiation is dependent on TFIIH-mediated promoter clearance and phosphorylation of the CTD repeats at serine 5 (Ser5-P). The Ser5-P CTD recruits capping enzyme to the 5′ region of nascent mRNA which triggers RNAPII promoter escape (Shandilya and Roberts, 2012).

The EEC undergoes continued rearrangements before becoming a productive elongation complex and this process is often accompanied with promoter transcriptional pausing near the promoter.

1.2.2.1 Promoter proximal pausing

Promoter proximal pausing is a key regulatory step of the post-initiation process, which was first described in *Drosophila* on uninduced heat-shock genes (Gilmour and Lis, 1986; Rougvie and Lis, 1988). Promoter-proximal pausing is a wide-spread phenomenon in *Drosophila* and mammals at the vast majority of genes but has not been observed in plants yet (Muse et al., 2007; Core et al., 2008). Promoter-proximal pausing describes the state when RNAPII, stimulated by certain signals, pauses in the 5' region of the transcription unit (Figure 4). Promoter-proximal pausing serves as a checkpoint and is rate-limiting before omitting to productive elongation (Giardina et al., 1992; Lis, 1998). The concrete mechanism behind promoter-proximal pausing is not completely understood. Site-specific pausing, cis elements and the first nucleosome downstream of the transcription start site have been proposed to be involved in transcriptional pausing, e. g. the modification state of the first nucleosome has been shown to be important for reaching a productive elongation state (Izban and Luse, 1991; Greive and von Hippel, 2005; Mavrich et al., 2008). In studies using the transcription inhibitor DRB (5,6-dichloro-1-β-D-ribofuranosyl-1H-benzimidazole) several factors implicated in promoter-proximal pausing have been identified. DRB is a nucleoside analogue and inhibits transcription of most protein-coding genes (Sehgal et al., 1976). Three elongation factors are involved in DRB-mediated transcription inhibition: DRB-sensitivity inducing factor (DSIF), Negative elongation factor (NELF) and Positive transcription elongation factor b (P-TEFb) (Price, 2000). DSIF consist of the transcription factors SPT4 and SPT5 (Suppressor of Ty 4 and 5). SPT5 is conserved among all three domains of life, whereas SPT4 is absent in bacteria (Hartzog et al., 1998). NELF comprises four subunits: NELF-1, B, C/D and E and is conserved between mammals and *Drosophila* but not present in *C. elegans*, yeast or *Arabidopsis* (Narita et al., 2003). DRB sensitivity-inducing factor (DSIF) and negative elongation factor (NELF) cooperatively induce transcriptional pausing by binding to RNAPII (Hartzog et al., 1998; Wada et al., 1998; Yamaguchi et al., 1999b). In species where NELF is not present, no transcriptional pausing has been observed (Yamaguchi et al., 2013). During transcriptional pausing capping enzymes associate with RNAPII CTD and SPT5, and the nascent RNA becomes capped (Wen and

Shatkin, 1999; Rodriguez et al., 2000). Promoter-proximal pausing may facilitate capping and a capped nascent RNA might be prerequisite for overcoming the pause (Pei et al., 2003).

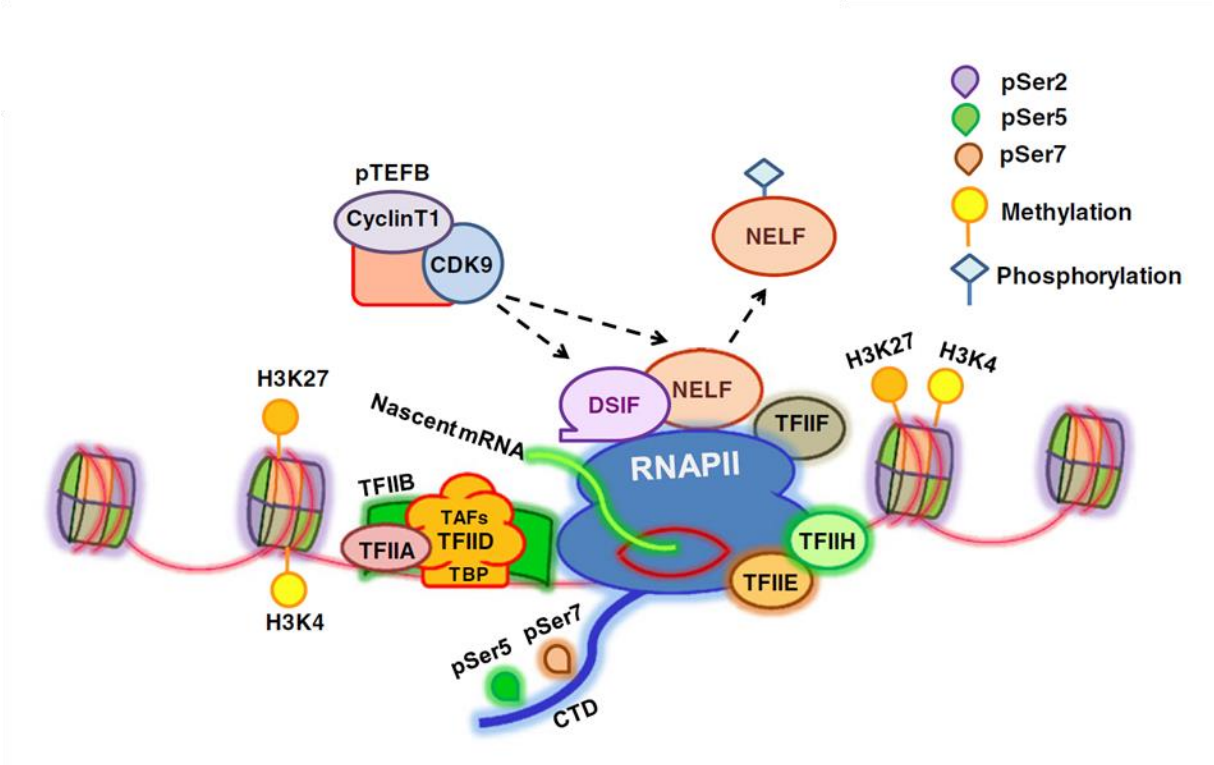

Figure 4. Abortive initiation and paused RNA polymerase II. Depending on the transcriptional competence of RNAPII, it can potentially enter a paused state. The presence of negative factors like NELF and DSIF inhibits productive transcription initiation resulting in abortive transcription or promoter proximal pausing. CDK9, the kinase subunit of P-TEFb, alleviates this repression via phosphorylation of NELF and DSIF. Nucleosomes around a paused polymerase are methylated at H3K4/27 (Shandilya and Roberts, 2012).

1.2.2.2 Productive transcription elongation

Promoter clearance and promoter-proximal pausing are rate-limiting steps in transcript elongation. Several factors are involved in release from pausing and beginning of productive elongation (Figure 5). The negative effects of DSIF and NELF on RNAPII are relieved by phosphorylation of RNAPII and SPT5 P-TEFb (Yamada et al., 2006). Evidence is also given that the capping enzymes counteract the negative effects of DSIF and NELF (Mandal et al., 2004). TFIIS is also important to stimulate the intrinsic RNA-cleavage activity of RNAPII to relieve backtracked polymerases during pausing (Reines et al., 1989). The dissociation of NELF from DSIF is a main step for productive elongation. DSIF stays associated with RNAPII, whereas NELF leaves the complex (Andrulis et al., 2000; Wu et al., 2005). After escape from the pause site, DSIF has a positive effect on elongation (Wada et al.,

1998; Zhu et al., 2007). The phosphorylation activity of P-TEFb is crucial. P-TEFb phosphorylates not only SPT5 but also the CTD of RNAPII at Ser2, which correlates with productive elongation (Fujita et al., 2009; Lenasi and Barboric, 2010). Several factors stimulate the activity of RNAPII, among others there is TFIIF, eleven-nineteen lysine-rich in leukaemia (ELL) and Elongin. Both ELL and Elongin have been shown to stimulate the elongation rate *in vitro*, whereas TFIIF is important for promoter clearance and stalled states (Zawel et al., 1995; Conaway and Conaway, 1999; Yan et al., 1999). Factors involved in processing, export and surveillance of the nascent mRNA like the THO/TREX complex have been shown to facilitate transcription in yeast. Additionally, topoisomerases have been shown to regulate the level of torsional stress due to transcription (Fleischmann et al., 1984; Huertas and Aguilera, 2003).

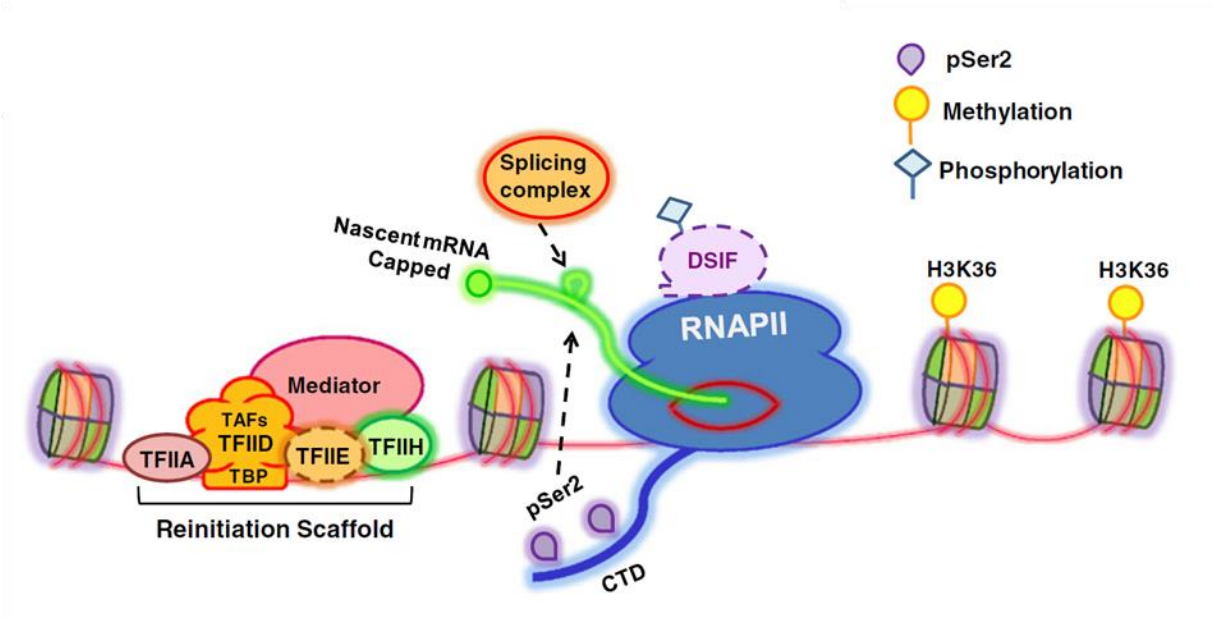

Figure 5. Transcription elongation. Following promoter clearance, RNAPII proceeds for elongation. Part of the PIC components remain associated at the promoter, forming a reinitiation scaffold. The elongating RNAPII CTD repeat is phosphorylated at Ser2 by cyclin-dependent kinase 9 (CDK9), while the SSU72 phosphatase removes Ser5-P. Splicing factors are recruited by Ser2-P CTD. H3K36 methylation marks active elongation (Shandilya and Roberts, 2012).

1.2.3 Termination of transcription

The recognition of a RNAPII termination signal leads to processing of the nascent RNA and the release of RNAPII from the DNA (Proudfoot and Brownlee, 1976; Proudfoot, 2011). Two well-studied pathways of transcription termination are known in yeast: the poly (A)-dependent pathway and the Nrd1-Nab3-Sen1-dependent pathway (Mischo and Proudfoot, 2013). Most protein-coding genes in eukaryotes

have a highly conserved poly (A) signal (PAS), 5'-AAUAAA-3', followed by a G/U-rich sequence. The formation of a defined 3' end of the transcribed RNA and the disengagement of the RNAPII from its DNA template are two closely connected processes to produce functional mRNAs (Birse et al., 1998). Several protein complexes facilitate the key events of transcription termination, including the cleavage and polyadenylation factor (CPSF), the cleavage stimulatory factor (CstF), and the poly (A) polymerase (Figure 6) (Kuehner et al., 2011). A pausing event in the vicinity of the PAS might correlate with the changes in the transcription complex and the recruitment of the mentioned factors upon termination and polyadenylation (Gromak et al., 2006; Grosso et al., 2012). The second termination pathway is utilised when RNAPII transcribes along non-coding RNA. The 3' ends of the non-coding RNAs are either processed by the nuclear exosome-TRAMP and lack a poly (A) tail or by the Nrd1-Nab3-Sen1 pathway, which leads to rapid degradation of the RNA (Vasiljeva and Buratowski, 2006). After release of the nascent RNA from RNAPII, the so-called pre-mRNA undergoes further maturation and processing and is exported into the cytoplasm for translation. For a subsequent round of initiation from the promoter region, the RNAPII itself needs to be reversed to its non-phosphorylated state (Shandilya and Roberts, 2012). To advance RNAPII recycling and a fast reinitiation, the terminal and promoter region can interact, which is known as gene looping (Calvo and Manley, 2003). TFIIB is one of the factors that has been shown to be involved in gene looping (Singh and Hampsey, 2007).

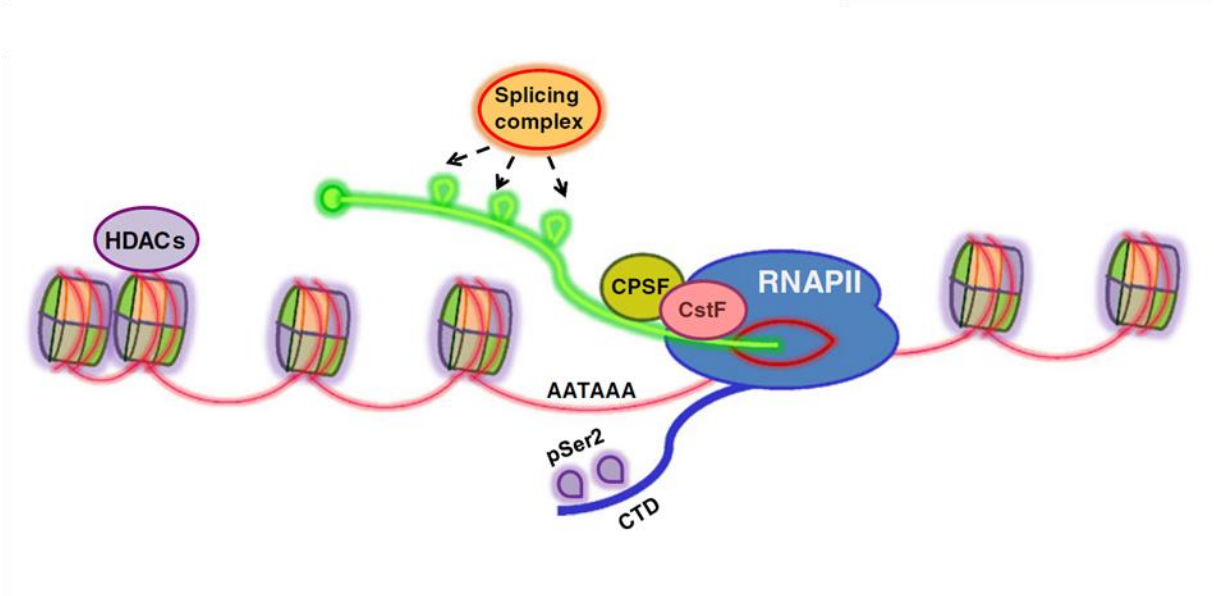

Figure 6. Transcription termination. As the RNAPII reaches the poly (A) signal at the 3′ end, processing and termination specific complexes such as CPSF and CstF are recruited. The CTD repeat is hyper-phosphorylated at serine 2 at the gene terminus (Shandilya and Roberts, 2012).

1.3 Phosphorylation cycle of RNA Polymerase II CTD during transcription

Rpb1, the largest subunit of RNAPII, evolved a unique, highly repetitive carboxy-terminal domain (CTD), which plays a complex role in regulation of the transcription cycle (Chapman et al., 2008). The CTD is composed of multiple tandem repeats with the consensus sequence YSPTSPS (Liu et al., 2010). The CTD differs in length correlating with the complexity of the organism: *S. cerevisae* has 26, mammalian 52, and *Arabidopsis* 34 repeats (Hajheidari et al., 2013). The CTD has been shown to be dispensable for catalytic activity of RNAPII but essential for viability (Serizawa et al., 1993; West and Corden, 1995). During transcription, the CTD serves as a docking platform for several factors. The capability to interact with a diverse set of factors is achieved by extensive post-translational modifications of the heptapeptide repeats. Tyr, Thr and Ser can be phosphorylated, the prolines can undergo isomerisation and methylations, also ubiquitinations and glycosylation have been observed (Li et al., 2007b; Egloff and Murphy, 2008; Sims et al., 2011). Specific CTD modifications are linked to certain stages of RNA transcription and processing (Figure 7). Ser5 phosphorylation is associated with promoter release and the recruitment of the 5’ capping machinery (Jiang et al., 1996; Cho et al., 1997). Besides Ser5, phosphorylation is also connected to histone modifications and chromatin remodelling (Krogan et al., 2003). Phosphorylation levels of Ser5 are enriched at the promoter region and decrease towards the 3’ end (Mayer et al., 2010). The cyclin dependent kinase subunit Cdk7 of TFIIH phosphorylates Ser5 and Ser7 early in transcription (Liu et al., 2004). Two phosphatases, SSU72 and RTR1, have been shown to remove these Ser5-P marks (Krishnamurthy et al., 2004; Mosley et al., 2009). Subsequent to Ser5-P at the promoter region, Ser2-P increases downstream of the transcriptional start site, which correlates with productive elongation (Heidemann et al., 2013). The increase of Ser2-P towards the 3’ end correlates with recruitment of factors and complexes involved in productive elongation and mRNA splicing (Morris and Greenleaf, 2000; Yoh et al., 2007). Additionally, 3’ processing, termination and export is associated to Ser2-P (Strasser and Hurt, 2001; MacKellar and Greenleaf, 2011). The kinase subunit Cdk9 of P-TEFb together with recently found Cdk12 and Cdk13 phosphorylates Ser2 in a Ser5-P-dependent manner (Bartkowiak and Greenleaf, 2011). Conversely, the RNAPII-associated phosphatase

FCP1 (TFIIF-associated CTD-phosphatase) removes Ser2 marks at the 3' region of the transcribed region (Cho et al., 2001). Ser7 is also dynamically phosphorylated during the transcription cycle and peaks early in transcription (Mayer et al., 2010; Schwer and Shuman, 2011). Ser7-P is mainly involved in snRNA maturation (Egloff et al., 2007).

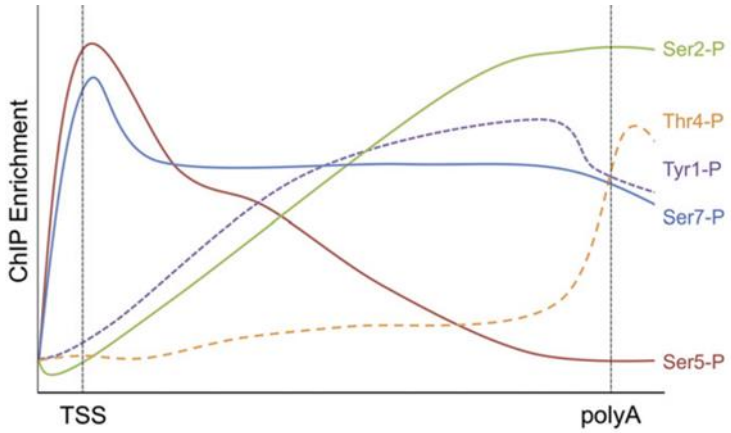

Figure 7. Phosphorylation profile among transcribed genes of several amino acid residues of the RNAPII CTD. Average profile of CTD phosphorylation marks in genes revealed by chromatin immunoprecipitation (ChIP) experiments. RNAPII attached to the cellular DNA is purified and correlated to defined gene sections using monoclonal antibodies, which target the specific CTD modifications (Heidemann et al., 2013).

1.4 mRNA processing

In addition to synthesis, the nascent RNA is also processed during transcription (Figure 8). Pre-mRNA processing is coordinated by the phosphorylation state of the CTD of the biggest subunit of RNAPII, Rbp1. Not only the phosphorylation cycle is important for proper recruitment of the processing factors, the CTD itself serves as loading platform of several transcription and mRNA processing factors (Chapter 1.3 and Aguilera, 2005). As the nascent RNA reaches a length of 22-25 nt and emerges from the exit channel, pre-mRNA capping takes place (Lenasi and Barboric, 2013). The formation of the 7-methylguanosine cap is catalysed by three enzymes: triphosphatase, guanylyltransferase and methyltransferase (Shuman, 2001). The capping reaction is reversible and driven by two enzymes in metazoans: The guanylyltransferase, which carries the triphosphatase and guanylyltransferase activity, and the methyltransferase. Both enzymes do not interact directly with each other but with the Ser5-P CTD of RNAPII (Shuman, 2001). After its formation, the cap is bound by the cap-binding proteins (CBP) CBP20 and CBP80 (Izaurralde et al., 1994). The cap-binding complex (CBC) is required for further post-transcriptional

modifications (Aguilera, 2005). The CBC links post-transcriptional modification to mRNA export by interaction with the export factor ALY of the TREX (transcription/export) complex and is also involved in nuclear mRNA decay (Das et al., 2003; Cheng et al., 2006a). CBC is also involved in the next step of modification, splicing, by increasing the efficiency of binding of the small nuclear ribonucleoprotein (snRNP) core components to the cap proximal 5' splice site (Bird et al., 2004). Most spliceosomes, including those for alternative splicing, are recruited during transcription, the splicing reaction itself occurs also rather co-transcriptionally than post-transcriptionally (Beyer and Osheim, 1988; Pandya-Jones and Black, 2009). The exon junction complex (EJC) is deposited to exon-exon junctions to mark the RNA for further processing steps as export, translation and nonsense-mediated decay (Reichert et al., 2002).

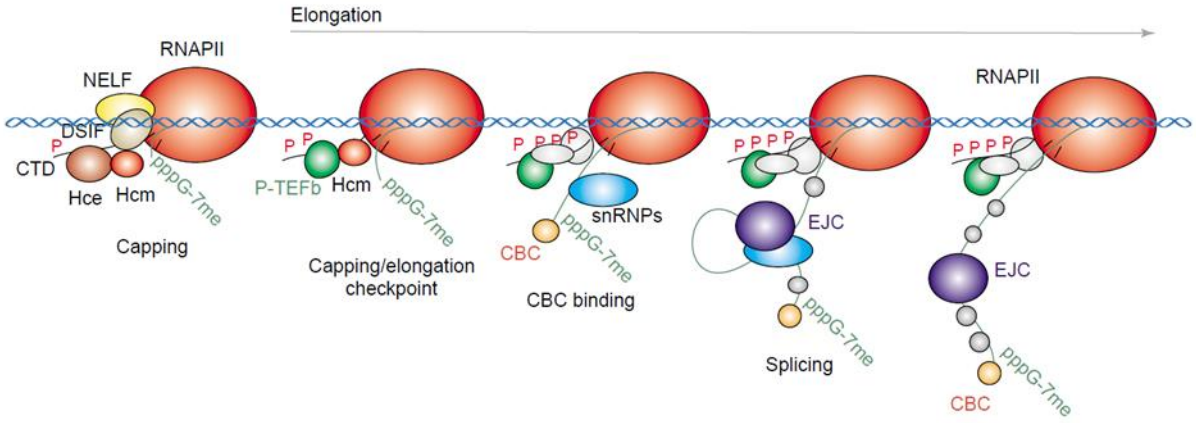

Figure 8. Schematic representation of the first steps of co-transcriptional mRNP assembly. Shown is the 5' capping, CBC (cap-binding protein complex) loading and the splicing-dependent assembly of the exon junction complex (EJC), as it may occur in humans (Heidemann et al., 2013).

The processing of the 3' end of the pre-mRNA is a two-step process: cleavage shortly after the 5'-AAUAAA-3' sequence, and polyadenylation of the exposed 3'-OH (Mandel et al., 2008). Several factors are involved in this process, including CstF and CPSF (1.2.3). Cleavage and early polyadenylation can occur co-transcriptional, but also post-transcriptional poly (A) site cleavage was reported (Bauren et al., 1998; Licatalosi et al., 2002). Co-transcriptional loading of RNA binding proteins (e. g. CBC and EJC) regulates different events, like mRNA export, translation, and the life span of the RNA, e. g. by recruiting factors involved in processing or protecting from nucleases (Daneholt, 2001). Nascent transcripts are packaged for export with export adapters, building so called mRNPs (messenger ribonuceloproteins) to become export competent. The packaging is tightly controlled, and only fully processed mRNPs become export competent (Schmid and Jensen, 2008). To ensure this, the

recruitment of export adapters is linked to several steps of the transcription cycle (Lei et al., 2001; Iglesias and Stutz, 2008). In the end the mRNA and associated factors are exported through nuclear pores and translated in the cytoplasm.

1.5 SPT4-5

The transcript elongation factor SPT5 or NusG in *E. coli* is the only transcription factor conserved in all three domains of life (Harris et al., 2003). SPT5 forms a complex with the small subunit SPT4, called SPT4-SPT5 or DSIF in mammals and *Drosophila* (Hartzog and Fu, 2013). SPT4 is found in eukaryotes and archaea but is absent in bacteria (Ponting, 2002). SPT4 and SPT5 were originally discovered in a genetic screen for mutations that supress the defects caused by insertions of the transposon Ty (Suppressor of Ty, SPT) (Winston et al., 1984). Studies in 1998 showed subsequently that SPT4 and SPT5 regulate transcription elongation (Hartzog et al., 1998).

Additional studies in yeast revealed that SPT4-SPT5 prevents pausing or arrest of the elongating RNAPII, and both SPT4-SPT5 and RNAPII must be coordinated for normal growth (Hartzog and Fu, 2013). Human homologs of SPT4-SPT5, in contrast to yeast, were found as inhibitors of elongation but were also described to stimulate transcription (Wada et al., 1998). The complex was termed DSIF in humans. The inhibitory function of SPT4-SPT5 has only been demonstrated in a few organisms and this inhibitor function correlates with the existence of NELF, a second multi-subunit complex (see 1.2.2.1), which is required for DSIF activity in mammals and *Drosophila* (Yamaguchi et al., 2013). It has become customary to use the term DSIF in organisms, in which its negative activity is known, whereas in all other organisms it is called SPT4-SPT5 (Hartzog and Fu, 2013). SPT5/NusG appears to be essential in all three domains of life, whereas SPT4 is for example dispensable in yeast but its importance in higher eukaryotes has not been clarified (Deuring et al., 2000; Pei and Shuman, 2002; Yamada et al., 2006).

1.5.1 Structure of the SPT4-SPT5 complex and the interaction with RNAPII

SPT4-SPT5 is a heterodimeric complex consisting of the large subunit SPT5 and the small subunit SPT4. The large subunit SPT5 is a multi-domain protein consisting of an N-terminal acidic domain, a NusG N-terminal (NGN) domain, multiple KOW (Kyprides, Ouzounis, Woese) domains and a set of short repeats at the C-terminus

(C-terminal repeats, CTR). The KOW domains mediate protein-protein interaction, whereas the NGN domain has been shown to interact both with the RNAPII and SPT4. Tyr, Ser and Thr residues of the SPT5-CTR have been shown to be phosphorylated, for example by the kinase activity of P-TEFb (Ponting, 2002; Yamada et al., 2006; Hartzog and Fu, 2013). In contrast to SPT5, SPT4 is a small zinc finger protein (Malone et al., 1993). SPT4 and SPT5 interact via the NGN domain of SPT5, where a large hydrophobic surface is created by the beta sheet shape of the interface (Guo et al., 2008). Binding of SPT5 to RNAPII is, like to SPT4, mediated by the NGN domain of SPT5. The affinity of SPT5-NGN alone to RNAPII is lower compared with the SPT4-SPT5 complex (Hirtreiter et al., 2010). Direct interactions of SPT4 and RNAPII have not been observed (Hartzog and Fu, 2013). SPT4 does not only increase the SPT5 binding affinity to RNAPII but it also increases the stability of the SPT5 protein itself. In yeast cells lacking SPT4, SPT5 protein levels drop to one third compared with wild-type (Ding et al., 2010). SPT5 binds to the clamp domain near the coiled-coil motif of RNAPII and thereby it spans the cleft elongating RNAPII, where the active centre of RNAPII, the nascent RNA, and the DNA are situated in (Figure 9).

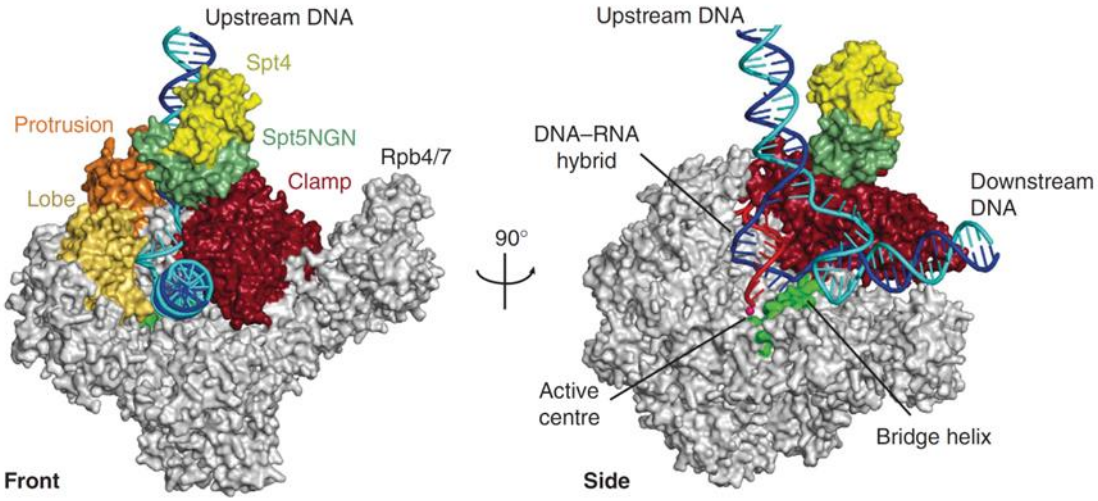

Figure 9. Model of the complete yeast RNAPII–SPT4/5 elongation complex. Proteins are shown as molecular surfaces with key domains highlighted in colour and labelled. Nucleic acids are shown as ribbon models with the DNA template, DNA non-template, and the RNA in blue, cyan, and red, respectively (Martinez-Rucobo et al., 2011).

SPT5 thereby encloses the DNA-RNA hybrid in the elongation complex and promotes processivity via allosteric mechanisms. The binding of SPT4-SPT5 to RNAPII completely encircles the DNA-RNA hybrid and leads to conformational

changes, which are necessary for enhanced processivity of RNAPII (Hartzog and Fu, 2013). Processivity may also be mediated by interaction of SPT5 with the non-coding strand and maintaining the transcription bubble, in which also the first KOW domain might be involved in (Klein et al., 2011; Martinez-Rucobo et al., 2011). Additionally, SPT4-SPT5 binds RNAPII at sites that are also bound by transcription initiation factors. TFIIE binds at the same site as SPT4-SPT5 predicting competition between these factors: TFIIE out-competes the inhibitory effect of SPT4-SPT5 on the pre-initiation complex, whereas SPT4-SPT5 displaces TFIIE from the elongation complex and stimulates processivity. The out-competition of TFIIE by SPT4-SPT5 is a crucial step for promoter escape and accomplishing a productive elongating state (Pokholok et al., 2002; Mayer et al., 2010; Grohmann et al., 2011).

1.5.2 SPT4-SPT5 in transcription elongation

SPT4-SPT5 is tightly associated to RNAPII in a transcription-dependent manner. This association begins just down-stream of the transcription start site and persists until the site of termination (Tardiff et al., 2007; Glover-Cutter et al., 2008). SPT4-SPT5 mirrors extensively the distribution of RNAPII on chromatin and primarily co-localises with RNAPII phosphorylated at Ser2 (Andrulis et al., 2000). The SPT4-SPT5 complex has also been shown to associate with RNAP I, regulating its transcript elongation as well as rRNA processing. These findings suggest a high conservation of SPT5 and an existence prior the divergence of the nuclear RNA polymerases of eukaryotes (Schneider et al., 2006; Anderson et al., 2011). In contrast to RNAP I and RNAPII, there is no evidence that SPT4-SPT5 associates with or regulates RNAPIII. Mutants of *SPT4* and *SPT5* have been shown to affect the translocation rate and the processivity of the elongating form of RNAPII (Quan and Hartzog, 2010). As SPT4-SPT5 is also involved in transcriptional pausing after promoter clearance, the positive functions of SPT4-SPT5 must be somehow triggered, which is mediated by P-TEFb. P-TEFb phosphorylates not only the CTD of RNAPII but also the CTR of SPT5 and NELF, if existent. This phosphorylation reverses the inhibitory function of SPT5 and stimulates its positive role in elongation (Yamada et al., 2006). SPT4-SPT5 promotes elongation by reducing the frequency of transcriptional pausing and arrest of the elongating RNAPII and thereby facilitating induced processivity, which is consistent with the findings that elongation is only promoted *in vitro* by SPT4-SPT5 when nucleotides are limiting (Zhu et al., 2007). Transcriptional processivity is maintained by interaction with the nascent RNA and the RNAPII directly. SPT4-SPT5 protects

the elongation complex from pausing and arrest, and assists RNAPII by overcoming such triggers or barriers like nucleosomes (Bourgeois et al., 2002; Zhu et al., 2007). These suggestions are supported by the findings that SPT4-SPT5 coordinates chromatin remodelling and histone modification during transcription elongation (Chen et al., 2009). The chromatin remodeller Chd1 (chromodomain helicase DNA-binding 1), the methyltransferases Set1 and Set2 (Su(var)3-9, Enhancer-of-zeste Trithorax 1 and 2) and the histone modifier Paf1 (RNA Polymerase-associated factor 1) complex have been shown to interact with SPT4-SPT5 (Squazzo et al., 2002; Simic et al., 2003). The Paf1 complex in particular interacts with the phosphorylated form of the SPT5 CTR, suggesting that the CTR acts as a phosphorylation state regulator of recruitment of factors involved in productive elongation (Liu et al., 2009). SPT4-SPT5 might protect elongating RNAPII from transcription arrest events due to nucleosomes and their modifications (Hartzog and Fu, 2013). In particular, the CTR of SPT5 has also been implicated to recruit RNA processing factors to the elongating RNAPII (Schneider et al., 2010). In yeast, *spt4* and *spt5* mutations cause capping and splicing defects, affect the poly-adenylation site choice, mRNA export, and rRNA processing (Cui and Denis, 2003; Burckin et al., 2005; Suh et al., 2010; Anderson et al., 2011). SPT4-SPT5 assists with recruitment of factors that co-transcriptionally modify the nascent RNA including 5’ capping, which has been reported to have a positive role in early elongation (Kim et al., 2004). The capping enzymes interact not only with the C-terminal domain of RNAPII but also with the SPT5 CTR. The capping enzymes of yeast directly interact with SPT5 dependent on the phosphorylation state of the CTR (Lindstrom et al., 2003). SPT4-SPT5 also binds RNA directly and can be cross-linked with the nascent RNA of 22 nt or longer (Missra and Gilmour, 2010). This leads to the suggestion that the SPT5-RNA interaction may influence RNA processing because recent studies showed that SPT4-5 assists processing factors to get access to the nascent RNA (Hartzog and Fu, 2013).

1.6 Aim of this thesis

Transcription of protein-coding genes by RNA polymerase II is not only regulated on the level of initiation but also on elongation level. Several transcription elongation factors have been identified in the recent years, especially in yeast and humans, which are necessary for productive elongation. The transcription elongation factor complex SPT4-SPT5, also called DSIF has been extensively studied from yeast to human, whereas in plants it has not been identified so far.

The aim of this thesis is to identify and characterise possible *Arabidopsis* orthologs of SPT4-SPT5. Analysis of these orthologs will be conducted by characterisation of knockout or knockdown mutant plants. A phenotypically characterisation of those mutants will give inside information in the function of SPT5 and SPT4 in overall growth and development. To further investigate a possible involvement of SPT4-SPT5 in specific developmental pathways the observed mutant phenotypes will be investigated in detail. These plants will be further analysed by genome-wide transcript profiling compared to wild-type, in order to identify possible genes involved in the development of the observed mutant phenotypes.

The possible SPT4-SPT5 complex will also be characterised biochemically. A possible physical interaction of SPT4 and SPT5 as complex and its possible interaction partners will be analysed by affinity purification. Antibodies against SPT4 and SPT5 will be created and used for identification of SPT4 and SPT5 proteins in *Arabidopsis* and to analyse the association of SPT4 and SPT5 and different forms of RNAPII to chromatin. In particular transcribed compared to non-transcribed regions, will be examined comparatively in wild-type and mutant plants by chromatin immunoprecipitation and immunostaining to elucidate a possible role of SPT4-SPT5 in transcription elongation.

CHAPTER 2

RESULTS

2. Results

2.1 Identification of *Arabidopsis SPT4* and *SPT5*

The subject of research in this thesis is the heterodimeric complex SPT4-SPT5. Possible *Arabidopsis* orthologs of the human and yeast SPT4 and SPT5 were identified with a BLASTP search of the *Arabidopsis* database (http://www.arabidopsis.org/) and the amino acid (aa) sequences of yeast and human SPT4 and SPT5 were used as a query for the search. The BLASTP search resulted in two hits for both SPT4 and SPT5. The two genes At5g08565 and At5g63670 code for the SPT4 orthologs and were termed *SPT4-1* and *SPT4-2*, respectively. The SPT5 ortholog is encoded by the two genes At2g34210 and At4g08350 which were termed *SPT5-1* and *SPT5-2*, respectively (Figure 10A).

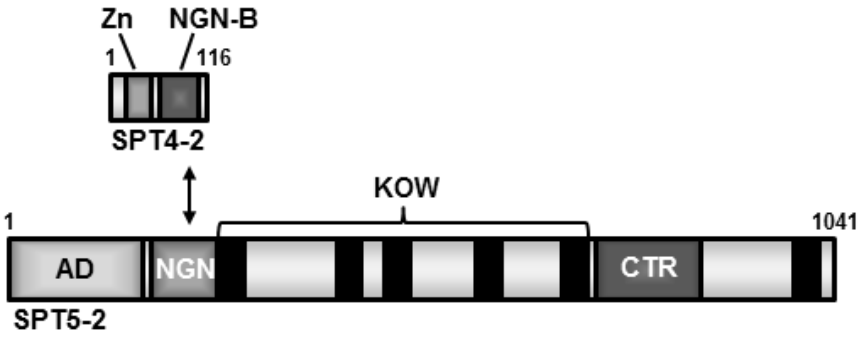

Figure 10. **Gene and protein models. (A)** The gene models of the *SPT4* and *SPT5* genes are adapted from the *Arabidopsis* database (http://www.arabidopsis.org/). Coding sequences are indicated by grey boxes, UTRs in black, while introns are depicted as lines. **(B)** Domain structure of SPT4 and SPT5.

Sequence identities of SPT4-1/2 and SPT5-1/2 were compared with a pairwise global sequence alignment (http://www.ebi.ac.uk/Tools/psa/emboss_needle/). SPT4-1 and SPT4-2 share 87.9% amino acid sequence identity and have both a size of ~13.4 kDa. SPT5-1 and SPT5-2 have 65.8% of their amino acid sequence conserved. SPT5-1 and SPT5-2 are ~110.3 kDa ~115.4 kDa in size, respectively. Comparing the amino acid sequence identity of SPT4-1 to its yeast, human and rice relatives, SPT4-1 is to 26.0%, 36.6% and 66.4% identical to its orthologs, respectively. The amino acid sequence of SPT4-2 is to 27.4%, 35.8% and 67.2% conserved comparing its yeast, human and rice relatives, respectively. SPT5-1 shares 20.9%, 30.6% and 46.7% identities to its yeast, human and rice relatives,

respectively. SPT5-2 is to 22.9%, 34.4% and 54.0% identical to its yeast, human and rice relatives, respectively. The comparison of SPT4 showed that the zinc-binding motif, including four invariant Cys residues, and the NGN-binding motif (NGN-B), which is important for interaction with SPT5, are highly conserved (Figure 10 and Figure 11).

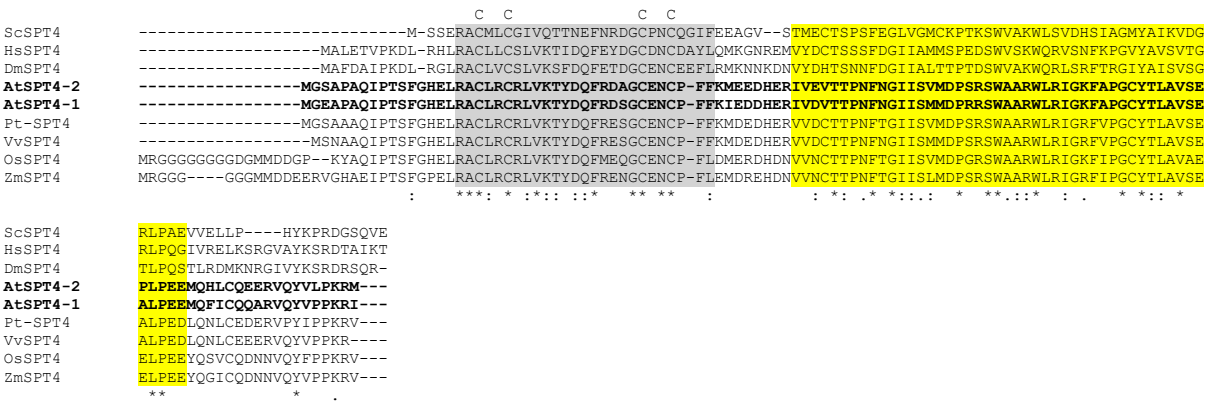

Figure 11. Amino acid sequence alignment of SPT4 from different species. The alignment was generated using Clustal Omega (http://www.ebi.ac.uk/Tools/msa/clustalo/) and the SPT4 amino acid sequences of *Saccharomyces cerevisiae* (Sc), *Homo sapiens* (Hs), *Drosophila melanogaster* (Dm), the dicot species *Arabidopsis thaliana* (At), *Populus trichocarpa* (Pt) , *Vitis vinifera* (Vv) and the monocot species *Oryza sativa* (Os) and *Zea mays* (Zm). The zinc-binding motif is highlighted in grey and the NGN-binding domain, mediating the interaction with SPT5, in yellow. The four Cys residues forming the zinc finger are depicted in red on top of the sequences, and the Ser residue critical for SPT5-interaction is indicated by an arrow (Guo et al., 2008). Asterisks below the sequences indicate invariant residues, while (:) indicate residues that are highly conserved.

Yeast and metazoan SPT5 displays an N-terminal acidic domain, the NGN and 5 to 6 KOW domains, which are conserved also in *Arabidopsis*. Besides the mentioned domains *Arabidopsis* has six KOW domains and a C-terminal repeat domain (CTR) like in humans or *Drosophila*. The CTR, which has been shown to be important for recruitment of factors that are involved in co-transcriptional processing and histone modification, shares similarity with human and Drosophila SPT5 and with its serine and threonine residues might be a target of phosphorylation as those aa residues are conserved among species (Hartzog and Fu, 2013). The NGN-domain has been shown to be important for interaction with SPT4 and the biggest subunit of RNAPII. The KOW domains are important for protein-protein and protein-RNA/DNA interaction. The CTR with its serine and threonine residues might be a target of phosphorylation as those amino acid residues are conserved among species (Figure 10 and Figure 12).


ScSPT5
HsSPT5
DmSPT5
AtSPT5-1
AtSPT5-2
PtSPT5
VvSPT5
OsSPT5
ZmSPT5

Figure 12. Amino acid alignment of SPT5 of different species. The alignment was generated using Clustal Omega (http://www.ebi.ac.uk/Tools/msa/clustalo/) and the SPT5 amino acid sequences of *Saccharomyces cerevisiae* (Sc), *Homo sapiens* (Hs), *Drosophila melanogaster* (Dm), the dicot species *Arabidopsis thaliana* (At), *Populus trichocarpa* (Pt), *Vitis vinifera* (Vv) and the monocot species *Oryza sativa* (Os) and *Zea mays* (Zm). The acidic N-terminal domain is highlighted in yellow, the NGN domain mediating the interaction with SPT4 (and RNAPII) in grey, and the KOW domains in blue. The (putative) phosphorylated Thr residues of the C-terminal repeats (CTR) (Yamada et al., 2006) are indicated in red, and the Glu residue within the NGN domain that is critical for SPT4-interaction is indicated by an arrow (Guo et al., 2008). Asterisks below the sequences indicate invariant residues, while (:) indicate residues that are highly conserved.

In addition to SPT5-1/2, the *Arabidopsis* genome encodes a third protein with similarity to SPT5, termed SPT5-like (SPT5L). SPT5L is plant-specific and has been implicated in siRNA-mediated RNA-directed DNA methylation pathway (Bies-Etheve et al., 2009; He et al., 2009; Rowley et al., 2011). SPT5L has a size of ~158 kDa and shares 17.9% amino acid sequence identity with SPT5-2 and 16.5% with SPT5-1. SPT5L has like SPT5 a (shorter) acidic domain, the NGN domain and three KOW motifs. In addition, SPT5L contains an extensive C-terminal domain with multiple WG/GW repeats.

2.2 Expression of SPT4 and SPT5 in *Arabidopsis*

The expression of *SPT4* and *SPT5* was analysed in *Arabidopsis* with the *Arabidopsis* transcript profiling data from http://www.arabidopsis.org/ which is based on a large set of publicly available microarray data of different tissues and developmental stages. According to this data *SPT4-1*, *SPT4-2* and *SPT5-2* genes are ubiquitously expressed throughout all tissues. *SPT4-1* seems to be expressed at

lower levels compared with *SPT4-2*. *SPT4-1* is highly expressed in mature pollen whereas *SPT4-2* shows a reduced expression in this tissue. *SPT5-1* appears to be expressed at very low levels (or not at all) in the majority of analysed tissues except for pollen, where the *SPT5-1* transcript is clearly detected (Figure 13).

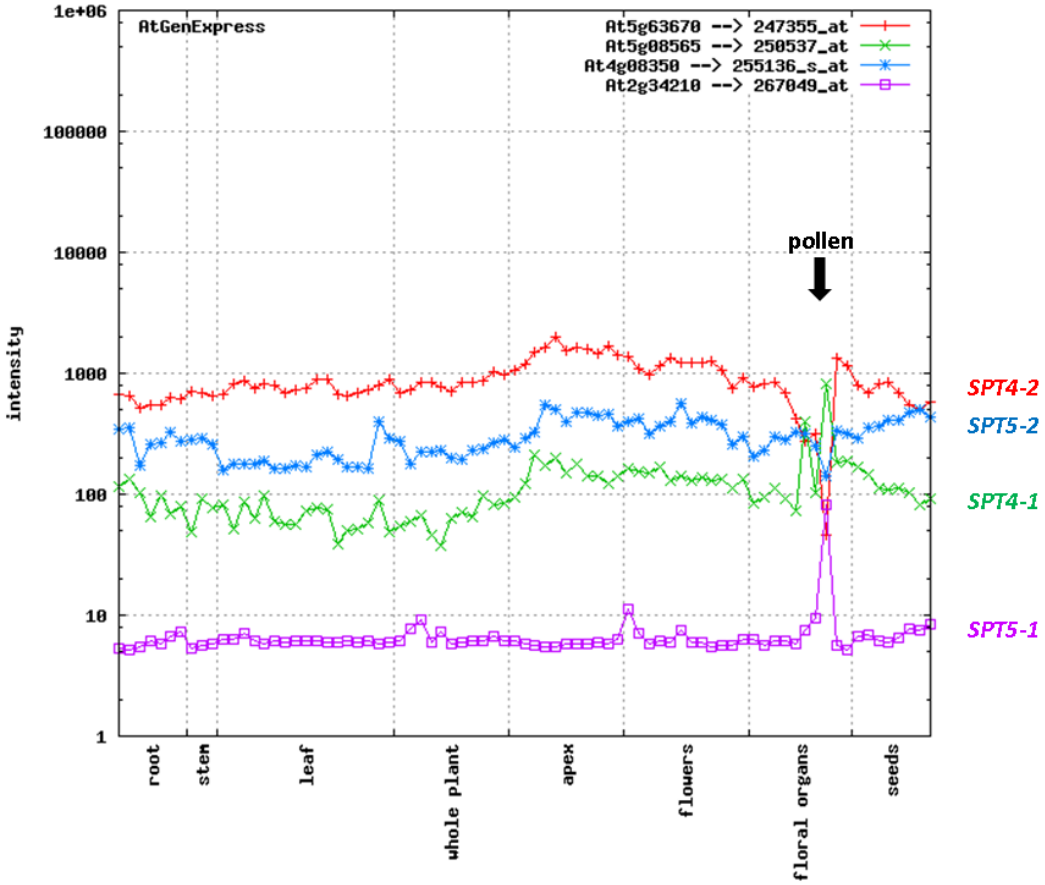

Figure 13. Transcript levels of *SPT4-1/2* and *SPT5-1/2*. The transcript levels in various tissues are displayed using the AtGenExpress tool (http://jsp.weigelworld.org/expviz/expviz.jsp) based on a large set of microarray transcript profiling data.

To validate the microarray data RT-PCR with primers specific for *SPT4-1/2* and *SPT5-1/2* has been performed in selected tissues. In line with the transcript profiling data, the transcripts of *SPT4-2* and *SPT5-2* were ubiquitously detected in in all samples. The *SPT4-1* transcript was detected at low levels in most tissues, whereas higher amounts were observed in stamen and pistil. The *SPT5-1* transcript was exclusively detected in stamen and pistils. Since stamen and pistils were isolated from open flowers where pollen were adhering to the pistil, it is possible that in line with the above-mentioned microarray data the signal detected in the RT-PCRs originated from pollen RNA. Therefore, the *SPT4-1, SPT4-2* and *SPT5-2* genes appear to be widely expressed in the plant, while *SPT5-1* expression likely is restricted to pollen and pistil (Figure 14).

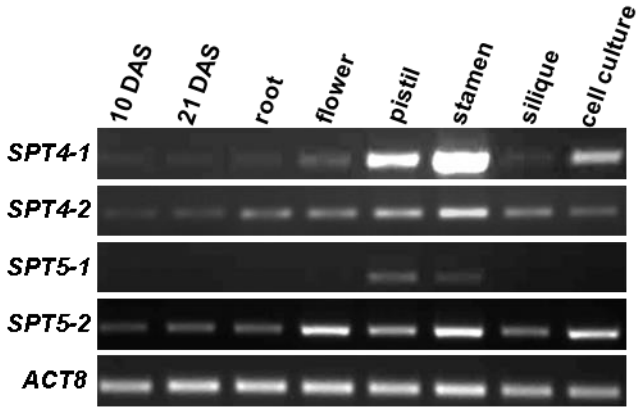

Figure 14. Expression of *SPT4-1/2 and SPT5-1/2*. Transcript levels of the *SPT4-1/2* and *SPT5-1/2* genes as well as of the reference gene *ACT8*, were examined by RT-PCR from RNA samples of selected tissues (aerial parts of 10 and 21 days after stratification (DAS) seedlings, roots, inflorescence heads, pistils, stamen, elongated siliques, and L*er* PSD-B suspension cultured cells) with gene-specific primers.

To analyse the expression pattern of *SPT4-1/2* and *SPT5-1/2* in detail, fusions of the GUS gene and eGFP-NLS with the putative promoter sequences of the four genes were cloned. As promoter sequence the sequence 5' of the ATG until the 3' UTR of the downstream gene was used. Unfortunately, transformed into the wild-type ecotype Columbia-0, neither the GUS nor the eGFP-NLS fusions showed any staining or fluorescence, respectively.

2.3 Characterisation of T-DNA insertion mutants in *SPT4-2* and *SPT5*

To examine the role of *SPT4* and *SPT5* in *Arabidopsis*, available T-DNA insertion lines were analysed. The lines were obtained from the Nottingham Arabidopsis Stock Centre (NASC). While no suitable lines were available for SPT4-1, we examined one line for SPT4-2 and SPT5-1 each, and several lines for SPT5-2 (Figure 15). The genetic background of all insertion mutants used in this study was the *Arabidopsis* ecotype Columbia-0 (Col-0).

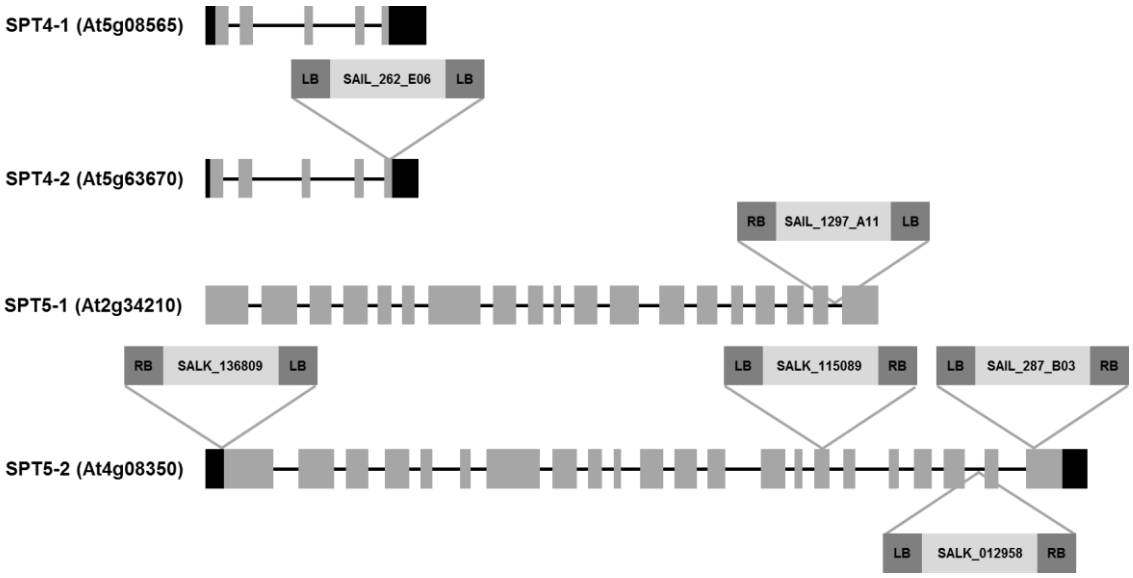

Figure 15. Gene models. The gene models of the *SPT4* and *SPT5* genes are adapted from the *Arabidopsis* database (http://www.arabidopsis.org/). Coding sequences are indicated by light grey boxes, UTRs in black, while introns are depicted as lines. The positions of T-DNA insertions are also indicated as annotated at *Arabidopsis* database.

2.3.1 Identification and characterisation of the *spt4-2* insertion allele

According to databases two T-DNA lines for *SPT4-1* were available at GABI KAT (University Bielefeld), GK-173A10-013459 and GK-879H10-026525. However the insertion positions, supposed to be in the second exon and in the putative promoter region of *SPT4-1*, respectively, could not be confirmed by GABI KAT. Accordingly, the *Arabidopsis* insertion line SAIL_262_E06 for *SPT4-2* was obtained from Syngenta Arabidopsis Insertion Library (SAIL) collection.

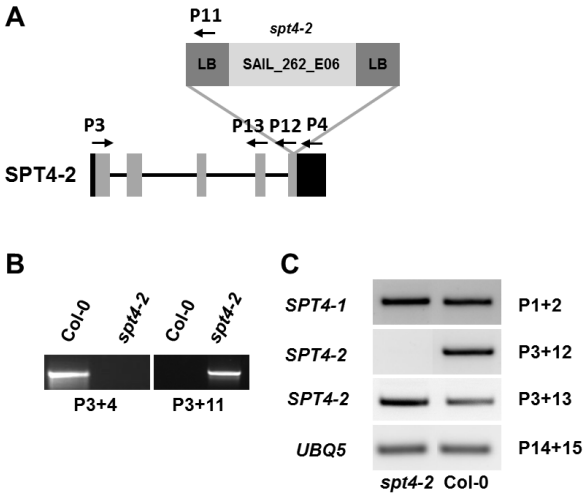

Figure 16. Genotyping and expression in *spt4-2*. (A) Gene model of *SPT4-2* with T-DNA and primers used for genotyping and expression. **(B)** Genotyping of wild-type and mutant (*spt4-2)* plants by PCR with the indicated primers. **(C)** In *spt4-2* plants no transcript of the *SPT4-2* gene is detectable by RT-PCR in RNA isolated from seedlings, while the transcripts of the *SPT4-1* gene and of the reference gene *UBQ5* are present approximately at wild-type levels.

According to the data provided at http://www.arabidopsis.org/ (TAIR) the SAIL_262_E06 T-DNA is inserted at the last exon of *SPT4-2* (At5g08565) at base pair 1200 downstream of the translational start codon with the left border (LB) of the T-DNA directed towards the 5'-end region of the gene (Figure 16A); this mutant is termed *spt4-2* in this thesis. The insertion position has been verified by PCR-based genotyping and sequencing of the PCR product. The T-DNA is situated 5 bp down-stream of the annotated position at the last exon, at base pair 1205 down-stream of the translational start codon. Homozygous T-DNA mutant plants were identified using PCR-based genotyping. The extracted DNA was used as a template for PCR reactions with primer specific for *SPT4-2* and the T-DNA for amplification of wild-type or T-DNA insertion alleles, respectively (Figure 16B).

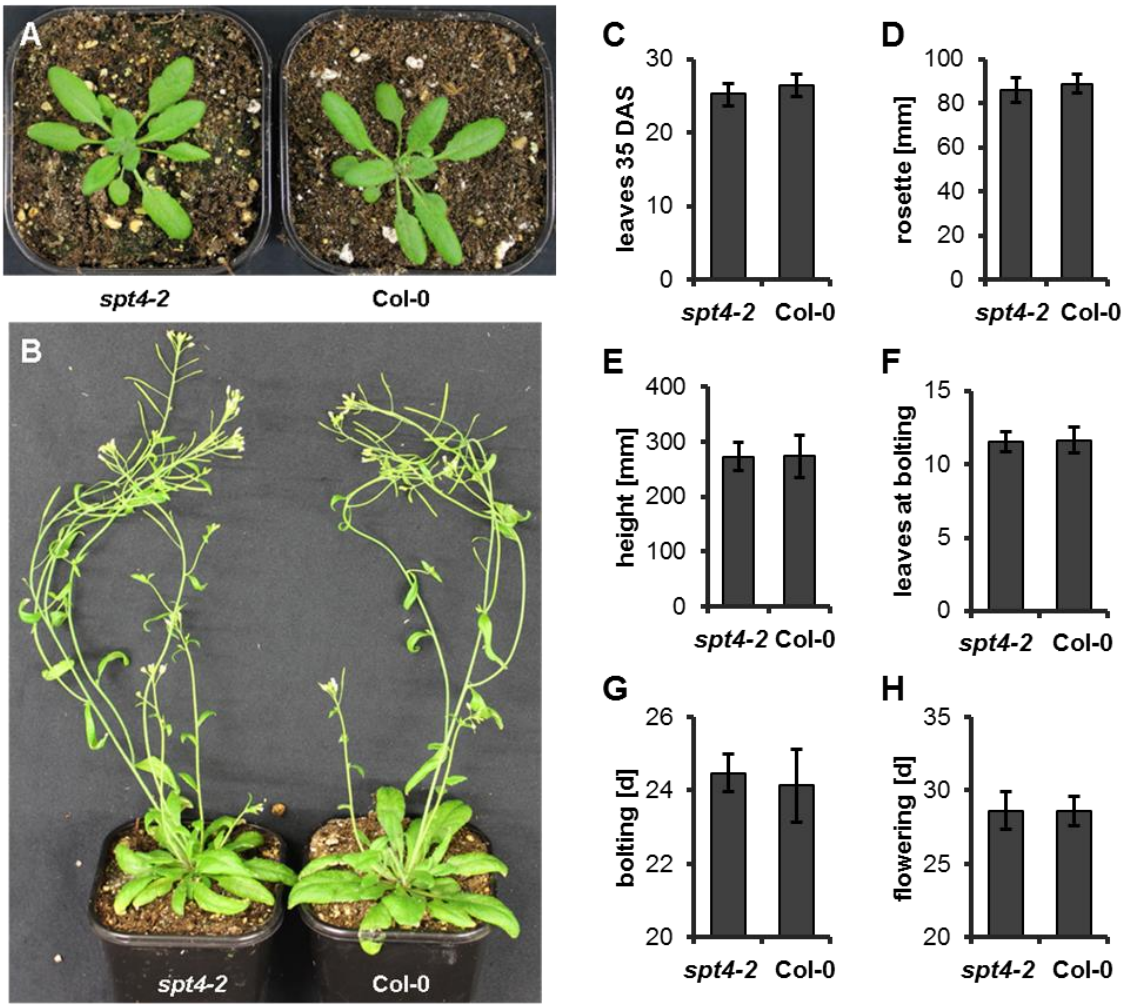

Figure 17. Phenotypic analyses of *spt4-2*. *spt4-2* plants (SAIL_262_E06) at **(A)** 21 DAS and **(B)** 35 DAS develop similar to Col-0 control plants. **(C)** The number of leaves at bolting, **(D)** bolting time, **(E)** flowering time, **(F)** number of leaves at 35 DAS, **(G)** rosette diameter 35 DAS and **(H)** height 15 DAB. The Data was analysed using a one-way ANOVA. Error bars indicate SD of at least 10 plants. Data sets marked with asterisks are significantly different from Col-0 as assessed by Dunnett's multiple comparison test: * $P < 0.05$, ** $P < 0.01$ or *** $P < 0.001$. The experiment was repeated twice.

The expression level of *SPT4-1* and *SPT4-2* was analysed in the *spt4-2* mutant by RT-PCR. The PCR showed that there is no expression of full length *SPT4-2* using primer from start to stop codon but using primer before the T-DNA showed expression of a truncated transcript. Besides, the expression level of *SPT4-1* is not altered in *spt4-2* (Figure 16C). Phenotypic analysis under long day and short day conditions showed no different phenotype compared with wild-type (Figure 17). This might be explained by the redundant function of *SPT4-1* or that truncated transcripts of *SPT4-2* are functional.

2.3.2 Identification and characterisation of the *spt5-1* insertion allele

For *SPT5-1* one line, SAIL_1297_A11, was available from the SAIL collection. Sequencing of the left border sequence revealed that the T-DNA is inserted 118 bp upstream of the annotated position in the last intron between exon 18 and exon 19 and the left border is directed towards the 3'-end region of the *SPT5-1* (At2g34210) gene (Figure 18A); this mutant is termed *spt5-1* in this thesis.

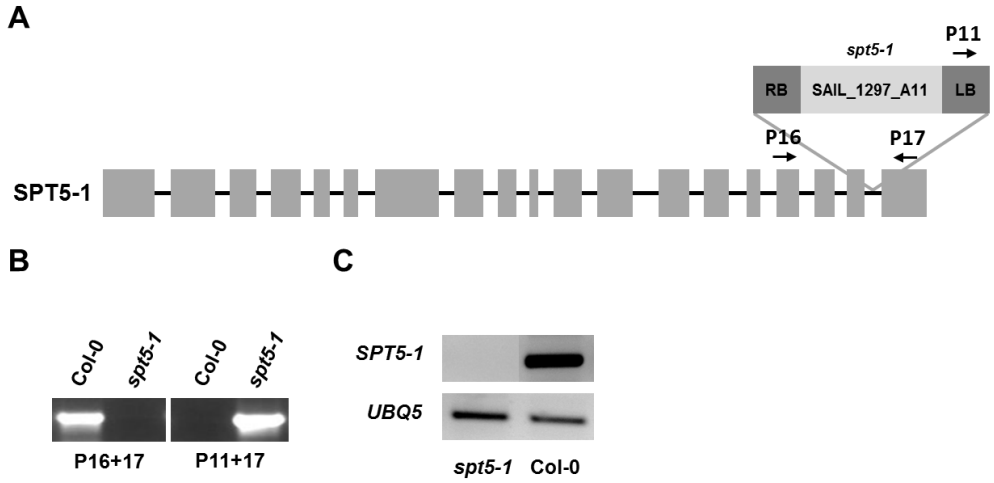

Figure 18. Genotyping and expression of *spt5-1*. (A) Gene model of *SPT5-1* with T-DNA and primers used for genotyping. **(B)** Genotyping of wild-type and mutant (*spt5-1)* plants by PCR with indicated primers. **(C)** In *spt5-1* plants no transcript of the *SPT5-1* gene is detectable by RT-PCR in RNA isolated from stamen, while the transcripts of the reference gene *UBQ5* are present approximately at wild-type levels.

Homozygous plants were identified using primers specific for *SPT5-1* and the T-DNA (Figure 18B). The expression of *SPT5-1* was tested in the *spt5-1* mutant with RT-PCR using cDNA from stamen. No expression of *SPT5-1* was detectable in *spt5-1* using primers spanning the T-DNA (Figure 18C). Phenotypic analysis of *spt5-1* plants compared with wild-type revealed that the knockout mutant of *SPT5-1* is viable (Figure 19). *spt5-1* shows a slight early flowering when measured in days. *spt5-1*

bolts and flowers earlier than wild-type but has no difference in the number of leaves at bolting (Figure 19F-H). The leaves of *spt5-1* have a rounder shape and a somewhat shorter petiole compared to wild-type (Figure 19A).

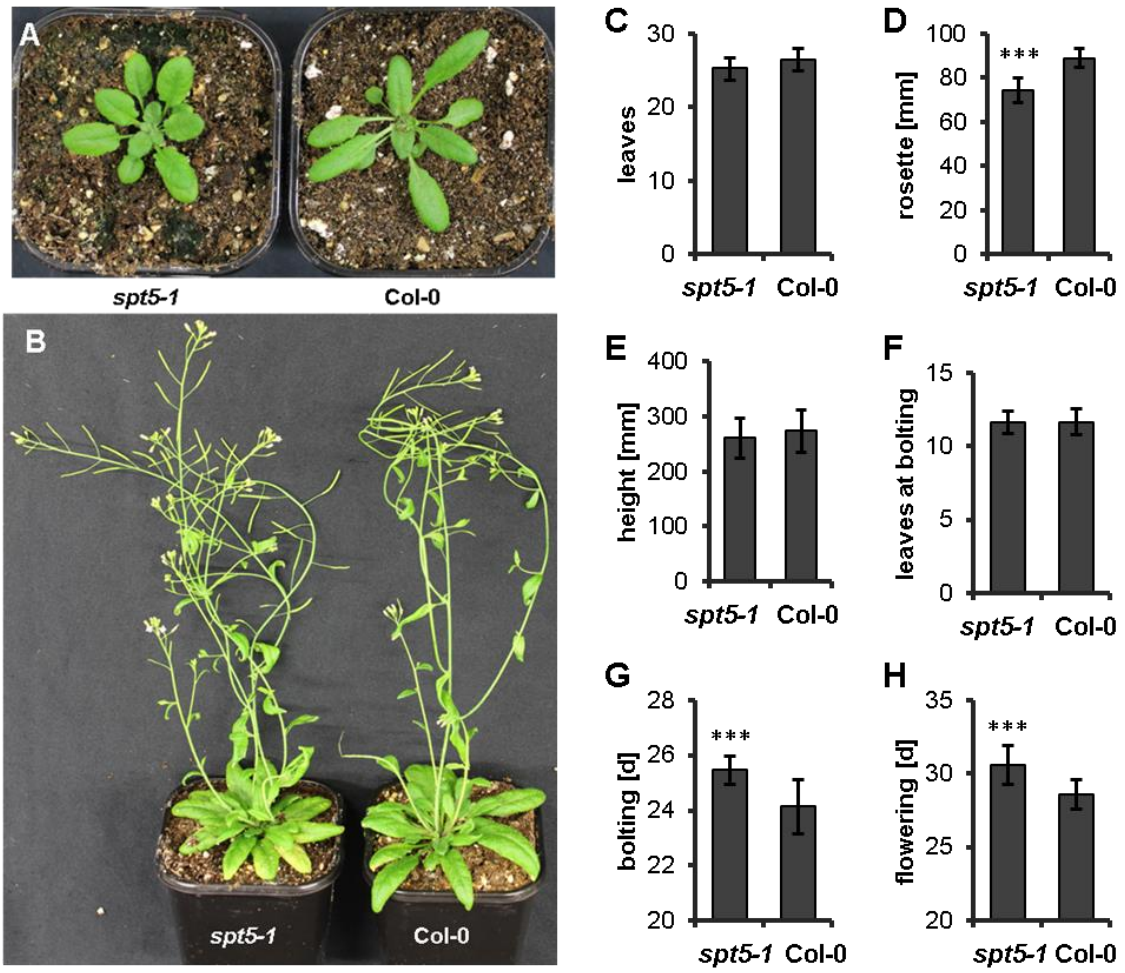

Figure 19. Phenotypic analyses of *spt5-1*. *spt5-1* plants (SAIL_1297_A11) at **(A)** 21 DAS and **(B)** 35 DAS develop similar to Col-0 control plants. **(C)** The number of leaves at bolting, **(D)** bolting time, **(E)** flowering time, **(F)** number of leaves at 35 DAS, **(G)** rosette diameter 35 DAS and **(H)** height 15 DAB were analysed using a one-way ANOVA. Error bars indicate SD of at least 10 plants. Data sets marked with asterisks are significantly different from Col-0 as assessed by Dunnett's multiple comparison test: * $P < 0.05$, ** $P < 0.01$ or *** $P < 0.001$. The experiment was repeated twice.

As the leaves were not smaller, the decreased petiole length could explain the smaller rosette diameter (Figure 19A+D). The overall appearance was essentially like wild-type as hereof the number of leaves and the rosette diameter at 35 DAS and the height 15 DAB are shown (Figure 19C-E). It is not possible to conclude if the minor flowering defect is due to the knockout of *spt5-1*, as no other T-DNA line was available to confirm this. It was also not possible to complement the phenotype because of the instability of the *SPT5-1* coding sequence in *Escherichia coli* and *Agrobacterium tumefaciens*.

Although *SPT5-1* is expressed only in reproductive organs no difference in fertility compared with wild-type was detected.

2.3.3 Identification and characterisation of *spt5-2* insertion alleles

For the ubiquitously expressed *SPT5-2*, four independent T-DNA insertion lines were analysed. Three lines were obtained from the Salk Institute Genomic Analysis Laboratory (SIGnAL), the lines SALK_136809, SALK_115089 and SALK_012958. The fourth line SAIL_287_B03 was obtained from the SAIL collection. The lines were named *spt5-2-1*, *spt5-2-2*, *spt5-2-3* and *spt5-2-4*, respectively. The T-DNA insertions for the four lines are located in the putative promoter region, the 16th exon, intron 20 and exon 22 as annotated in the *Arabidopsis* database, respectively (Figure 20A). The mutant lines were genotyped using a gene specific primers and a primer combination binding in the T-DNA (Figure 20B).

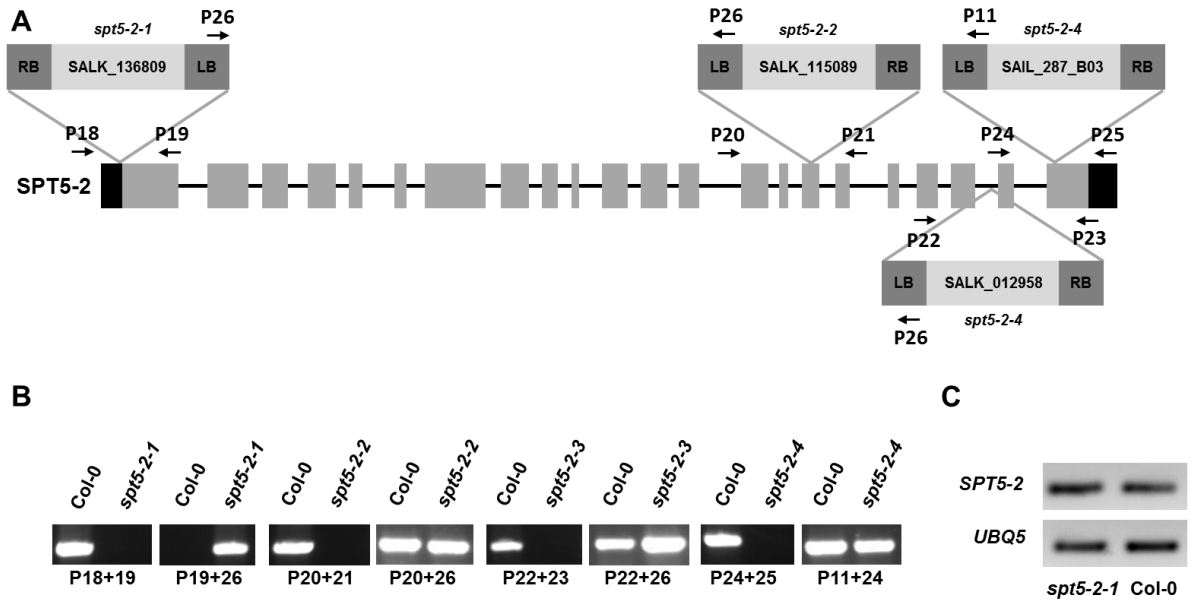

Figure 20. Genotyping and expression of T-DNA insertion mutants in *SPT5-2*. (A) Gene model of *SPT5-2* with T-DNAs and primers used for genotyping. **(B)** Genotyping of segregating plants by PCR with the indicated primers. Shown are results for a wild-type plant (left) and a plant homozygous for the T-DNA insertion. **(C)** In *spt5-2-1* plants transcript of the *SPT5-2* gene is detectable by RT-PCR in RNA isolated from leaves approximately at wild-type levels.

In *spt5-2-1* plants, *SPT5-2* transcript levels were not reduced and accordingly the plants had wild-type appearance (Figure 20C). However, for the other three lines (*spt5-2-2, spt5-2-3, and spt5-2-4*) despite great efforts no plants homozygous for the T-DNA insertions could be identified (Figure 20B). The segregation pattern of the viable plants indicated that *SPT5-2* is an essential gene and individuals homozygous

for the T-DNA insertion are not viable. For all three lines approximately 33% were wild-type and 67% hemizygous for the T-DNA insertion. The line *spt5-2-2* was further analysed. The analysis of the seed-set revealed that 99.2% of the seed looked fully developed whereas 0.8% did not develop, which corresponded to wild-type. The germination rate for *spt5-2-2* was ~80%. These results indicate that the knockout of *SPT5-2* has effect on very early development.

To study the role of *SPT5-2* in plant growth and development, an RNAi strategy was implemented to obtain knockdown lines for SPT5-2. RNAi and amiRNA (artificial microRNA) strategies with constructs under control of the CaMV 35S promoter were used but no plants harbouring the full length construct were obtained.

2.3.4 Identification and characterisation of inducible RNAi lines for *SPT5-2*

In view of this outcome a new strategy was used, an RNAi construct under the control of a β-estradiol-inducible expression system. Therefore, a two component system was used (Brand et al., 2006). The system contained an activation and a responder unit. The activation unit consist of the chimeric XVE element under a promoter of choice. In this study the *UBQ10* (At4g05320) promoter was used, which is ubiquitously expressed in all tissues. The XVE element is a fusion of the DNA-binding domain of the bacterial repressor LexA (X), the acidic transactivation domain of VP16 (V) and the regulatory region of the human estrogen receptor (E). The XVE element can be activated by β-estradiol (Zuo et al., 2000). By activation, the XVE element can induce the expression of the *SPT5*-RNAi cassette fused to the XVE-responsive promoter on the responder unit (For vector maps see Figure 78).

Both constructs were transformed simultaneously into Col-0. The T0 seeds were selected on plates with kanamycin and basta (pMDC150-pUBQ10 and pMDC160-SPT5-RNAi) or kanamycin and hygromycin basta (pMDC150-pUBQ10 and pMDC221-SPT5-2-RNAi). Positive transformants were genotyped using a primer combination specific for *UBQ10* promoter and the pMDC150 plasmid and a combination specific for the *SPT5*-RNAi construct and the plasmids pMDC160 and pMDC221, respectively (Figure 21).

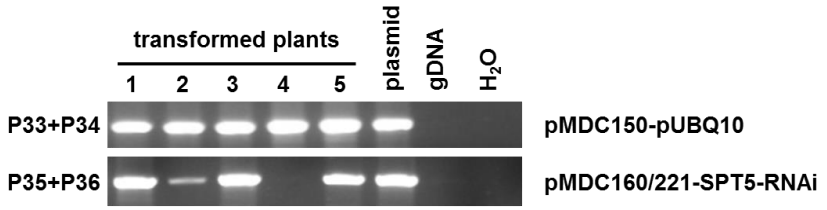

Figure 21. Identification of inducible *SPT5*-RNAi mutant plants. Construct-specific primers were used to identify the presence of the transformed pMDC150-pUBQ10 (P35+P36) and pMDC160-SPT5-RNAi or pMDC221-SPT5-RNAi construct in transgenic plants. An example of five positively selected plants is shown.

To test the system, leaves from positively genotyped plants were induced with 20 µM β-estradiol solution or mock treated applied by a paintbrush. The leaves were harvested after 48 h and 70 h and the *SPT5-2* expression was analysed using RT-PCR. After 48 h almost no down-regulation of *SPT5-2* was detectable but after 70 h a clear down-regulation of *SPT5-2* was detectable (Figure 22).

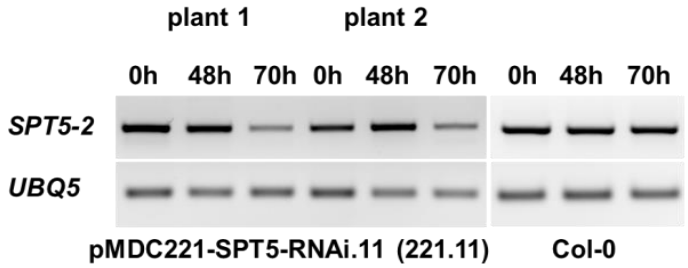

Figure 22. Expression of *SPT5-2* after induction. Transcript level of *SPT5-2* and *UBQ5* as determined by RT-PCR at various time points after induction in the line 221.11 are shown.

To analyse the effects of the induced down-regulation of *SPT5-2* on growth and development, two approached were used. For the first approach seedlings were grown in liquid medium with or without β-estradiol and the fresh-weight of ten plants was measured. These plants were used for RNA extraction and the expression level of *SPT5-2* was determined. For the second approach seeds were directly sown out on medium containing 2 µM β-estradiol or no β-estradiol. This approach was used to analyse the effect of the *SPT5-2* knockdown on early development of the seedlings. After 14 days the growth of the seedlings was documented (Figure 23B). The induction of RNAi in seedlings grown in liquid culture by applying β-estradiol resulted in down-regulation of *SPT5-2* transcript levels (Figure 23A). The reduced expression of *SPT5-2* correlated with decreased growth of the RNAi lines that was also evident from a reduction in fresh weight of the plants by ~60-70%. No growth difference was

observed for the line *160.5* as also no down-regulation of *SPT5-2* could be detected (Figure 23C).

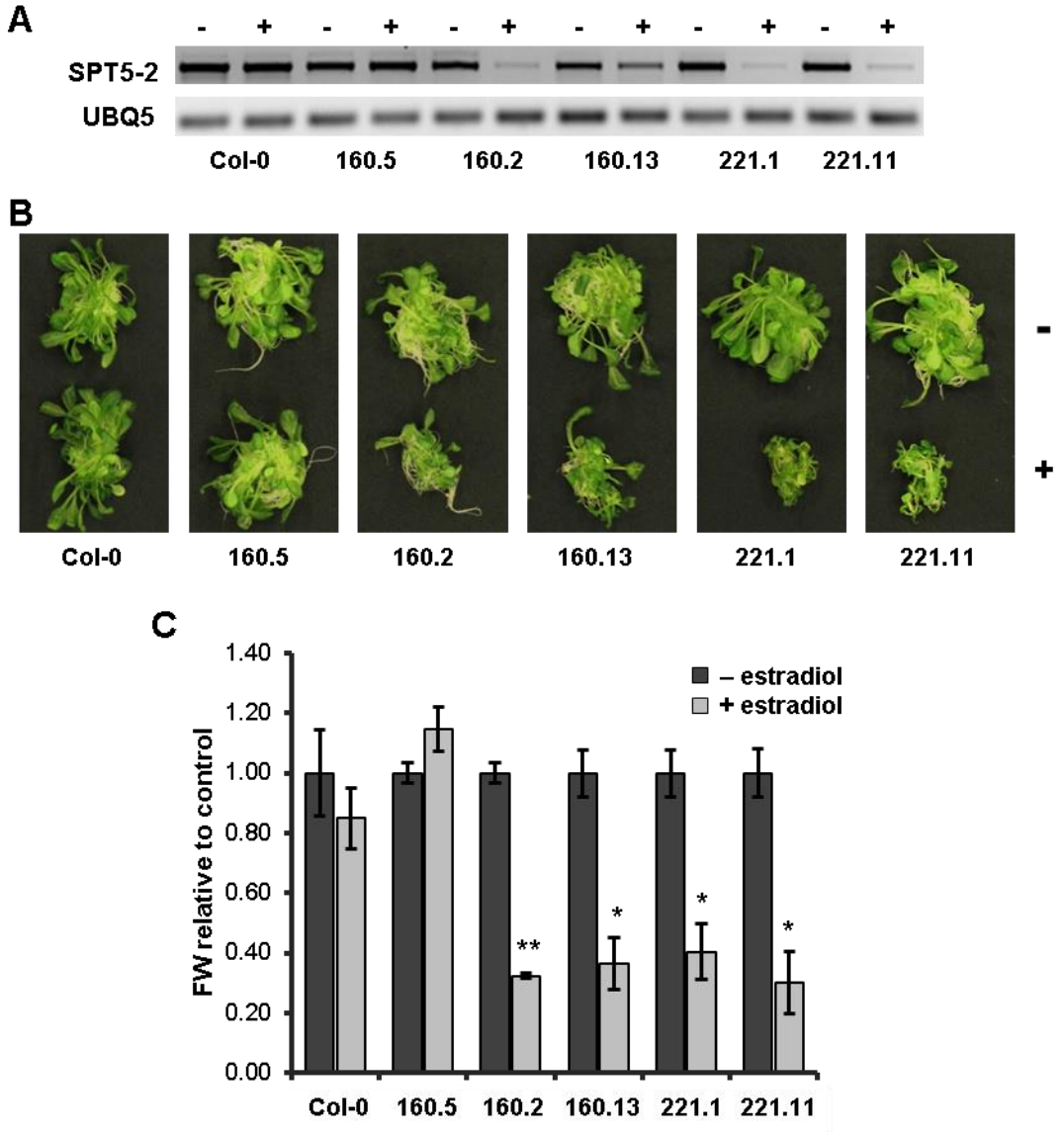

Figure 23. Induced expression of a *SPT5*-RNAi construct affects plant growth. (A) Transcript level of *SPT5-2* and *UBQ5* as determined by RT-PCR in untransformed Col-0 and various independent transformed lines expressing the *SPT5*-RNAi construct under control of a β-estradiol-inducible system. The application of β-estradiol is indicated by (+), while the mock controls are indicated by (-). **(B)** The images depict each 10 seedlings that are grown in liquid MS medium in the absence of β-estradiol, or that were treated with β-estradiol. **(C)** Fresh-weight (FW) of seedlings grown in liquid MS medium with or without β-estradiol. FW of each line was normalised to the mock treatment. Relative FW was analysed using a one-way ANOVA and error bars indicate SD of two replicates. Data sets marked with asterisks are significantly different from Col-0 as assessed by Dunnett's multiple comparison test: * $P < 0.05$, ** $P < 0.01$. The experiment was performed twice with similar results.

Similarly, the reduced growth of the seedlings upon induction of RNAi expression was also observed when the plants were grown on solid medium (Figure 24). These experiments revealed that *SPT5-2* is an essential gene in *Arabidopsis*, as

knockout of leads to embryonic lethality and induced down-regulation of its expression severely impairs plant growth.

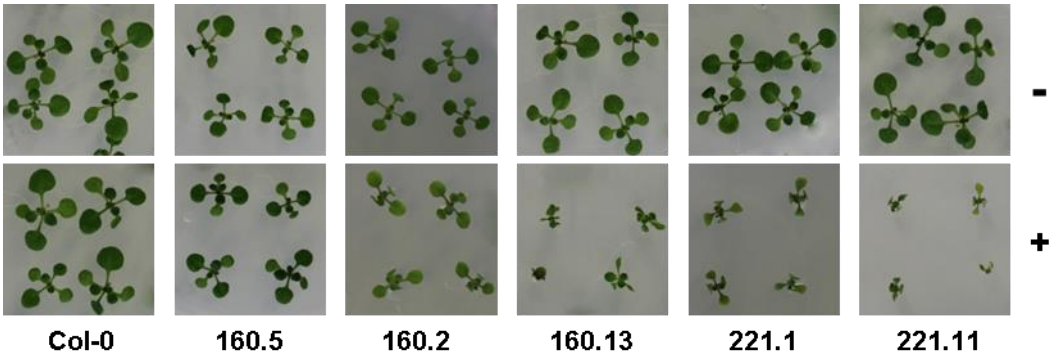

Figure 24. Induced expression of a *SPT5*-RNAi construct affects plant growth. Seedlings were grown on solid MS medium in the absence (-) or presence (+) of β-estradiol. Pictures were taken 14 DAS. The experiment was performed twice with similar results with approximately 20 plants per plate.

2.4 Characterisation of *SPT4* knockdown lines

The *SPT4-2* knockout line shows no essential difference in growth compared with wild-type and for *SPT4-1* no line was available to create a double knockout mutant of *SPT4-1* and *SPT4-2*. An RNAi approach was used to knockdown both *SPT4-1* and *SPT4-2*. The RNAi construct was directed against full length *SPT4-2* under the control of the viral 35S overexpression promoter. The vector pFGC5941-SPT4-RNAi (Figure 25A) and the line *SPT4-R1* were previously created in our laboratory (Lolas, 2009). Four additional independent lines were created during this study.

2.4.1 Molecular characterisation of *SPT4* knockdown lines

The construct pFGC5941-SPT4-RNAi was transformed into Col-0 with the floral dip method. The presence of the transformed construct in seedlings surviving the subsequent selection was confirmed by PCR using two sets of primers, producing a fragment of ~500 bp (Figure 25B). The lines *SPT4-R1*, *SPT4-R3*, *SPT4-R7*, *SPT4-R16* and *SPT4-R17* were chosen for further analysis. The expression levels of *SPT4-1* and *SPT4-2* were analysed with RT-PCR (Figure 25C). The RT-PCR experiments demonstrated that due to the sequence similarity the transcript levels of both *SPT4-1* and *SPT4-2* were reduced in the transgenic lines. Moreover, the transcript levels were reduced to different extent in the various lines. The expression level of *SPT5-2* was not altered in the different *SPT4*-RNAi lines (Figure 25C).

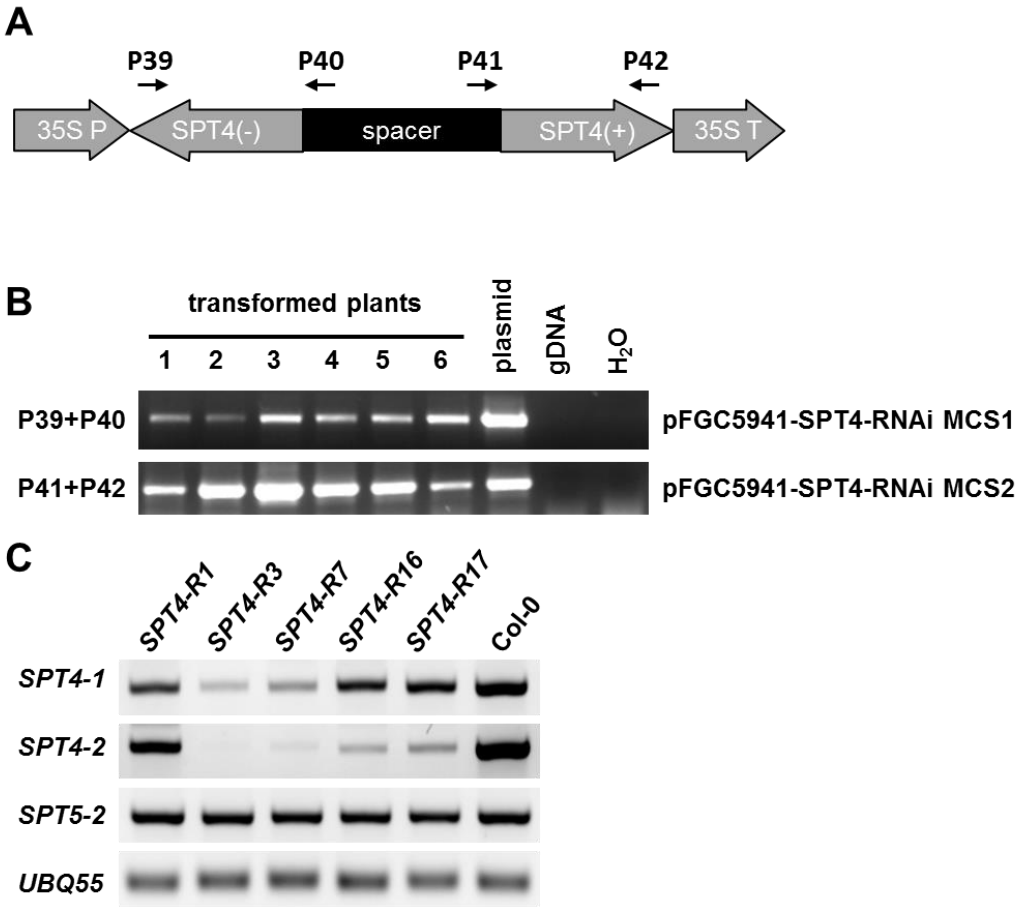

Figure 25. Identification and expression analysis of *SPT4*-RNAi lines. (A) Schematic representation of pFGC4591 plasmid harbouring the *SPT4-2* coding sequences. **(B)** Genotyping of positively selected plants. Construct specific primers were used to identify the presence of the MCS1 (P55+P56) and the MCS2 (P57+P58). An example of six positively selected plants is shown. **(C)** The transcript levels of *SPT4-1/2*, *SPT5-2* and the reference gene *UBQ5* in the RNAi lines and Col-0 were examined by RT-PCR with gene-specific primers. The RNA was isolated from 10 DAS plants.

2.4.1.1 Analysis of the SPT4 knockdown on plant development under long-day conditions

The phenotypic analysis was based on a series of defined developmental stages which has been described in details (Boyes et al., 2001). The basic time-course analysis covers plant development from 21 days after stratification (DAS) until late stages of flowering and seed maturation. The *SPT4*-RNAi lines and Col-0 plants were grown under 16h light and 8h darkness. The overall growth of the *SPT4*-RNAi lines was reduced compared with wild-type (Figure 26 and Figure 28) and growth reduction corresponded with the degree of down-regulation to the two *SPT4* genes (Figure 25C). Thus, plants of line *R3* were smallest and displayed the lowest *SPT4* transcript levels.

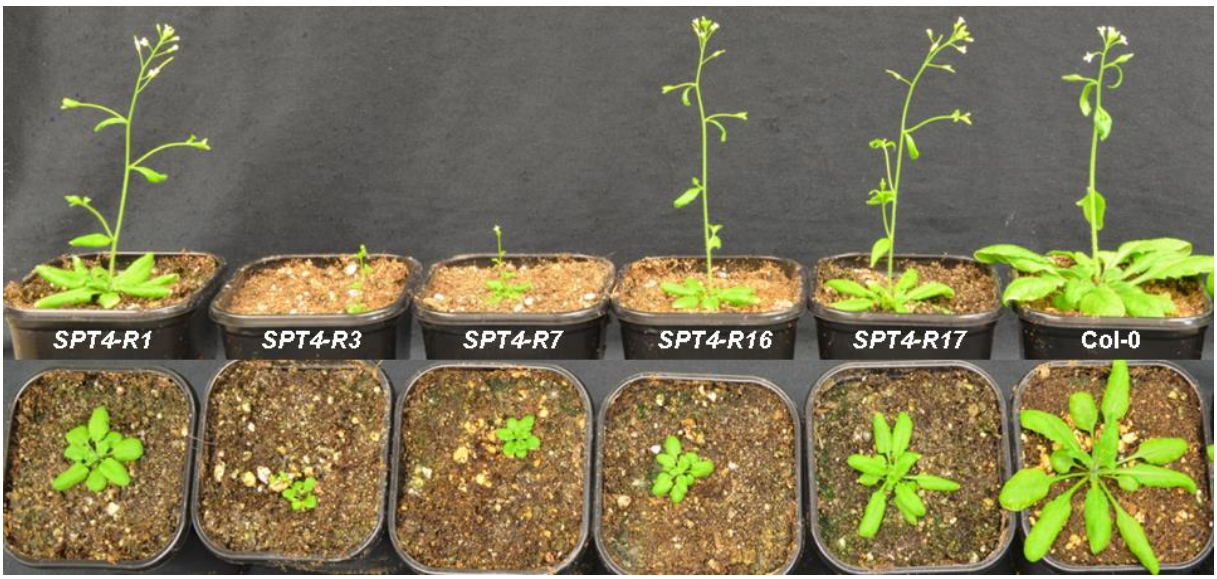

Figure 26. Phenotype of *SPT4*-RNAi plants. Representative individuals of the different RNAi lines relative to Col-0 (28 DAS top, 21 DAS bottom) are shown.

The degree of growth reduction of the individual plant lines relative to Col-0 is also evident from the differences in the size of the leaves (Figure 27), number of rosette leaves, rosette diameter, and plant height at flowering and 15 days after bolting (Figure 28A-D). The effects observed were most severe for the RNAi lines *R3* and *R7*, while the other RNAi lines were more mildly affected, which correlates with the transcript level of *SPT4*.

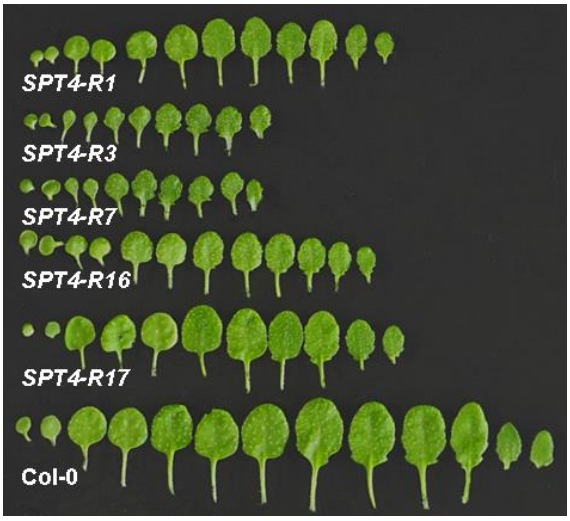

Figure 27. Phenotype of *SPT4*-RNAi plants. Pictures of leaves were taken of 26 DAS plants grown on solid MS.

In addition to the defects during vegetative development, the *SPT4*-RNAi lines exhibited differences during the reproductive phase compared to Col-0. The *SPT4*-RNAi had fewer primary and secondary inflorescences than the control plants

(Figure 28 E, F). Additionally the *SPT4*-RNAi plants had fewer leaves at bolting but the bolting time and flowering time was similar to Col-0 (Figure 28G-I).

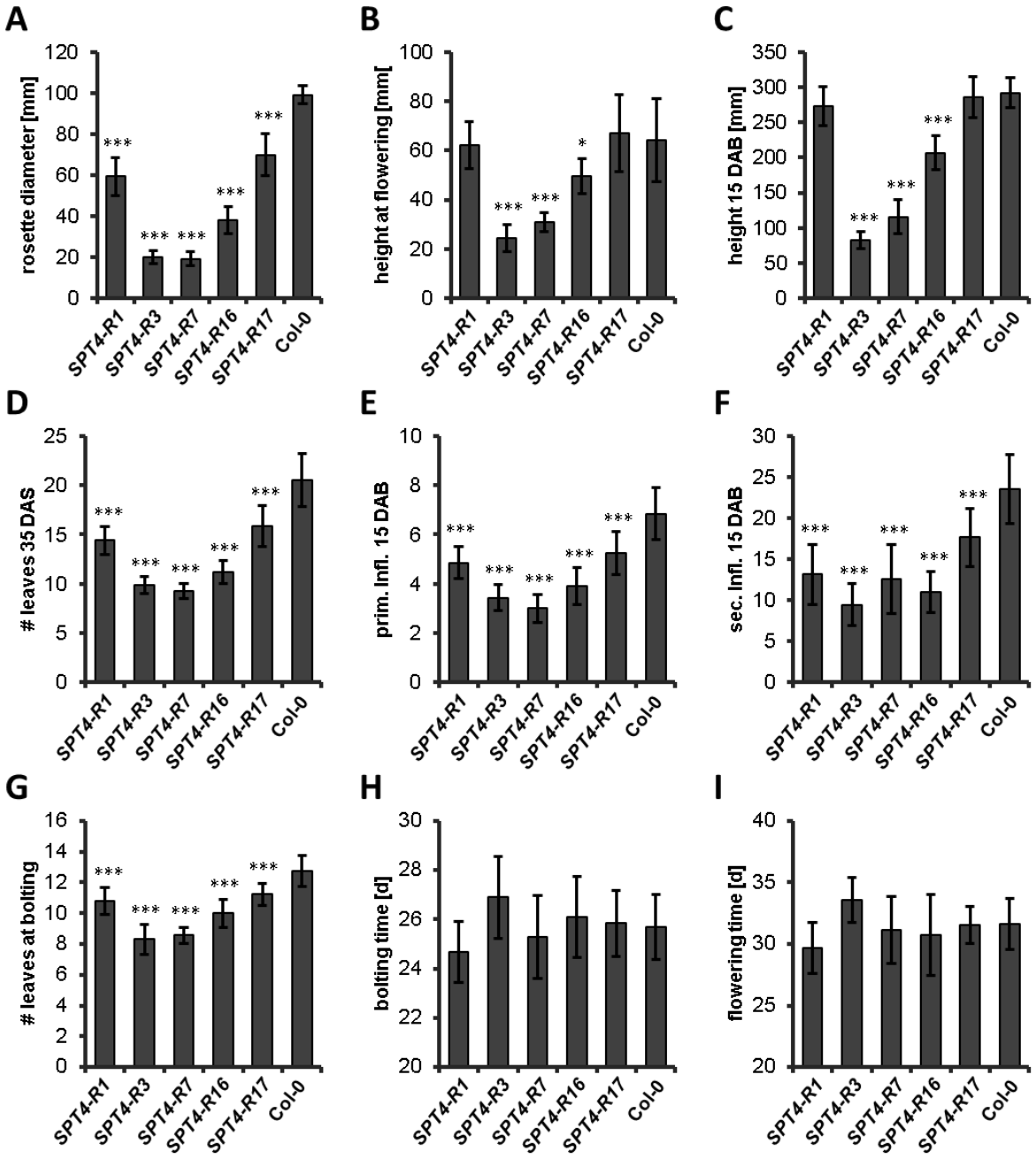

Figure 28. Phenotypic analysis of *SPT4*-RNAi plants. (A) The rosette diameter 35 DAS, **(B)** height at flowering, **(C)** height 15 days after bolting, **(D)** number of leaves at 35 DAS, **(E)** primary inflorescence 15 DAB, **(F)** secondary inflorescence, **(G)** leaves at bolting, **(H)** bolting time and **(I)** flowering time were analysed using a one-way ANOVA. Error bars indicate SD of at least 10 plants. Data sets marked with asterisks are significantly different from Col-0 as assessed by Dunnett's multiple comparison test: * $P < 0.05$, ** $P < 0.01$ or *** $P < 0.001$. The experiment was performed at least three times.

The fresh and dry-weight of seedlings 21 DAS grown on solid MS medium was also clearly reduced compared to wild-type (Figure 29).

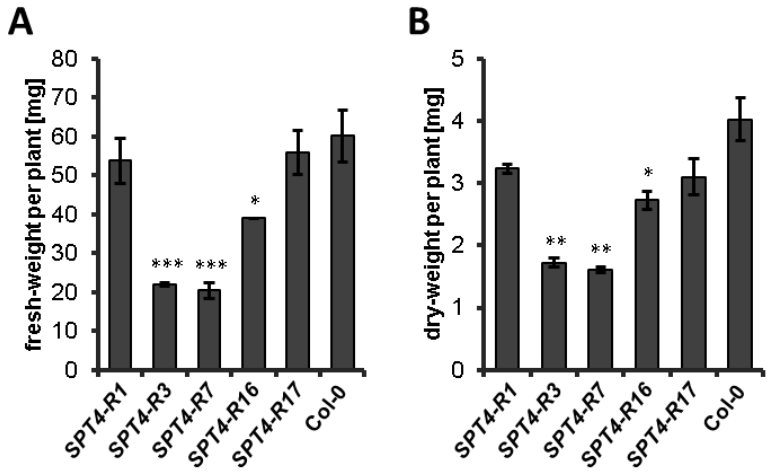

Figure 29. Phenotypic analysis of *SPT4*-RNAi plants. (A) Fresh- and **(B)** dry-weight of 26 DAS plants grown on solid MS. Fresh and dry-weight were analysed using a one-way ANOVA. Error bars indicate SD of two independent experiments with at least 35 plants per experiments (C, D). Data sets marked with asterisks are significantly different from Col-0 as assessed by Dunnett's multiple comparison test: * $P < 0.05$, ** $P < 0.01$ or *** $P > 0.001$.

2.4.1.2 Analysis of the SPT4 knockdown on plant development under short-day conditions

To study the effect of the photoperiod on the development and flowering time of mutant plants, all five *SPT4*-RNAi lines and Col-0 plants were grown under short-day conditions. In general, growing *Arabidopsis* plants at short-day conditions results in an extended vegetative stage accompanied with late bolting and flowering time. Plant development of was observed until flowering. The overall growth of the *SPT4*-RNAi lines compared to wild-type was clearly smaller at all stages (Figure 30).

Figure 30. Phenotype of *SPT4*-RNAi plants under short-day conditions. Representative individuals of the different RNAi lines relative to Col-0 at **(A)** at 60 DAS, **(B)** 110 DAS and **(C)** 135 DAS are shown.

The *SPT4*-RNAi lines 1, 16 and 17 bolted and flowered like wild-type and in contrast to long day conditions, under short day the lines 3 and 7 bolted and flowered later compared to wild-type. Like under long day conditions, all lines had fewer rosette leaves both at bolting time and at day 70. Like the difference in rosette leaf number between mutant plants and Col-0, the rosette diameter at day 70 and the height at flowering was clearly reduced compared to Col-0 (Figure 31).

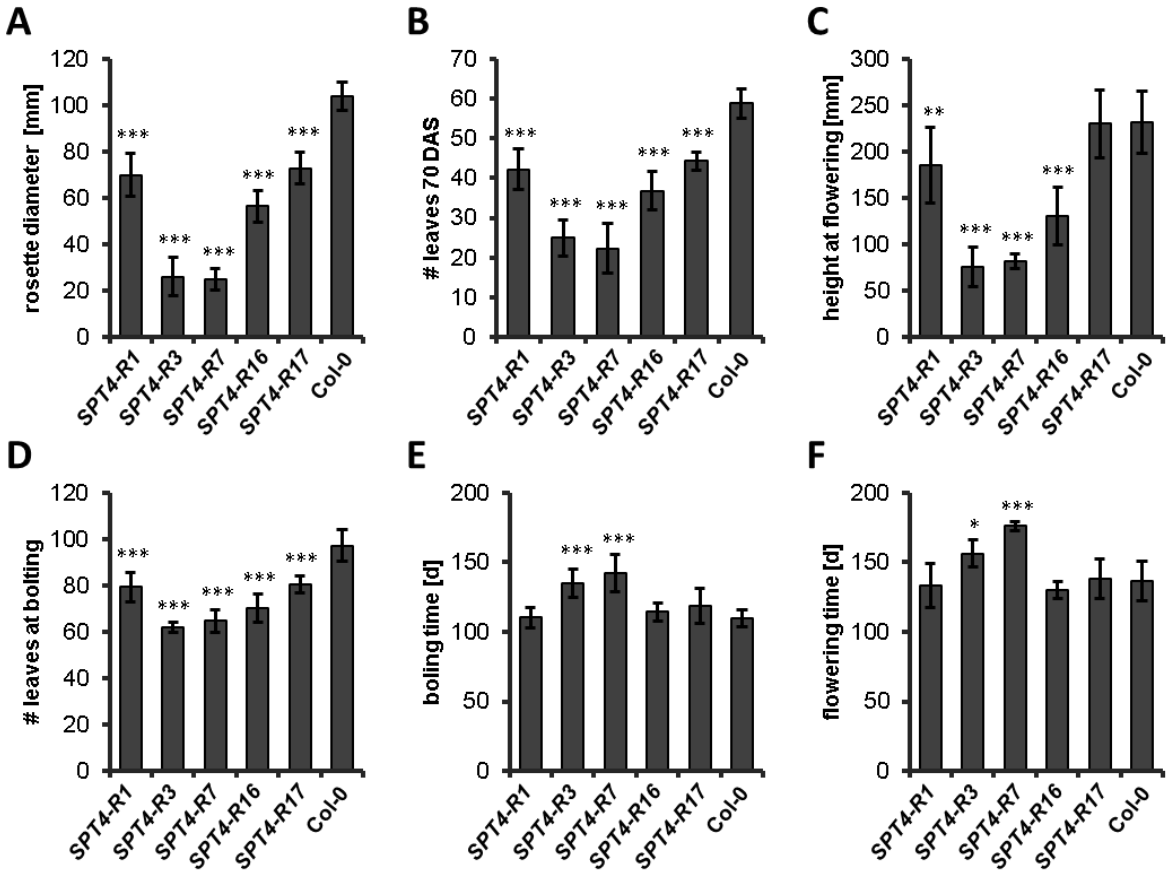

Figure 31. Phenotypic analysis of *SPT4*-RNAi plants under SD conditions. (A) The rosette diameter 70 DAS, **(B)** number of leaves at 70 DAS **(C)** height at flowering, **(D)** leaves at bolting, **(E)** bolting time and **(F)** flowering time were analysed using a one-way ANOVA. Error bars indicate SD of at least 10 plants. Data sets marked with asterisks are significantly different from Col-0 as assessed by Dunnett's multiple comparison test: * $P < 0.05$, ** $P < 0.01$ or *** $P < 0.001$. The experiment was at least three times.

2.4.2 *SPT4*-RNAi mutant plants show a cell proliferation defect

To examine whether defects in cell proliferation and/or cell expansion are responsible for the reduced growth of the plants with decreased *SPT4* expression, leaf sections of the *SPT4*-RNAi lines and Col-0 were analysed. For analyses of cell proliferation and/or cell expansion effects this study concentrates on the strongly affected RNAi line R3 and the less severely affected lines R1 and R16 relative to Col-0. In line with the reduced size of the leaves (Figure 27), fewer palisade parenchyma cells were counted across leaf blade sections of *SPT4*-RNAi plants. For example in the line *SPT4-R3* the number of palisade parenchyma cells was reduced to approximately 60% compared to wild-type (Figure 32).

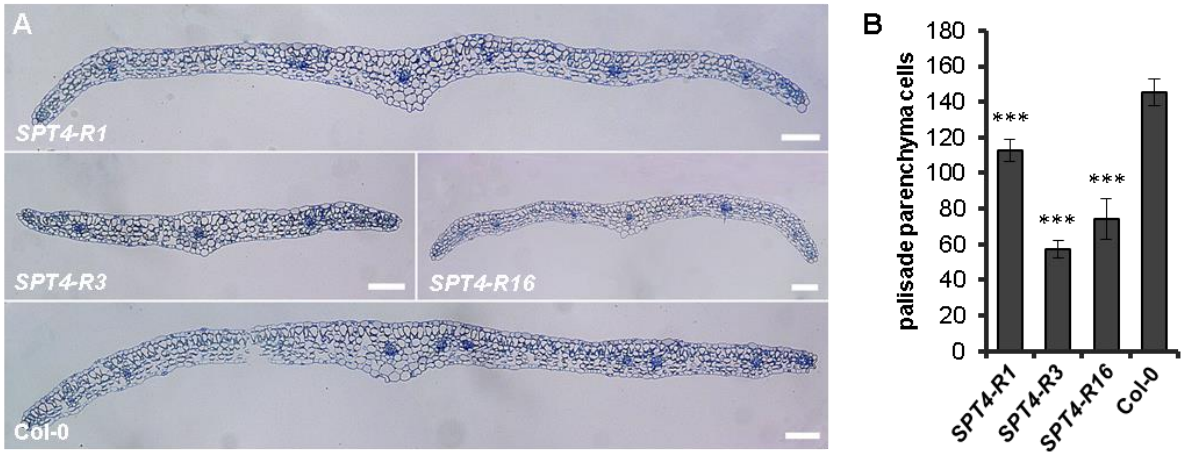

Figure 32. Palisade parenchyma cells in leave sections. (A) Microscopic images of transverse sections of 12 DAS leaves. Scale bar represents 100 µm. **(B)** Quantification of palisade parenchyma cell number per leaf across the leaf blade based on light microscopic images. The number of palisade parenchyma cells was analysed using a one-way ANOVA. Error bars indicate SD of at least four sections. Data sets marked with asterisks are significantly different from Col-0 as assessed by Dunnett's multiple comparison test: * $P < 0.05$, ** $P < 0.01$ or *** $P < 0.001$.

Quantification of the cell size revealed that palisade cells of *SPT4*-RNAi plants were enlarged relative to Col-0 and less tightly packed (Figure 32 and Figure 33), but still because of the reduced cell number leaves of RNAi plants were clearly smaller than those of Col-0 (Figure 32A). Microscopic pictures of leave sections were made by Dr. Michael Melzer at IPK Gatersleben (Figure 33A).

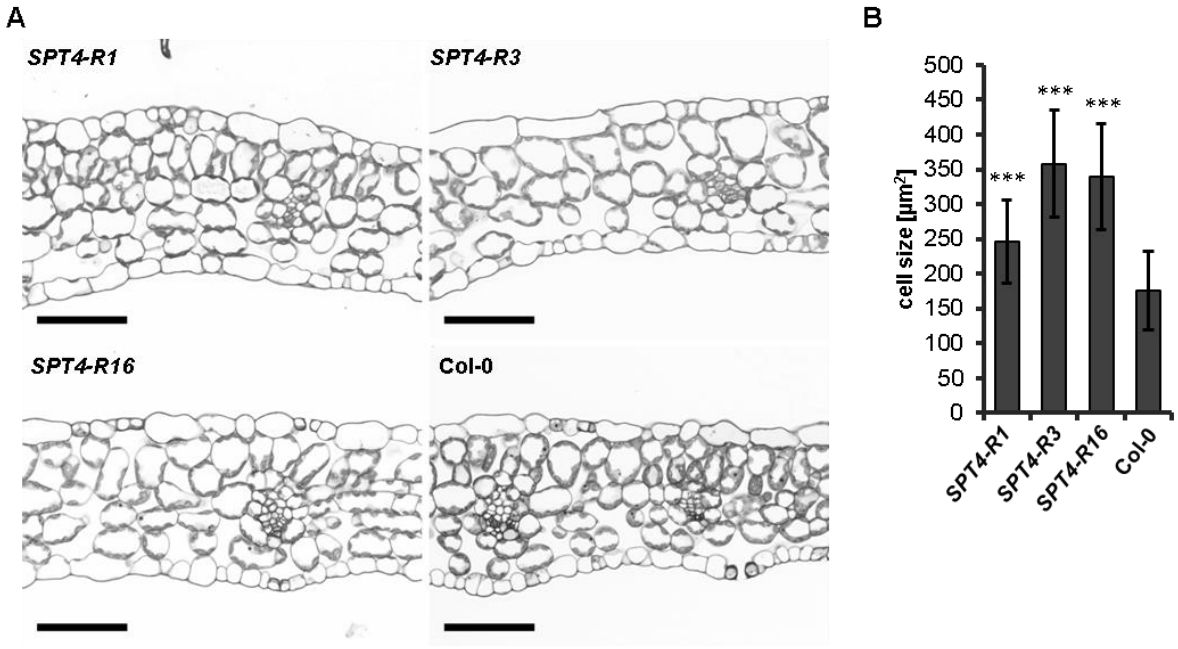

Figure 33. Cell size of palisade parenchyma cells. (A) Leave sections of different *SPT4*-RNAi plant lines and Col-0. Size bars represent 20 µm. **(B)** Quantification of palisade parenchyma cell size based on light microscopic images. Cell size was analysed using a one-way ANOVA. Error bars indicate SD of at least 57 cells. Data sets marked with asterisks are significantly different from Col-0 as assessed by Dunnett's multiple comparison test: * $P < 0.05$, ** $P < 0.01$ or *** $P < 0.001$.

Consistent with the reduced leaf parenchyma cell size also the size of epidermis cells was reduced in *SPT4*-RNAi plants. Analyses of cells of the adaxial epidermis of 14 DAS seedlings revealed that the *SPT4*-RNAi mutant plant had larger epidermis cells (Figure 34).

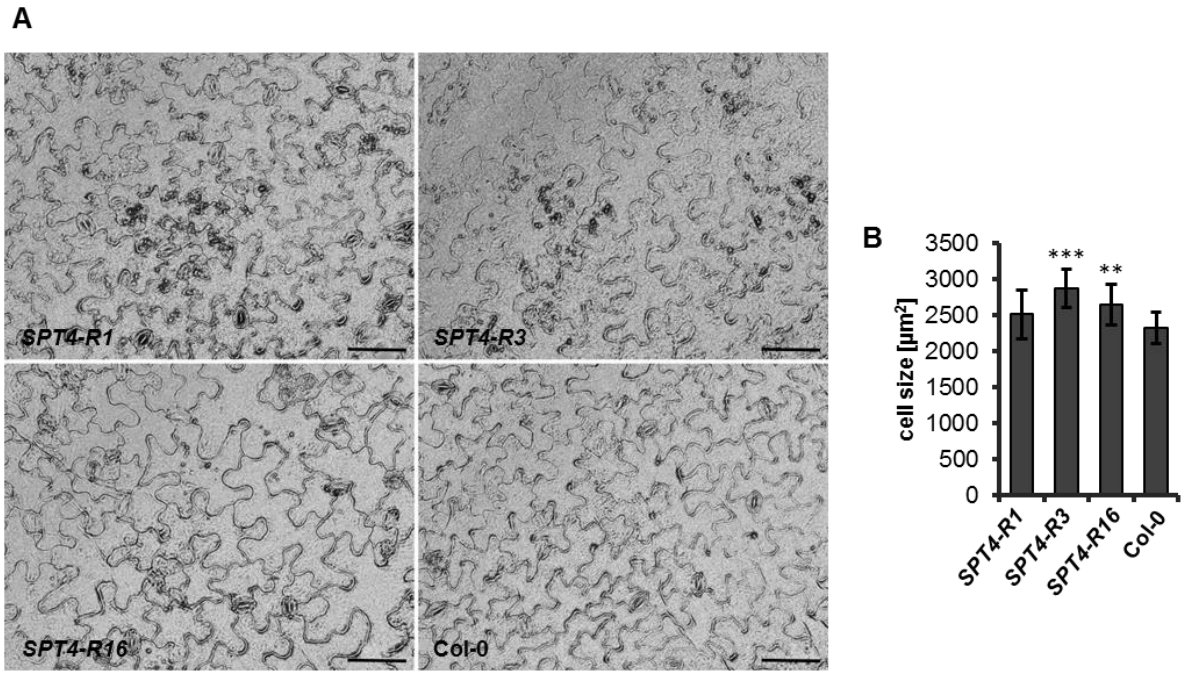

Figure 34. Cell size of epidermis cells. (A) Light microscopic pictures of adaxial epidermis cells of 14 DAS seedlings. **(B)** Quantification of the cell size of epidermis cells based on the light microscopic images. For counting purposes the background was subtracted with ImageJ. Size bars represent 50 µm. The cell size was analysed using a one-way ANOVA. Error bars indicate SD of at least 20 leaves. Data sets marked with asterisks are significantly different from Col-0 as assessed by Dunnett's multiple comparison test: * $P < 0.05$, ** $P < 0.01$ or *** $P < 0.001$.

The root apical meristematic zone was analysed to further investigate a possible cell proliferation defect in the *SPT4*-RNAi mutants. The number of cells and the length of the meristematic zone was measured using ImageJ software. The *SPT4*-RNAi lines had less cells in the proliferation zone, which leads to a reduced proliferation zone compared to wild-type (Figure 35), indicating a cell proliferation defect (Zhou et al., 2011).

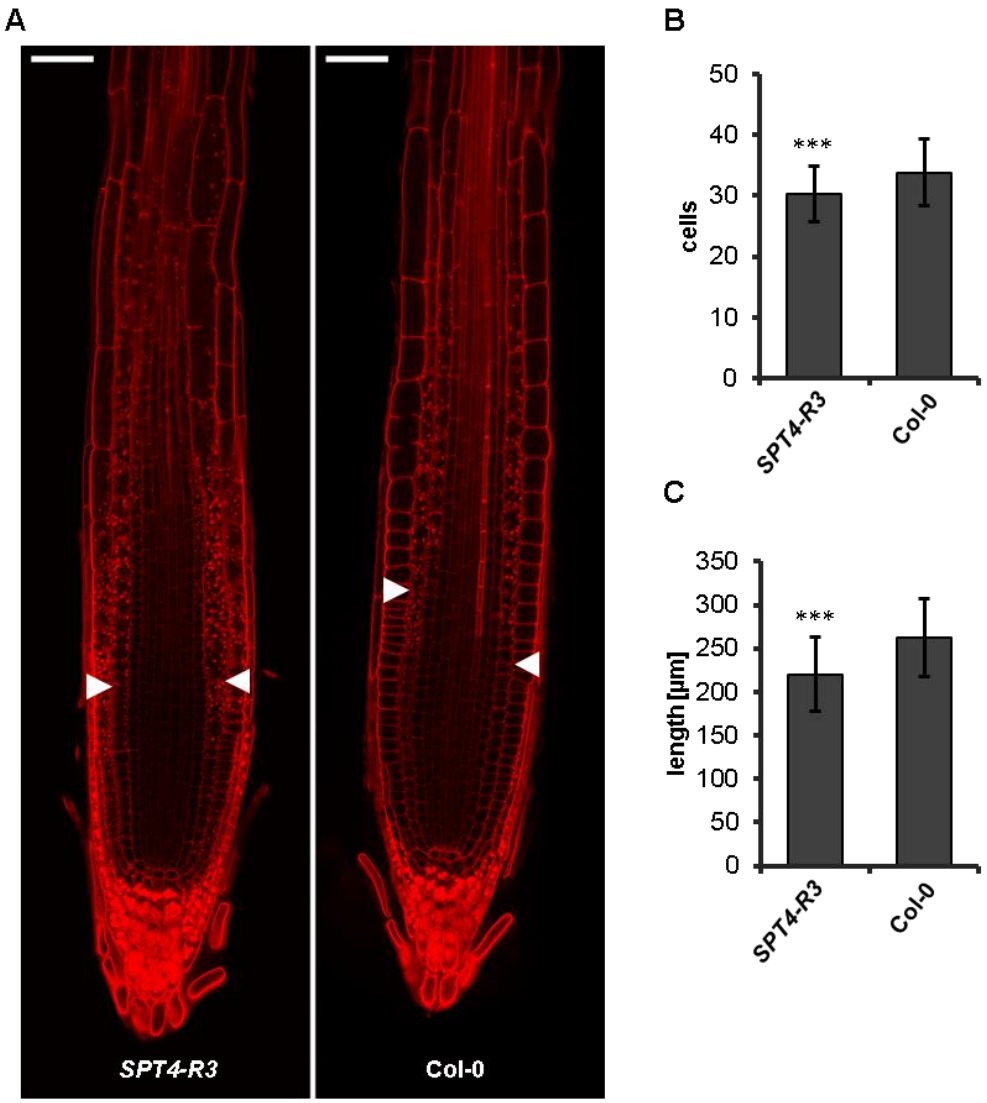

Figure 35. Meristematic zone of primary roots. (A) CLSM of propidium iodide stained primary root tips of *SPT4-R3* and wild-type (5 DAS). Size bars represent 20 µm. **(B)** Quantification of the cells and **(C)** length of the meristematic zone based on CLSM images. The number of cells and the length of the meristematic zone were analysed using a one-way ANOVA. Error bars indicate SD of at least 23 roots of three independent experiments. Data sets marked with asterisks are significantly different from Col-0 as assessed by Dunnett's multiple comparison test: * $P < 0.05$, ** $P < 0.01$ or *** $P < 0.001$.

To further investigate cell proliferation, *SPT4*-RNAi and Col-0 plants were crossed with a *pCYCB1;1::CYCB1;1-GFP* marker line, which allows visualisation of cells at the G2-M phase of the cell cycle (Ubeda-Tomas et al., 2009). Scoring the number of GFP-expressing cells in the root meristem demonstrated fewer mitotic cells in the *SPT4*-RNAi lines as compared to Col-0 (Figure 36), indicating that cell proliferation is reduced in the plants with decreased *SPT4* expression.

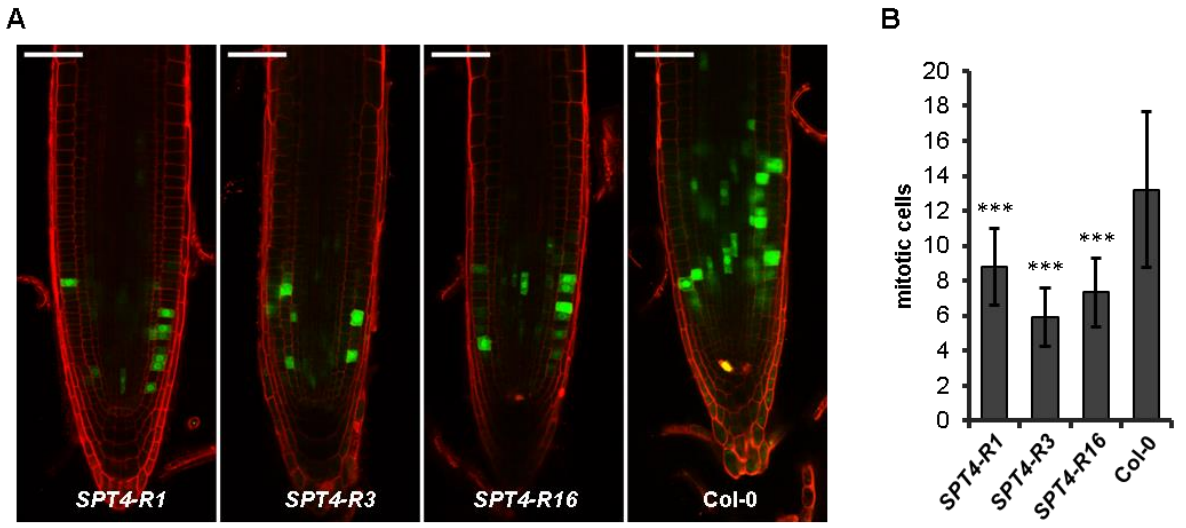

Figure 36. Mitotic cells in primary roots. CLSM images of primary root tips of the different plant lines (5 DAS) harbouring a *pCYCB1;1-CYCB1;1-GFP* reporter (GFP fluorescence in green and propidium iodide staining in red). The number of GFP-expressing mitotic cells was analysed using a one-way ANOVA. Error bars indicate SD of at least 23 roots of three independent experiments. Data sets marked with asterisks are significantly different from Col-0 as assessed by Dunnett's multiple comparison test: * $P < 0.05$, ** $P < 0.01$ or *** $P < 0.001$.

2.4.3 Mutant plants show defects in reproduction

In addition to the defects during vegetative development, the *SPT4*-RNAi lines exhibited differences during the reproductive phase compared to Col-0. Besides the effects described in 2.4.1.1 and 2.4.1.2, analysis of the flowers revealed that the floral organs of the *SPT4*-RNAi plants had a reduced size and the inflorescences had fewer flowers buds compared to wild-type (Figure 37A, B). Also, petals of mutants, especially line 3 and 7, flowers opened incompletely relative to the pedicle, whereas those of Col-0 flowers opened to an approximately 90° angle (Figure 37B). At stage 14 of flower development, anthers supposed to extend above the stigma (Smyth et al, 1990). However, pistils of lines 3 grew out of the flower before stamens have reached them (Figure 37C). Beside these finding it is also obvious that the stigma in line 3 and 7 was covered with pollen to a lesser extent. By dissecting the different organs of the wild-type and mutant flower, it could be observed that flowers of *SPT4*-RNAi plants, especially of line 3 and 7, showed an overall reduction in various flower organs. For example, petals of mutant plants were smaller in size than wild-type petals (Figure 37D) and the filaments of stamens were shorter than those of the wild-type (Figure 37E). Also, the mutant gynoecium was smaller compared to that of wild-type (Figure 37F).

Figure 37. Flower morphology of *SPT4*-RNAi plants relative to Col-0. (A) Flower buds, **(B)** top view of detached flowers showing and **(C)** side view of detached flowers where one or two petals were removed. Detached **(D)** petals, **(E)** pistils and **(F)** stamen of *SPT4-1*, *SPT4-R3*, *SPT4-R7*, *SPT4-R16*, *SPT4-R17* and Col-0 (from left to right) flowers.

A detailed look showed that freshly harvested siliques of the RNAi lines were smaller than Col-0 siliques and they displayed a reduced abscission of floral organs (Figure 38A). In line with their decreased size, clearing of fully elongated siliques showed that the RNAi lines contained a markedly reduced number of seeds per silique (Figure 38B, C). A significant fraction of the ovules did not develop compared to wild-type (Figure 38D, E). Hence, the combination of a decreased number of inflorescences and the reduced seed set result in a distinctly affected fertility of the *SPT4*-RNAi plants.

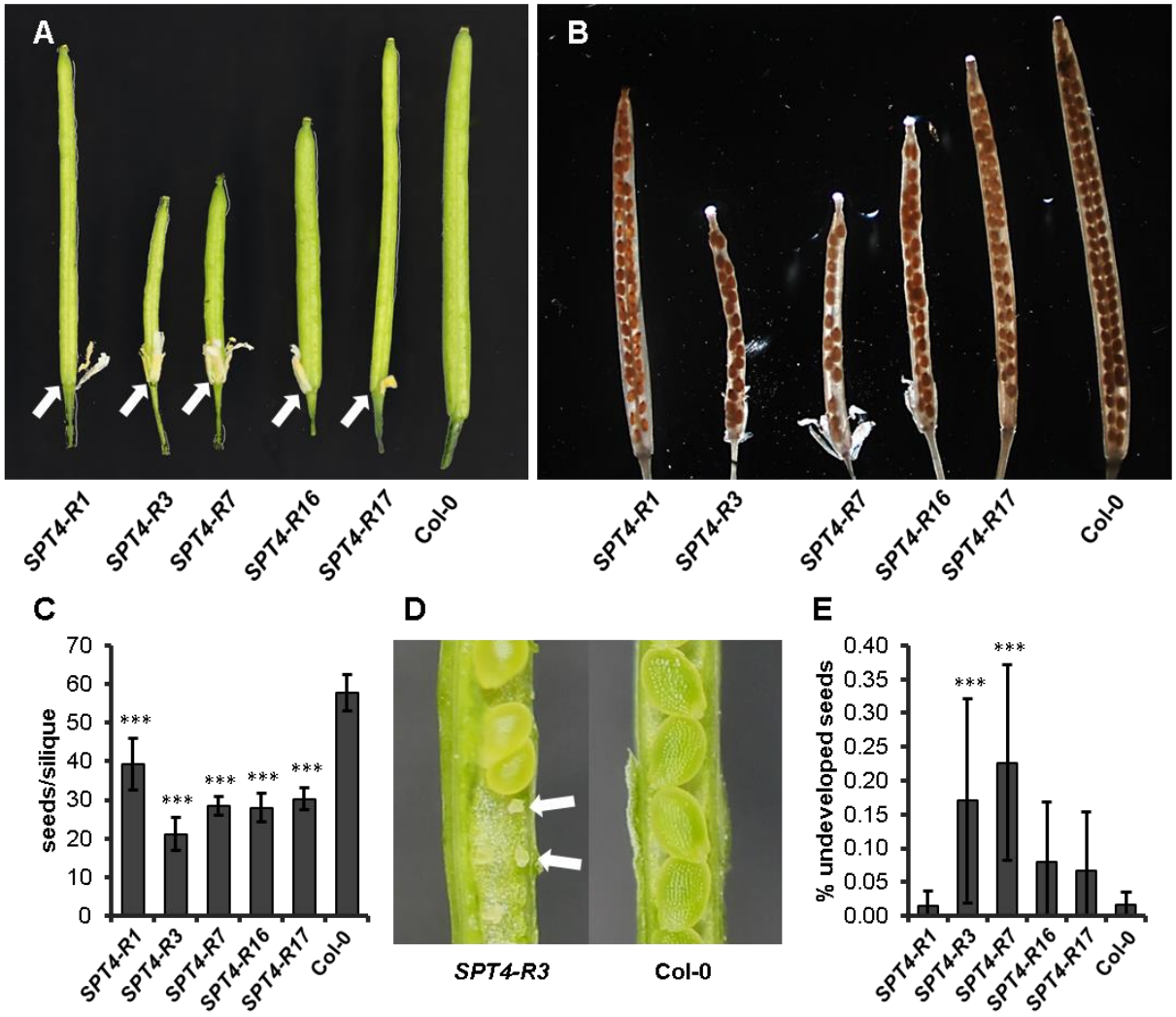

Figure 38. Reproductive defects of *SPT4*-RNAi plants relative to Col-0. (A) Documentation of freshly harvested elongated siliques with arrows indicated the defect in shedding floral organs, and **(B)** cleared siliques illustrate the number of seeds produced. **(C)** Average number of seeds per silique. **(D)** Open siliques, illustrating fully developed seeds and ovules that did not develop in an *SPT4-R3* silique (indicated by arrows). **(E)** Percentage of seeds which did not fully develop. Seeds per siliques and % undeveloped seeds were analysed using a one-way ANOVA. Error bars indicate SD of at least 16 siliques. Data sets marked with asterisks are significantly different from Col-0 as assessed by Dunnett's multiple comparison test: * $P < 0.05$, ** $P < 0.01$ or *** $P < 0.001$.

To analyse whether these reproductive defects and reduced fertility are beside the slower stamen growth due to reduced fertility of pollen, pollen were stained with Alexander stain, which stains viable pollen red and aborted pollen green (Alexander, 1969). The experiment shows that a high proportion of pollen was stained and thus is viable (Figure 39).

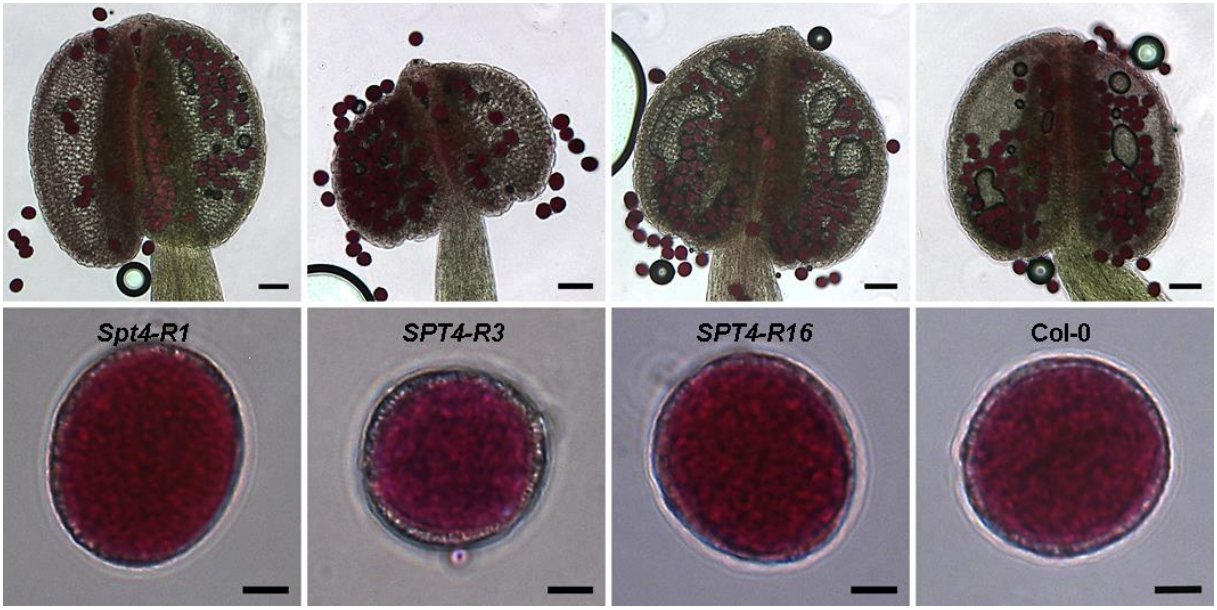

Figure 39. Pollen viability. Pollen stained with Alexander stain is shown. Red staining of pollen shows viability. Representative anthers (upper panel) and pollen (lower panel) are shown. The size bars correspond to 50 µm (upper panel) and 5 µm (lower panel).

2.5 Transcriptome analysis of the line *SPT4-R3*

In view of the transcription-related function of SPT4 and the growth defects of the RNAi plants defective in *SPT4* expression, genome-wide transcript profiling was performed to identify possible alterations in gene expression relative to wild-type. Total RNA isolated from aerial parts of 10-day old *SPT4-R3* and Col-0 seedlings was comparatively examined by microarray hybridization using the ATH1 gene chip (Affymetrix) representing 22800 *Arabidopsis thaliana* genes. After summarisation and normalisation with Robust Multi-chip Analysis (RMA), 501 genes were found ≥2-fold up-regulated, while 662 genes were ≥2-fold down-regulated (p-value < 0.01) in *SPT4-R3* relative to Col-0. Gene ontology (GO) analysis was performed for the up- and down-regulated genes to gain insight in the biological processes the misexpressed genes are involved in.

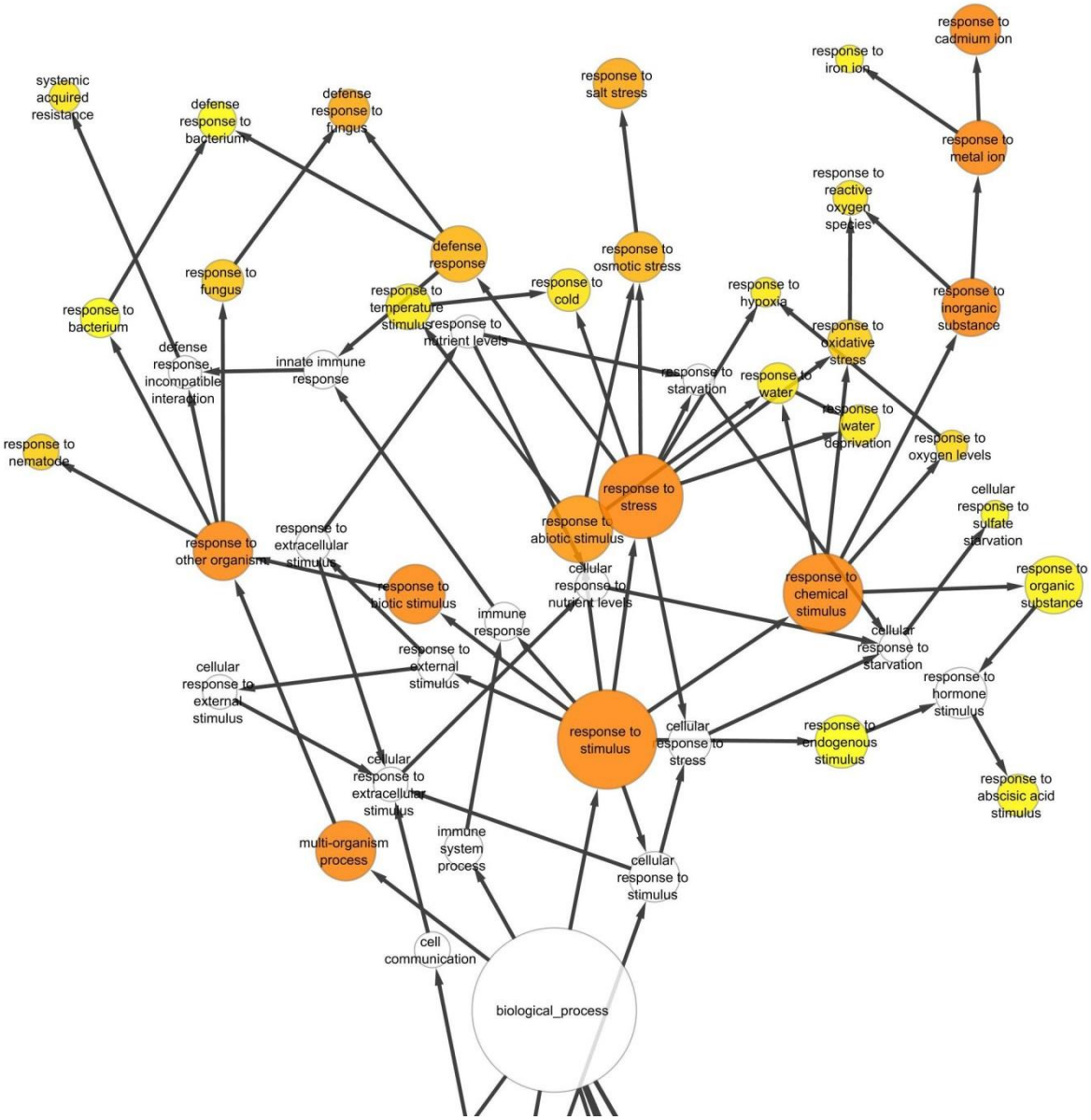

Figure 40. Gene ontology analysis of genes up-regulated in *SPT4-R3* relative to Col-0. The analysis was performed in Cytoscape using the BiNGO plugin version (Shannon et al., 2003; Maere et al., 2005). GO categories were identified that were significantly overrepresented among >2-fold up-regulated genes. The different grades of orange of the circles correspond to the level of significance of the overrepresented GO category ($P < 0.05$). The size of the circles is proportional to the number of genes in each category. Note that for clarity, only the part of the entire network related to the stimulus responsive categories is shown.

Among the up-regulated genes, the category of genes involved in response to stimulus was clearly over-represented. The sub-categories: response to other organism, biotic stimulus, abiotic stimulus, chemical stimulus and response to stress were among the most over-represented (Figure 40). For the down-regulated also the main category response to stimulus was down-regulated more striking than others, which comprises genes involved in “response to auxin stimulus” (Figure 41).

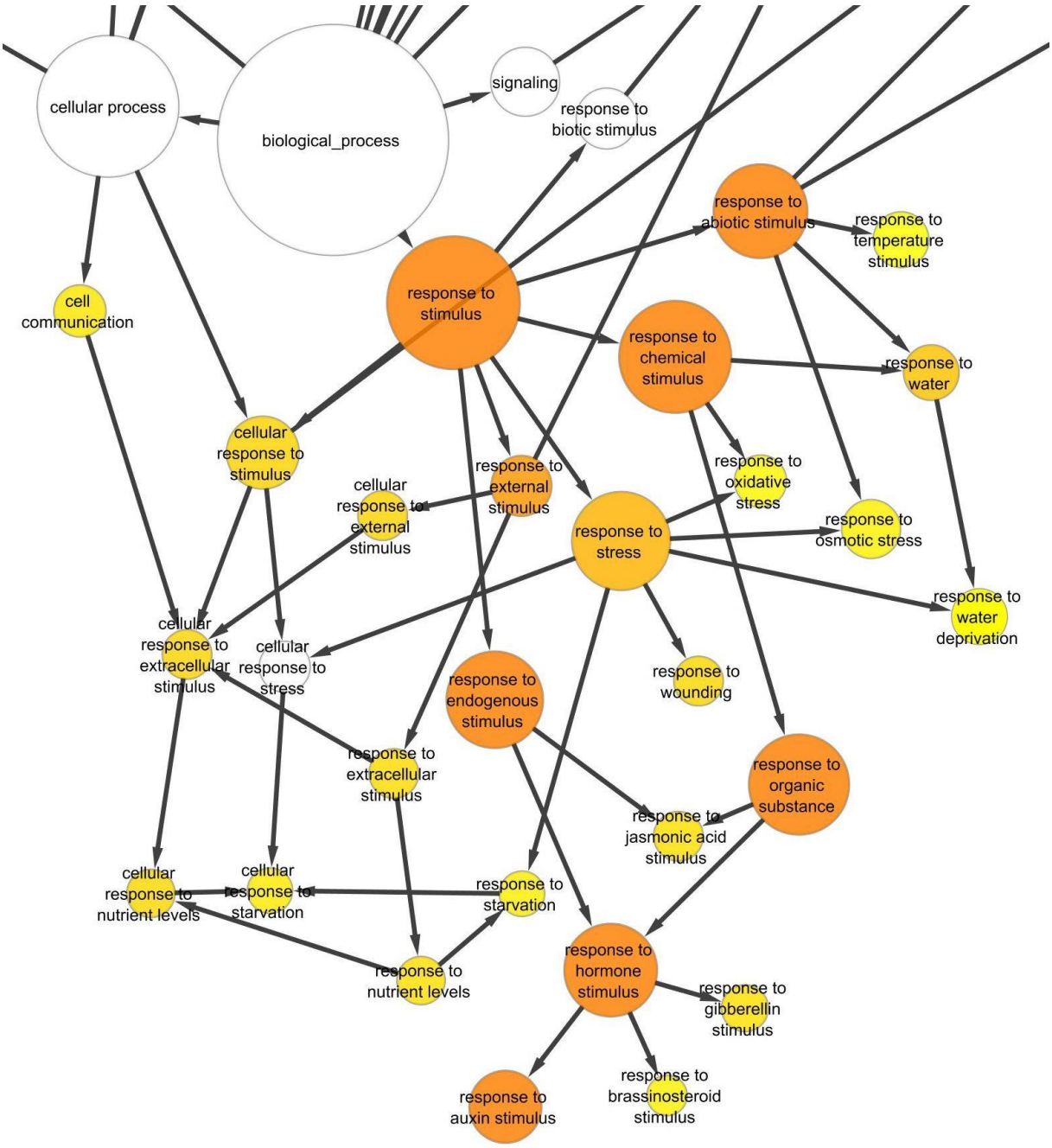

Figure 41. Gene ontology analysis of genes down-regulated in *SPT4-R3* relative to Col-0. GO categories were identified that were significantly overrepresented among the >2-fold down-regulated genes. Note that for clarity, only the part of the entire network related to the stimulus responsive categories is shown.

The differentially expressed auxin-related genes were summarised in Table 6. Remarkably many *Aux/IAA* genes were detected. Most prominent was the subgroup of *Aux/IAA* genes, whose expression is inducible by auxin in *Arabidopsis* seedlings by a short-term IAA application (Overvoorde et al., 2005; Paponov et al., 2008). Eight of ten genes of this group were at least two-fold down-regulated (Table 1).

Table 1. Regulation of *Aux/IAA* genes in *SPT4-R3* plants relative to Col-0.

AGI	gene	auxin[1] inducible	fold change microarray	fold change qRT-PCR
At4g14560	IAA1	+	-8.42	-9.14
At3g23030	IAA2	+	-5.14	-4.10
At1g04240	IAA3	+	-2.66	-3.72
At5g43700	IAA4	+	-3.08	-2.73
At1g15580	IAA5	+	-3.41	-10.14
At1g52830	IAA6	+	-6.63	-4.70
At3g23050	IAA7		1.13	
At2g22670	IAA8		1.14	
At5g65670	IAA9		1.36	
At1g04100	IAA10		1.02	
At4g28640	IAA11	+	-1.12	
At1g04550	IAA12		-1.21	
At2g33310	IAA13	+	-1.51	
At4g14550	IAA14		-4.69	
At1g80390	IAA15		n.d.	
At3g04730	IAA16		-2.31	
At1g04250	IAA17	-	-1.73	-1.02
At1g51950	IAA18		-1.28	
At3g15540	IAA19	+	-6.97	-8.66
At2g46990	IAA20		-1.12	
At3g16500	IAA26		1.15	
At4g29080	IAA27		1.41	
At5g25890	IAA28	-	1.00	
At4g32280	IAA29	+	-24.61	-56.12
At3g62100	IAA30		-1.57	
At3g17600	IAA31		1.11	
At2g01200	IAA32		-1.01	
At5g57420	IAA33		-1.15	
At1g15050	IAA34		-1.01	

[1] *Aux/IAA* genes that are auxin-inducible according to (Overvoorde et al., 2005; Paponov et al., 2008) are indicated by +, and those which are not auxin-inducible are indicated by -.

A comprehensive list of genes induced or repressed due to an auxin stimulus (Overvoorde et al., 2005) was compared to the genes misexpressed in *SPT4-R3*. This revealed that genes only in the groups “auxin related” and “induced by auxin treatment”, were misexpressed. This comparison shows that the *Aux/IAA* genes were not down-regulated due to a general lack of auxin because only a small proportion of auxin inducible genes was differentially expressed, restricted to the group of “auxin related genes” (Table 7 and Table 8).

2.6 Transcript level analysis of differentially expressed genes in *SPT4-R3* mutant plants

To validate the microarray results, quantitative real-time RT-PCR was performed. For qRT-PCR like for the microarray experiments total RNA of the aerial part of ten day old seedlings was taken. Beside the down-regulation of auxin-related genes an up-regulation of pathogen-relate gens was observed (Figure 40 and Figure 41). Therefore, the expression of genes involved in pathogen response and auxin inducible Aux/IAA genes was analysed.

2.6.1 *SPT4-R3* shows changes in pathogen-related genes

The GO analysis of the microarray data showed that the category response to other organism was among the over-represented. Therefore, the gene *PR3*, *PR5* and *GH3.2* where analysed further by qRT-PCR. The pathogenesis-related (PR) genes *PR3* and *PR5* are involved in systemic acquired resistance (SAR). The expression of *PR5* is salicylic acid (SA) dependent, whereas *PR3* is independent of SA signalling and depends on a jasmonic acid (JA) dependent pathway (Clarke et al., 2000; Durrant and Dong, 2004). Both genes are up regulated upon infection by pathogens. Although PR proteins have antimicrobial activity *in vitro* their physiological functions have not been clearly defined in most cases (van Loon et al., 2006). The family of GH3 (GRETCHEN HAGEN 3) proteins catalyse the conjugation of IAA to aspartate and the knockout of *GH3.2* has be shown to reduce pathogen susceptibility (Gonzalez-Lamothe et al., 2012).

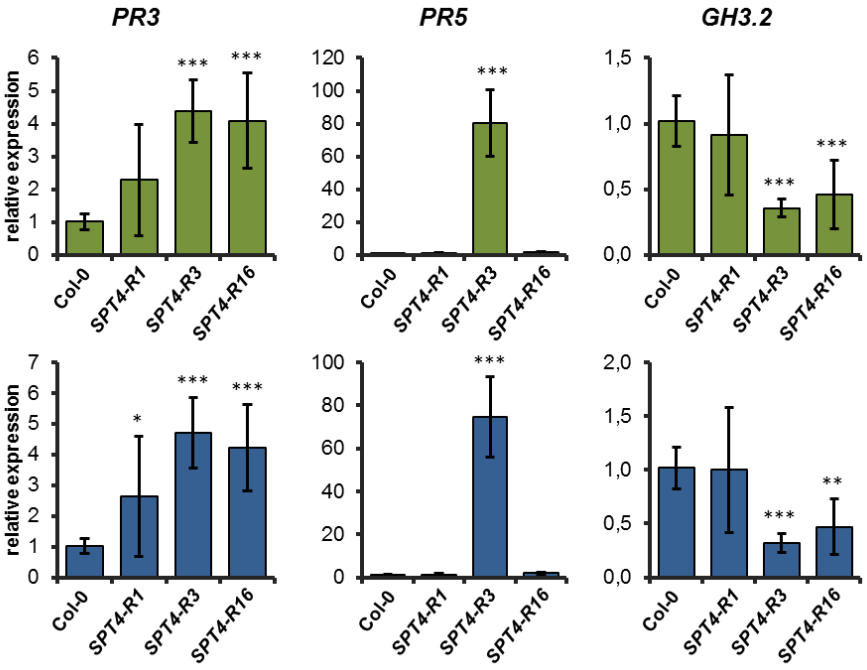

Figure 42. qRT-PCR analysis of transcript levels of pathogen-related genes. Quantitative RT-PCR analysis of the *SPT4*-RNAi plants relative to Col-0 using *ACT8* (green bars) or *EF1α* (blue bars) for normalisation. Relative expression was analysed using a one-way ANOVA. Error bars indicate SD of at least three biological and three technical replicates. Data sets marked with asterisks are significantly different from wild-type as assessed by Dunnett's multiple comparison test: * $P < 0.05$, ** $P < 0.01$ or *** $P < 0.001$.

These experiments demonstrated that the two pathogen responsive genes *PR3* and *PR5* are 4.7 and 75-times up-regulated, respectively. The expression of the *GH3.2* gene is 3.2 times down-regulated (Figure 42), indicating a lower susceptibility to pathogens. Pathogen infection assays are supposed to be performed by a collaborating laboratory but were not finished until the end of this thesis.

2.6.2 Auxin inducible *Aux/IAA* genes are down-regulated in *SPT4* knockdown lines

The expression of several *Aux/IAA* genes was examined by qRT-PCR. Eight auxin-inducible *Aux/IAA*s, which were also down-regulated according to the microarray experiment were tested (Table 1). The different *Aux/IAA* genes were 2.7- to 56-fold down-regulated in *SPT4-R3* relative to Col-0 plants (Figure 43). *IAA17*, which expression has been shown not to be affected by auxin treatment (Overvoorde et al., 2005), shows no difference compared to wild-type (Figure 44). In plants of the less severely affected *SPT4-R1* and *SPT4-R16* lines the *Aux/IAA* genes were also down-regulated, albeit to a lesser extent (Figure 43).

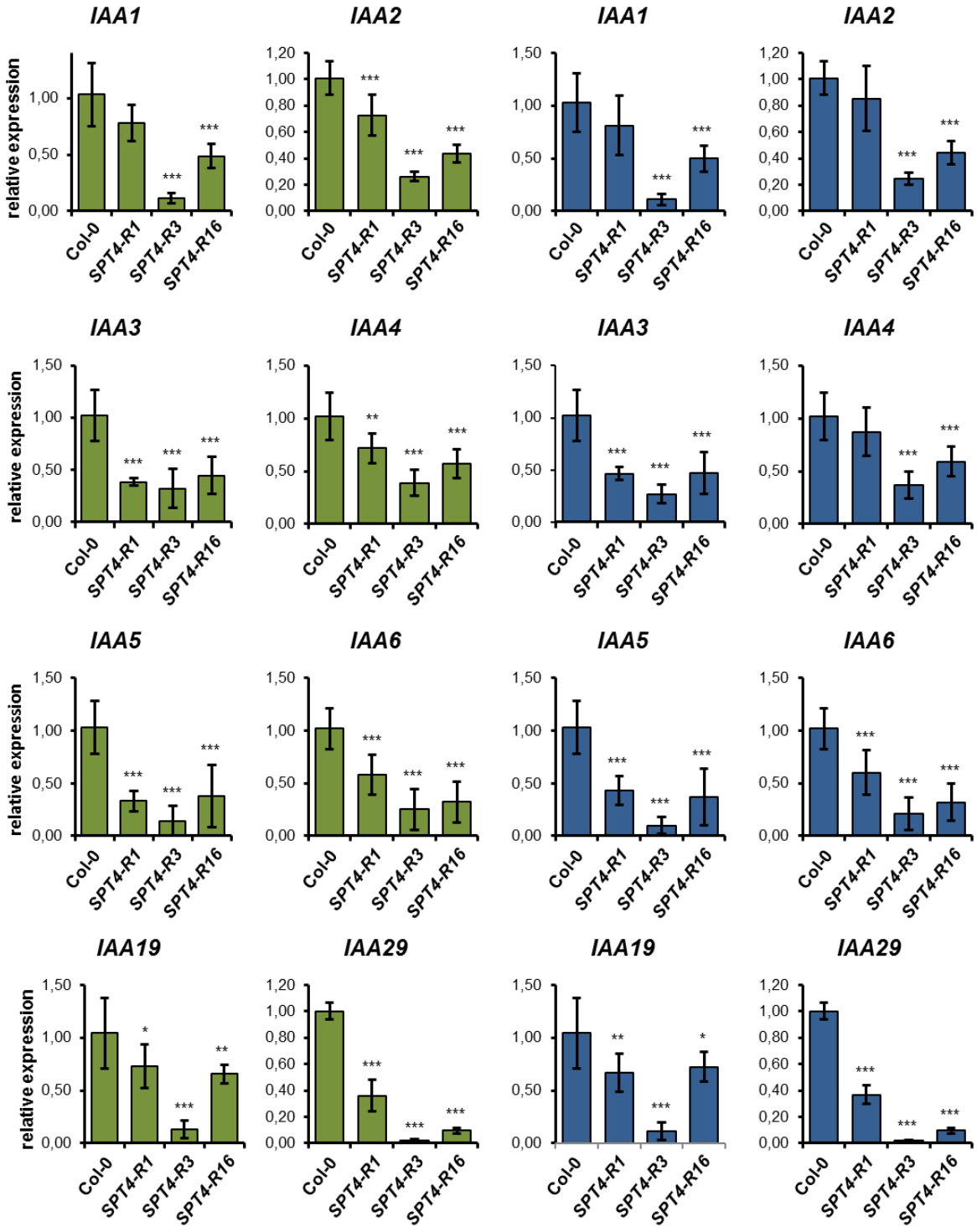

Figure 43. qRT-PCR analysis of transcript levels of *Aux/IAA* genes. Quantitative RT-PCR analysis of the *SPT4*-RNAi lines relative to Col-0 using *ACT8* (green bars) or *EF1*α (blue bars) for normalisation. Relative expression was analysed using a one-way ANOVA. Error bars indicate SD of at least three biological and three technical replicates. Data sets marked with asterisks are significantly different from wild-type as assessed by Dunnett's multiple comparison test: * $P < 0.05$, ** $P < 0.01$ or *** $P < 0.001$.

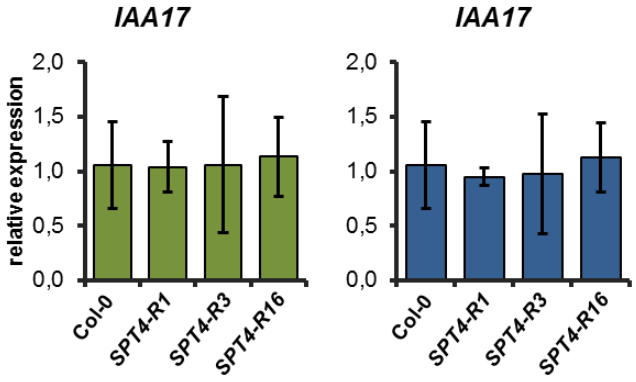

Figure 44. qRT-PCR analysis of transcript levels of *IAA17*. Quantitative RT-PCR analysis of the *SPT4*-RNAi plants relative to Col-0 using *ACT8* (green bars) or *EF1α* (blue bars) as a reference. Relative expression was analysed using a one-way ANOVA. Error bars indicate SD of at least three biological and three technical replicates. Data sets marked with asterisks are significantly different from wild-type as assessed by Dunnett's multiple comparison test: * P < 0.05, ** P < 0.01 or *** P < 0.001.

2.6.2.1 The induction by IAA is reduced in the line SPT4-R3

As several *Aux/IAA* genes have been shown to be up-regulated upon auxin treatment, the inducibility of several *Aux/IAA*s by auxin was tested by qRT-PCR (Overvoorde et al., 2005; Paponov et al., 2008). Total RNA was extracted from 6 DAS seedlings grown in liquid MS after 2 h IAA induction. It was examined whether the inducibility of the *Aux/IAA* genes was affected in plants of the *SPT4-R3* line, when compared to Col-0. Quantitative RT-PCR demonstrated that relative to Col-0 in *SPT4-R3* plants, the transcripts of the tested *IAA1, IAA5, IAA19* and *IAA29* genes were induced to a lesser extent after treatment of the plants with IAA (Figure 45).

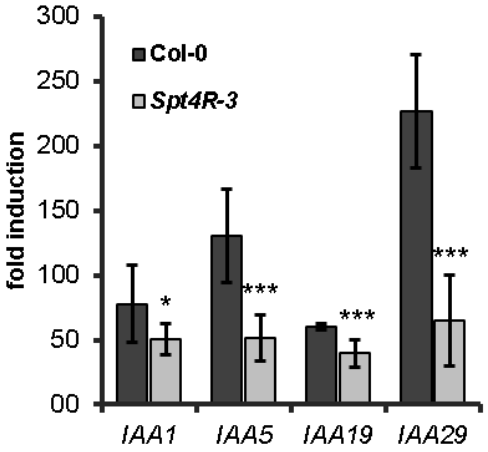

Figure 45. Reduced IAA-inducibility of *Aux/IAA* genes. 6 DAS seedlings were treated for 2 h with 20 µM IAA. Transcript levels of the indicated *Aux/IAA* genes were measured using qRT-PCR. Fold change in transcript levels after IAA treatment was analysed using a one-way ANOVA. Error bars indicate SD of at least three biological and three technical replicates. Data sets marked with asterisks are significantly different from Col-0 as assessed by Dunnett's multiple comparison test: * P < 0.05, ** P < 0.01 or *** P < 0.001.

2.6.3 Expression of *AUX1/LAX* genes in *Arabidopsis* roots

To test if the misregulation of *Aux/IAA* expression has something to do with impaired auxin transport the expression of auxin transporter in the microarray experiment was analysed. While the expression of transporter of the PIN-Formed and the P-GLYCOPROTEIN family was not changed, the AUX1/LAX (AUXIN1/LIKE AUX1) family of auxin influx carrier was down-regulated. *AUX1* belongs to a small multigene family comprising four highly conserved genes (i.e., *AUX1* and *LAX1*, *LAX2*, and *LAX3*). All four have been reported to be auxin influx carrier and have been described to regulate various auxin related developmental processes (Swarup et al., 2008; Peret et al., 2012). The expression of the four different genes was tested by qRT-PCR with total RNA extracted from roots of *SPT4-R3* and wild-type. The analysis showed no clear pattern like in the microarray experiment. *AUX1* and *LAX3* are both significantly down-regulated, whereas the down-regulation of *LAX1* and the up-regulation of *LAX2* are only significant with one reference gene (Figure 46).

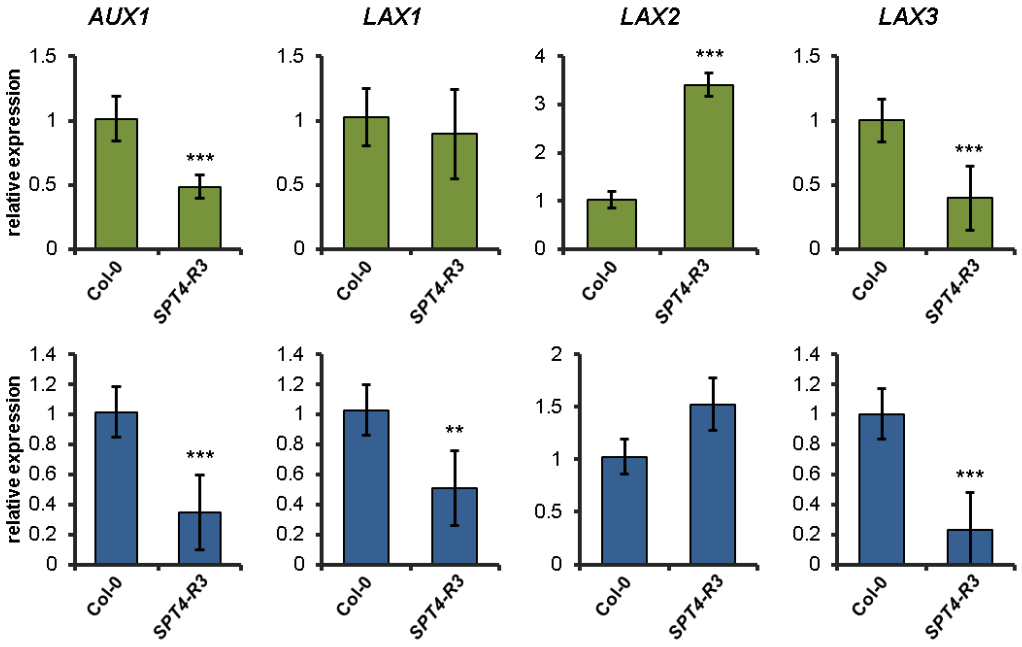

Figure 46. qRT-PCR analysis of transcript levels of *AUX1/LAX1 genes*. Quantitative RT-PCR analysis of the *SPT4*-RNAi plants relative to Col-0 using as a reference *ACT8* (green bars) or *EF1a* (blue bars). Relative expression was analysed using a one-way ANOVA. Error bars indicate SD of at least three biological and three technical replicates. Data sets marked with asterisks are significantly different from wild-type as assessed by Dunnett's multiple comparison test: * $P < 0.05$, ** $P < 0.01$ or *** $P < 0.001$.

2.7 Auxin-related phenotypes of the *SPT4*-RNAi lines

To examine the biological relevance of the altered expression of auxin-related genes and in particular the down-regulation of several *Aux/IAA* genes other plant characteristics known to be influenced by auxin were analysed. Vein patterning has been reported to be highly regulated by auxin (Wenzel et al., 2007; Rolland-Lagan, 2008; Scarpella et al., 2010; Sawchuk et al., 2013). Therefore, the vein patterning of cotyledons, first to third rosette leaf and also sepals and petals of flowers have been analysed. Beside the vein patterning also root growth has been shown to be strongly dependent on auxin signalling (Rahman et al., 2007; Benjamins and Scheres, 2008; Chapman and Estelle, 2009), thus primary root length, root gravitropism and lateral root density have been analysed.

2.7.1 Knockdown of *SPT4* causes a vein patterning defect

Vein patterning of leaves and flowers was studied in chloral hydrate cleared leaves, sepals and petals of *SPT4*-RNAi and Col-0 plants. The venation of cotyledons was hardly affected in the *SPT4*-RNAi lines. In the first and second leaves differences were observable. The severity of the vein patterning phenotype correlated with the strength of down-regulation of *SPT4*. The effect was severe within *SPT4-R3* and *R7* leaves and clearly weaker in *SPT4-R1*, *R16* and *R17* plants. The *SPT4-R3* and *R7* leaves had clearly less veins and lacked most of the tertiary and higher-order veins. In addition to the reduced vein branching, the leaves showed more free-ending veins (Figure 47). Also third leaves of *SPT4*-RNAi plants compared to wild-type showed differences in vein patterning but the difference is not as severe as seen in the first and second leaf.

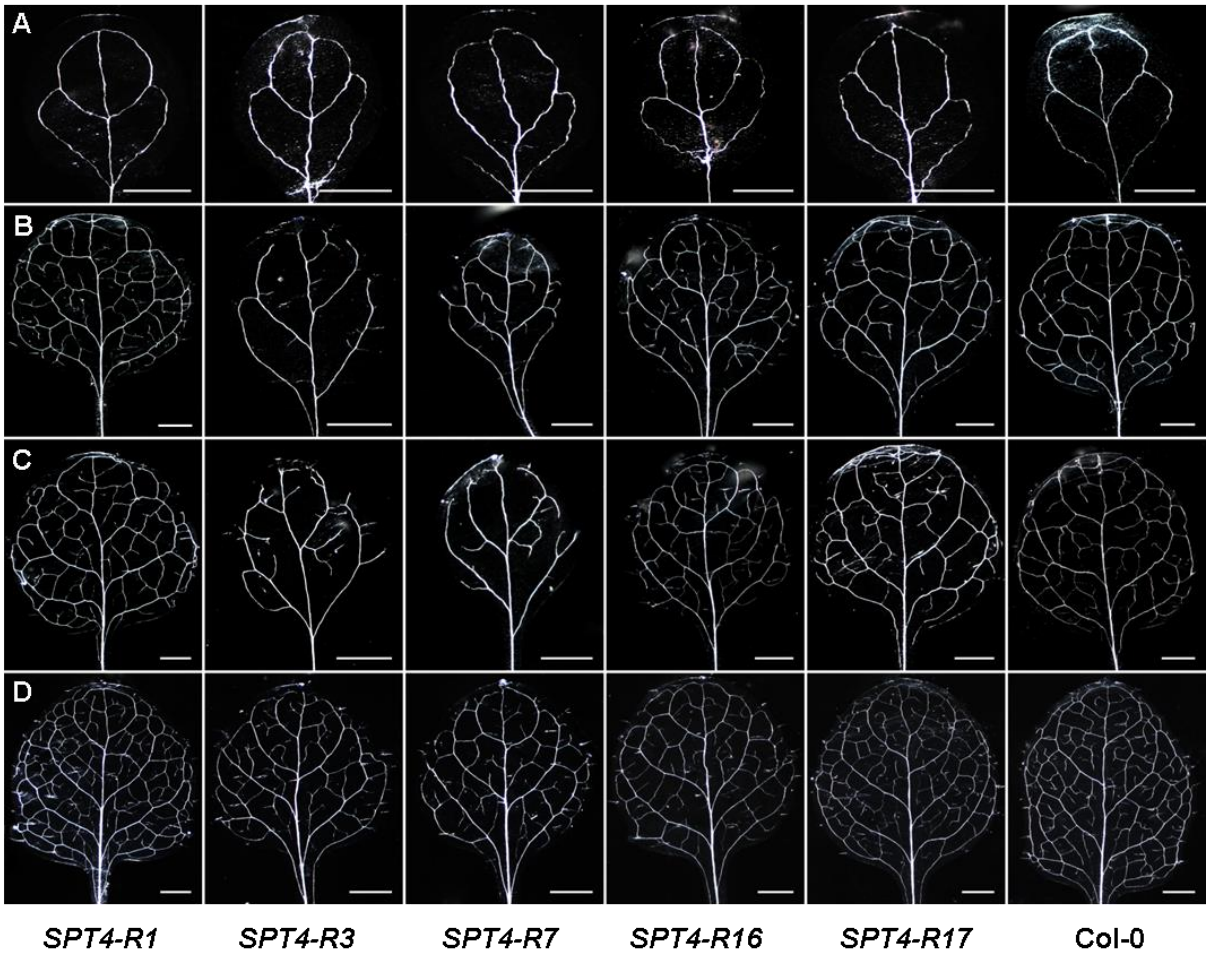

Figure 47. Leaf vein patterning *SPT4*-RNAi plants relative to Col-0. Vein pattern of cleared leaves of the indicated plant lines. Representative leaves of 26 d old plants are shown: **(A)** Cotyledon, **(B)** first leaf, **(C)** second leaf and **(D)** third leaf. Size bars indicate 1 mm.

Sepals and petals showed also a vein patterning defect, which was stronger in *SPT4*-RNAi lines 3 and 7 compared to lines 1, 16 and 17. In both sepal and petals clearly more free-ending veins and reduced vein branching was detectable in lines *R3* and *R7* compared to wild-type and the other three *SPT4*-RNAi lines (Figure 48).

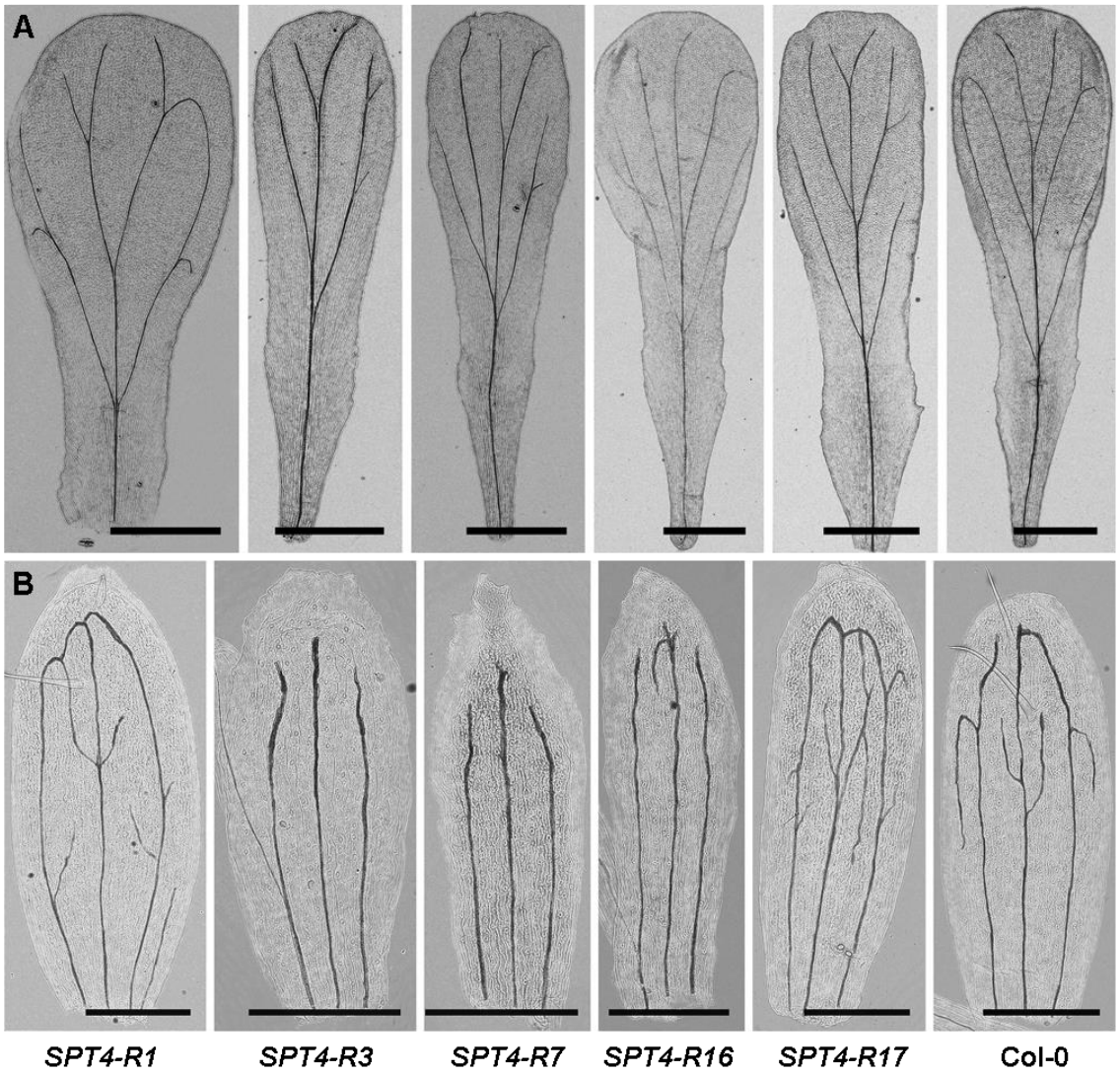

Figure 48. Sepal and petal vein patterning of *SPT4*-RNAi plants relative to Col-0. Vein pattern of cleared petals and sepals of the indicated plant lines: **(A)** Petals and **(B)** sepals. Size bars indicate 0.5 mm.

2.7.1 Knockdown of *SPT4* causes a defect in root growth and a higher sensitivity to exogenous auxin

Root growth was observed on vertically growing plants in a plant incubator under long day conditions. The length and the amount of lateral roots of the primary root were measured every second day for two weeks starting with the fourth and sixth day, respectively. The results revealed that the roots of the RNAi lines, especially the lines 3 and 7, grew more slowly compared to wild-type (Figure 49A). In addition to the reduced growth rate the RNAi plants exhibited fewer lateral roots and also the density of lateral roots was significantly reduced, severest again within line 3 and 7 (Figure 49B, C).

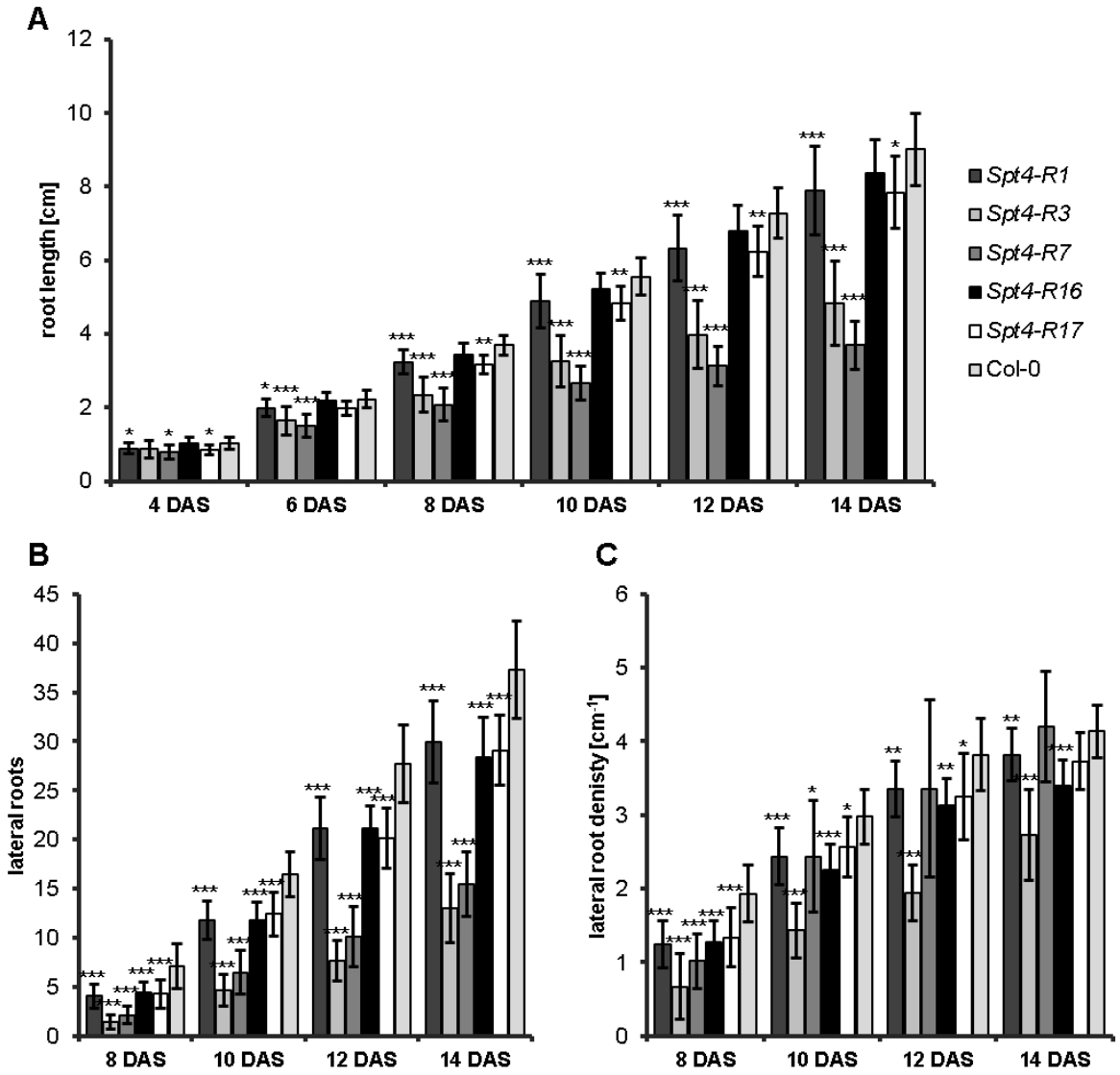

Figure 49. Primary root growth and lateral roots. (A) The length of the primary root of plants and **(B)** the number of lateral roots grown on MS medium was measured at the indicated DAS. **(C)** The number of lateral roots per cm of primary root was scored at the indicated DAS. Root length, number of lateral roots and lateral root density were analysed using a one-way ANOVA. Error bars indicate SD of at least 14 plants. Data sets marked with asterisks are significantly different from Col-0 as assessed by Dunnett's multiple comparison test: * $P < 0.05$, ** $P < 0.01$ or *** $P < 0.001$. Each experiment was performed three times with similar results.

Besides the reduced root growth especially the line *SPT4-R3* showed gravitropism defects and had a more wavy root growth compared to wild-type (Figure 50).

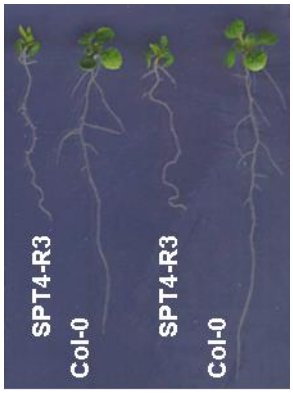

Figure 50. Gravitropism defect of *SPT4-R3*. Shown are 10 DAS plants grown vertically on solid MS.

The reduced root growth and the reduced IAA inducibility (2.6.2.1) indicate alterations in auxin signalling in *SPT4*-RNAi plants, therefore the response to the application of exogenous IAA was tested. IAA is known to inhibit *Arabidopsis* root elongation (Rahman et al., 2007). To test this hypothesis, plants were treated with different concentrations of IAA. The elongation rate of the primary root of RNAi plants was determined relative to untreated plants as described in 5.4.7. Root elongation was significantly more severely inhibited by IAA treatment in the *SPT4*-RNAi plants than in Col-0 (Figure 51), suggesting that the *SPT4*-RNAi plants are more sensitive to the application of exogenous IAA.

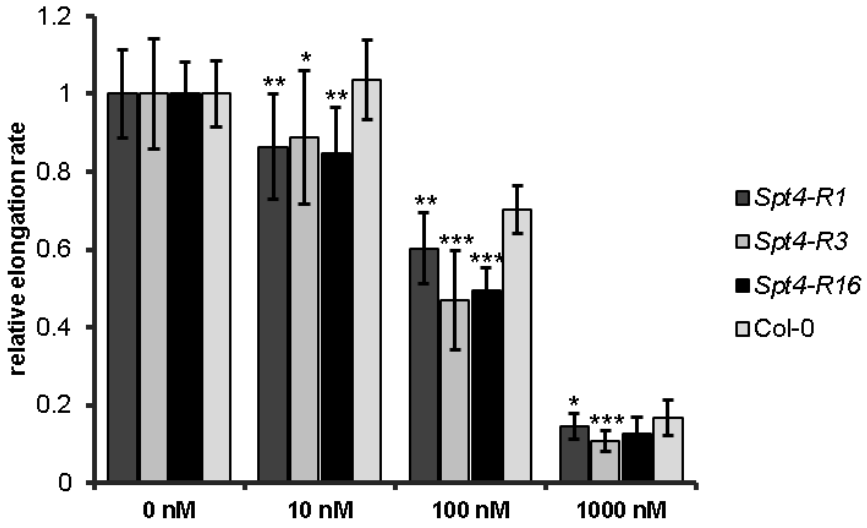

Figure 51. Elongation rates of primary roots at different IAA concentrations relative to untreated plants. The relative elongation rate was analysed using a one-way ANOVA. Error bars indicate SD of at least 13 plants. Data sets marked with asterisks are significantly different from wild-type as assessed by Dunnett's multiple comparison test: * P < 0.05, ** P < 0.01 or *** P < 0.001. The experiment was performed twice with similar results.

2.7.2 *SPT4-R3* plants have a stronger auxin response

The analyse the auxin response, the line *SPT4-R3* was crossed with wild-type plants harbouring a *DR5-GUS* reporter construct. The *DR5* promoter consists of tandem direct repeats of 11 bp that included the auxin-responsive TGTCTC element. The reporter construct can be used to visualize the auxin response through the auxin response factors (ARF) binding to the synthetic *DR5* promoter (Ulmasov et al., 1997b). Comparative histochemical staining for GUS activity was made for the aerial part and roots of wild-type and *SPT4-R3*. The plants were stained until a first staining of the wild-type was visible to have a comparative staining. The aerial parts of the plants showed in general a more intense staining in *SPT4-R3* plants than in Col-0 (Figure 52). The GUS staining in Col-0 was restricted to the leaf margins and hydathodes, while in *SPT4-R3* the staining was additionally visible across the leaf blade and veins.

Figure 52. Response to auxin with *DR5* promoter. Response to auxin as visualised using the *DR5-GUS* reporter. Col-0 and *SPT4-R3* plants harbouring the *DR5-GUS* reporter were histochemically stained for GUS activity. Aerial part of plants (18 DAS), cotyledon, first and second leaf (from left to right) were analysed. Size bars correspond to 1 mm.

Similarly, to the staining of the aerial part, in the primary root tip of *SPT4-R3* showed a more intense and spatially less defined staining compared to Col-0. Contrary to the root tip in lateral roots of different developmental stages no marked differences were visible (Figure 53). These experiments revealed that in *SPT4-R3* plants the auxin response is stronger and spatially less confined than in Col-0.

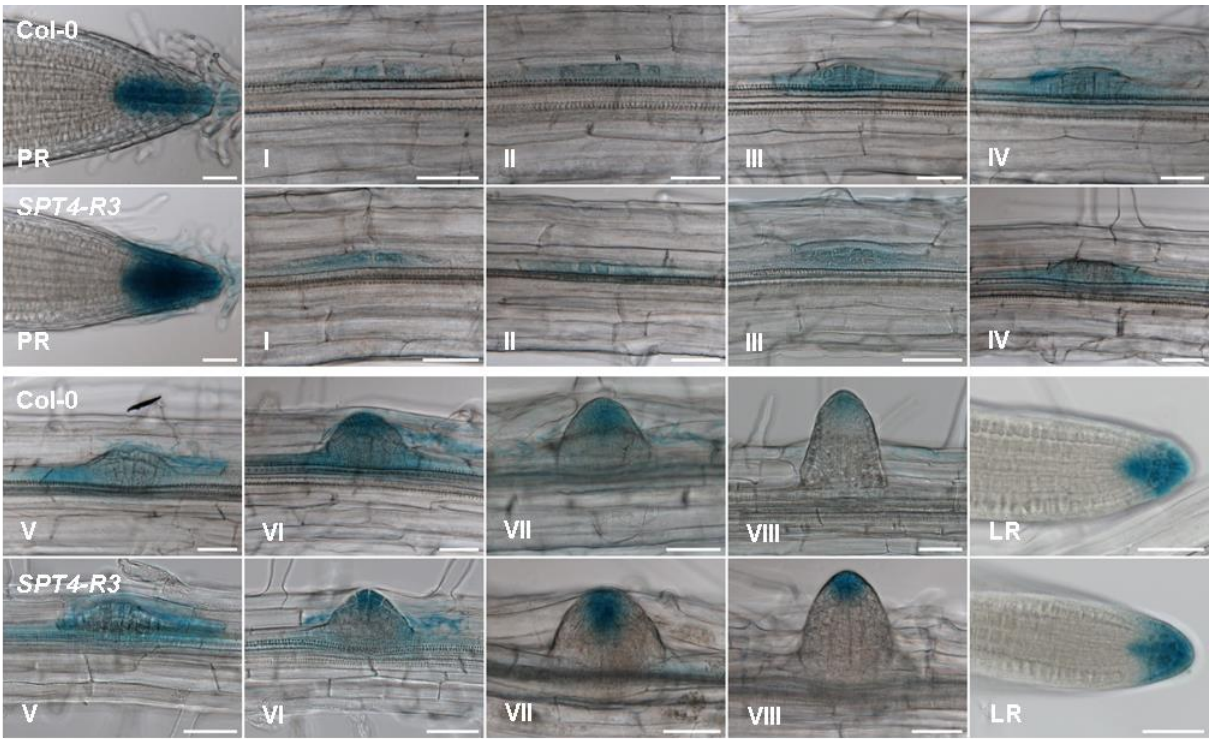

Figure 53. Auxin response in the primary root. Auxin response visualised by the *DR5-GUS* reporter. Col-0 and *SPT4-R3* plants harbouring the *DR5-GUS* reporter were histochemically stained for GUS activity. Primary root tip **(PR)**, the different stages of lateral roots **(I – VIII)** and elongated secondary roots **(LR)** were examined of 12 DAS plants. Size bars correspond to 50 µm.

2.8 SPT4-SPT5 complex in *Arabidopsis*

From yeast to human and interaction of SPT4 and SPT5 and as a complex to RNAPII has been identified. SPT5 was found to be situated along transcribed regions in yeast, *Drosophila* and human (Hartzog and Fu, 2013). For analysis of SPT4-SPT5 proteins in *Arabidopsis thaliana*, antibodies (AB) were raised against SPT4 and SPT5 that could be used for immunoblot and immunoprecipitation experiments. To analyse the association of SPT5 with transcribed genes in *Arabidopsis* chromatin immunoprecipitation (ChIP) and affinity purification experiment were performed using SPT5 and RNAPII antibody.

2.8.1 Purification of the C-terminal part of SPT5 for antibody production

For immunisation the last 250 aa of SPT5-2 (~ 30 kDa) were used as the C-terminal region of SPT5 has been shown to be exposed (Martinez-Rucobo et al., 2011; Martinez-Rucobo and Cramer, 2013). For this purpose the corresponding coding sequence was cloned into the pQE expression vector for expression in *E. coli*. After pilot experiments of the expression and purification of the recombinant protein it was produced in larger quantities with Ni-NTA affinity purification via the N-terminal His-tag. The purified protein used for commercial immunisation in rabbit (Figure 54).

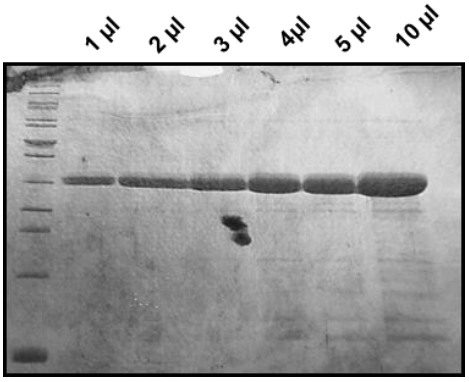

Figure 54. Purified SPT5. The last 250 aa of SPT5-2 (~ 30 kDa) were purified with the N-terminal His-tag. Different amount of the eluate are shown.

2.8.2 Initial testing of the SPT4 and SPT5 antibodies

Besides the antiserum against the C-terminal part of SPT5-2, an antiserum raised against recombinant full-length SPT4-2 was also available in the group. Both antisera were tested by Western blot if they could detect the recombinant protein they were raised against. The SPT5 antibody detected the recombinant protein to a concentration of ~12.5 ng (Figure 55A). With the SPT4 antiserum it was not possible to detect a signal at the corresponding size of the recombinant protein (data not shown), therefore it was not further used in this study. To further analyse the specificity of the SPT5 antibody it was tested against nuclear protein extracts of 21 DAS *Arabidopsis* seedlings (5.5.13) and total protein extracts of cell culture (5.5.9). The Western blot showed a clear signal in both extracts at the corresponding size of SPT5 of approximately 115 kDa (Figure 55B). Also additional bands were detected and the most prominent of the unspecific band had a size of approximately 55 kDa which correlated with the size of the big subunit of Rubisco. Possible degradation of SPT5 could be also a cause for the additional bands.

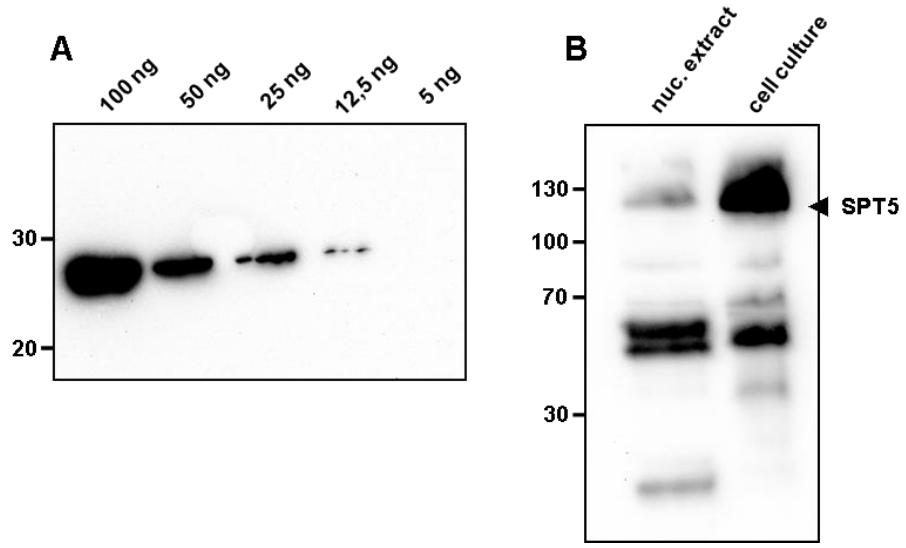

Figure 55. Immunoblot analysis with anti-SPT5 serum. (A) Immunoblot of different concentrations of recombinant protein used for immunization. **(B)** Immunoblot with anti-SPT5 serum of nuclear extracts of 21 DAS seedlings and total protein extract for *Arabidopsis* cell culture.

2.8.3 Identification of interaction partners of SPT4

2.8.3.1 SPT4 interacts with SPT5 in a complex

It has been shown that SPT4 interacts with SPT5 in other organisms for example yeast and human (Hartzog and Fu, 2013). To test whether the interaction of SPT4 and SPT5 is conserved in plants and to identify possible additional interaction partners of the complex, affinity purification using a protein extract of *Arabidopsis* cell culture was performed (5.5.9). For purification the GS-tag (Figure 56A) was favoured over the TAP-tag as the GS-tag has been shown to be superior to the TAP-tag both concerning specificity and complex yield (Van Leene et al., 2008). SPT4-2 was N-terminally fused to the GS-tag and both, the free GS-tag and SPT4-2-GS under control of the 35S promoter were transformed into *Arabidopsis* suspension cultured cells (Van Leene et al., 2011). This approach was already used to identify other nuclear protein complexes (Nelissen et al., 2010; Pauwels et al., 2010). SPT4-2-GS and the free GS-tag were purified by IgG affinity purification using commercially available IgG agarose beads. This method was further improved regarding specificity by coupling rabbit IgG to metal-beads (Figure 56B). The protocol therefore was kindly provided by Dr. Joachim Griesenbeck.

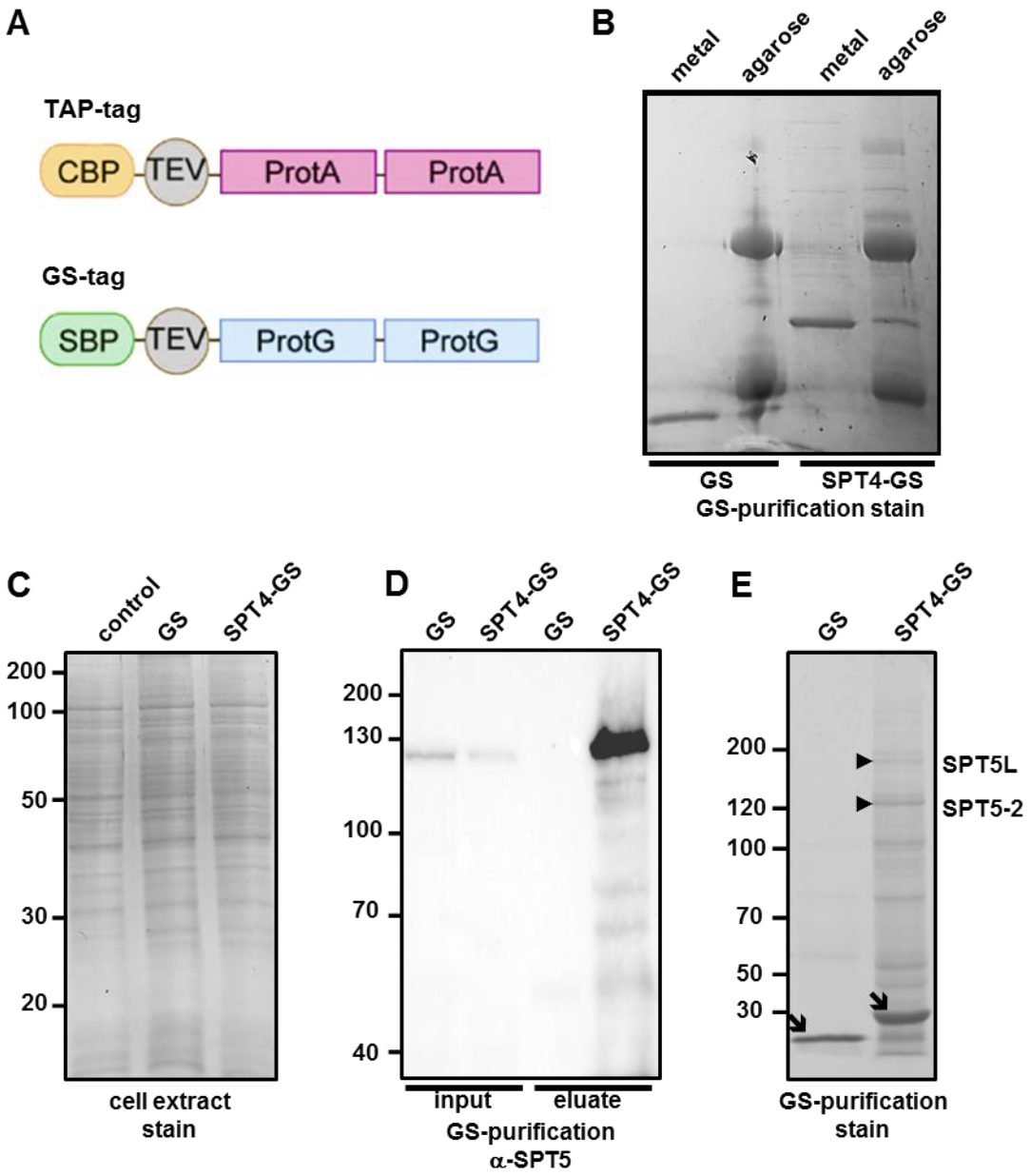

Figure 56. SPT4 occurs in a complex with SPT5 and SPT5L. (A) Overview of TAP and GS tags. (Abbreviations: ProtA: immunoglobulin G (IgG)-binding domain of protein A; ProtG: IgG-binding domain of protein G; TEV: tobacco etch virus (TEV) protease cleavage site; CBP: calmodulin-binding peptide; SBP, streptavidin-binding peptide. **(B)** Eluates of the affinity purifications comparing metal beads and agarose beads after SDS-PAGE and Coomassie-staining of the gel. **(C)** Protein extracts of untransformed cells and of cells expressing free GS or SPT4-GS after SDS-PAGE and Coomassie-staining of the gel. **(D)** Immunoblot analysis with an anti-SPT5 serum of input samples and eluates of the GS/SPT4-GS affinity purifications. **(E)** Eluates of the affinity purifications after SDS-PAGE and Coomassie-staining of the gel. The free GS-tag and SPT4-GS are indicated by arrows, while the bands corresponding to SPT5-2 and SPT5L, identified by mass spectrometry in the SPT4-GS eluate, are indicated by arrowheads.

As control, the total protein extracts of non-transformed cells and of cells expressing SPT4-2-GS or GS before purification is shown. The Coomassie-stained band pattern after SDS-PAGE was similar and the bands corresponding to GS and

GS-SPT4-2 did not stand out in the extracts of the transformed cell lines (Figure 56C). To identify possible interaction partners of SPT4, both SPT4-2-GS and the free GS-tag were comparatively isolated from the same amount of cell extract according to Bradford-assay. The input and elution fractions of the immune-purified proteins were tested with the SPT5 antibody. The SPT5 antiserum marked specifically a protein of the expected size of approximately 115 kDa in the SPT4-2-GS and GS input samples but in the eluates SPT5 was only detectable using SPT4-2-GS for precipitation and not in the GS control (Figure 56D). The immunoblot analysis indicated that SPT4 and SPT5 occur in a protein complex in *Arabidopsis* cell culture.

2.8.3.2 Identification of possible interaction partners of the SPT4-SPT5 complex

Mass spectrometry was performed to identify possible interaction partner of the SPT4-SPT5 complex in *Arabidopsis*. The proteins of the affinity purification were separated by SDS-PAGE (Figure 56E). The gel was cut into slices, proteins were digested with trypsin and analysed by mass spectrometry with a MaXis 4G UHR-Q TOF-system in the laboratory of Prof. Dr. Deutzmann. Both SPT4-GS and GS eluates were analysed comparatively. Several proteins were identified and are listed in Table 2 (For complete list see Table 9).

Table 2. Mass spectrometry results of the SPT4-GS affinity purification.

AGI	#IPs[1]	mass [kDa]	Mascot mean score	description
At4g08350	5	115.3	2115.30	SPT5-2
At5g04290	5	157.9	1103.76	SPT5L
At5g63670	5	13.4	330.78	SPT4-2
At5g08565	5	13.4	223.97	SPT4-1
At5g13680	5	146.5	176.90	ELO2
At1g02080	4	269.7	712.05	CCR4-NOT subunit 1
At5g50320	3	63.1	222.10	ELO3
At4g35800	2	204.9	393.60	NRPB1
At4g21710	1	134.9	667.08	NRPB2

[1]numbers indicate in how many out of a total of 5 experiments the respective protein was identified.

In line with the immunoblot analysis, we identified by mass spectrometry SPT5-2 with a high score in every affinity purification. Interestingly, SPT5L was also identified in all SPT4-GS eluates with high scores. Both were not detected in the GS control samples. Single bands were analysed by mass spectrometry. The bands

corresponding to SPT5-2 and SPT5L are among the most prominent bands in the Coomassie-stained gel of the SPT4-GS eluates, except for the bands corresponding to the tagged SPT4-GS and GS proteins. This indicates that both proteins are interactors of SPT4-2. Beside the two SPT5 proteins the subunit 1 of the putative *Arabidopsis* CCR4-NOT (Carbon catabolite repression 4-Negative on TATA) complex was reproducibly identified. In yeast the CCR4-NOT complex acts as a positive transcription factor and interacts directly with the RNA polymerase II (Kruk et al., 2011). Moreover, the ELO2 and ELO3, two subunits of the Elongator complex, were identified reproducibly. The Elongator complex is well characterised in *Arabidopsis* and co-purifies with RNAPII. The Elongator complex has histone acetyltransferase activity and is formed out of six subunits. The ELO3 subunit carries the histone acetyltransferase activity (Nelissen et al., 2005; Nelissen et al., 2010). The two largest subunits of RNAPII, NRPB1 and NRPB2 (Nuclear RNA Polymerase II), could also be identified as possible interactors of SPT4-GS with somewhat lower mean score. To prove these results, similar affinity purification experiments with a SPT5-2-GS fusion should also be performed but despite great efforts it was not possible to generate the required constructs due to the genetic instability of the *SPT5* coding sequence in both in *E. coli* and *A. tumefaciens*.

2.8.3.3 SPT4-2 interacts directly with SPT5-2 and SPT5L

One question, which could not be answered by the affinity purification experiments, was if SPT4 and SPT5 interact directly. To assess this question, *in vitro* pull-down experiments were performed with recombinant GST and with GST fused to SPT4 (GST-SPT4). The N-terminal part of both, SPT5-2 and SPT5L were cloned into the pBC-SK vector containing the T7 promoter and translated *in vitro*. Both constructs had the NGN domain, which has been shown to be the interacting domain with SPT4 in yeast. The N-terminal part of SPT5-2 was incubated with glutathione-agarose immobilized GST-SPT4-2 and as a negative control with GST. Bound proteins were eluted and analysed by SDS-PAGE. SPT5-2 was clearly bound to GST-SPT4 and only background level was detected with GST (Figure 57). Similarly, the N-terminal part of SPT5L specifically interacted with GST-SPT4 and not with GST. Therefore, both SPT5-2 and SPT5L can directly interact *in vitro* with SPT4.

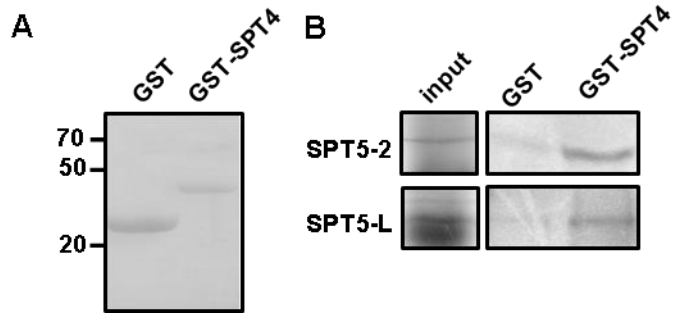

Figure 57. SPT4 interacts with SPT5-2 and SPT5L directly. (A) Pull-down assays with recombinant GST and GST-SPT4. **(B)** The N-terminal regions of *in vitro* translated ^{35}S-Met-labelled SPT5-2 (aa1-314) and SPT5L (aa1-294) were incubated with immobilised GST and GST-SPT4-2. After washing the glutathione beads, eluted proteins were analysed by SDS-PAGE and detected by phosphoimaging. Aliquots of the protein input samples (25%) are also shown.

2.9 Cellular localisation of SPT4 and SPT5

To analyse the cellular localisation of SPT4, the coding sequence of SPT4-2 was fused N- and C-terminally to GFP. As control free GFP and nuclear HMGB14 fused to GFP was used (Grasser et al., 2006). Protoplasts of tobacco BY-2 cell culture were transformed with those constructs and analysed for its sub-cellular localisation SPT4-GFP fluorescence was found in the nucleus and in the cytoplasm when overexpressed under control of the 35S promoter (Figure 58).

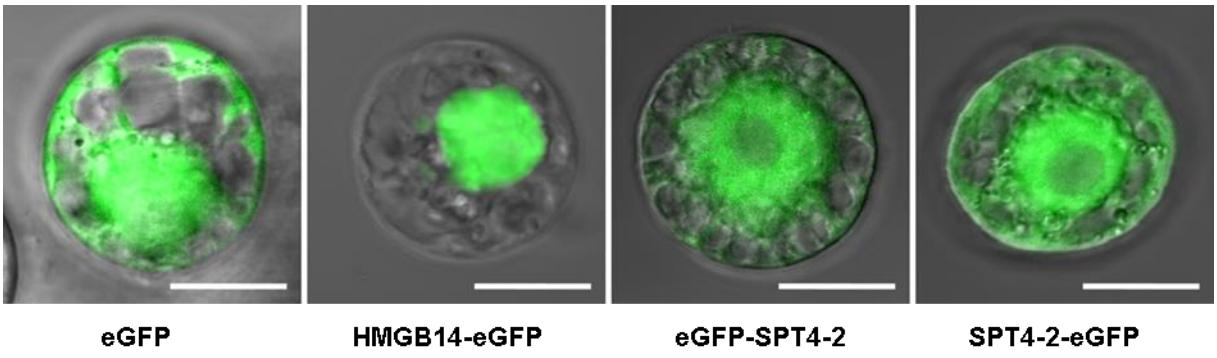

Figure 58. SPT4 localisation. 5'- and 3'-fusions of GFP to SPT4-2 show localisation of SPT4 in tobacco protoplasts. Size bars correspond to 10 µm.

Due to the genetic instability of SPT5 no GFP fusion construct could be created, therefore its cellular localisation was analysed by immunostaining of *Arabidopsis* root nuclei using the SPT5 antibody. Besides the SPT5 antibody an antibody against the non-phosphorylated C-terminal repeats of RNAPII was used. To counterstain the DNA of the nucleus DAPI was used. The immunostaining showed

that SPT5 localised to the nucleus but not to the nucleolus. And it partially co-localises with the RNAPII (Figure 59).

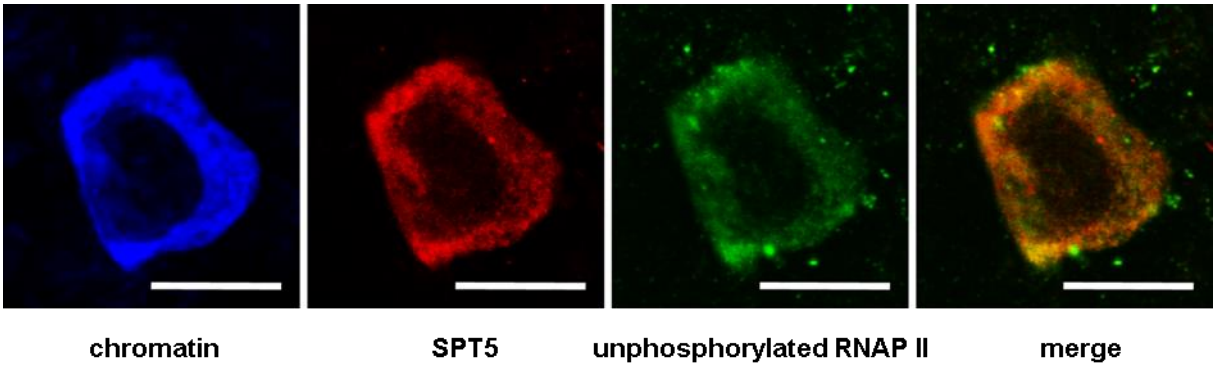

Figure 59. SPT5 localisation. Co-localisation analysis of SPT5 (red) and inactive RNAPII (non-phosphorylated CTD) (green) within euchromatic regions of the nucleus of a root cell visualised by CLSM. The DNA of the nucleus was counterstained with DAPI (blue). Size bars correspond to 10 µm.

To gain a detailed insight into the SPT5 localisation also in view of the co-localisation with the RNAPII super-resolution, structured illumination microscopy (SIM) was performed with the immunostained meristematic cells of the *Arabidopsis* root tip. SIM was performed by Dr. Veit Schubert in the laboratory of Dr. Andreas Houben. The SPT5 signal was exclusively detected in the nucleus (Figure 60). This demonstrates that SPT5 is a nuclear protein of interphase cells. The sub-nuclear distribution of SPT5 was investigated in comparison to the phosphorylated and non-phosphorylated forms of RNAPII. Therefore, cells were simultaneously labelled with the respective antibodies and counterstained with DAPI. The antibody specific against the non-phosphorylated RNAPII was raised against non-phosphorylated heptamer repeats of the carboxy-terminal domain. For the active form an antibody against the CTD repeats phosphorylated at Ser2 was used. Like SPT5 both forms of the RNAPII were absent from the nucleolus and heterochromatin (Figure 60). After applying super-resolution microscopy it became obvious that SPT5 and both forms of RNAPII composed separate networks within the euchromatin. Further analysis of the degree of co-localisation between SPT5 and the RNAPII signals revealed that SPT5 is more frequently associated with the active (CTD-Ser2P) than with the non-phosphorylated form of RNAPII. The overlap coefficient (OC) was determined as the degree of co-localisation between SPT5 and the RNAPII. The analysis of SPT5 and RNAPII and signals revealed that SPT5 is more clearly associated with the active (OC=0.86; n=18; SD=0.0240) than with the non-phosphorylated (OC=0.71; n=18;

SD=0.0212) form of RNAPII. The preferential association of SPT5 with the active rather than the inactive form of RNAPII is also obvious from the insets.

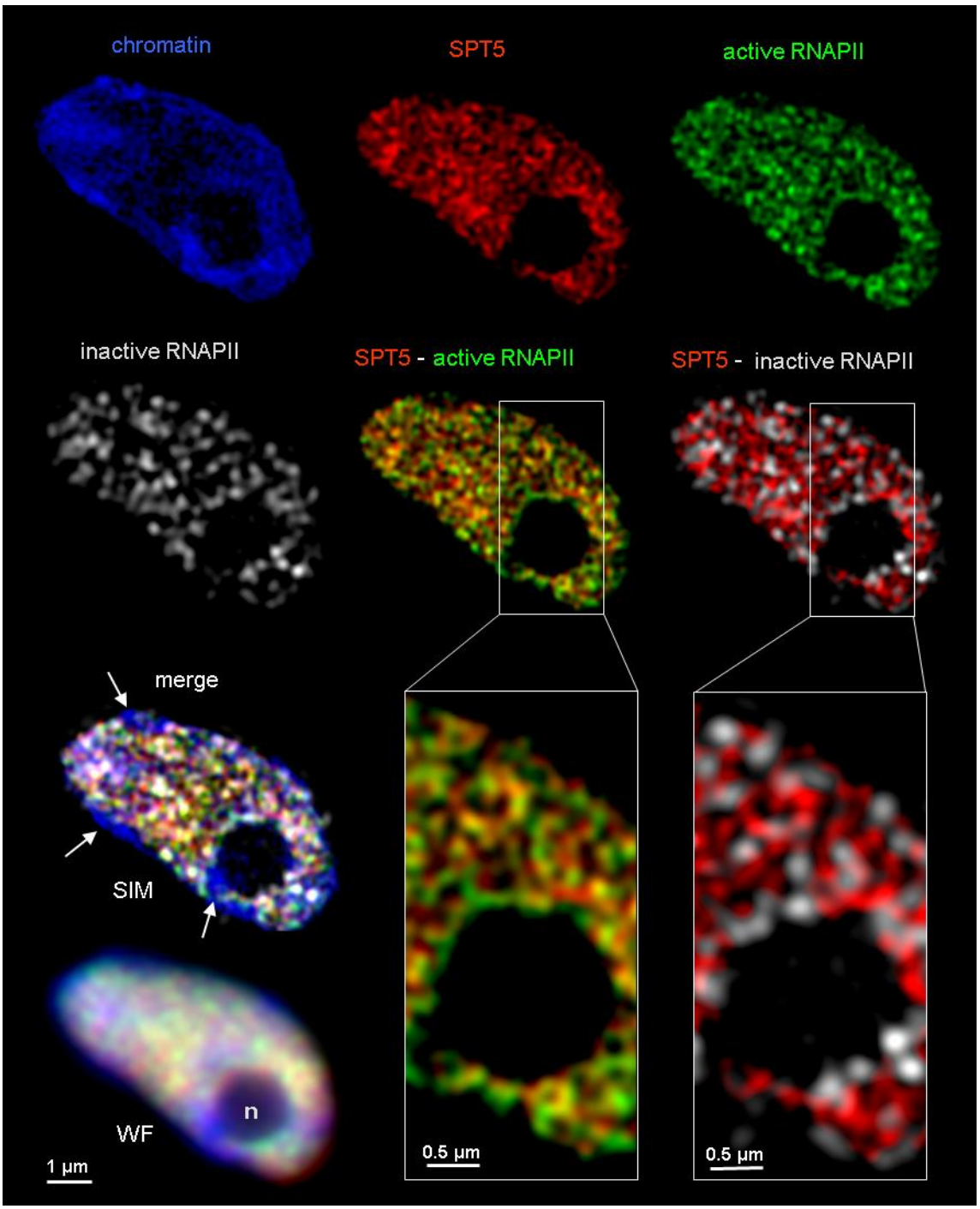

Figure 60. SPT5 localises to transcriptionally active euchromatin. Co-localisation analysis of SPT5 with active RNAPII (CTD-Ser2P) and inactive RNAPII (non-phosphorylated CTD) within euchromatic regions of the nucleus of a meristematic cell visualised by SIM. The nucleus was counterstained with DAPI (blue). They are not present in the nucleolus (n) and within heterochromatin (arrows). As a comparison to the SIM images the merged nucleus (four colours) is also shown in wide-field (WF) illumination.

2.10 Chromatin immunoprecipitation

2.10.1 Quality control

Chromatin immunoprecipitation with antibodies against SPT5 and RNAPII was performed to examine the association of SPT5 with transcribed genes in more detail. For every ChIP experiment a quality control was performed by normal PCR. With primers against the housekeeping gene *ACT8* and the transposon *TA3* the specificity of the samples was tested. *ACT8* was used as a control for actively transcribed gene and the transposon *TA3* as a control for silenced regions (Konieczny et al., 1991). As SPT5 and RNAPII have been shown to locate to actively transcribed regions, therefor a signal was expected for *ACT8* but not for *TA3.* Both the input and H3 were used as positive controls and signals for *ACT8* and *TA3* were expected. In contrast the pre-immune serum (PI) was used as negative control and neither a signal for *ACT8* nor for *TA3* was expected. A typical gel is shown (Figure 61).

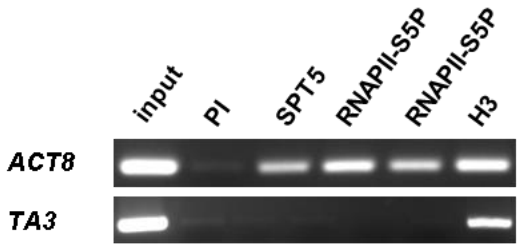

Figure 61. ChIP quality control. A representative PCR against the actively transcribed *ACT8* and the non-transcribed transposon *TA3* is shown.

2.10.2 SPT5 is associated with actively transcribed genes

The distribution of SPT5 was studied at two long genes, for simple discrimination between different gene regions. The gene At3g02260 has a transcribed region of ~17.5 kb and the gene At1g48090 has a transcribed region of 26.4 kb. For these experiments the SPT5 antiserum was used in comparison to the pre-immune serum. The ChIP efficiency of different gene regions (Figure 62A) was quantified by qPCR. SPT5 was detected along the entire transcribed region of At3g02260 and At1g48090 with increasing levels towards the 3´end of the gene (Figure 62B, C). As a control the intergenic region 6 down-stream of At3g02260 and the *DOG1* (*DELAY OF GERMINATION 1*) gene were used because both regions are not transcribed in the used tissue and no signal significantly above background was detected in the ChIP material. (Figure 62B). *DOG1* is expressed seed-specifically (Bentsink et al., 2006).

For comparison, ChIP assays were performed using a histone H3-specific antibody, revealing a similar association of H3 at all tested regions including the intergenic region and the *DOG1* gene (Figure 62D). Therefore, in these assays typical for TEFs, SPT5 is found along the entire region transcribed by RNAPII but not along non-transcribed regions.

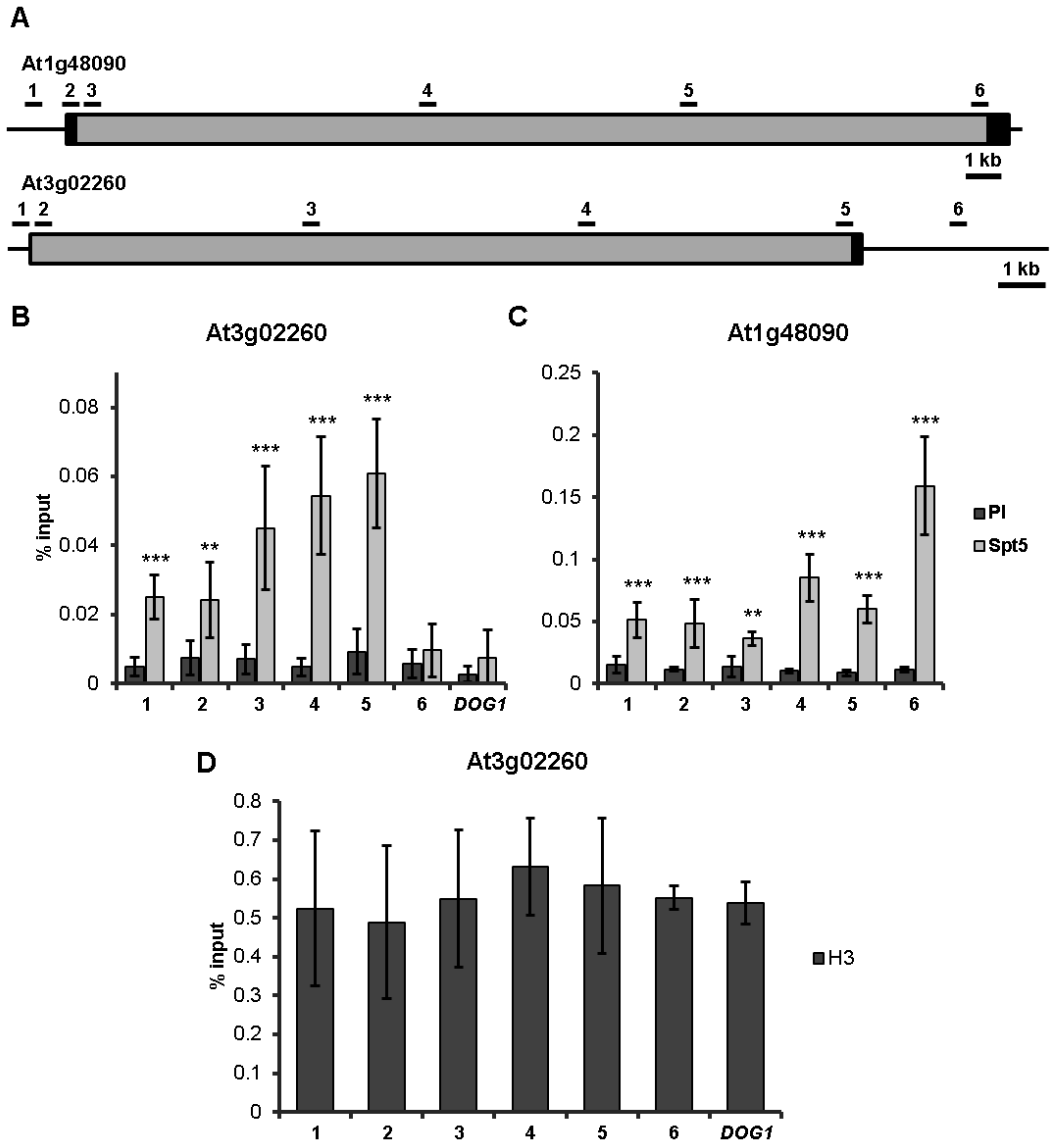

Figure 62. SPT5 associates with RNAPII transcribed regions. **(A)** Schematic representation of At3g02260 and At1g48090 with the transcribed region (exons and introns) marked by boxes. The Bars above indicate the relative positions of the regions analysed by ChIP. **(B)** ChIP analyses of At3g02260 and **(C)** At1g48090 with SPT5 anti-serum. **(D)** ChIP with the antibody against H3 was used as control. For the ChIP experiments, percentage input was determined by qPCR and analysed using one-way ANOVA. Error bars indicate SD of at least three biological and three technical replicates. Data sets marked with asterisks are significantly different from PI as assessed by Dunnett's multiple comparison test: * $P < 0.05$, ** $P < 0.01$ or *** $P < 0.001$.

2.10.3 *SPT4-R3* exhibits elevated levels of SPT5

To analyse the effects of the *SPT4* down-regulation, the association of SPT5 was determined comparatively in *SPT4-R3* and Col-0 chromatin. For comparison the association of SPT5 with the At3g02260 gene was tested. The transcript levels of At3g02260 are similar according to our microarray experiment in Col-0 and *SPT4-R3*.

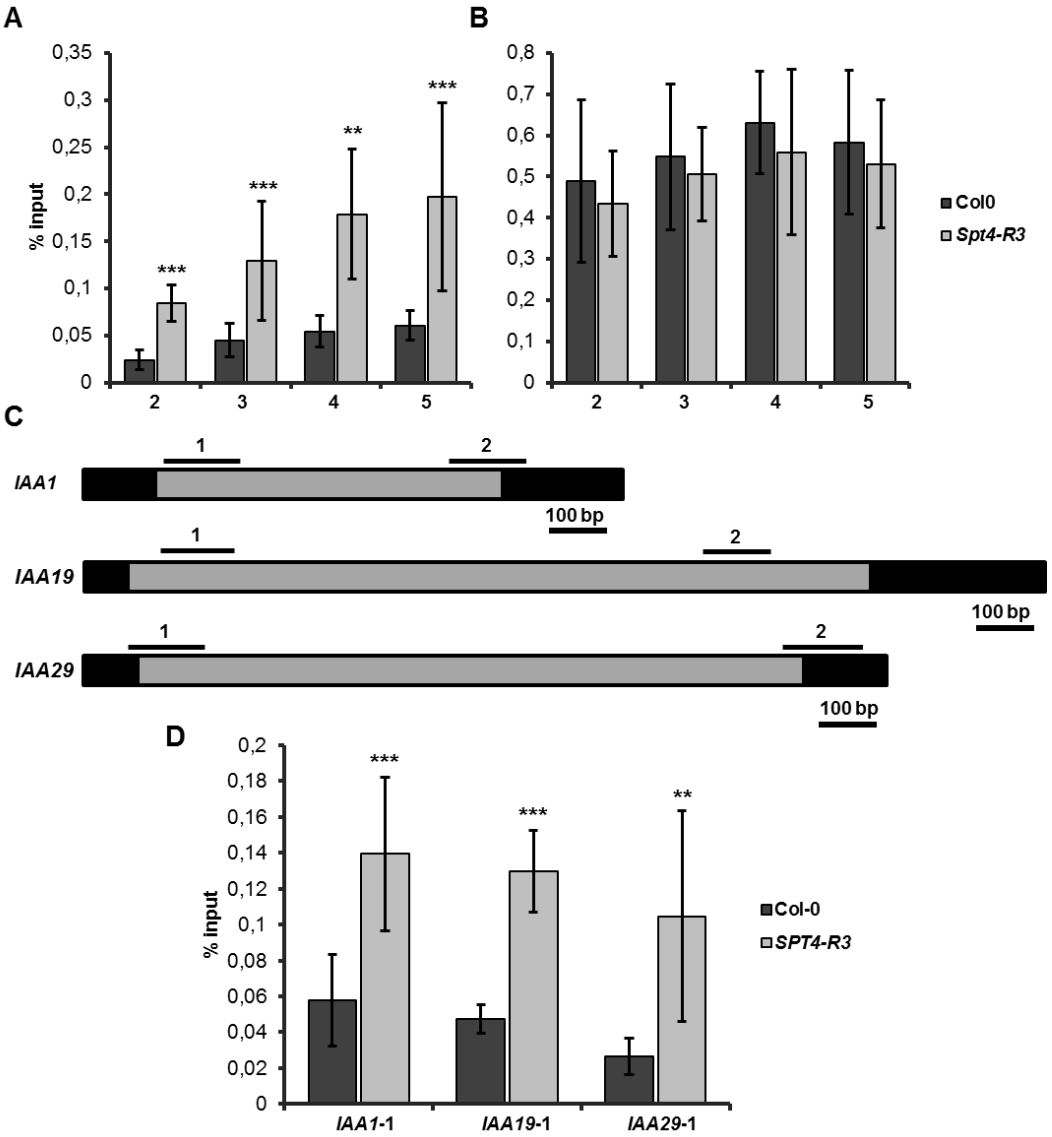

Figure 63. *SPT4-R3* exhibits elevated levels of SPT5. ChIP analyses of At3g02260 with the SPT5 **(A)** and H3 **(B)** anti-serum comparing *SPT4-R3* and wild-type. Numbers correspond to regions depicted in Figure 62A. **(C)** Schematic representation of *IAA1*, *IAA19* and *IAA29* with the boxed region indicating the transcribed region (exons, introns) and the bars above indicate the relative positions of the regions analysed by ChIP. **(D)** ChIP analyses of *IAA1*, *IAA19* and *IAA29* with the SPT5 anti-serum comparing *SPT4-R3* and wild-type. For the ChIP experiments, percentage input was determined by qPCR and analysed using one-way ANOVA. Error bars indicate SD of at least three biological and three technical replicates. Data sets marked with asterisks are significantly different from wild-type as assessed by Dunnett's multiple comparison test: * $P < 0.05$, ** $P < 0.01$ or *** $P < 0.001$.

Elevated levels of SPT5 were detected along the whole transcribed region of At3g02260 in *SPT4-R3* compared with Col-0 (Figure 63A), whereas the levels of H3 are the same in both Col-0 and *SPT4-R3* (Figure 63B). As the Histone H3 is equally distributed among chromatin this results suggest comparability of all samples used in this comparison of *SPT4-R3* and Col-0. Additionally the association of SPT5 to the genes *IAA1*, *IAA19* and *IAA29,* down-regulated in *SPT4-R3*, was analysed. In line with the elevated levels along At3g02260, SPT5 was significantly enriched in the 5´region of the *Aux/IAA* transcription units comparing Col-0 and *SPT4-R3* chromatin (Figure 63C, D).

2.10.4 RNAPII Ser2P and Ser5P is associated with actively transcribed genes

As SPT5 is a transcription elongation factor further ChIP analyses were performed using antibodies against the elongating forms of RNAPII. The antibodies were against the RNAPII phosphorylated within the CTD at positions Ser2 or Ser5. For comparison of the results, ChIP experiments with an antibody against histone H3 were performed (Figure 62D). In these experiments, RNAPII-Ser5P was more enriched towards the 5´end of the transcription unit in wild-type chromatin (Figure 64A, B), whereas RNAPII-Ser2P occurs with slightly higher tendency towards the 3´end of the transcribed region (Figure 64C, D). This distribution was detectable along both long genes, At3g02260 and At1g48090. Subsequently, the distribution of both RNAPII-Ser2P and RNAPII-Ser5P was examined at the three *Aux/IAA* genes, *IAA1, IAA19* and *IAA29*. RNAPII-Ser5P was found enriched at the 5´end of the transcription units like observed with At3g02260 and At1g48090. RNAPII-Ser2P was detected with a tendency towards the 3´end (Figure 64E, F). These differential distributions among transcribed genes of RNAPII-Ser5P and RNAPII-Ser2P are well-documented in yeast and metazoan (O'Brien et al., 1994; Komarnitsky et al., 2000; Buratowski, 2009). In plants, details of the RNAPII-CTD phosphorylation during the transcription cycle are not known but recently kinases were identified that catalyse the phosphorylation of specific serine residues within the CTD (Hajheidari et al., 2012). A distribution of RNAPII-Ser2P/Ser5P comparable to the observation in this thesis was found at *Arabidopsis* genes recently (Ding et al., 2011).

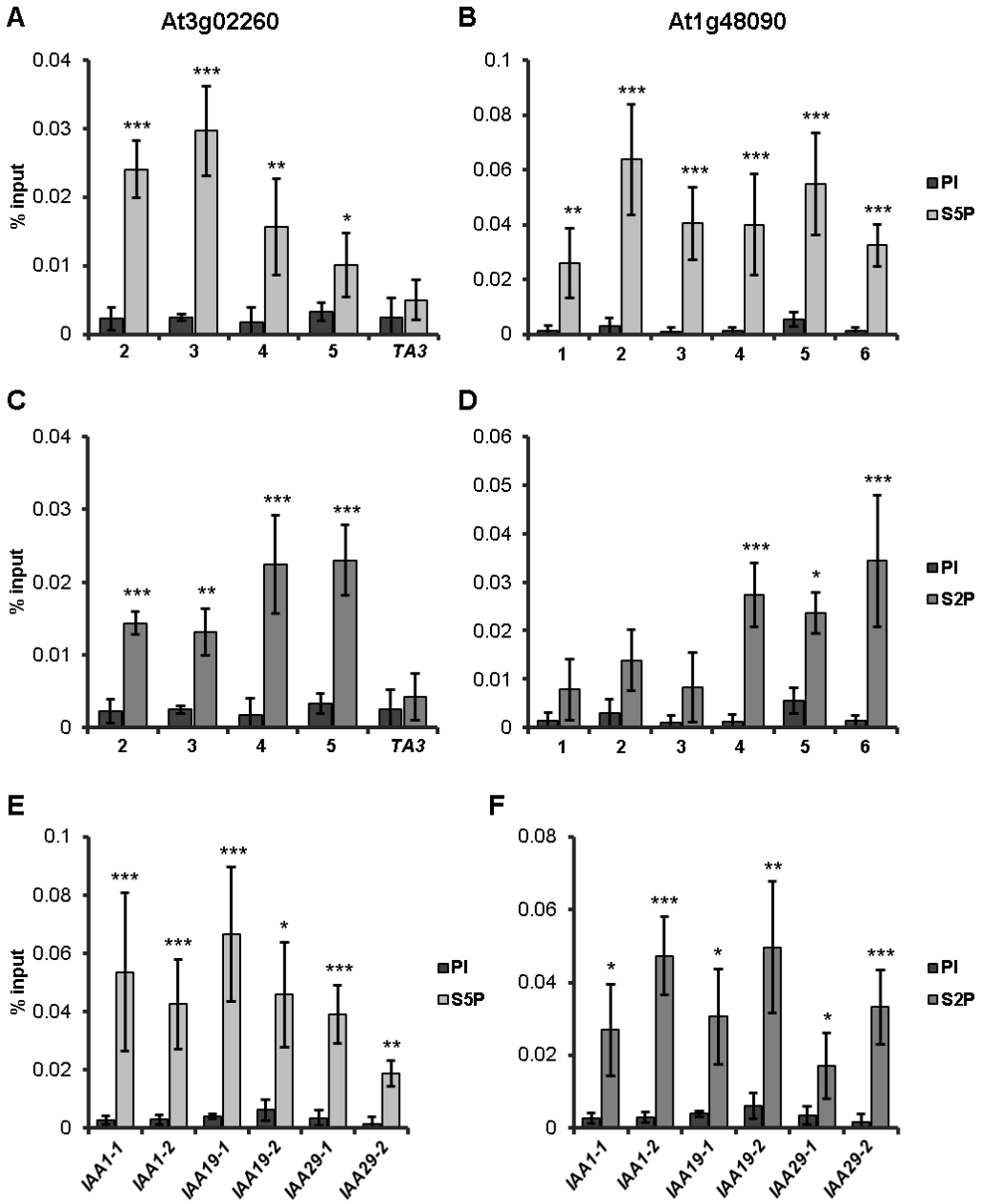

Figure 64. Association of RNAPII-Ser5P and -Ser2P to wild-type chromatin. (A-D) ChIP analyses of At3g02260 **(A, C)** and At1g48090 **(B, D)** with an anti-serum against RNAPII-Ser5P **(A, B)** and RNAPII-Ser2P **(C, D)**. **(E, F)** Association of RNAP-Ser5P **(E)** and RNAP-Ser2P **(F)** to three different IAAs. For the ChIP experiments, percentage input was determined by qPCR and analysed using one-way ANOVA. Error bars indicate SD of at least three biological and three technical replicates. Data sets marked with asterisks are significantly different from PI as assessed by Dunnett's multiple comparison test: * $P < 0.05$, ** $P < 0.01$ or *** $P < 0.001$.

2.10.5 *SPT4-R3* exhibits elevated levels of RNAPII-Ser2P and -Ser5P

Like for SPT5, the level of RNAPII association to genes was analysed comparing Col-0 and *SPT4-R3*. In accordance with the observations of elevated SPT5 association along transcribed regions of At3g02260 and At1g48090 in *SPT4-R3*, RNAPII-Ser2P and RNAPII-Ser5P were also detected at significantly increased levels

at the same gene regions (Figure 65A-D). The association of Histone H3 was not significantly altered between Col-0 and *SPT4-R3* (Figure 63C). As the Histone H3 is associated to the analysed chromatin regions this results suggest comparability of all samples, which is necessary to compare *SPT4-R3* and Col-0 samples.

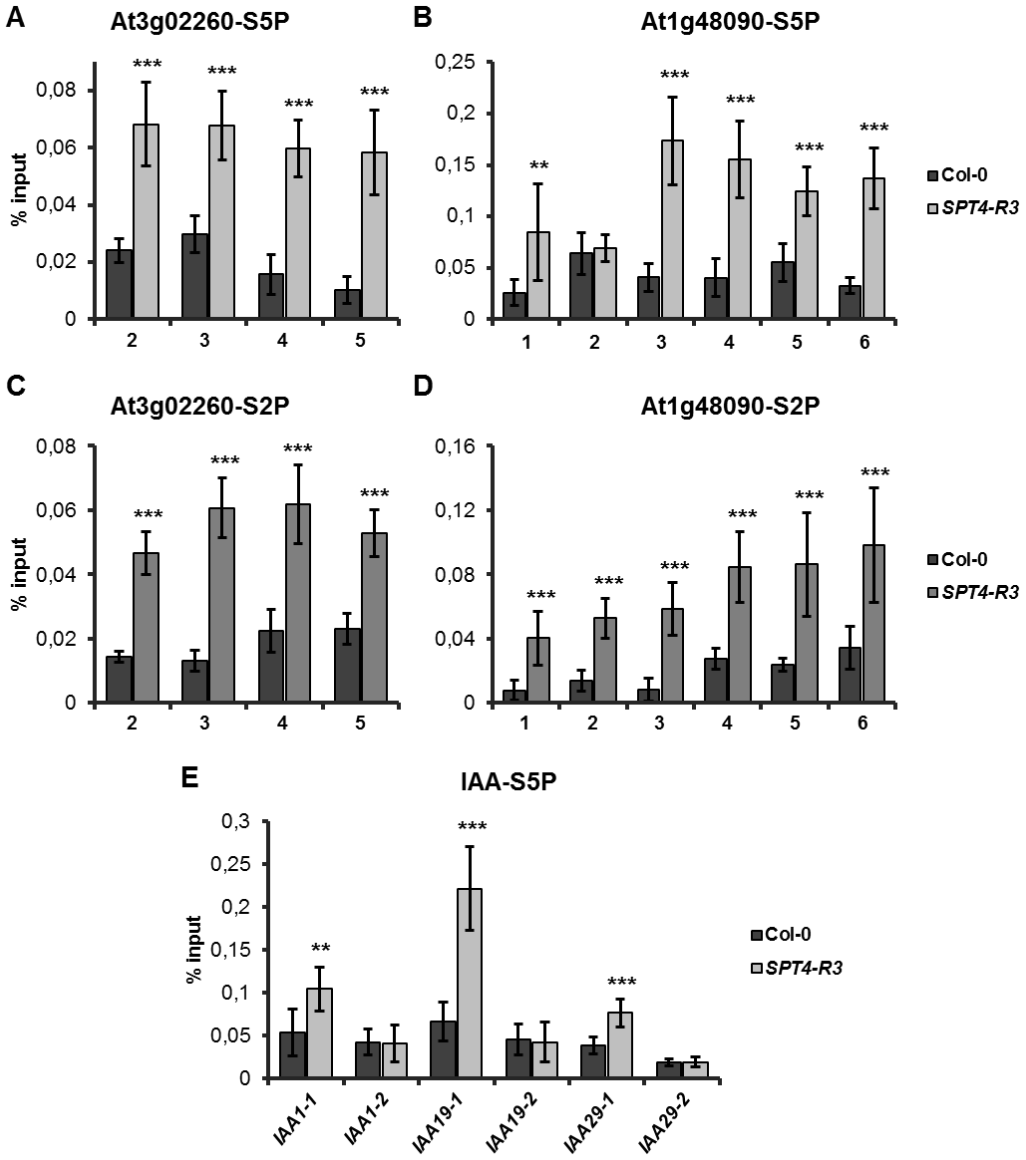

Figure 65. *SPT4-R3* exhibits elevated levels of RNAPII. (A-D) ChIP analyses of At3g02260 **(A, C)** and At1g48090 **(B, D)** using an anti-serum against RNAPII-Ser5P **(A, B)** and RNAPII-Ser2P **(C, D)** comparing the ChIP signal in *SPT4-R3* and wild-type. **(E)** Association of RNAP-Ser5P to three different *IAA*s comparing *SPT4-R3* and wild-type. For the ChIP experiments, percentage input was determined by qPCR and analysed using one-way ANOVA. Error bars indicate SD of at least three biological and three technical replicates. Data sets marked with asterisks are significantly different from wild-type as assessed by Dunnett's multiple comparison test: * $P < 0.05$, ** $P < 0.01$ or *** $P < 0.001$.

The association of RNAPII-Ser5P with the *IAA1, IAA19* and *IAA29* genes, which are down-regulated in *SPT4-R3*, was compared in Col-0 and *SPT4-R3* plants.

Comparing *SPT4-R3* and wild-type, RNAPII-Ser5P was enriched in *SPT4-R3* only in the 5´region of the transcription units of the different IAAs, but not in the 3´region, which is different from At3g02260 and At1g48090 (Figure 65E).

2.11 Double-mutants of *SPT4*-RNAi lines

In other organisms SPT4/5 has been shown to interact genetically or physically with several transcription factors like SPT6 and with factors that modify the mRNA co-transcriptionally (Lindstrom et al., 2003). To assay whether other transcription factors and modifying enzymes interact genetically with SPT4/5, double-mutants were created. Crosses of *SPT4*-RNAi lines with T-DNA insertion lines affected in the expression of TFIIS, the subunits SSRP1 and SPT16 of the FACT complex and as well as the two cap binding proteins CBP20 and CBP80 were created with standard genetic crossings. The mutant lines used for this crosses were genotyped using gene specific primers and a primer combination binding in the T-DNA, revealing that all double-mutants used in this thesis were homozygous for both T-DNA insertions (Figure 66).

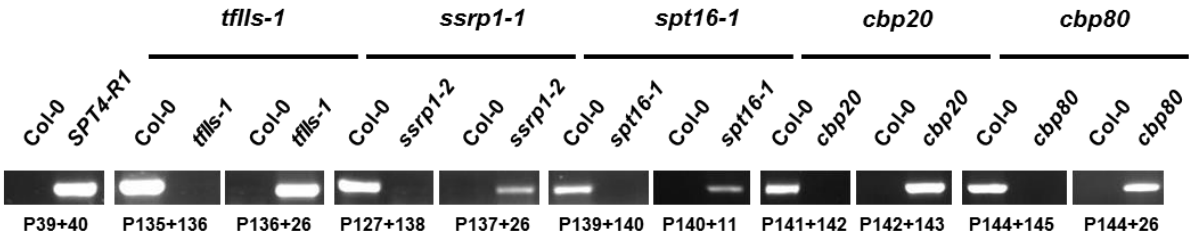

Figure 66. Genotyping of wild-type and mutant plants by PCR with the indicated primers. Shown are results for a wild-type plant and a plant homozygous for the T-DNA insertion.

2.11.1 Analysis of *SPT4-R1* and *tfIIs-1* double-mutant

The transcript elongation factor TFIIS promotes efficient transcription by RNA polymerase II. TFIIS helps the RNAPII to overcome transcriptional blocks or arrest sides by stimulating the intrinsic cleavage activity of RNAPII (Reines et al., 1989; Fish and Kane, 2002). In *Arabidopsis*, a putative TFIIS homolog to human TFIIS had been identified by amino acid sequence comparisons (Grasser, 2005). Plants homozygous for the T-DNA inserted in the coding sequence of the *TFIIS* locus (At2g38560) have essentially wild-type phenotype but display reduced seed dormancy (Grasser et al.,

2009). In yeast *spt4* and *spt5* mutants combined with *TFIIS* mutants show genetic interaction (Fish and Kane, 2002). In light of the interest in elongation factors and their role in plant development, a double-mutant of *SPT4-R1* and *tfIIs-1* was created. Phenotyping experiments showed that the *SPT4-R1/tfIIs-1* double-mutant looks essentially like wild-type and *tfIIs-1* (Figure 67).

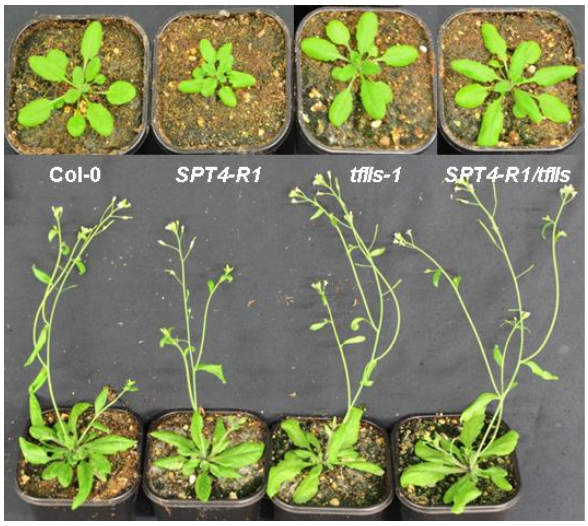

Figure 67. Phenotype of *SPT4-R1* and *tfIIs-1* and the double-mutant *SPT4-R1xtfIIs*. Representative individuals, single- and double-mutants of *SPT4* and *TFIIS* relative to Col-0 (21 DAS top, 35 DAS bottom) are shown.

For the phenotypic analysis, different vegetative and reproductive traits were measured (Figure 68). This analysis and the statistical evaluation with a two-way ANOVA and a Tukey's post test showed that at vegetative stage *tfIIs-1* contributes to the phenotype, and at reproductive stages both TFIIS and SPT4 contribute to the phenotype. To sum up, *TFIIS* is epistatic to *SPT4* looking at vegetative growth resembling the *tfIIs-1* mutant phenotype. Additive effects were observed for reproductive traits like flowering, bolting and the number of inflorescences.

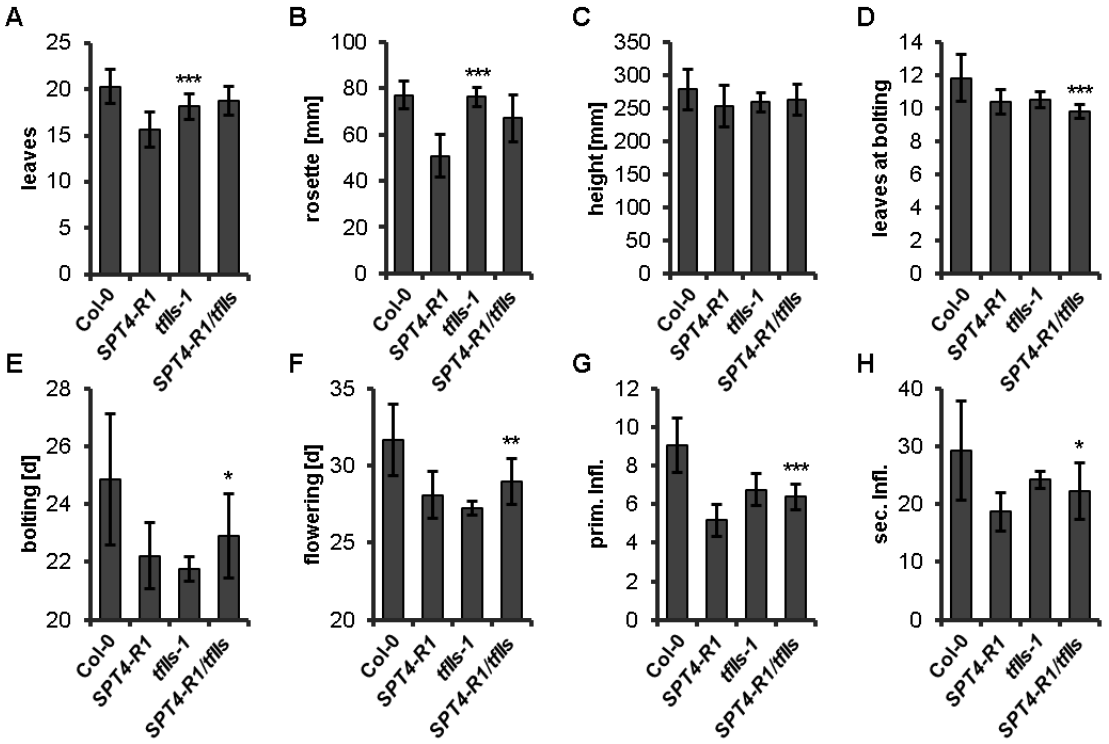

Figure 68. Phenotypic analysis of *SPT4-R1*/*tflls-1* double-mutant plants. (A) The number of leaves 35 DAS, **(B)** rosette diameter 28 DAS, **(C)** height 15 days after bolting, **(D)** number of leaves at bolting, **(E)** bolting time, **(F)** flowering time, **(G)** primary inflorescence 15 DAB, and **(H)** secondary inflorescence were analysed using a two-way ANOVA. Error bars indicate SD of at least ten plants. Data sets marked with asterisks show significant differences of the single-mutants to the double-mutant and of the double-mutant to wild-type as assessed by Tukey's multiple comparisons of means test with a 95% family-wise confidence level: * $P < 0.05$, ** $P < 0.01$ or *** $P < 0.001$. The experiment was performed at least two times.

The germination rate of seeds harvested 15 days after flowering was analysed. At this stage seeds are immature and wild-type seeds are not able to germinate in the same degree as *tfiis-1* seeds which are defective in dormancy (Grasser et al., 2009). The experiment showed that the line *SPT4-R1* germinates less compared to wild-type, whereas the germination rate of the double-mutant lies in between *tflls-1* and *SPT4-R1* (Figure 69).

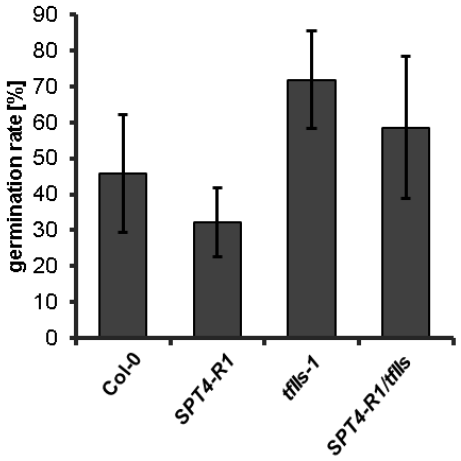

Figure 69. Germination rate of *SPT4-R1* and *tflls-1* double-mutant plants. Seeds have been harvested 15 DAF and the germination rate has been determined using ImageJ. Error bars indicate SD of eight independent experiments with at least 130 seeds per experiment per line.

2.11.2 Analysis of *SPT4-R1* and *ssrp1-2* or *spt16-1* double-mutants

The transcript elongation factor Facilitates chromatin transcription (FACT) consists of the two subunits SSRP1 and SPT16. FACT is a histone chaperone that assists the progression of transcribing RNA polymerase on chromatin templates by destabilizing nucleosomes (Belotserkovskaya et al., 2003). A putative homologue of the human SSRP1 has been identified in *Arabidopsis* (Duroux et al., 2004). Both SSRP1 and SPT16 are essential and plants with reduced levels of either SSRP1 or SPT16 show defects in both vegetative and reproductive development (Lolas et al., 2010). It has also been shown in yeast that FACT can alleviate transcriptional inhibition by DSIF and NELF (Wada et al., 2000). In view of these results double-mutants of *SPT4-R1* and *ssrp1-2* or *spt16-1* have been created and phenotypically analysed. The overall growth reveals that the *SPT4-R1/ssrp1-2* double-mutant looks essentially like the *ssrp1-2* single-mutant, whereas contrarily the *Spt4-R1/spt16-1* double-mutant looks essentially like the *SPT4-R1* single-mutant (Figure 70).

Figure 70. Phenotype of double-mutants of *SPT4-R1* and the FACT complex. Representative individuals, single-and double-mutants of *SPT4* and *SSRP1* or *SPT16,* relative to Col-0 (21 DAS top, 42 DAS bottom) are shown.

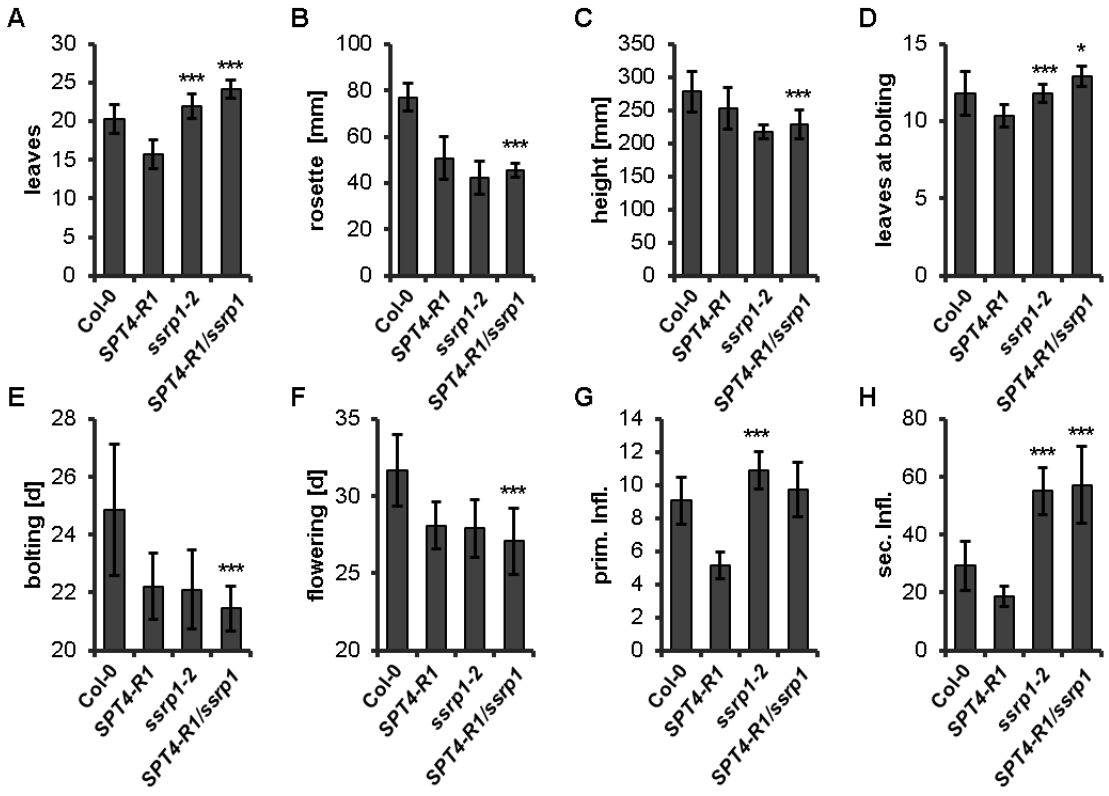

Figure 71. Phenotypic analysis of *SPT4-R1*/*ssrp1-2* double-mutant plants. (A) The number of leaves 35 DAS, **(B)** rosette diameter 28 DAS **(C)** height 15 days after bolting, **(D)** number of leaves at bolting, **(E)** bolting time, **(F)** flowering time, **(G)** primary inflorescence 15 DAB, and **(H)** secondary inflorescence were analysed using a two-way ANOVA. Error bars indicate SD of at least ten plants. Data sets marked with asterisks show significant differences of the single-mutants to the double-mutant and of the double-mutant to wild-type as assessed by Tukey's multiple comparisons of means test with a 95% family-wise confidence level: * $P < 0.05$, ** $P < 0.01$ or *** $P < 0.001$. The experiment was performed at least two times.

This observation was confirmed by detailed phenotypic analysis of the *SPT4-R1/ssrp1-2* (Figure 71) and the *SPT4-R1/spt16-1* (Figure 72) double-mutants. Analysis of *SPT4-R1/ssrp1-2* shows that *SSRP1* is epistatic over *SPT4* for number of leaves, leaves at bolting, primary and secondary inflorescences (Figure 71A, D, G, H), whereas for rosette diameter, height, bolting and flowering an additive effect (Figure 71B, C, E, F) is seen. The analysis of *SPT4-R1/ssrp1-2* indicates an epistatic effect between *SSRP1* and *SPT4* since the double-mutant essentially resembled the phenotype of *ssrp1-2*. In contrast to these findings the analysis *of SPT4-R1/spt16-1* showed that *SPT4* is epistatic to *SPT16* and the double-mutant resembled the phenotype of *SPT4-R1* (Figure 72).

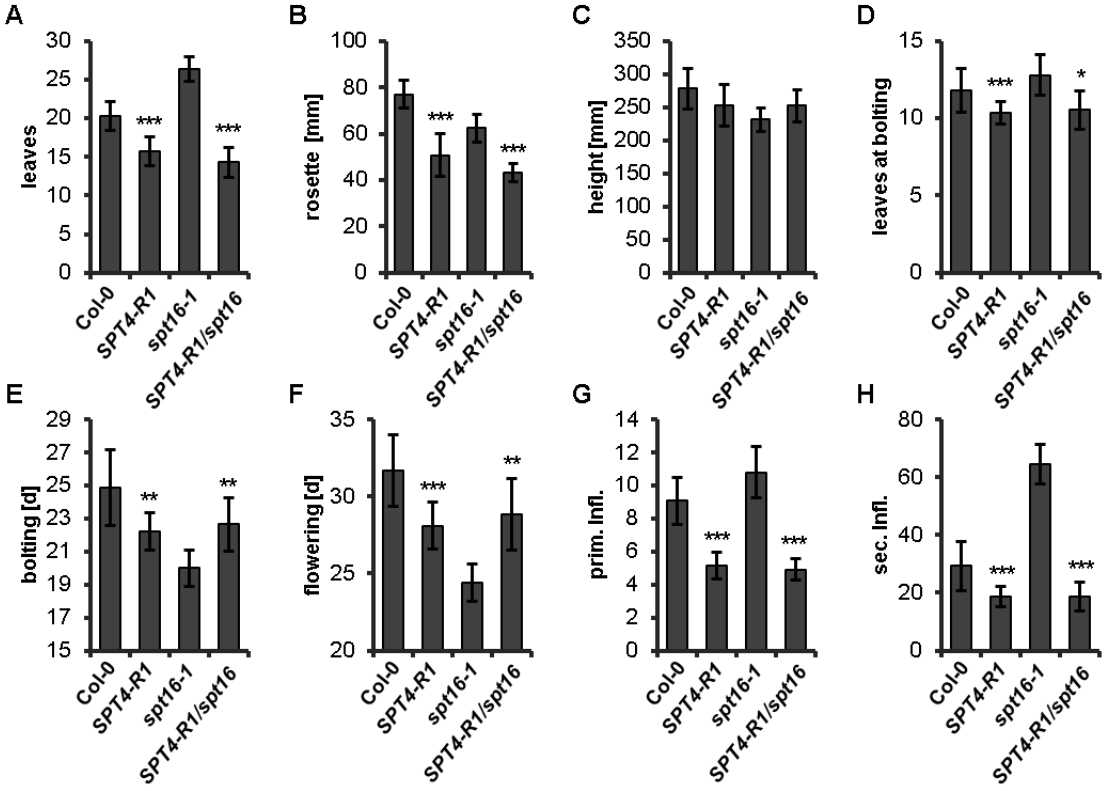

Figure 72. Phenotypic analysis of *SPT4-R1*/*spt16-1* double-mutant plants. (A) The number of leaves 35 DAS, **(B)** rosette diameter 28 DAS, **(C)** height 15 days after bolting, **(D)** number of leaves at bolting, **(E)** bolting time **(F)** flowering time, **(G)** primary inflorescence 15 DAB, and **(H)** secondary inflorescence were analysed using a two-way ANOVA. Error bars indicate SD of at least ten plants. Data sets marked with asterisks show significant differences of the single-mutants to the double-mutant and of the double-mutant to wild-type as assessed by Tukey's multiple comparisons of means test with a 95% family-wise confidence level: * $P < 0.05$, ** $P < 0.01$ or *** $P < 0.001$. The experiment was performed at least two times.

2.11.3 Analysis of *SPT4-R1* and *cbp20* or *cbp80* double-mutants

SPT4/5 has been shown to be involved in post-transcriptional modification of the nascent mRNA (Wen and Shatkin, 1999; Pei and Shuman, 2002; Xiao et al., 2005). The C-terminal region of SPT5 serves as a platform, e. g. for capping enzymes and splicing factors (Schneider et al., 2010). The cap binding complex (CBC) is a heterodimeric complex of the small subunit CBP20 and the large subunit CBP80. CBC binds the 5'-cap of the nascent mRNA and protects it from decapping. The CBC has also been shown to be involved in splicing and mRNA export (Lee et al., 1983; Worch et al., 2005; Balatsos et al., 2006). Mutants of the *Arabidopsis* homologue of CBP20 have a late flowering phenotype, serrated leaves, and is involved in drought tolerance (Papp et al., 2004; Jager et al., 2011). The large subunit CBP80 has been reported to be involved in pre-mRNA and alternative splicing and in processing of microRNAs. Mutants of CBP80 look essentially like *cbp20* and have serrated leaves and a late flowering phenotype (Laubinger et al., 2008; Bush et al., 2009; Raczynska et al., 2010). To gain insight in the genetic interacting of the cap binding proteins CBP20 and CBP80 with SPT4 in *Arabidopsis,* mutants of both *CBP20* and *CBP 80* have been crossed with the *SPT4-R17* line.

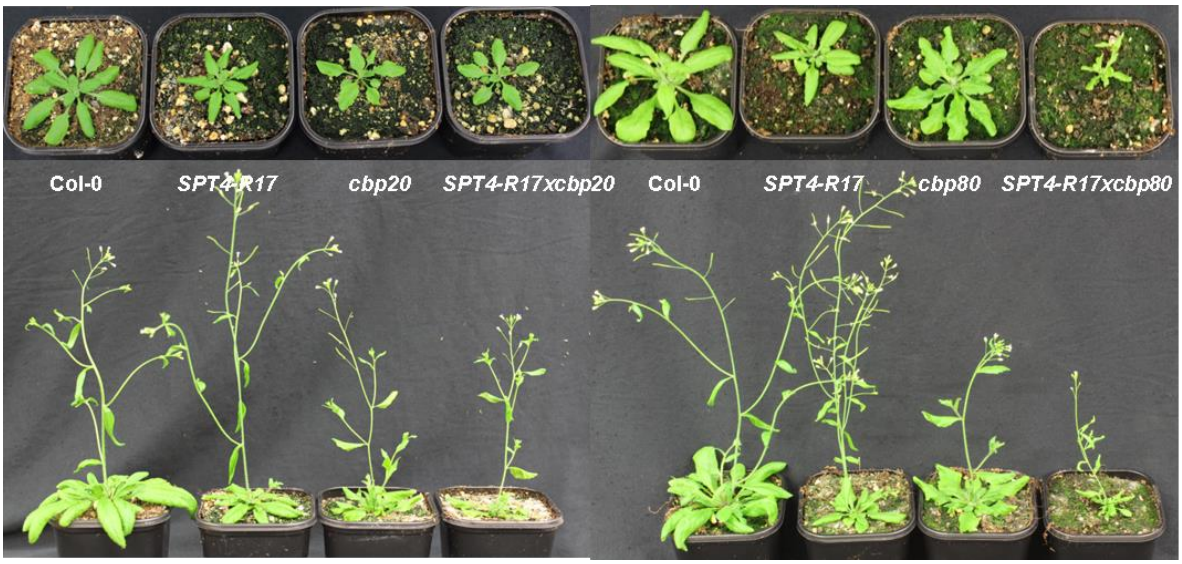

Figure 73. Phenotype of double-mutants of *SPT4-R1* and the cap binding proteins *cbp20* and *cbp80*. Representative individuals, single- and double-mutants of *SPT4* and *CBP20* or *CBP80,* relative to Col-0 (21 DAS top, 35 DAS bottom) are shown.

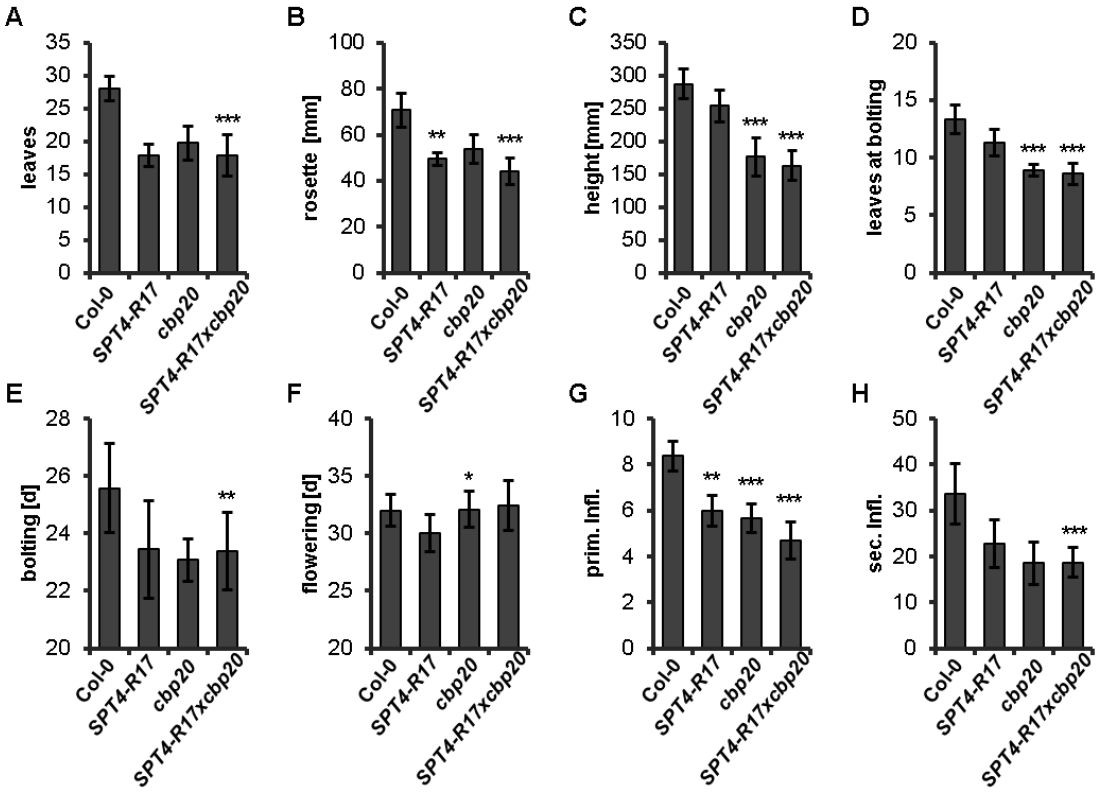

Figure 74. Phenotypic analysis of *SPT4-R17*/*cbp20* double-mutant plants. (A) The number of leaves 35 DAS, **(B)** rosette diameter 28 DAS **(C)** height 15 days after bolting, **(D)** number of leaves at bolting, **(E)** bolting time, **(F)** flowering time, **(G)** primary inflorescence 15 DAB, and **(H)** secondary inflorescence were analysed using a two-way ANOVA. Error bars indicate SD of at least 10 plants. Data sets marked with asterisks show significant differences of the single-mutants to the double-mutant and of the double-mutant to wild-type as assessed by Tukey's multiple comparisons of means test with a 95% family-wise confidence level: * $P < 0.05$, ** $P < 0.01$ or *** $P < 0.001$. The experiment was performed at least two times.

The overall growth of both *SPT4-R17*/*cbp20* and *SPT4-R17*/*cbp80* is reduced compared to the single-mutants and the wild-type (Figure 73). The line *SPT4-R17xcbp20* shows like the *cbp20* single-mutant serrated leaves and late flowering phenotype and is slightly smaller than *cbp20* or *SPT4-R17* (Figure 73). *SPT4-R17xcbp80* in contrast has a severe pleiotropic phenotype with small curled leaves and is clearly smaller than both single-mutants (Figure 73). The detailed phenotypic analysis showed contrary results for *SPT4-R17xcbp20.* In case of leave number, bolting time and secondary inflorescences *SPT4-R17xcbp20* displayed additive effects (Figure 74A, E, H), whereas for primary inflorescences a synergistic effect was observed (Figure 74G). The other analysed traits showed epistatic effects, either resembling the *cbp20* (Figure 74C, D, F), or the *SPT4-R17* phenotype (Figure 74B). The *SPT4-R17xcbp80* double-mutant displayed mainly synergistic (Figure 75B, C, G,

H) or epistatic effects of *CBP80* over *SPT4*, resembling the phenotype of *cbp80* (Figure 75A, F).

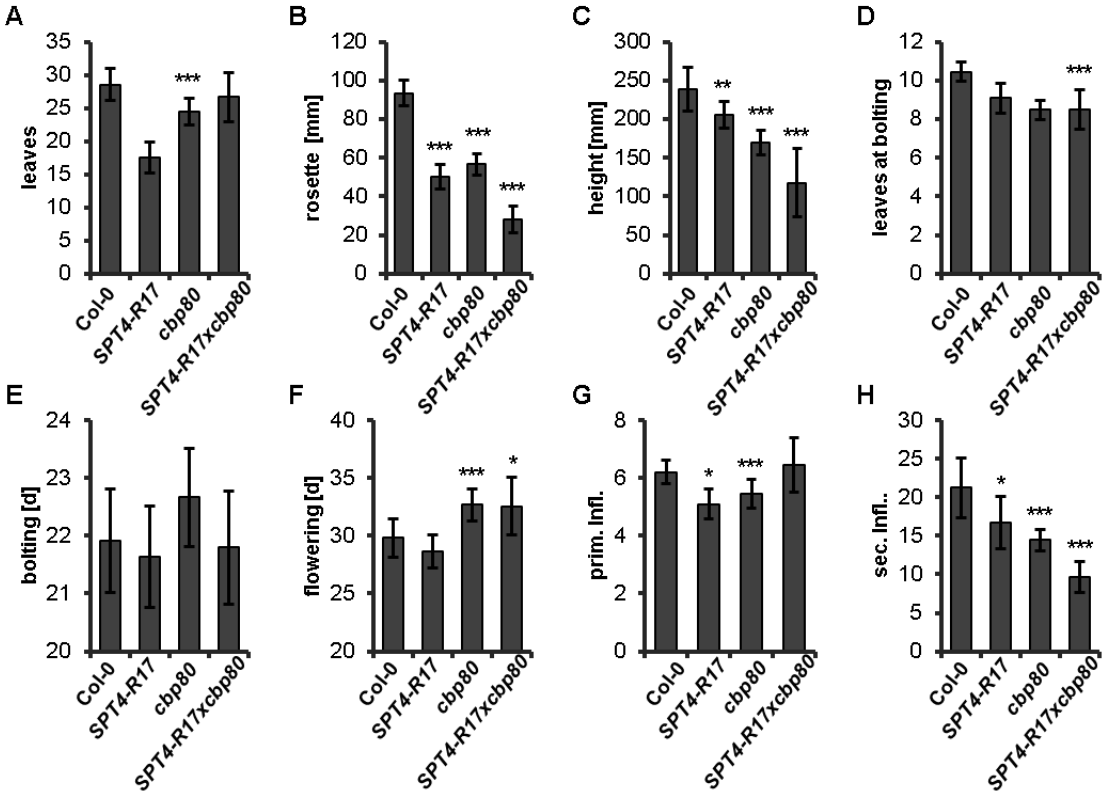

Figure 75. Phenotypic analysis of *SPT4-R17*/*cbp80* double-mutant plants. (A) The number of leaves 35 DAS, **(B)** rosette diameter 28 DAS, **(C)** height 15 days after bolting, **(D)** number of leaves at bolting, **(E)** bolting time, **(F)** flowering time, **(G)** primary inflorescence 15 DAB, and **(H)** secondary inflorescence were analysed using a two-way ANOVA. Error bars indicate SD of at least ten plants. Data sets marked with asterisks show significant differences of the single-mutants to the double-mutant and of the double-mutant to wild-type as assessed by Tukey's multiple comparisons of means test with a 95% family-wise confidence level: * $P < 0.05$, ** $P < 0.01$ or *** $P < 0.001$. The experiment was performed at least two times.

CHAPTER 3

DISCUSSION

3. Discussion

In the last years it became more and more obvious that not only transcription initiation is crucial for regulation of mRNA transcription but that transcription elongation is also a tightly regulated process (Grasser, 2005). The RNA polymerase II itself is regulated by differential phosphorylation of the uniform C-terminal domain. Several transcription elongation factors interact through the CTD directly or indirectly with the transcription elongation complex and thereby regulate the transcription. Three types of transcript elongation factors are known: factors that modulate the activity of RNAP II, factors that modify histones in transcribed regions and factors that facilitate transcription through chromatin (Figure 76).

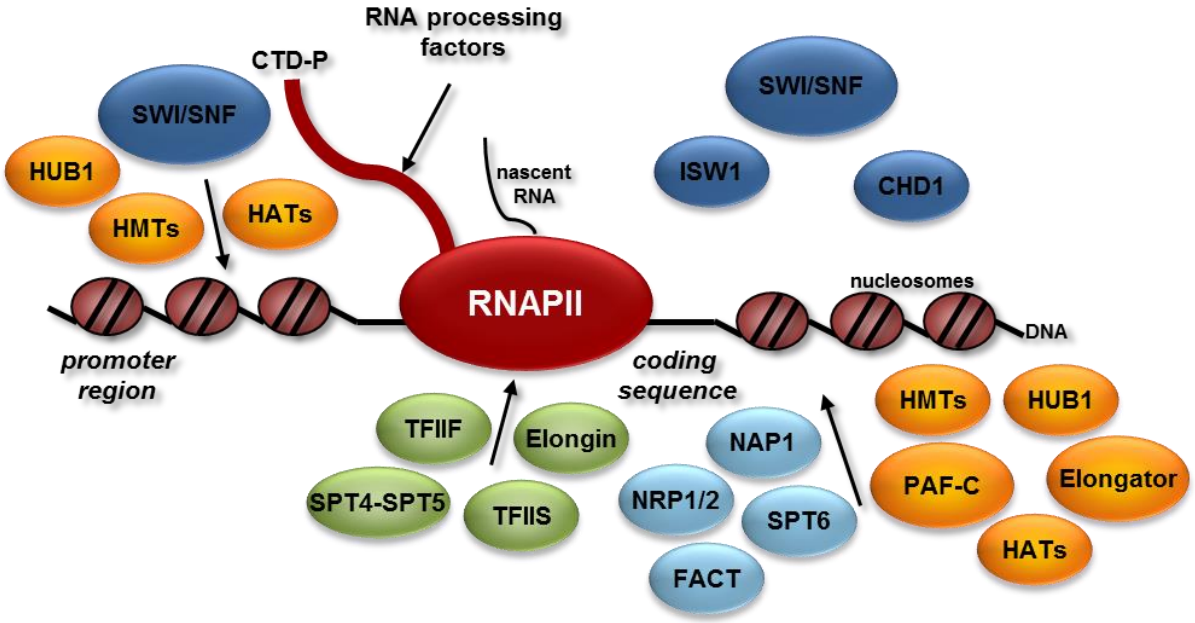

Figure 76. Factors involved in transcription elongation. Factors that modulate the activity of RNAP II (green), that modify histones in transcribed regions (yellow), and that facilitate transcription through chromatin ATP-dependent (dark-blue) and ATP-independent (light-blue) are shown (Grasser, 2005).

The transcription elongation factor SPT4-SPT5 is one of the factors that modulate the activity of RNAPII. SPT4-SPT5 interacts directly with RNAP II and thereby regulates the activity of RNAPII both positively and negatively. From bacteria to human, SPT4-SPT5 has been extensively studied but in plants nothing is known so far (Hartzog and Fu, 2013; Yamaguchi et al., 2013). The aim of this thesis was to identify and characterise orthologs of SPT4-SPT5 in *Arabidopsis*. For both subunits, SPT4 and SPT5, two orthologs were identified in *Arabidopsis*, demonstrating that SPT4-SPT5 is conserved in plants. A third SPT5 protein, SPT5-like (SPT5L), showing minor protein identity with the two other *Arabidopsis* SPT5 proteins, was

also part of this study. The plant specific SPT5L has previously been described in *Arabidopsis* and is involved in the gene silencing pathway RNA-directed DNA methylation. Expression analysis among different tissues showed that one ortholog of both, SPT4-2 and SPT5-2, is ubiquitously expressed in all tested tissues. The other homolog is poorly or not at all expressed in most tissues but highly expressed in stamen and pistils (Figure 13 and Figure 14).

3.1 SPT4-SPT5 in development

SPT5 (NusG in bacteria) has been shown to be essential in most analysed organisms, as knockout of SPT5 are lethal, e. g. in yeast, humans and *Drosophila*. In yeast RNAPII transcription elongation is impaired in different SPT5 mutants (Hartzog et al., 1998; Wada et al., 1998; Kaplan et al., 2000). SPT4 in not essential in yeast, as knockout mutants are viable but its importance in higher eukaryotes has not been clarified (Hartzog and Fu, 2013). To analyse the effects of SPT4 and SPT5 in *Arabidopsis*, different T-DNA insertion alleles of *SPT4* and *SPT5* were analysed in this study. The *spt4-2* T-DNA insertion line showed no pronounced effects on plant growth and development. The plants look essentially like wild-type, leading to the suggestion that SPT4-2 is not essential for viability in *Arabidopsis* as there might be a redundancy with SPT4-1 (Figure 17). Analysis of *SPT4-2* expression in *spt4-2* compared to wild-type showed that no full length but a truncated mRNA is expressed in *spt4-2* in higher amounts as in wild-type. This observation might also favour the idea that a truncated version of SPT4-2 may be sufficient for viability but the existence of a truncated protein was not analysed. Analysing the line *spt4-2*, it cannot be clearly determined if SPT4-2 is essential for viability. No further insertion lines were available for *SPT4-2* or *SPT4-1*, so knockout of these two genes could not be analysed in more detail.

To characterise the function of *SPT5-1* in development, the T-DNA line SAIL_1297_A11 (*spt5-1*) was analysed. The knockout line *spt5-1* looks essentially like wild-type, showing minor developmental differences (Figure 19). It could not be confirmed that the observed phenotypes are due to knockout of *SPT5-1*, as no other independent T-DNA line for *SPT5-1* was available. Complementation of SAIL_1297_A11 was not possible due to unspecific recombination of the complementation construct when transformed into *E. coli*. Even if it cannot be shown

that the observed phenotypes is due to the down-regulation of *SPT5-1* expression, it indicates that *SPT5-1* is not essential as no *SPT5-1* transcript was expressed.

3.1.1 Knockout of *SPT5-2* is embryonic lethal

The knockout of *SPT5-2* has severe effects on development and is embryonic lethal in *Arabidopsis*, as shown with the lines *spt5-2-2*, *spt5-2-3* and *spt5-2-4* (Figure 20). Detailed analysis of the allele *spt5-2-2* showed a normal seed set with almost 100% of the seeds looking fully developed. Germination experiments revealed a germination rate of ~80%, suggesting a developmental defect early in embryonic development before germination and after fertilisation. Similar embryonic lethal phenotypes have been observed for other transcription elongation factors in *Arabidopsis* like SSRP1, a subunit of the chromatin remodelling complex FACT, and SPT6, an ortholog of human SPT6 (Lolas et al., 2010; Gu et al., 2012). Additionally an RNAi approach was utilised to knockdown *SPT5*-2, in order to gain viable plants showing a phenotype. Unfortunately, no plants harbouring the complete *SPT5*-RNAi construct without recombinations under the control of the viral 35S promoter could be identified. A second approach using a amiRNA approach with different sequences was also unsuccessful. In line with the possible lethality of plants harbouring a *SPT5*-RNAi construct is that tetracycline-mediated knockdown of hSPT5 in HeLa cells causes G1 arrest and apoptotic cell death (Komori et al., 2009). In contrast siRNA-mediated depletion of either *SPT4* or *SPT5* in human B-cells reduced IgA class switch recombination without significant cell death (Stanlie et al., 2012). Conclusively the generally expressed SPT5-2 is essential in *Arabidopsis*, which is in line with most of the findings in other organisms (Hartzog and Fu, 2013).

3.1.2 Induced knockdown of *SPT5-2* is viable

To overcome the problem of the embryonic lethality of *spt5-2-2* and the RNAi approach, an inducible RNAi system was utilised to analyse the function of SPT5 in later stages. After induction with β-estradiol the *SPT5*-RNAi construct was expressed in all tissues under the ubiquitous *UBQ10* promoter. A clear down-regulation of *SPT5-2* has been observed in leaves 70 h after application of β-estradiol. Growth on solid MS-Medium with or without β-estradiol showed a drastic growth defect but the plants were viable (Figure 23 and Figure 24). Growth in liquid MS first under non-inducing conditions and later induced with β-estradiol showed also growth defects and reduced fresh weight of 30 to 40% relative to the mock treated control. These

results showed a drastic growth defect of the *SPT5-2* knockdown but in contrast to knockout and permanent knockdown, induced knockdown of SPT5-2 is not embryonic lethal. These results lead to the assumption that SPT5 seems to be essential in the early stages of embryonic development and an inducible knockdown of *SPT5* shows severe growth and developmental defects but is viable until day 14. Later developmental stages have to be analysed but an induction is complicated due to the nature of β-estradiol as it is not transported inside the plant and has to be sprayed. β-estradiol-inducible expression systems have been frequently used to analyse the overexpression of genes that are lethal if constitutively overexpressed (Mehrnia et al., 2013; Takada et al., 2013).

3.1.3 Knockdown of *SPT4* leads to defects in vegetative and reproductive development

3.1.3.1 Vegetative development

Simultaneous down-regulation of *SPT4-1* and *SPT4-2* expression in *Arabidopsis* by RNAi resulted in severe growth defects and the severity correlated with the extent of reduction in *SPT4* transcript levels. The independent *SPT4*-RNAi lines analysed in this thesis study were clearly smaller than wild-type, and showed pleiotropic growth defects both under short and long-day conditions (Figure 26 and Figure 30).

The reduced leave size of *SPT4*-RNAi plants is caused by a reduced number of cells as shown by palisade parenchyma and epidermis cells (Figure 32). Although the cell size is slightly increased in the *SPT4*-RNAi plants, the decreased growth is caused by reduced cell proliferation (Figure 33 and Figure 34). This has been observed in other studies with mutant alleles of genes involved in transcription, e. g. in mutants of the histone monoubiquitinase HUB1 (HISTONE MONOUBIQUITINATION1), an ortholog of yeast BRE1 and mutants of subunits of the Mediator complex (Autran et al., 2002; Fleury et al., 2007). HUB1 promotes H2B monoubiquitination in plants, a posttranslational histone modification, which plays a crucial role in formation of active chromatin (Pavri et al., 2006; Fleury et al., 2007; Lolas et al., 2010). Interestingly, HUB1 was shown to play a role in the regulation of the cell cycle during early organ growth in plants (Fleury et al., 2007). Mutation in the HUB1 gene resulted in a reduction in leaf size caused by a decrease in cell number, proposing a general role for HUB1 as a regulator of cell divisions. HUB1 has also been shown to interact with the Mediator complex (Dhawan et al., 2009). It is

interesting that HUB1 and SPT4 share some of the same cell cycle defect phenotypes, as both SPT5 and HUB1 have shown a functional interplay with the Mediator complex. Mediator has also been shown to regulate the activity of RNAPII (Kremer et al., 2012). The *struwwelpeter* (*swp*) mutant, an ortholog of yeast *MED14* (*Mediator complex subunit 14*), shows reduced cell numbers in all aerial organs, and this defect is partially compensated by an increase in final cell size in *Arabidopsis* (Autran et al., 2002). The proliferation defect shown in *SPT4*-RNAi leaves could also been observed in roots. Root growth is determined by the balance between cell division and cell elongation (Beemster and Baskin, 1998). To assess the role of SPT4 in root growth, the length and the number of cells in the meristematic zone was measured. This analysis showed that the meristematic zone in *SPT4*-RNAi roots is smaller and exhibits less cells compared to wild-type. This indicates that *SPT4*-RNAi exhibits a cell cycle deficiency (Figure 35). Possible effects of *SPT4* knockdown on the cell cycle were studied by analysing the expression of the CYCB1;1-GFP under its native promoter (Colon-Carmona et al., 1999). CYCB1;1-GFP allows the visualization of cells at the G2-M phase of the cell cycle. The number of GFP-stained cells was significantly reduced in *SPT4*-RNAi plants when compared with the wild-type (Figure 36), which could reflect a slower progression and/or a delayed G2/M transition of the cell cycle. The observed phenotypes in *SPT4*-RNAi mutants therefore suggest that SPT4-SPT5 plays a role in promoting normal cell proliferation, showing a defect in the cell cycle. The mentioned factors are all involved in promoting productive transcription in *Arabidopsis* or other organisms by either modulating the activity of RNAP II (SPT4-5, Mediator), or modifying histones in transcribed regions (HUB1).

The intrinsic leaf size is determined by the number of cells produced by cell division activities during the early stages of primordium. In line with the reported defects in HUB1 and Mediator, in *SPT4*-RNAi plants the cell division rate was severely reduced during the early stage of leaf development possibly due to a block at the G2/M transition. To clarify this, the ploidy level *SPT4*-RNAi compared to wild-type has to be measured. Although the primary cause of *SPT4*-RNAi phenotypes was due to the reduction of the cell division rate, SPT4 rather represents a regulator higher upstream connected with its proposed function in allowing processive transcription. The knockdown of *SPT4* might lead to an alteration of the expression of genes involved in cell cycle progression and coordination of growth in multiple organ

types, as several genes involved in the cell cycle are down-regulated in the microarray experiment.

3.1.3.2 Reproductive development

Besides vegetative development, the *SPT4*-RNAi plants exhibit strong alterations in the development of reproductive organs, resulting in smaller size and reduced fertility (Figure 37 and Figure 38). The reduced size of the floral organs correlates with the overall reduced growth, whereas the reduced fertility might be due to the alteration of floral organ size or defects in egg cell development, as the pollen seems to be viable, shown by Alexander stain (Figure 39). The reduced size of the filaments combined with reduced size of the anthers and a reduced amount of pollen might lead to a reduced number of pollinations and thereby to a reduced fertility. The defects in flowering and reproduction might also be due to defects in the cell cycle, as reproductive defects are also known for the mentioned HUB1 mutant and other mutants of factors involved in transcription, e. g. mutants of both subunits of the FACT complex, SPT16 and SSRP1 (Fleury et al., 2007; Lolas et al., 2010)

SPT4-RNAi plants flowered late under short day conditions but no significant difference has been observed under long day conditions. In *Arabidopsis*, the transition to flowering stage is controlled by four major pathways, the autonomous, vernalisation, gibberellic-acid-dependent and LD pathways. FLOWERING LOCUS T (FT) integrates outputs of the photoperiodic pathway, the autonomous, and vernalisation pathways. The transcriptional regulator FLOWERING LOCUS C (FLC), which is a central player in the *Arabidopsis* floral transition, represses expression of FT in the leaf (Sheldon et al., 1999). In *SPT4*-RNAi plants FLC expression was not altered (Data not shown). Another endogenous signal affecting flowering time in *Arabidopsis* is gibberellic-acid. Gibberellic-acids are plant growth regulators, which can act directly at the level of meristem identity genes to induce flowering. In *Arabidopsis*, gibberellins are dispensable for flowering under LD, but essential under SD conditions (Zeevaart, 2008). Although an involvement of the *SPT4*-RNAi mutants in gibberellin pathways has not been studied in this thesis, the mutant phenotype indicates that this could be an area of interest for further studies.

3.2 Genome-wide expression analysis of *SPT4*-RNAi mutants

Genome-wide microarray experiments were performed on wild-type and *SPT4*-RNAi to gain insights into the molecular mechanisms of the observed phenotypes. The transcript profiling experiment revealed that the expression of only a small proportion (~5.1%) of the genes was altered more than 2-fold. The role of SPT4 in global gene expression has not been analysed in other organisms up to date, whereas global gene expression of SPT5 has been examined by genome-wide transcript profiling in zebrafish and in HeLa cells. Both studies revealed that a relatively small number of genes were differentially expressed in the samples depleted in SPT5, for instance in zebrafish only <5% of the genes were affected. In HeLa cells the misregulated genes participated mainly in transcription related processes, whereas in zebrafish the expression of genes involved in diverse biological processes from stress response to cell fate specification is affected (Krishnan et al., 2008; Komori et al., 2009). Similarly, the transcript levels of only a relatively small proportion of genes were affected in *Arabidopsis* mutants of TFIIS and Elongator. (Grasser et al., 2009; Wang et al., 2013).

In contrast, genome-wide chromatin association studies in yeast imply that transcription elongation factors are found at all genes during transcription (Mayer et al., 2010). An explanation for the contradictory finding that only a subset of genes is incorrectly expressed in the absence of a certain TEF, like SPT5 directly before apoptosis in HeLa cells, indicates that a number of genes appear to be more sensitive to the loss or depletion of a specific TEF (Grasser, 2005; Yamaguchi et al., 2013). Transcript elongation is a non-uniform process as many factors are involved, therefore the comparison of elongation rates of different genes show a degree of nonuniformity (Palangat and Larson, 2012). Currently, it is still poorly understood to which extent different characteristics of a gene like DNA sequence, inducibility, expression level, RNAPII density, chromatin structure, and co-transcriptional mRNA processing determine RNAPII elongation, or which transcript elongation factors are required for productive transcription elongation (Perales and Bentley, 2009; Palangat and Larson, 2012; Danko et al., 2013).

Most likely the down-regulation of SPT4 or other factors involved in promoting processive transcription elongation results in the misregulation of certain genes. This misregulation then leads to the development of a phenotype different from wild-type

when the expression of critical genes of a certain pathway is affected to a crucial amount.

3.3 Possible involvement of SPT4 in pathogen response

Gene ontology (GO) analysis of misregulated genes in *SPT4-R3* plants showed a noticeable enrichment in the functional categories related to pathogen response, which could be confirmed by qRT-PCR (Figure 42). This has led to the suggestion that the SPT4-SPT5 complex might have a role in regulating plant pathogenesis response genes. Higher plants defence barriers mainly rely on innate immune systems counteracting microbial infection (Berr et al., 2012). The response is triggered by receptors recognising pathogen-related patterns like proteins, lipopolysaccharides or cell wall components, including a signalling pathway involving the hormones salicylic acid (SA), jasmonic acid (JA) and ethylene (ET), which finally activate transcription of defence genes, like the *Pathogenesis-Related* (*PR*) genes (Dong, 2004; Jones and Dangl, 2006; Verhage et al., 2010). Recently chromatin remodelling and histone modification gained interest as potential transcriptional regulators of plant innate immunity. Mutants of the histone deacetylase STR2 and the ATP dependent chromatin remodelling complex SWR1-like have been shown to be more resistant to pathogens, whereas mutants of the H2B ubiquitin-ligase HUB1 and ATP dependent chromatin remodelling complex SYD (SPLAYED) exhibited a higher sensitivity upon pathogen infection (March-Diaz et al., 2008; Walley et al., 2008; Dhawan et al., 2009; Wang et al., 2010; Berr et al., 2012). Together with these findings our data suggests reduced pathogen susceptibility in the line *SPT4-R3*. Even though it has to be proven by pathogen infection experiments, this observation suggests that chromatin remodelling and also general transcription factors may play a more pronounced role in regulating *Arabidopsis* defence response.

3.4 SPT4 is involved in auxin response

The microarray and subsequent GO analysis of the *SPT4*-RNAi plants indicated that genes involved in auxin signalling were over-represented among the down-regulated genes in *SPT4-R3*. Most striking was the down-regulation of *Aux/IAA* genes (Figure 43).

The plant hormone auxin plays a central role in plant development. The predominantly occurring form, indole-3-acetic acid (IAA), regulates cell division, cell elongation and triggers differentiation events leading to diverse developmental processes. A few examples are the establishment of embryo polarity, vascular differentiation, apical dominance and tropic responses to light and gravity (Woodward and Bartel, 2005; Hayashi, 2012). Auxin responses are regulated at three major steps: auxin metabolism, directional auxin transport, and signal transduction (Benjamins and Scheres, 2008; Chapman and Estelle, 2009).

3.4.1 Auxin biosynthesis and transport

Auxin synthesis is dependent on tryptophan and Cytochrome P450 and the *YUCCA* gene have both been suggested to be involved in auxin biosynthesis (Zhao et al., 2002; Cheng et al., 2006b, 2007). Not only biosynthesis itself is important but also modifications because only 1% of total auxin is present as free auxin, whereas the remaining part is conjugated to amino acids and sugars (Ouyang et al., 2000; Zazimalova and Napier, 2003). The regulation of auxin likely depends on the hydrolysis of those conjugated auxin forms (Benjamins and Scheres, 2008).

Important for the role of auxin in development is its temporal and spatial distribution in the plant. Long distance transport of auxin is mediated in the phloem, whereas for short distances the polar transport is mediated by carrier proteins (Hayashi, 2012). Auxin is a weak acid and can therefore freely enter the cell but is then trapped inside the cell because of its protonation. Specific auxin efflux carriers are necessary to transport auxin out of the cell (Rubery and Sheldrake, 1973). Three families of proteins are involved in auxin transport, the PIN FORMED (PIN) and MULTIDRUG RESISTANCE (MDR)–p-glycoprotein (PGP) family of auxin efflux carrier and auxin influx carrier of the AUXIN RESISTANT1 (AUX1) family (Bennett et al., 1996; Friml et al., 2003; Reinhardt et al., 2003; Paponov et al., 2005; Swarup et al., 2005).

3.4.2 Auxin signalling

The expression analysis of *Aux/IAA* genes revealed that a significant part of the auxin inducible *Aux/IAA* genes were down-regulated in *SPT4-R3* (Figure 43). In contrast, the expression of *IAA17*, which has been reported to be insensitive upon auxin treatment, was not altered within the *SPT4*-RNAi lines (Figure 44). The gene families *AUXIN/INDOLE ACETIC ACID* (*Aux/IAA*) and *AUXIN RESPONSE FACTOR*

(*ARF*) are the best studied factors involved in auxin signalling (Figure 77). *Aux/IAAs* are primary auxin response genes and most of them are rapidly up-regulated by auxin application. The *Arabidopsis* genome contains 29 *Aux/IAA* genes and the encoded proteins comprise four conserved domains (Hagen and Guilfoyle, 2002). Domain II is target for ubiquitination followed by degradation by the 26S proteasome, domain III is supposed to exert repressor function and mediates together with domain IV homodimerisation or heterodimerisation with ARF proteins (Abel et al., 1994; Ulmasov et al., 1997b). The interaction of Aux/IAAs with ARFs leads to the repression of the ARF function. 23 ARF are encoded in the *Arabidopsis* genome, which exert an N-terminal DNA-binding region. This domain is necessary for binding to so called auxin response elements (AuxRE) in promoter sequences. Depending on the type of ARF they can act as transcriptional repressor or activator (Ulmasov et al., 1997a; Luerssen et al., 1998).

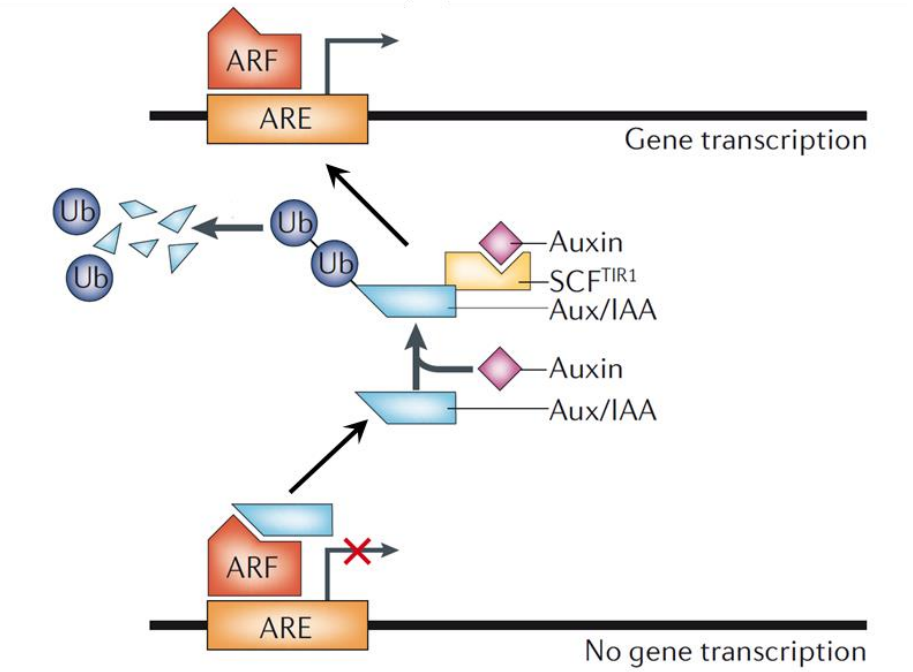

Figure 77. Auxin signal transduction pathway. Aux/IAA transcriptional repressors are bound to the corresponding ARF (auxin response factor) transcription factor, and target genes of auxin remain switched off. When auxin (pink) binds to the TIR1 auxin receptor, TIR1 interacts with Aux/IAA proteins, which leads to ubiquitination and degradation of Aux/IAAs by a SCFtype E3 ubiquitin ligase. When Aux/IAA proteins bind to auxin-modified TIR1/AFBs, the ARF transcription factor is no longer repressed, resulting in the expression of target genes (Teale et al., 2006).

Specific pairs of Aux/IAAs and ARFs are suggested to determine auxin dependent developmental processes. A well-characterised example for such a pair is the auxin response factor MONOPTEROS (ARF5) and its corresponding Aux/IAA protein BODENLOS (IAA12), which are crucial for embryo pattern formation (Przemeck et

al., 1996; Weijers et al., 2005). The degradation of Aux/IAAs is mediated by TRANSPORT INHIBITOR RESISTANT 1 (TIR1) or another member of the family, which are subunits of a Skp1-Cullin-F-box (SCF) class E3 ubiquitin ligase complex (Kepinski and Leyser, 2004; Dharmasiri et al., 2005). Auxin promotes the interaction of TIR1 and Aux/IAA proteins by binding to TIR1 and enhancing the affinity to its Aux/IAA substrate (Tan et al., 2007). The high number of Aux/IAAs, ARFs and homologs of TIR1 provides an enormous range of transcriptional regulators with potentially distinct specificities, although it is still unclear to which extent these protein interactions occur in the plant (Guilfoyle and Hagen, 2012). However, in SPT4-RNAi plants not only the transcript levels of auxin-inducible *Aux/IAA*s were down-regulated, but also their inducibility by IAA was affected (Figure 45). Leading to the suggestion that the knockdown of SPT4 affects expression of only a subset of *IAA*s, this may be due to the nature of the auxin inducible IAA, as their expression is rapidly changed upon auxin treatment.

3.4.3 Auxin in leaf vascular development

The microarray analysis of the *SPT4*-RNAi line 3 showed that a high proportion of auxin-related genes were misexpressed compared to wild-type. Therefore, the venation patterning was analysed, showing a severe venation pattern defects from cotyledons to third leaves and also in sepals and petals of flowers (Figure 47 and Figure 48). Aerial organs such as leaves and flowers are generated by the shoot apical meristem. Auxin and especially auxin transport has been shown to be involved in the formation of plant organs and also the leaf vasculature. The organ initiation starts with a local auxin maximum, which induces polar transport leading to canalisation of the auxin flow along a narrow column of cells.

The defects in vascular and root (3.4.4) development are probably also due to a reduced cell proliferation rate. Auxin promotes cell division by providing the necessary competence to enter into the cell cycle. Auxin acts on multiple targets, influencing directly or indirectly both transcription and post-transcriptional regulation (Redig et al., 1996; Perrot-Rechenmann, 2010). Auxin is important for the activity of certain cyclin-dependent kinases (CDK) involved in the cell cycle, and AuxREs can be found in promoter region of various cyclins suggesting that they are primary auxin responsive genes (Harashima et al., 2007; Perrot-Rechenmann, 2010). Little is known about the involvement of *Aux/IAA* or *ARF* genes, also because the Aux/IAAs seem to be redundant and knockout mutants of several *Aux/IAAs* show no distinct

phenotype. In contrast, gain-of-function mutants of *Aux/IAA* display pleiotropic phenotypes, e. g. defects in cell division (Overvoorde et al., 2005; Peret et al., 2009). The reduced transcript levels of *Aux/IAA* genes in *SPT4*-RNAi plants most likely result in lower Aux/IAA repressor levels that may cause elevated activity of activating ARFs. In agreement with that, enhanced auxin response was visualised in leaves of *SPT4*-RNAi plants using the *DR5-GUS* reporter. Recently, a gain-of-function mutant of *MONOPTEROS* (*MO*) uncoupled from regulation by Aux/IAA proteins has been identified, displaying a number of semi-dominant traits affecting auxin signalling and organ patterning, e. g. defects in the differentiation of vascular tissue (Krogan et al., 2012). Theoretically a gain-of-function *ARF* mutant would correspond to a loss-of-function *Aux/IAA* mutant. As several *Aux/IAA* have been shown to be down-regulated in the *SPT4*-RNAi mutants and the vascular patterning phenotype correlates with the MO gain-of-function, this observed vascular patterning phenotype in *SPT4*-RNAi plants might be triggered by the alteration in *Aux/IAA* expression.

In line with *SPT4*-RNAi mutants similar results have been shown in mutant plant of ELO3, a subunit of the histone acetlytransferase complex Elongator, showing a defective venation patterning with disconnected primary loops and reduced secondary and tertiary veins. Several *Aux/IAA* were down-regulated in the *elo3* mutants and the down-regulation was related to reduced acetylation levels of histone H3K14 in their promoter and/or coding regions, a marker for active genes (Nelissen et al., 2010).

3.4.4 Auxin in root development

SPT4-RNAi plants exhibit also defects in root development and the reduced levels of Aux/IAA may cause this defect (Figure 49 and Figure 50). As in leaf development, regional auxin gradients and local maxima are crucial for establishing the root primordia (Benjamins and Scheres, 2008). As auxin is mainly produced in apical part, it has to be transported to the root mediated by the phloem, where structured auxin maxima are established by the auxin efflux carrier of the PIN family and the auxin influx carrier of the AUXIN1/LIKE AUXIN1 (AUX1/LAX) family in sink tissues (Sabatini et al., 1999; Grieneisen et al., 2007; Petersson et al., 2009; Vanneste and Friml, 2009). Also for the development of lateral roots, an auxin maximum is necessary, whereas the auxin for the establishment of the lateral root primordia is also synthesised in the root (Benkova and Hejatko, 2009). The analysis of the expression level of the *AUX1/LAX* influx carrier in *SPT4-R3* mutants showed reduced level of

AUX1 and *LAX3* expression in the roots. Both *AUX1* and *LAX3* are involved in lateral root development and emergence, whereas *AUX1* is also involved in root gravitropism response. LAX1 and LAX2 seem to be redundant with AUX1, as single- and double-mutants show no root related effects and triple-mutants with AUX1 display the *aux1* phenotype (Swarup et al., 2008; Peret et al., 2012). This finding suggests that the misregulation of *AUX1* and *Aux/IAA*s might explain the gravitropism defects of *SPT4-R3*, and together with the misregulation of *LAX3* it might be the cause for the reduced number of lateral roots and the lower lateral root density. Experiments with exogenously applied auxin showed that *SPT4*-RNAi plants are more sensitive, as the root elongation rate of the *SPT4*-RNAi plants relative to Col-0 is decreased by IAA. This is in agreement with the suggestion that *SPT4*-RNAi exhibits lower levels of the Aux/IAA repressors compared with wild-type, which are destabilised upon auxin treatment. The finding leads to the suggestion that the misexpression of Aux/IAA repressors and *AUX1/LAX* influx carrier in *SPT4*-RNAi plants is one major reason for the observed auxin-related phenotypes.

In addition to SPT4-SPT5, several other *Arabidopsis* chromatin factors were identified that affect auxin signalling, raising the possibility that auxin-related gene expression is particularly sensitive to misregulation of transcript elongation in the chromatin context. The chromatin remodelling factor PICKLE is involved in IAA14-mediated repression of ARF7/19 in lateral root initiation (Fukaki et al., 2006). Aux/IAA expression and auxin signalling was perturbed in mutant plants affected in SDG2, a histone methyltransferase that catalyses H3K4 trimethylation (Yao et al., 2013). The chromatin factor PROPORZ1 is required for acetylation of accurate H3K9/14 within promoter and transcribed region at auxin-controlled loci (Anzola et al., 2010). Both H3K4me^3 and H3K9/14ac are histone mark characteristic of transcribed genes.

3.5 Interactions of SPT4 with SPT5 and as complex

A physical interaction of the two subunits of the heterodimeric transcription elongation factor SPT4-SPT5 has been shown in various organisms but not in plants so far. Besides the direct interaction in a complex, SPT4-SPT5 interacts physically or genetically with other general transcription factors, histone modifying proteins, and pre-mRNA processing factors like the capping enzymes, or splicing factors, to only mention a few (Hartzog and Fu, 2013; Yamaguchi et al., 2013). A direct interaction of

SPT4 and SPT5 has been shown by affinity purification from suspension cultured cells transformed with GS-tagged SPT4-2, which resulted in efficient co-purification of SPT5-2 (Figure 56). This finding strongly indicates that the SPT4-SPT5 heterodimer occurs *in planta*.

Interestingly, also SPT5L has been identified as interactor of SPT4-2 (Figure 56 and Table 2). SPT5L is a chromatin-associated protein implicated in siRNA mediated RNA-directed DNA methylation (Bies-Etheve et al., 2009; He et al., 2009; Rowley et al., 2011). SPT5L displays only limited protein identity to SPT5 (17.9% with SPT5-2 and 16.5% with SPT5-1), but the two proteins show high identities in the NGN domain (49.4% with SPT5-2), which mediates the interaction between SPT5 and the NGN-binding domain of SPT4. Additionally, both proteins share the conserved glutamate which has been shown to be crucial for SPT4-SPT5 interaction (Guo et al., 2008). Therefore, an interaction between SPT4 and SPT5L is not unexpected but in view of the three-dimensional structure of the RNAPII-SPT5NGN-SPT4 complex it is unlikely that SPT5 and SPT5L are found in the same complex (Klein et al., 2011; Martinez-Rucobo et al., 2011). One would rather expect that the two proteins occur in different complexes, which would be in agreement with the different mechanisms, in which SPT5 and SPT5L appear to be involved in. A further hint for an *in vivo* interaction of SPT4-2 with SPT5L is the finding that also AGO4, which has been shown to be involved in siRNA mediated RNA-directed DNA methylation and physical interacts with SPT5L, has also been co-purified.

However, although SPT4 is overexpressed in the cell suspension culture, no outstanding protein band for SPT4-GS is visible on Coomassie stained gels of total proteins extracts (Figure 56). Due to the nature of the experiment it shows no direct interaction, therefore direct interactions of SPT4 and SPT5 were analysed with another method, *in vitro* GST-pull-downs. These results confirmed interaction of SPT5 and SPT4 shown by the GS-pull-downs, demonstrating that SPT4 interacts with the N-terminal parts (including their NGN domains) of SPT5 and SPT5L. (Figure 57). In further experiments it will be attractive to elucidate whether SPT4 in combination with SPT5L plays a role in gene silencing.

Additionally the two largest subunits of RNAPII (NRPB1, NRPB2) were co-purified with SPT4-2 (Table 2). Based on structural studies in archaea NRPB1 would be expected to be linked to SPT4 indirectly via the NGN domain of SPT5 (Martinez-Rucobo et al., 2011; Martinez-Rucobo and Cramer, 2013). Moreover, a subunit of the

TEF complexes CCR4-NOT and two subunits of the Elongator complex were found to elute reproducibly with SPT4-GS (Table 2). CCR4-NOT is targeted to the coding region of genes in a transcription-dependent manner similar to RNAPII, and in yeast promotes elongation by interacting directly with elongating RNAPII (Liang et al., 2009; Kruk et al., 2011). The Elongator complex was identified as a histone acetyltransferase complex that activates RNAPII-mediated transcription in yeast and is also well characterised in plants (Otero et al., 1999; Wittschieben et al., 1999; Nelissen et al., 2005; Nelissen et al., 2010). A direct interaction of SPT4-SPT5 with Elongator is supported by the speculation that SPT4-SPT5 serves as a platform for the recruitment of histone modifiers and thereby contributing to productive elongation, as e. g. a direct interaction of the Paf1 complex to SPT5-CTR has been shown in yeast (Squazzo et al., 2002; Hartzog and Fu, 2013). An interaction with CCR4-NOT and Elongator directly or indirectly through RNAPII with SPT4-SPT5, seems to be likely even though it has neither been observed in *Arabidopsis* nor in other organisms, as they are both involved in RNAPII mediated transcription elongation.

3.6 SPT4-SPT5 localisation to chromatin

To analyse the function of SPT4-SPT5 in transcription, the sub-cellular localisation was analysed. Typical for a transcription elongation factor that facilitates transcription by RNAPII, SPT5 localises to the transcriptionally active euchromatin in *Arabidopsis* nuclei and not within heterochromatic regions (Figure 59 and Figure 60). Interestingly, SPT4 was found not only in the nucleus but also in the cytoplasm (Figure 58), which contrasts the observation in humans and yeast, where localisation is restricted to the nucleus (Hartzog et al., 1996; Huh et al., 2003). The cytoplasmic localisation could also be due to the overexpression of SPT4-GFP or the instability of the fusion protein. Immunostaining experiments with SPT5 antibody and an antibody against the non-phosphorylated form of the RNAPII CTD showed a partial co-localisation of both (Figure 59), which was analysed in more detail by super-resolution microscopy (Figure 60). These analyses showed a co-localisation with RNAPII, which is independent from the phosphorylation status of RNAPII CTD. SPT5 more clearly co-localises with the transcribing RNAPII phosphorylated at Ser2 within the CTD repeats, compared with the non-phosphorylated RNAPII. This nuclear

localisation of SPT5 was also described in *Drosophila*, yeast and human (Yamaguchi et al., 1999a; Kaplan et al., 2000; Huh et al., 2003).

3.7 SPT5 localises to transcribed regions

A side specific localisation study of SPT5 to specific genes was performed by chromatin immunoprecipitation (ChIP) in *Arabidopsis* seedlings. The ChIP experiments revealed that SPT5 associates with the entire RNAPII-transcribed regions of At3g02260 and At1g48090 but not with an intergenic region or the non-transcribed gene *DOG1*. SPT5 appeared to be enriched towards the 3´ end of the transcribed region of At3g02260 and At1g48090 (Figure 62). These findings are partly in line with genome-wide chromatin occupancy experiments of the transcription machinery in yeast (Mayer et al., 2010), which showed that SPT4 and SPT5 association is enriched towards the 3´ end of transcribed regions, like for At3g02260 and At1g48090 but displays also a peak at the 5´ end of the transcription units, which has not been observed for At3g02260 and At1g48090. To further evaluate an involvement of *Arabidopsis* SPT4-SPT5 in transcription elongation, the association of SPT5 to chromatin was analysed comparative in *SPT4-R3* and Col-0 plants. This comparison showed increased levels of SPT5 at transcribed regions in *SPT4-R3* compared to Col-0 at At3g02260 and At1g48090, and also in the 5' region of several *Aux/IAA*s (*IAA1*, *IAA19* and *IAA29*) that are down-regulated in *SPT4-R3* (Figure 63). The increased levels of SPT5 at transcribed regions in *SPT4-R3* indicate a lower activity of SPT5 in promoting transcription elongation due to the reduced level of SPT4, as more SPT5 is associated along transcribed regions suggesting a reduced RNAPII processivity, which has also been observed in other organisms. In yeast SPT4 depletion leads to reduced RNAPII processivity (Mason and Struhl, 2005). Additionally a decreased transcript elongation rate was observed in a *spt5* mutant, which may be related to a function of SPT4-SPT5 in facilitating RNAPII transcription through triggers of transcriptional pausing such as nucleosomes by the recruitment of factors that modify histones (Quan and Hartzog, 2010).

Besides SPT5, also the occupancy of the elongating forms of RNAPII, phosphorylated at Ser5 and Ser2 of the CTD, were analysed by chromatin immunoprecipitation. The ChIP experiments showed an enrichment of the Ser5 phosphorylated form at the 5' region, whereas the Ser2 phosphorylated form was

enriched at the 3’ region of the transcribed unit (Figure 64). This pattern was observed at long genes as well as at three different *Aux/IAA*s in wild-type, correlating with previous studies in other organisms (Mayer et al., 2010). A similar pattern of RNAPII association has also been observed in *Arabidopsis* at genes of plant stress memory responses, and genes which are regulated by the *Arabidopsis* thrithorax-like protein ATX1, a histone methyltransferase (Ding et al., 2011; Ding et al., 2012). In these studies, an induction of transcription of several genes led to an increase of association of RNAPII Ser5P and Ser2P forms to the transcribed regions, whereas a transcriptional repression led to a decrease of RNAPII association. Comparison of the RNAPII levels associated to chromatin in *SPT4-R3* and wild-type revealed elevated levels of both Ser5P and Ser2P RNAPII at the coding region of the two long genes in *SPT4-R3*, whereas at the three tested *Aux/IAA*s only the Ser5P form was enriched at the 5’ region (Figure 65).

The enrichment of RNAPII along transcribed regions, which has been observed in *SPT4-R3*, has been suggested in other organisms as defects in transcript elongation such as decreased elongation rates (Saunders et al., 2006; Palangat and Larson, 2012). The differences in RNAPII association show in line with the microarray experiments and the observations for other TEFs that although SPT4-SPT5 is a general transcription factor. its impact on the transcription of genes is not uniform (Grasser, 2005; Wang et al., 2013). In line with yeast, *Drosophila*, and zebrafish, the ChIP experiments indicate that decreased levels of SPT4 cause transcript elongation defects also in *Arabidopsis*, as evident from the enhanced RNAPII (and SPT5) density within transcription units (Hartzog et al., 1998; Wada et al., 1998; Kaplan et al., 2000; Chen et al., 2009). A possible explanation for enriched SPT5 and phosphorylated RNAPII at transcribed regions in *SPT4-R3* may be a reduction in the processivity of RNAPII. The reduced level of SPT4 may lead to a reduction of SPT5 activity in promoting productive elongation and this in turn may then slow down transcribing RNAPII. An equal rate in transcription initiation in *SPT4-R3* and wild-type and a reduced processivity with a lower RNAPII transcription rate may cause elevated level of RNAPII at transcribed regions.

The high level of Ser5 phosphorylated RNAPII with *SPT4-R3* compared to wild-type at the 5’ region of the three tested *Aux/IAA*s might be an indication for enhanced transcriptional stalling with *SPT4-R3* because of reduced activity of SPT4-SPT5 due to the strongly reduced levels of SPT4. The enhanced level of RNAPII-Ser5P at the

5’ region compared to the 3’ region in *SPT4*-R3 is not seen at At3g02260 and At1g48090, which leads to the suggestion that it only occurs at a subset of genes, or that the effect of SPT4-SPT5 is only crucial at a specific subset of genes, e. g. the *Aux/IAA* genes, which expression can be rapidly altered by auxin. Stalling of RNAPII at a specific subset of genes has been suggested previously in *Arabidopsis* on drought responsive genes (Ding et al., 2012).

3.8 Double-mutants analysis

Double-mutants in this study have been created to analyse possible genetic interaction. The double-mutant phenotype can be considered as: (i) additive, when it exhibits a combination of traits present in the single-mutants; (ii) epistatic, when it resembles the phenotype of one of the single-mutants, but not the other; (iii) suppressed, when it is closer to the wild- type condition than either of the single-mutants; or (iv) synergistic, when the double-mutants phenotype made by both mutations is greater than the sum of their individual phenotypes (Pérez-Pérez et al., 2009).

3.8.1 Analysis of *SPT4-R1/tfIIs-1* double-mutants

SPT4-SPT5 has been shown to interact genetically with *TFIIS* in yeast, as *spt4* and *spt5* mutations exhibited enhanced growth defects when combined with mutations in elongation factor TFIIS. TFIIS functions in rescuing RNAPII from transcription arrest suggesting that they are both required to overcome pausing during elongation (Hartzog et al., 1998; Lindstrom and Hartzog, 2001; Fish and Kane, 2002). In contrast to yeast, no synergistic effects were observed in *SPT4-R1/tfIIs-1* mutant plants. The double-mutant displayed epistatic effects between *TFIIS* and *SPT4* regarding vegetative growth whereas additive effects were observed for reproductive traits (Figure 67 and Figure 68). In yeast and *Arabidopsis* the lack of TFIIS has only minor effects on development, whereas disruption of TFIIS in mice leads to embryonic lethality (Malagon et al., 2004; Ito et al., 2006; Grasser et al., 2009). The results observed by phenotypic analysis of *SPT4-R1/tfIIs-1* lead to the suggestion that SPT4-SPT5 and TFIIS are involved in the same pathway in *Arabidopsis.* The two processes facilitating productive transcription by having a positive role on elongation rate of RNAPII and activation of the intrinsic cleavage

activity of RNAPII to overcome backtracking are linked in *Arabidopsis* as they are in yeast (Lindstrom and Hartzog, 2001).

3.8.2 Analysis of *SPT4-R1/ssrp1-2* and *SPT4-R1/spt16-1* double-mutants

FACT and *SPT4-SPT5* have been shown to interact genetically in human, as FACT is important to relieve RNAPII from pausing, mediated by SPT4-SPT5 and NELF *in vitro* (Wada et al., 2000). *SPT4*-RNAi mutants and mutants of the subunits SSRP1 and SPT16 of the FACT complex all show reduced cell proliferation and reduced fertility. In contrast to *SPT4*-RNAi mutants, *ssrp1-2* and *spt16-1* exhibit a rather 'bushy' phenotype, as the shoot meristem of all homozygous mutants produced more reproductive tissues (Lolas et al., 2010). Although *ssrp1-2* and *spt16-1* have essentially similar phenotypes, the double-mutants with *SPT4-R1* were not uniform as *SSRP1* is epistatic to *SPT4*, whereas *SPT4* is epistatic to *SPT16*, resembling the *ssrp1-2* and *SPT4-R1* mutant phenotype, respectively (Figure 70). Interestingly, this difference of double-mutant phenotypes affecting the two FACT subunits has also been observed for double-mutants of *ssrp1-2* and *spt16-1* with *tfIIs-1* (Mortensen, unpublished data). A possible explanation for the non-uniform phenotype might be the correlation with the observation that SSRP1 and SPT16 have independent roles in gene regulation in humans, as knockdown of SSRP1 and SPT16 showed that a subset of genes was regulated by SSRP1 independently of SPT16. (Li et al., 2007c) The difference of the two FACT mutants might be not observable in the single-mutant but in combination with other mutant alleles. The phenotypical analysis shows that both FACT and SPT4-SPT5 are involved in the same pathway, and that SSRP1 has a role upstream of SPT4-SPT5 and probably also down-stream together with SPT16.

3.8.3 Analysis of *SPT4-R17/cbp20* and *SPT4-R17/cbp80* double-mutants

The cap binding complex (CBC) comprising the subunits CBP20 and CBP80 binds the 5' cap structure of the produced mRNAs and is involved in transcription elongation as CBP80 has been shown to interact directly with P-TEFb and the RNAPII phosphorylated at Ser2 and a depletion of CBC reduces total levels of Ser2-P RNAPII (Lenasi et al., 2011). SPT4-SPT5 has been shown to be involved in the recruitment of capping enzymes but a genetic interaction with the cap binding complex has not be shown (Lindstrom et al., 2003). Single-mutants of CBP20 and CBP80 look essentially alike, have serrated leaves, and display some minor

phenotypes in organ development. Double-mutants of the cap binding complex subunits *CBP20* and *CBP80* with the *SPT4*-RNAi mutant line 17 showed synergistic effects, which was best seen with *SPT4-R17/cbp80* (Figure 73). The difference in the severity of the phenotypes of *SPT4-R17/cbp20* and *SPT4-R17/cbp80* double-mutants correlates with the observations that rather *CBP80* than *CBP20* seems to be involved in mediating genetic or physical interactions with other factors like the mRNA export machinery (Cheng et al., 2006a). These results show that there might be a genetic interaction between SPT4-SPT5 and CBC, whereas the interaction is more pronounced with *cbp80* than with *cbp20*.

3.9 Outlook

In this thesis, an *Arabidopsis* ortholog of SPT4-SPT5 was identified, and an involvement in auxin related gene expression was suggested. To further analyse the function of SPT4-SPT5 in auxin-related gene expression, it would be of interest to analyse the localisation of PIN and Aux/LAX carrier in detail by immunostaining, to analyse if an alteration in the distribution of the auxin carrier might contribute to the mutant phenotypes. Although in *SPT4-R3* several *Aux/IAA*s are down-regulated, it would be of interest to analyse a possible suppression of the *SPT4*-RNAi phenotype by introducing gain-of-function Aux/IAA alleles like *msg2* (IAA19) of *axr5* (IAA5) to further elucidate if the *SPT4*-RNAi phenotype results from reduced expression of *Aux*/IAA.

SPT4-2 has been shown to interact directly with SPT5L *in vitro*. It would be interesting to further analyse if SPT4 has a role in RNA-mediated DNA methylation or other small RNA mediated processes. Also other factors involved in transcription elongation have been shown to be involved in small RNA dependent processes, e. g. the cyclin-dependent kinase CDKF phosphorylating RNAPII at Ser2, which is involved in microRNA maturation (Hajheidari et al., 2012).

SPT4 has been shown to interact with SPT5 and e. g. the RNAPII to improve the affinity purification DNase and/or RNase digestion before purification, which might be appropriate as SPT5 has been shown to interact with both the nascent RNA and the DNA strand (Hartzog and Fu, 2013). A reduction of the contaminating proteins, which bind to the RNA or DNA, found after elution would therefore increase the sensitivity of the mass spectrometry. SPT5 is phosphorylated in various organisms and the

phosphorylation sites are conserved in *Arabidopsis* and are important for SPT5 function (Yamada et al., 2006). As it is possible to purify sufficient amounts of SPT5 in SPT4-GS purification it should be possible to identify possible phospho-peptides of *Arabidopsis* SPT5.

SPT4-SPT5 is involved in transcriptional pausing, which has not been discovered in *Arabidopsis* so far but hints of the existence of promoter proximal stalling of RNAPII are given (Ding et al., 2012). SPT4-SPT5 is among the factors involved in transcriptional pausing in humans and *Drosophila*. Therefore, the *SPT4*-RNAi and inducible *SPT5*-RNAi lines display a perfect tool to further elucidate the existence of RNAPII stalling in *Arabidopsis*.

4. Summary

SPT4-SPT5 is a general transcription elongation factor that facilitates productive transcription by RNA polymerase II in various organisms. It is a heterodimeric complex assembled of the small subunit SPT4 and the large subunit SPT5. SPT4-SPT5 is essential for processive elongation, which is carried out by assisting RNAPII in overcoming transcriptional barriers like nucleosomes. SPT5 interacts directly with the largest subunit of RNAPII, Rbp1, and thereby stabilises the RNA-DNA hybrid inside the RNA polymerase which, is inevitable for productive elongation.

This work focuses on the characterisation of an SPT4-SPT5 complex in *Arabidopsis thaliana*. The two subunits SPT4 and SPT5 are encoded by two genes each: SPT4-1/2 and SPT5-1/2. A mutant affected in the tissue-specifically expressed SPT5-1 is viable, whereas inactivation of the generally expressed SPT5-2 is embryonic lethal. Inducible knockdown of *SPT5* expression leads to severe growth defects and a reduction of plant weight to about 40% of wild-type. Simultaneous down-regulation of both SPT4-1 and SPT4-2 by RNAi gives rise to severe growth and development defects caused by decreased cell proliferation. Additionally, these plants displayed auxin-related phenotypes, e. g. distorted gravitropism, reduced root growth, and impaired vein patterning. Consistently, genome-wide transcript profiling revealed that several auxin-related genes are down-regulated in the line *SPT4-R3* compared with wild-type. Among those auxin-related genes the group of *Aux/IAA* genes was further analysed, showing a down-regulation especially within the group of auxin-inducible *Aux/IAA*s. The reduction of Aux/IAA repressor levels leads to an enhanced auxin response in *SPT4*-RNAi plants.

Furthermore, this thesis provides evidence that SPT4-SPT5 forms a complex in *Arabidopsis* and interacts with the transcription elongation complex. Immunostaining revealed that SPT5 localises to the transcriptionally active euchromatin, and essentially co-localises with transcribing RNAPII phosphorylated at Ser2. Chromatin immunoprecipitation showed a SPT5 distribution over the entire transcription unit of RNAPII-transcribed genes. In *SPT4*-RNAi plants, elevated levels of RNAPII and SPT5 are detected within transcribed regions, indicating transcript elongation defects in these plants. Therefore, this study provides evidence that *Arabidopsis* SPT4-SPT5 is conserved in plants, acts as a transcription elongation factor, and has a critical role in auxin-related gene expression.

CHAPTER 5

MATERIAL AND METHODS

5. Material and Methods

5.1 Materials

5.1.1 Chemicals and enzymes

Laboratory grade chemicals and reagents were purchased from Carl Roth (Germany), Fluka (Switzerland), Applichem (Germany), Life Technologies (UK) and Sigma Aldrich (Germany). L-[35S] methionine was obtained from Hartmann analytic (Germany). MS medium and plant agar were obtained from Duchefa (Netherlands). Enzymes were purchased from Thermo Fisher Scientific (USA), PEQLAB (Germany) or New England Biolabs (USA) if not otherwise stated.

5.1.2 Oligonucleotides

Oligonucleotides used in this study were purchased either from MWG-Biotech (Germany) or Metabion International AG (Germany). All oligonucleotide primers (providing also the required restriction enzyme cleavage sites for cloning) are listed in Table 10.

5.1.3 Plasmids

All plasmid used in this study are listed in Table 3. For plasmid maps see Figure 78, Figure 79 and Figure 80.

Table 3. List of plasmids.

Plasmid	Description	Insert
3'-GFP-SPT4 *	transient expression of SPT4-2-GFP fusion in tobacco protoplasts	*Spt4-2* full length CDS
5'-GFP-SPT4 *	transient expression of GFP-SPT4-2 fusion in tobacco protoplasts	*Spt4-2* full length CDS
pBC-SK-SPT5-2N *	*in vitro* translation insertion of *SPT5-2* N-terminal CDS	*SPT5-2* N-terminal CDS
pBC-SK-SPT5LN *	*in vitro* translation insertion of *SPT5L* N-terminal CDS	*SPT5L* N-terminal CDS
pCambia2300-GS *	stable expression of GS	GS-tag
pCambia2300-SPT4-2-GS *	stable expression of SPT4-2-GS fusion in *Arabidopsis* cell culture	*Spt4-2* full length CDS

pFGC5941-SPT4-RNAi	stable expression of *SPT4*-RNAi construct	*SPT4-2* fragment
pFGC5941-SPT5-RNAi *	stable expression of *SPT5*-RNAi construct	*SPT5-2* fragment
pGEX5x.1-SPT4-2 *	expression of GST-SPT4-2 fusion in *E. coli*	*Spt4-2* full length CDS
pMDC150-pUBQ10 *	stable ubiquitous expression of *XVE* element	*UBQ10* promoter
pMDC160-SPT5-RNAi *	inducible expression of *SPT5*-RNAi construct	*SPT5*-RNAi fragment of pFGC5941-SPT5-2
pMDC221-SPT5-RNAi *	inducible expression of *SPT5*-RNAi construct	*SPT5*-RNAi fragment of pFGC5941-SPT5-2
pQE-SPT5-2C *	expression of C-terminal part of *SPT5-2* in *E. coli*	C-terminal part of *SPT5-2*

* Plasmids generated in this work

5.1.4 Seed stocks

Arabidopsis thaliana seeds, ecotype Columbia (Col-0), were obtained from the Nottingham Arabidopsis Stock Centre (NASC, UK). All mutant seed stocks have a Columbia (Col-0) genetic background. The following mutant seeds were used in this project (Table 4):

Table 4. List of seed stocks.

Name	T-DNA	AGI	Seed stock ID	Publication
spt4-2	SAIL_262_E06	At5g08565	NASC ID: 812248	this work
spt5-1	SAIL_1297_A11	At2g34210	NASC ID: N848561	this work
spt5-2-1	SALK_136809	At4g08350	NASC ID: N636809	this work
spt5-2-2	SALK_115089	At4g08350	NASC ID: N615089	this work
spt5-2-3	SALK_012958	At4g08350	NASC ID: N512958	this work
spt5-2-4	SAIL_287_B03	At4g08350	NASC ID: N813305	this work
tfIIs-1	SALK_056755	At2g38560	NASC ID: N556755	Grasser et al., 2009
ssrp1-2	SALK_001283	At3g28730	NASC ID: N501283	Lolas et al., 2010
spt16-1	SAIL_392_G06	At4g10710	NASC ID: N818083	Lolas et al., 2010
cbp20	pPCV6NFHyg	At5g44200		Papp et al., 2004
cbp80	SALK_024285	At2g13540	NASC ID: N859834	Laubinger et al., 2008

5.1.5 Software

Adobe ® Photoshop® CS5 Extended Version 12.0.4 x64 (Adobe Systems Incorporated)

Alpha view® Software Version 3.0.3.0 (Alpha Innotech Corporation)
AxioVision40 V4.8.0.0 (Zeiss)
Cytoscape version 2.8.3 with BiNGO plugin V2.44
(http://www.psb.ugent.be/cbd/papers/BiNGO/)
EndNote X6.0.1 (Thomson Reuters)
ImageJ version 1.45d3 (http://rsbweb.nih.gov/ij/)
LAS AF V 3.1.0 build 8587 (Leica Microsystems)
Laser Scanning Microscope LSM 510 V 4.2SP1 (Zeiss)
LSM Image Browser V4.2.0.121 (Zeiss)
R version 2.15.3 (http://www.r-project.org)
realplex software version 2.2 (Eppendorf)
VectorNTI 10.3.0 (Life Technologies)

5.2 Bacterial work

5.2.1 Generation and transformation of electro-competent cells

An 80 µl glycerol stock of *Agrobacterium tumefaciens* or *Escherichia coli* cells were grown overnight at 30 °C (*A. tumefaciens*) or 37 °C (*E. coli*) at 200 g in 15 ml LB medium with the corresponding antibiotics. The culture was used to inoculate 1 L LB medium with antibiotics and grown until OD_{600} of 0.750. During harvesting and washing all steps were performed on ice. The cells were harvested by centrifugation for 30 min at 5000 g. The pellet was washed twice by resuspending it in a volume of 1 L and 500 ml H_2O. The washed pellet was resuspended in 20 ml 10% glycerol (v/v) and centrifuged for 15 min at 5000 g. In the end the pellet was then resuspended in 2 ml 10% glycerol (v/v) and stored in 80 µl aliquots at -80 °C.

For transformation one aliquot was used and either half of the ligation reaction (5.3.3) or 100 ng plasmid was added to a 2 ml electroporation cuvette and electroporated (Voltage: 2.5 kV, Resistance 200 Ω, Capacitance: 250 µFD). 1 ml of LB medium was added to the electroporation reaction, incubated for 1 h at the corresponding temperature and plated out on solid LB plates with selection.

5.2.2 Generation and transformation of chemically competent *E. coli* cells

The protocol was adopted from Inoue et al., 1990. A single colony of an *E. coli* strain was grown in LB medium overnight at 37 °C. The culture was diluted the next

day in 250 ml SOB to about 1:100. This culture was grown at 18 °C until an OD_{600} of about 0.6. Afterwards, the cells were cooled quickly in an ice water bath for ten minutes before harvested at 4 °C. The pellet was resuspended in ice-cold TB buffer and kept on ice for ten minutes. Following an additional harvesting step (30 min, 4000 g, 4 °C), the pellet was gently taken up in 20 ml ice-cold TB buffer. Afterwards DMSO (v/v) was added to a final concentration of 7%. The cells are then aliquoted, immediately frozen in liquid nitrogen and stored at -80 °C. For transformation, an aliquot of 100 µl was used together with either half of the ligation reaction (5.3.3), or 100 ng plasmid and a heat-shock was applied (42 °C, 45 sec). 1 ml of LB medium was added to the reaction, incubated for 1 h at 37 °C and plated out on solid LB plated with selection.

5.3 Molecular biological methods

5.3.1 Genomic DNA extraction of *A. thaliana*

For extraction of genomic DNA, a small piece of leaf tissue was frozen in liquid nitrogen and homogenized. For extraction of DNA, 400 µl of Edward buffer (200 mM Tris HCl, 250 mM NaCl, 0.5% SDS (w/v) and 25 mM EDTA) was added and the cell debris was centrifuged (full speed, 5 min). 350 µl of the supernatant was taken and the DNA was precipitated by adding the same amount of 100% isopropanol and a 15 min centrifugation step with full speed. After the precipitation the pellet was washed once with 70% ethanol (v/v), dried and dissolved in 75 µl ddH_2O.

5.3.2 Polymerase chain reaction (PCR)

5.3.2.1 Taq Polymerase

The Taq Polymerase (PEQLAB) was used for normal PCRs like genotyping and RT-PCR. The amount of DNA used as a template was dependent on the nature of the DNA: 100 ng of plasmid DNA, 1.5 µl of genomic DNA, and 5 µl of cDNA was used. The extension time t_E was calculated upon the length of the amplicon, given an amplification rate of the Taq-Polymerase of 1 kb/min.

Reactions

2.5 µl	10x Taq-Buffer
0.75 µl	dNTP (2 mM)
0.75 µl	Primer Forward (10 µM)
0.75 µl	Primer Reverse (10 µM)
x µl	DNA Template
0.15 µl	Taq DNA-polymerase
ad 25 µl	H_2O

Program

95 °C	3 min	
95 °C	30 sec	35x
53 °C	30 sec	
72 °C	t_E	
72 °C	5 min	
10 °C	pause	

5.3.2.2 KAPAHIFI-Polymerase

Due to its proof-reading activity, the KAPAHIFI Polymerase (PEQLAB) was used for fragments which were used for cloning. The amount of DNA used as a template was dependent on the nature of the DNA: 100 ng of plasmid DNA, and 5 µl of cDNA was used. The extension time t_E was calculated upon the length of the amplicon, given an amplification rate of the KAPA-Polymerase of 2 kb/min.

Reactions

10 µl	5x KAPA Polymerase-Buffer
1.5 µl	dNTP (2 mM)
1.5 µl	Primer Forward (10 µM)
1.5 µl	Primer Reverse (10 µM)
x µl	DNA Template
0.5 µl	KAPAHIFI DNA-polymerase
ad 50 µl	H_2O

Program

98 °C	3 min	
98 °C	20 sec	35x
53 °C	15 sec	
72 °C	t_E	
72 °C	5 min	
4 °C	pause	

5.3.2.3 Quantitative PCR

QPCR was performed with KAPA™ SYBR® FAST QPCR MasterMix Universal (PEQLAB) and a Mastercycler ep realplex^2 with realplex software version 2.2 (Eppendorf) according to the manufacturer's instructions.

For expression analysis, total RNA was extracted with the RNeasy Mini Plant kit supplied with RNase-Free DNase set (Qiagen) according to the manufacturer's instructions. The cDNA was synthesized like described in 5.3.8 with RevertAid™ H Minus M-MuLV Reverse Transcriptase (Thermo Fisher Scientific). Expression levels

were normalized to *ACT8* (AT1G49240), and *EF1α* (AT5G60390), taking the primer efficiency into consideration.

For ChIP (5.5.13), 5µl precipitated DNA (diluted 1:50 for input, 1:10 for H3 and 1:5 for SPT5, RNAPII-CTD-Ser2P and RNAPII-CTD-Ser5P) was analysed with locus-specific primers. The IP data were normalized to the input. For primer sequences, see Table 10.

Reactions

10 µl	2x
0.4 µl	Primer Forward (10 µM)
0.4 µl	Primer Reverse (10 µM)
5 µl	DNA Template
ad 20 µl	H_2O

Program

98 °C	3 min	
98 °C	3 sec	40x
60 °C	20 sec	
95 °C	15 sec	
60-95 °C	70x 15 sec	
95 °C	15 sec	

5.3.3 Plasmid construction

Gel electrophoresis and cloning was performed according to Sambrook et al., 1989. Gel electrophoresis was performed with a 1% agarose (w/v) gel in 160 ml TAE buffer (40 mM Tris, 20 mM acetic acid, and 1 mM EDTA) and 7 µl 1% ethidium bromide (w/v). DNA clean-up was performed with the NucleoSpin® Gel and PCR Clean-up kit (Macherey-Nagel). Restriction digest, dephosphorylating and ligation were performed according to the manufacturer's protocol. Subcloning of Gateway® compatible PCR fragments into the pENTR™/D-TOPO® Vector for and later Gateway® reactions were performed according to the manufacturer's (Life Technologies) manual.

5.3.4 Mini Prep

For Mini Prep of plasmids, 5 ml of LB medium with selection were inoculated with a positive transformed colony. The next day cells were harvested (5 min, 5000 g, 4 °C) and resuspended in 200 µl resuspension buffer (50 mM Tris-HCl pH 8.0, 10 mM EDTA, 100 µg/ml RNase A). Subsequently 300 µl lysis buffer were added (200 mM NaOH, 1% SDS (w/v)), incubated at room temperature for 5 min and the lysis was stopped by adding 300 µl neutralization buffer (3 M KAc pH 4.8 pH with glacial acetic acid). After incubation on ice for 10 min, the cell debris was spun down at full speed

for 10 min. The supernatant was taken, and the DNA was precipitated by adding equal amounts of isopropanol. After precipitation the pellet was washed once with 70% ethanol (v/v), dried and resuspended in 100 µl H_2O.

5.3.5 Midi Prep

For Midi Preps the remaining culture of the corresponding Mini Prep or a new positive colony was used to inoculate a 100 ml culture. For plasmid isolation the NucleoBond® Xtra Midi kit (Macherey-Nagel) was used according to the manufacturer's instructions. After precipitation the pellet was resuspended in 200 µl H_2O.

5.3.6 Sequencing

Sequencing was performed by either Eurofins MWG Operon (Ebersberg) or GATC Biotech (Konstanz). Plasmids were prepared as described in 5.3.5 and sent in the demanded concentrations.

5.3.7 RNA Extraction

5.3.7.1 Extraction of total RNA

Total RNA was extracted with the RNeasy Mini Plant kit supplied with RNase-Free DNase set (Qiagen) according to the manufacturer's instructions or with a protocol adopted from Logemann et al., 1987. 100 – 200 mg plant material was homogenised, resuspended in 600 µl Z6 buffer (8 M guanidium HCl, 20 mM MES, 20 mM EDTA and 100 mM β-mercaptoethanol) and 500 µl phenol/chloroform/isoamyl alcohol (25/24/1) pH 4.5 was added. After centrifugation for 10 min at 16000 g at 4 °C the supernatant was transferred in a new tube and 1/20 volume 1 N acidic acid and 0.7 volume 100% ethanol were added. The RNA pellet was precipitated (10 min, 16000 g, 4 °C) and washed with 500 µl 3 M NaAc pH 5.2 and 80% ethanol (v/v), and then dried and resuspended in 50 µl H_2O. 3.5 µg total RNA was treated for 2 h with DNaseI according to the manufacturer's instructions

5.3.7.2 Extraction of mRNA

The mRNA of stamen and pistils was extracted using Dynabeads® mRNA Direct™ Kit (Life Technologies) supplied with magnetic Dynabead Oligo $(dT)_{25}$. Approximately 50 mg tissue was homogenised in a 0.5 ml tube with a mortar frozen in liquid nitrogen. Afterward 300 µl lysis/binding buffer (100 mM Tris HCl pH 7.5, 500

mM LiCl, 10 mM EDTA, 1% LiDS (w/v) and 5 mM DTT) were added and mixed for 15 min. The beads were washed two times in wash buffer A (10 mM Tris HCl, pH 7.5, 150 mM LiCl, 1 mM EDTA and 0.1% LiDS (w/v)) and two times in wash buffer B (10 mM Tris HCl pH 7.5, 150 mM LiCl and 1 mM EDTA). The bead-bound mRNA was stored in 10 mM Tris HCl pH 7.5 at -20 °C.

5.3.8 Synthesis of cDNA

The cDNA was prepared from DNase treated total RNA extracts with RevertAid™ H Minus M-MuLV Reverse Transcriptase (Thermo Fisher Scientific). 2 µg RNA were incubated with 0.2 µg random hexamer primer for 5 min at 70 °C in a total volume of 11.5 µl. Subsequently 4 µl 5x reaction buffer, 2 µl dNTP (10 mM), 0.5 µl RNase Inhibitor (20 U) (Thermo Fisher Scientific) were added and incubated for 5 min at 25 °C. The Reverse Transcriptase was added and incubated for 90 min at 42 °C with a 10 min 70 °C deactivation step in the end. For PCR the cDNA was diluted 1:25.
For cDNA Synthesis of Dynabeads-extracted mRNA, the SuperScript® III Reverse Transcriptase (Life Technologies) was used according to the manufacturer's protocol. For PCR the cDNA was diluted 1:5.

5.3.9 Genome-wide transcript profiling by microarray

Total RNA was isolated from the aerial part of ten day old seedlings with RNeasy Mini Plant kit supplied with RNase-Free DNase set (Qiagen) according to the manufacturer's instructions. The quality of the DNA was analysed with a 2100 Bioanalyzer (Agilent Technologies) and the microarray experiment was performed by the Kompetenzzentrum für Fluoreszente Bioanalytik (Regensburg, Germany; http:// http://www.kfb-regensburg.de/) with the *Arabidopsis* ATH1 Genome Array chip (Affymetrix) of 22800 probe sets designed for *Arabidopsis* (Nelissen et al., 2005). The experimental design comprised three replicates of each genotype, with one replicate corresponding to one RNA extraction on an independent pool of plants. The raw data from the Affymetrix GeneChip arrays (CEL files) were summarized with the Robust Multi-chip Analysis (RMA) using a baseline to the median of all samples followed by quality control with principal component analysis (Bolstad et al., 2003). Transcripts showing a significant differential gene expression were identified by pair-wise comparison using a Student's t-test with a p-value <0.01. Only significantly changed transcripts also displaying a least two fold change of gene expression were accepted for further analysis. For analysis of significantly overrepresented GO

categories among up- and down regulated genes, we used the BiNGO plugin version 2.44 for Cytoscape version 2.8.3 with a p-value < 0.05 (http://www.psb.ugent.be/cbd/papers/BiNGO/; Maere et al., 2005).

5.4 Cell biological methods and plant work

5.4.1 Plant growth

Arabidopsis thaliana Col-0 plants, various T-DNA insertion mutant lines from the SALK and SAIL collections were kindly provided by Nottingham Arabidopsis Stock Centre (NASC, http://arabidopsis.info/) and additional transgenic lines all with the Col-0 background were grown on soil in a phytochamber under long day (LD) (16 h light and 8 h dark at constantly 22 °C) or short day (SD) conditions (8 h light at 22 °C and 16 h dark at 18 °C) rhythm. Plants transformed with the *bar* or *pat* gene (Phosphinotricin-Acetyltransferase) as a selection marker conferring BASTA® resistance were sprayed with BASTA® (Bayer Crop Science) with a concentration of 100 mg/l glufosinate ammonium seven days after germination. Spraying was repeated two more times with an interval of two days.

For plant growth under sterile conditions seeds were surface sterilized with chloric gas (50 ml 12.5% hypochloric acid (w/v) and 2 ml 37% HCl (v/v)) in an exsiccator. The seeds were grown on solid MS medium (4.4 g/L MS salts and 0.8% phytoagar (w/v)) in a plant incubator (Percival Scientific) under LD conditions. For selection antibiotics and herbicides were added.

5.4.2 Stable transformation of *Arabidopsis*

Stable transformation of *Arabidopsis* was performed by using the “Floral Dip” method described in by Clough and Bent, 1998.

5.4.3 Soil-based phenotyping

Overall plant development and flower morphology have been observed and documented for the various genotypes of plants used in this project. The phenotypic analysis was based on a series of defined growth stages which has been described in detail (Boyes et al., 2001). Bolting time was measured by counting the days after stratification (DAS) until flower bud became visible. Flowering time was measured by counting the days after stratification until the opening of the first flower. Pictures of

plants were taken with the CANON EOS 600D with a CANON MACRO LENS EF-S 60 mm 1:2.8 USM or a CANON ETS 18-55 mm objective (Canon).

5.4.4 Crossing of *Arabidopsis*

For crossing of different mutant lines all opened and young flowers were removed. From the remaining unopened flowers sepals, petals and stamens were gently removed, leaving behind only the carpel. After two days pollen from an open flower was brushed onto the carpel and the carpel was led to develop into a silique which was harvested at maturation.

5.4.5 Germination test

For germination tests flowers were labelled the day they opened, and 15 days later the siliques were harvested and sown out on petri dishes with water-soaked paper without stratification. Pictures were taken at day 0 and at day 7. The germination-rate was determined using ImageJ version 1.45d3 (http://rsb.info.nih.gov/ij/). The images were converted to 8-bit and the background was subtracted with a rolling ball radius of 10 px. Afterwards the threshold was set to 225 and the number of particles was counted with a particle size of 10 px or more to count the number of total seeds (picture at day 0), or a particle size of 300 px or more to count the number of germinated seeds (picture at day 7).

5.4.6 Phenotypic analysis of roots

Phenotypic analysis of roots was performed on solid ½ MS (2.2 g/L MS salt and 0.8% phytoagar (w/v)) with 1% sucrose (w/v) on square petri dishes (13 x 13 cm). Plates were grown vertically in a plant incubator. For confocal microscopic images of roots, the roots were stained by adding 20 µM propidium iodide to the microscope slide for 10 min prior analysis.

5.4.7 Growth under auxin-inducing conditions

For auxin (IAA) induction in liquid medium, sterilized seeds were sown out on solid MS. After five days plants were transferred to liquid MS with 1% sucrose (w/v). One day later the plants were mock treated with ethanol or with 20 µM IAA dissolved in ethanol for 2 h, harvested and frozen in liquid nitrogen (Overvoorde et al., 2005).
For root growth on auxin-inducing medium, surface-sterilized seed were sown out on plates with ½ MS with 1% sucrose (w/v). After three days the plants were moved to

plates with the corresponding auxin concentrations (10 nM, 100 nM or 1000 nM), or without auxin. Root length was measured after 6 and after 14 days with ImageJ. Relative root elongation rate was determined by normalization of the growth between day 6 and 14 for every IAA concentration with the corresponding mock control (Nelissen et al., 2010).

5.4.8 Growth under β-estradiol-inducing conditions

Seedlings were grown on MS with 1% sucrose with or without 2 µM β-estradiol. Pictures were taken after 14 days.

For β-estradiol induction in liquid medium, plants were grown on MS with 1% sucrose without β-estradiol, and moved after 7 days into 25 ml liquid MS with 1% sucrose (10 plants per Erlenmeyer flask). After one additional day seedlings were either mock treated with 0.1% DMSO (v/v), or treated with 2 µM β-estradiol dissolved in DMSO. After 6 additional days the plants were harvest dried on paper and the fresh-weight was determined (Brand et al., 2006).

5.4.9 Chloral hydrate clearing

Leaves of 26 DAS (~ bolting) seedlings grown on solid MS, or fully elongated siliques of ~ 35 DAS plants were fixed in 30% ethanol (v/v) and 70% acidic acid (v/v) overnight prior to clearing. After washing with 70% ethanol (v/v), the plant material was cleared in chloral hydrate solubilised in 30% glycerol (v/v) (1.8g chloral hydrate in 1 ml 30% glycerol) also overnight. The chloral hydrate was removed and the samples were mounted on a microscope slide in 30% glycerol (v/v).

5.4.10 Leaf surface analysis

Fully elongated first leaves of 26 DAS plants grown on solid MS were fixed and cleared in 100% methanol overnight. The next day the methanol was removed, the samples were incubated with 90% lactic acid (v/v) overnight, and mounted on a microscope slide.

5.4.11 GUS-staining

Roots, leaves, or whole plants of different ages were used for GUS staining. Roots were stained for 1 h, leaves and whole plants for 3 h in GUS staining solution (50 mM $NaHPO_4$ pH 7.2, 0.5 mM $K_3Fe(CN)_6$, 0.5 mM $K_4Fe(CN)_6$, 1% Triton X-100 (v/v) and 2 mM X-Gluc) at 37 °C. After staining, leaves and whole plants were

washed several times with 70% ethanol (v/v) at 37 °C until the leaves were cleared. After clearing, leaves or whole plants were mounted on a microscope slide. Roots were directly mounted on a slide without clearing.

5.4.12 Fixation and semi-thin sections of leaves

Fixation and semi-thin sections of leaves were made in the laboratory of Dr. Michael Melzer. For the primary fixation, sections of leaf tissue were incubated for 2.5 h at 25 °C in 50 mM cacodylate buffer pH 7.2, containing 0.5% (v/v) glutaraldehyde and 2.0% (v/v) formaldehyde, followed by one wash with buffer and two washes with distilled water. After primary fixation, samples were transferred into a solution of 1% (w/v) OsO_4 for secondary fixation. After 1 h, samples were washed three times with distilled water. Dehydration at 25 °C was performed stepwise by increasing the concentration of ethanol as follows: 30% (v/v), 50% (v/v), 60% (v/v), 75% (v/v), 90% (v/v), and twice 100% (v/v) ethanol for 1 h each. After additional dehydration with propylene oxide for 1 h, the samples were infiltrated with Spurr resin (Plano) as follows: 33% (v/v), 50% (v/v), and 66% (v/v) Spurr resin in propylene oxide for 4 h each and then 100% (v/v) Spurr resin overnight. Samples were transferred into embedding molds, incubated there for 3 h in fresh resin, and polymerized at 70 °C for 24 h. Semi-thin sections with a thickness of ~3 µm were mounted on slides and stained for 2 min with 1% (w/v) methylene blue and 1% (w/v) Azur II in 1% (w/v) aqueous borax at 60 °C before light microscopic examination.

5.4.13 Alexander-stain of pollen

Pollen viability was tested using Alexander stain (Alexander, 1969). 4 – 6 anthers were excised and mature pollen from the detached anthers were then collected by dipping the whole anther onto a microscope slide containing 1 drop of Alexander stain (10% ethanol (v/v), 25% glycerol (v/v), 0.01% malachite green (w/v), 0.05% acid fuchsin (w/v), 0.005% Orange G (w/v), 5% phenol (w/v) and 5% chloral hydrate (w/v), acidified with 20µl glacial acetic acid). The slide was then covered with a coverslip and analysed with a microscope.

5.4.14 PEG-mediated transformation of tobacco protoplasts

Tobacco BY-2 cell culture was used to isolate protoplasts. The cells were grown in BY-2 medium (4.4 g/L MS salt, 30 g/L sucrose, 100 mg/L myo-inositol, 1 mg/L thiamine HCl, 0.2 mg/L dichlororphenoxyacetic acid (2,4-D) and 255 mg/L K_2PO_4),

and diluted once a week by transferring 2 ml of one week old culture into 70 ml fresh medium. For transformation, 20 ml 3 day old cell culture was spun down (400 g, 5 min) and resuspended first in 25 ml wash buffer (5 g/L BSA, 10 mM β-mercaptoethanol, 50 mM $CaCl_2$, 10 mM NaOAc and 250 mM mannitol) and afterwards incubated overnight in 13 ml digest solution (13 ml wash buffer with 1% cellulose (w/v), 0.5% macerocyme (w/v), and 0.1% pectinase (w/v)) in darkness. Protoplasts were handled with greatest care and every centrifugation step was performed for 4 min at 90 g. The supernatant was removed and the protoplasts were washed twice with 25 ml wash solution, with 10 ml and 5 ml W5 buffer (154 mM NaCl, 125 mM $CaCl_2$, 5 mM KCl and 5 mM glucose) and twice with 10 ml MMM buffer (0.1% MES-KOH pH 5.8 (w/v), 15 mM $MgCl_2$, and 500 mM mannitol). Viability of the protoplasts was tested with Evan's blue, and the cells were counted using a haemocytometer. The pellet was resuspended in MMM buffer to a concentration of $2x10^6$ cells/ml. For every transformation, 300 µl PEG buffer (40% PEG 4000 (v/v), 0.4 M mannitol, 0.1 M $Ca(NO_3)_2$) and 30 µg plasmid were added to 300 µl cells and incubated for 20 min. The cells were washed with 10 ml W5 buffer, resuspended in 0.7 ml MS medium with 400 mM sucrose, incubated overnight in darkness, and mounted on microscope slide for analysis.

5.4.15 *Agrobacterium*-mediated transformation of *Arabidopsis* suspension cell culture

Arabidopsis suspension cell culture (PSB-D) was grown in MSMO medium (4.4 g/L MS salts with minimal organics (Duchefa), 30 g/L sucrose, 0.5 mg/L NAA and 0.05 mg/L kinetin) and diluted once a week by transferring 7 ml of one week old culture into 43 ml fresh medium. For affinity purification of transcription factor complexes, the cell culture was transformed with constructs for expression of SPT4-2 coupled with the GS-tag and the GS-tag only as described previously (Van Leene et al., 2008; Van Leene et al., 2011).

5.4.16 Microscopy

5.4.16.1 Transmitted light microscopy

Morphological details of plants were examined by light microscopy using a Zeiss Discovery V8 stereomicroscope or a Zeiss Axioscope, and documented using a Zeiss Axiocam MRC5.

5.4.16.2 Confocal Microscopy

All microscopic studies were performed with a LSM510 META from Zeiss® or a SP8 from Leica. The pictures were analysed by the confocal software Laser Scanning Microscope LSM 510 and Leica LAS AF, respectively. The following table (Table 5) depicts the used excitation wavelengths and filters, depending on the fluorescent protein.

5.4.16.3 Super-resolution microscopy

Super-resolution, structured illumination microscopy (SIM) was performed by Dr. Veit Schubert in the laboratory of Dr. Andreas Houben at the IPK Gatersleben.

Table 5. Fluorescent proteins and dyes.

Fluorescent protein/dye	Excitation wavelength	Emission filter
DAPI	405 nm	410 – 495 nm
FITZ	488 nm	495 – 550 nm
GFP	488 nm	585 – 615 nm
Cy3	514 nm	550 – 610 nm
Propidium iodide	561 nm	570 – 650 nm

5.5 Biochemical methods

5.5.1 SDS-PAGE

Depending on the size of protein that has to be analysed, different separation gels were made with either 9% (w/v), 12% (w/v) or 18% (w/v) acrylamide:bisacrylamide (30:0.15), 0.75 M Tris-HCl pH 8.8, 0.2% SDS (w/v), 0.1% ammonium persulfate (APS) and 0.02% N,N,N‟,N‟-tetramethylethylenediamine (TEMED (v/v)) in a Bio-RAD Mini-Protean® 3 Multicaster system (Bio-Rad). The stacking gels were made of 10% acrylamide:bisacrylamide (30:0.8) (w/v), 0.14 M Tris-HCl pH 6.8, 0.23% SDS (w/v), 0.11% APS (w/v) and 0.06% TEMED (v/v). Before loading, the sample was mixed with 1x SDS loading buffer (150 mM Tris-HCl pH 7.0, 150 mM DTT, 5% SDS (w/v), 25% glycerol (v/v), and 0.1% bromophenol blue (w/v)) and denatured by boiling for 5 min at 95ºC. The SDS polyacrylamide gel electrophoresis (PAGE) was run in a Bio-RAD Mini-Protean® 3 running chamber in Laemmli running buffer (0.1% SDS (w/v), 3.03 g/L Tris, and 14.41 g/L glycine) at 160 V. The gels were either stained

with Coomassie brilliant blue (30% ethanol (v/v), 10% acetic acid (v/v) and 5 g/L Coomassie Brilliant Blue B-250) or used for Western blotting.

5.5.2 Western Blot

The protein samples for Western blotting were first separated by SDS-PAGE and then blotted onto Immobilon™-P Polyvinylidene Fluoride (PVDF) Transfer Membrane in blotting buffer (20% methanol (v/v), 200 mM glycine, 20 mM Tris-HCl and 0.01% SDS (w/v)) using a Semidry Mini Trans-Blot Blotter (Bio-Rad) at 100 mA per gel for 2.5 to 3 h. After blotting, the membrane was incubated in blocking buffer (5% skimmed milk powder (w/v), 20 mM Tris-HCl pH 7.5, 150 mM NaCl and 0.05% Tween 20 (v/v)) for 1 h at 4 °C with gentle agitation. To the blocking buffer primary antibody (1:2000 and 0.04% timerosal (w/v)) was added and incubated at 4 °C on a rotation wheel overnight. Afterwards, the membrane was washed with washing buffer (20 mM Tris-HCl pH 7.5, 150 mM NaCl, 0.05% Tween 20 (v/v) and 1% Triton X100 (v/v)) three times for 10 min. The membrane was then incubated for 1 h at 4 °C with rotation with the secondary IgG antibody (Anti-Rabbit IgG-Peroxidase – Sigma-Aldrich) in blocking buffer and 0.04% timerosal (w/v) at 4 °C with rotation. Finally, the membrane was washed again as described before. Protein signals were visualized using SuperSignal® West Pico Chemiluminescent Substrate (Thermo Fisher Scientific) and a FluorChem FC2 (Alpha Innotech).

5.5.3 Small scale expression and purification of proteins

For small scale expression of His- or GST-tagged proteins, 5 ml LB medium with selection was inoculated with transformed *E. coli* BL21-gold, and grown overnight at 37 °C and 200 g. Subsequently, 100 ml LB medium with selection was inoculated with the pre-culture to an OD_{600} of 0.1 and grown at 37 °C. At an OD_{600} of 0.75 – 1 protein expression was induced with IPTG of a final concentration of 1 mM. 2 h after induction the culture was harvested by centrifugation for 15 min at 5000 g at 4 °C. Before and after induction, a sample was taken to check the expression of recombinant proteins by SDS-PAGE (5.5.1).

5.5.3.1 His-tagged proteins

The pellet was resuspended in 5 ml lysis buffer pH 8 (100 mM NaH_2PO_4, 8 M urea, 10 mM Tris HCl) and sonicated six times for 15 s at 50% output with 30 sec pause in between (Bandeln Sonoplus HD 2070 and a MS 73 tip). The cells

were centrifuged (10 min, 20000 g, at 4 °C), and supernatant was incubated for 1 h at 4 °C with 40 µL 50% Ni-NTA agarose bead slurry (Qiagen). After incubation, the beads were washed three times with His-tag wash buffer pH 6.3 (100 mM NaH_2PO_4, 8 M urea, 10 mM Tris-HCl). After washing the bound proteins were eluted with elution buffer and analysed by SDS-PAGE (5.5.1).

5.5.3.2 GST-tagged proteins

The pellet is re-dissolved in 1x PBS (137 mM NaCl, 2.7mM KCl, 10 mM Na_2HPO_4*2 H_2O and 2 mM KH_2PO_4 pH 7.4) with 2% sarkosyl (v/v) and sonicated six times for 15 s at 50% output with 30 sec pause in between (Bandeln Sonoplus HD 2070 and a MS 73 tip). The cells were spun down for 10 min at 20000 g at 4 °C, and Triton X-100 was added to the supernatant to a final concentration of 2% (v/v). 100 µl of GST-beads were washed three times with 1x PBS and added to the cleared protein extract. After 1 h incubation at 4 °C under gentle agitation, the beads were washed three times. The washed beads were either used for pull-down experiments with *in vitro* translated proteins (5.5.12), or the bound protein was eluted by adding SDS loading buffer and analysed by SDS-PAGE (5.5.1).

5.5.4 Large scale expression and purification of His-tagged proteins

500 µL of the remaining inoculum (5.5.3) was used to inoculate a new 200 ml pre-culture for large scale protein expression. The starter culture was grown o/n at 37 °C and 200 g in LB with selection. The next day the starter culture was used to inoculate 6x 1 L LB medium with selection to an OD_{600} of 0.1 and grown at 37 °C to OD_{600} = 0.75 – 1, and then induced with IPTG to a final concentration of 1 mM. 2 h after induction, the culture was harvested by centrifugation (6000 g, 7 min, and 4 °C). Cells were resuspended in 35 ml lysis buffer and sonicated six times for 30 s at 50% output with 1 min pause in between (Bandeln Sonoplus HD 2070 and a MS 73 tip). The cells were centrifuged (10 min, 20000 g, at 4 °C) and the supernatant was incubated for 1 h at 4 °C with 3 ml washed 50% Ni-NTA agarose bead slurry (Qiagen). After incubation the beads were washed three times with His-tag wash buffer. After washing, the bound proteins were eluted with elution buffer and analysed by SDS-PAGE (5.5.1).

5.5.5 Desalting of proteins

A PD-10 column (GE Healthcare) was used to change buffers and desalt proteins after purification according to the manufacturer's description.

5.5.6 Antibody production

For generation of polyclonal antibody in rabbit, four samples (each 500 µl corresponding to at least 100µg) of the recombinant protein were sent to Eurogentec, Life Science Park (Seraing, Belgium) for immunization.

5.5.7 Acetone precipitation

For acetone precipitation to 300 µl of sample volume 1.2 ml ice-cold acetone was added and incubated overnight at -20 °C. After precipitation of proteins (10 min, full speed, 4 °C), the pellet was washed two times with ice-cold acetone and finally resuspended in 25 µl 1x PBS.

5.5.8 Coupling of rabbit-IgG to Epoxy-activated BcMag-beads

300 mg beads (Bioclone 1 µm BcMag Epoxy-activated Magnetic Beads No. Fc102, 1.7x 10^8 beads/mg) were resuspended in 50% acetone (v/v) (30 mg/ml) and vortexed vigorously. The tube was placed in the magnetic separator, the supernatant was removed and the beads were washed four times in 10 ml 0.1 M $NaPO_4$ buffer (pH 8.5). The residual beads were resuspended in 4 ml 0.1 M $NaPO_4$ buffer (pH 8.5) and incubated for 10 min under gentle shaking at RT.

The AB-mix was prepared during that time. 100 mg rabbit IgG (SIGMA I5006-100MG) were resuspended with 7 ml H_2O (final concentration of 14 mg/ml). 3.5 ml of the AB-mix were centrifuged for 10 min (13000 g, 4 °C) and the unused AB were stored at -20 °C. The supernatant was transferred in a 50 ml tube and 9.85 ml 0.1 M $NaPO_4$ buffer pH 8.5 and 6.65 ml 3 M ammoniumsulfate (3M $(NH_4)_2SO_4$ in 0.1 M $NaPO_4$ buffer pH 8.5) was added. The AB-mix was centrifuged 3 min at 2000 g; the supernatant was added to the precipitated beads and incubated for at least 18 h at 25 °C on a rotating wheel.

After incubation with the AB-mix the beads were washed with 20 ml 100 mM glycine pH 2.5, 20 ml 10 mM Tris HCl pH 8.8, 20 ml freshly prepared triethylamine solution for 5 min, 4x with 20 ml 1x PBS for 5 min, with 2x 20 ml 1x PBS with 0.5% Triton X-100 (v/v) for 5 and 15 min. Finally the beads were pooled in 16 ml 1x PBS with 0.02% sodiumazide (v/v) and stored in aliquots at 4 °C.

5.5.9 Affinity purification of GS-tagged proteins

For affinity purification, 15 g frozen cell suspension culture transformed with constructs harbouring a expression cassette for Spt4 tagged with GS or the GS tag only was grinded in liquid nitrogen (Van Leene et al., 2008). The ground material was divided into 50 ml tubes and 10 ml extraction buffer (25 mM HEPES pH 7.4, 100 mM NaCl, 0.05% NP-40 (v/v), 1 mM DTT, 2 mM MgCl2, 5 mM EGTA, 10% glycerol (v/v), 1 mM PMSF and proteinase inhibitor cocktail [2 µg/ml Antipain, 4 µg/ml Benzamidin, 2 µg/ml Leupeptin, 6 µg/ml N-α-Tosyl-L-phenylchlormethylketon, 0.25 µg/ml Aprotinin, 0.5 µg/ml Pepstatin A and 1.5 µg/ml Tosyl-L-phenylalanin-chlormethylketon]) was added to each tube and thoroughly mixed. The mixture was thawed at RT, pooled, and sonicated on ice (5x 30 sec at 30%) with a Bandeln Sonoplus HD 2070 and a MS 73 tip. The extract was centrifuged (1 h, 40000 g, 4 °C) and the supernatant was filtered through a 0.45 µm filter. Afterwards the protein concentrations of sample and control were measured with Bradford and the volumes and concentrations were adjusted. An aliquot was frozen for further analysis. The IgG-coupled magnetic beads (5.5.8) were washed with water and three times with extraction buffer. 100 µl IgG-beads slurry was added to each sample and incubated for 1.5 h at 4 °C under gentle agitation. The beads were centrifuged 5 min with 2000 g at 4 °C and eluted with 300 µl 0.1 M glycine pH 2.8 for 5 min under gentle shaking. The eluate was precipitated with acetone (5.5.7) and resuspended in 25 µl 1x PBS. For analysis, 6 µl of 6x SDS loading dye was added and the sample was loaded on a 9% SDS-Polyacrylamide (w/v) gel (5.5.1). The gel was only run until the front reached 1/3 of the gel and stained with Coomassie stain. Every lane was cut in six pieces and analysed with mass spectrometry (5.5.10).

5.5.10 Protein identification Mass spectrometry

Mass spectrometry was done in the laboratory of Prof. Dr. Rainer Deutzmann.

5.5.10.1 Protein digestion

After rinsing Coomassie-stained SDS-gels with distilled water for several hours, protein bands were cut out using a scalpel and transferred into clean microtubes (Eppendorf). To remove substances interfering with trypsin digestion and/or mass spectrometry, the gel pieces were washed sequentially with 50 mM NH_4HCO_3, 50 mM NH_4HCO_3/acetonitrile (3/1), 25% acetonitrile (w/v), and 50% acetonitrile (w/v) for 30 min, respectively. After drying by lyophilisation for 1 h, proteins were digested

by 2 µg trypsin (sequencing grade, Roche)/100 µl gel volume in 50 mM NH_4HCO_3 overnight at 37 °C. Peptides were eluted by two extractions with 100 mM NH_4HCO_3, followed by one extraction with 50 mM NH_4HCO_3 in 50% acetonitrile (w/v). The combined extracts were lyophilized, resuspended in 50 µl H_2O and lyophilized again to reliably remove any residual NH_4HCO_3, which might interfere with the following procedures.

5.5.10.2 LC-MS/MS

Peptides were separated on a Ultimate 3000 RSLC nano HPLC System (Dionex) by reversed phase chromatography using an AcclaimPepmap 100 C18 nano column (15 cm long, 5µm in d meter, flow rate 300 nl/min, Thermo Fisher Scientific), with a binary buffer system consisting of 0.1% formic acid (v/v) (eluent A) and 80% acetonitril in 0.1% formic acid (v/v) (eluent B). The peptides were separated by a linear gradient form 10 to 60% in 80 min. The LC-System was coupled to a MaXis 4G UHR-Q TOF-system (Bruker Daltonik) via a nano electrospray source (Bruker Daltonik). The mass spectrometer was operated in the data dependent mode with MS and MS/MS scans acquired at a resolution of minimal 60000, the scan rate for MS spectra was 2 Hz. Up to five most abundant precursor ions were selected for fragmentation by collisional dissociation.

5.5.10.3 Data analysis

The data (mgf-files) were launched to Mascot using the ProteinScape software (Bruker Daltonics). Mascot (v2.3.02, Matrix Science) was used as a search engine to search a local copy of the NCBInr protein data base. The criterion for reliable protein identification were Mascot scores >85. This value defines a cut off value, where the probability of false positive identification is 5% ($P < 0.05$; score: -10*log (P)). Typically the proteins were identified unambiguously with Mascot scores above 100.

5.5.11 *In vitro* transcription and translation

For *in vitro* transcription and translation, the TNT R Coupled Wheat Germ Extract System (Promega) was used. For protein expression, the Plasmid pBC-SK-Spt5-2-NGN and pBC-SKSpt5L-NGN were used. Both plasmids have a T7 promoter but no T7 terminator, so the plasmids have been linearized before transcription. The proteins were expressed according to the manufacturer's instruction with 500 ng plasmid and 4 µCi [^{35}S] methionine. After every synthesis 20% of the reaction was analysed with SDS-PAGE (5.5.1).

5.5.12 Pull-down with *in vitro* expressed proteins

For the pull-down, 50 µl purified GST-SPT4-2 agarose beads slurry (5.5.3.2) and 20 µl *in vitro* expressed SPT5-2-NGN or 10 µl SPT5L-NGN (5.5.11) were used. SPT4-2 and the *in vitro* expressed protein was incubated for 4 h at 4 °C in a total volume of 300 µl reaction buffer (25 mM HEPES pH 7.4, 100 mM NaCl, 0.05% NP-40 (v/v), 5 mM DTT, 50 µg/ml BSA, 10% glycerol (v/v), 2 mM $MgCl_2$, 0.1 mg/ml AEBSF and proteinase inhibitor cocktail). After incubation the beads were washed three times with washing buffer (25 mM HEPES pH 7.4, 200 mM NaCl, 0.1% NP-40 (v/v), 5 mM DTT, 50 µg/ml BSA, 10% glycerol (v/v), 2 mM $MgCl_2$, 0.1 mg/ml AEBSF and proteinase inhibitor cocktail), loaded on an SDS-Gel (5.5.1), dried (Gel Dryer: Model 583), and detected on a phosphor-screen with a Cyclone™ Storage System (Packard).

5.5.13 Plant chromatin immunoprecipitation

For chromatin immunoprecipitation, three week old seedlings were used. 1.5 g of plant material were cross-linked in 36 ml extraction buffer 1 (0.4 M sucrose, 10 mM HEPES pH 8.0, 5 mM β-mercaptoethanol, 0.1 mg/ml AEBSF and proteinase inhibitor cocktail) with 1% formaldehyde (v/v) (1 ml of 37% stock). The seedlings were cross-linked in vacuum for 10 min. The cross-linking was stopped by adding glycine to a final concentration of 0.125 M and incubation in vacuum for 10 min. The seedlings were washed with water and frozen in liquid nitrogen.

The seedlings were ground in liquid nitrogen and 30 ml extraction buffer 1 was added. After the ground material was thawed, it was filtered through a double-layer of Miracloth (Calbiochem) and spun down (20 min, 3000 g, 4 °C). After centrifugation, the pellet was resuspended in 1 ml extraction buffer 2 (0.25 M sucrose, 10 mM HEPES pH 8.0, 1% Triton X-100 (v/v), 10 mM $MgCl_2$, 5 mM β-mercaptoethanol, 0.1 mg/ml AEBSF and proteinase inhibitor cocktail) and centrifuged for with 12000 g for 10 min at 4 °C. The supernatant was removed afterwards, and the pellet was resuspended in 300 µl extraction buffer 3 (1.7 M sucrose, 10 mM HEPES pH 8.0, 0.15% Triton X-100 (v/v), 2 mM $MgCl_2$, 5 mM β-mercaptoethanol, 0.1 mg/ml AEBSF and proteinase inhibitor cocktail). In a new 1.5 ml tube, 300 µl extraction buffer 3 were added, and the resuspended pellet was gently added that it stays as a top layer. Subsequently, it was spun down 1 h at 16000 g at 4 °C, and the pellet was resuspended in 300 µl Nuclei Lysis buffer (50 mM HEPES pH 8.0, 10 mM EDTA,

1% SDS (w/v), 0.1 mg/ml AEBSF and proteinase inhibitor cocktail) and incubated on ice for 30 min. Following the incubation on ice, the nuclei solution was diluted ten times with ChIP dilution buffer (1.1% Triton X-100 (v/v), 1.2 mM EDTA, 16.7 mM HEPES pH 8.0, 167 mM, 0.1 mg/ml AEBSF and proteinase inhibitor cocktail) and sonicated eight times for 30 sec with 53% output with a 30 sec pause between each sonication with a Bandeln Sonoplus HD 2070 and a MS 73 tip. Before and after sonication a 200 µl aliquot was taken to check the sonication efficiency. The approximately 2.5 ml were split into two 1.5 ml tubes and centrifuged for 10 min at full speed at 4 °C. In the meantime, Protein A agarose beads were washed three times with ChIP dilution buffer. The supernatant was pre-cleared with 35 µl Protein A agarose beads per 1.5 ml. After 1 h at 4 °C incubation with gentle agitation, the supernatant was taken and 12 µl or 5 mg antibody was added and incubated overnight at 4°C under gentle agitation.

The next day Protein A agarose beads (35 µ per sample) were washed with ChIP dilution buffer and incubated for 3 h at 4 °C with the protein extract-antibody mixture. After 3 h, the beads were pelleted and 500 µl of the mock control was taken as input DNA. The pellet was washed with Low Salt Wash buffer (150 mM NaCl, 0.1% SDS (w/v), 1% Triton X-100 (v/v), 2 mM EDTA and 20 mM HEPES pH 8.0), High Salt Wash buffer (500 mM NaCl, 0.1% SDS (w/v), 1% Triton X-100 (v/v), 2 mM EDTA and 20 mM HEPES pH 8.0), LiCl Wash buffer (0.25 M LiCl, 1% NP-40 (v/v), 1% sodium deoxycholate (w/v), 1 mM EDTA and 10 mM HEPES pH 8.0) and twice with TE buffer (10 mM Tris HCl pH 8.0 and 1mM EDTA) for 10 min for every washing step. After washing, the immune complexes were eluted by adding 250 µl elution buffer (1% SDS (w/v) and 0.1 M $NaHCO_3$) for 15 min at 65 °C with agitation (1000 g). The supernatant was transferred to another tube and the elution was repeated once. To reverse cross-linking, 20 µl 5 M NaCl were added to the eluate and incubated for at least 6 h at 65 °C with agitation (1000 g). Proteinase K (20 µl 5 M NaCl, 20 µl 1 M Tris HCl and 0.9 U Proteinase K) was used to digest the proteins for 3 h at 45 °C with agitation (1000 g).

The DNA was recovered with Phase Lock Gel tubes (5Prime). Therefore, the tubes were spun down for 30 sec at 16000 g and an equal amount (500 µl) of 25/24/1 phenol/chloroform/isoamyl alcohol was added to the eluate and poured onto the phase lock gels. The phases were separated by 5 min centrifugation with 16000 g and subsequently, 500 µl of 1-brom-3-chlorpropane was added and again centrifuged

for 5 min with 16000 g. 400 µl of the upper phase was taken off, and the DNA was precipitated by adding 40 µl 3 M NaAc pH 5.8 and 1 ml Ethanol and centrifuged for at least 30 min with full speed at 4 °C. The pellet was washed with 1 ml 70% Ethanol (v/v), dried and resuspended in 40 µl TE buffer with 10 µg/ml RNase A.

For PCR, the input was diluted 1:250, H3 1:10, all other AB and PI 1:5, and 5 µl were used per PCR reaction. Every sample was tested with primers against *ACT8* and the transposon *TA3*.

5.5.14 Immunostaining of root-nuclei

For immunostaining plants were grown on filter paper. After 3 days, the plants were fixed in fixation solution (4% paraformaldehyde (w/v) in 1x PBS adjusted to pH 7.5 with H_2SO_4) for 20 – 30 min on ice (vacuum was applied for the first two minutes). Subsequently the seedlings were washed three times for 5 min with 1x PBS and digested with digesting mixture (0.7% cellulase R-10, 0.7% cellulose (w/v), 1% pectolyase (w/v) and 1% cytohelicase (w/v)) for 20 – 30 min at 37 °C. The enzyme mix was removed and 1x PBS was added. The root tips were collected with a pipette and applied to an object slide. The remaining 1x PBS was removed and 15 µl 1x PBS with 0.1% Tween 20 (v/v) was added. The coverslip was carefully added to avoid air bubbles, and the root tips were squeezed with a toothpick avoiding sliding of the coverslip. The object slide was frozen in liquid nitrogen and the coverslip was removed using a razor blade. The slides were blocked for 1 h (1x PBS, 4% BSA (w/v), 0.1% Tween 20 (v/v) and 0.1% Triton X-100 (v/v)) and afterwards washed three times with 1x PBS. 100 µl of primary AB-solution was added (1x PBS, 1% BSA (w/v) and 1:200 AB) covered with parafilm and incubated overnight at 4 °C. The samples were again washed three times with 1x PBS and 100 µl secondary AB-solution was added and incubated for 1 h. After three last washing steps with 1x PBS, 15 µl DAPI antifade (Millipore) was added and the samples were analysed with a Leica SP8 confocal microscope.

6. Bibliography

Abel, S., Oeller, P.W., and Theologis, A. (1994). Early auxin-induced genes encode short-lived nuclear proteins. Proc Natl Acad Sci U S A **91,** 326-330.

Adelman, K., Marr, M.T., Werner, J., Saunders, A., Ni, Z., Andrulis, E.D., and Lis, J.T. (2005). Efficient release from promoter-proximal stall sites requires transcript cleavage factor TFIIS. Mol Cell **17,** 103-112.

Aguilera, A. (2005). Cotranscriptional mRNP assembly: from the DNA to the nuclear pore. Curr Opin Cell Biol **17,** 242-250.

Alexander, M.P. (1969). Differential staining of aborted and nonaborted pollen. Stain technology **44,** 117-122.

Anderson, S.J., Sikes, M.L., Zhang, Y., French, S.L., Salgia, S., Beyer, A.L., Nomura, M., and Schneider, D.A. (2011). The transcription elongation factor Spt5 influences transcription by RNA polymerase I positively and negatively. J Biol Chem **286,** 18816-18824.

Andrulis, E.D., Guzman, E., Doring, P., Werner, J., and Lis, J.T. (2000). High-resolution localization of Drosophila Spt5 and Spt6 at heat shock genes in vivo: roles in promoter proximal pausing and transcription elongation. Genes Dev **14,** 2635-2649.

Ansari, K.I., Mishra, B.P., and Mandal, S.S. (2009). MLL histone methylases in gene expression, hormone signaling and cell cycle. Frontiers in bioscience **14,** 3483-3495.

Anzola, J.M., Sieberer, T., Ortbauer, M., Butt, H., Korbei, B., Weinhofer, I., Mullner, A.E., and Luschnig, C. (2010). Putative Arabidopsis transcriptional adaptor protein (PROPORZ1) is required to modulate histone acetylation in response to auxin. Proc Natl Acad Sci U S A **107,** 10308-10313.

Autran, D., Jonak, C., Belcram, K., Beemster, G.T., Kronenberger, J., Grandjean, O., Inze, D., and Traas, J. (2002). Cell numbers and leaf development in Arabidopsis: a functional analysis of the STRUWWELPETER gene. EMBO J **21,** 6036-6049.

Balatsos, N.A., Nilsson, P., Mazza, C., Cusack, S., and Virtanen, A. (2006). Inhibition of mRNA deadenylation by the nuclear cap binding complex (CBC). J Biol Chem **281,** 4517-4522.

Bartkowiak, B., and Greenleaf, A.L. (2011). Phosphorylation of RNAPII: To P-TEFb or not to P-TEFb? Transcription **2,** 115-119.

Basehoar, A.D., Zanton, S.J., and Pugh, B.F. (2004). Identification and distinct regulation of yeast TATA box-containing genes. Cell **116,** 699-709.

Baumann, M., Pontiller, J., and Ernst, W. (2010). Structure and basal transcription complex of RNA polymerase II core promoters in the mammalian genome: an overview. Molecular biotechnology **45,** 241-247.

Bauren, G., Belikov, S., and Wieslander, L. (1998). Transcriptional termination in the Balbiani ring 1 gene is closely coupled to 3'-end formation and excision of the 3'-terminal intron. Genes Dev **12,** 2759-2769.

Beemster, G.T., and Baskin, T.I. (1998). Analysis of cell division and elongation underlying the developmental acceleration of root growth in Arabidopsis thaliana. Plant Physiol **116,** 1515-1526.

Belotserkovskaya, R., Oh, S., Bondarenko, V.A., Orphanides, G., Studitsky, V.M., and Reinberg, D. (2003). FACT facilitates transcription-dependent nucleosome alteration. Science **301,** 1090-1093.

Benjamins, R., and Scheres, B. (2008). Auxin: the looping star in plant development. Annu Rev Plant Biol **59,** 443-465.

Benkova, E., and Hejatko, J. (2009). Hormone interactions at the root apical meristem. Plant Mol Biol **69,** 383-396.

Bennett, M.J., Marchant, A., Green, H.G., May, S.T., Ward, S.P., Millner, P.A., Walker, A.R., Schulz, B., and Feldmann, K.A. (1996). Arabidopsis AUX1 gene: a permease-like regulator of root gravitropism. Science **273,** 948-950.

Bentsink, L., Jowett, J., Hanhart, C.J., and Koornneef, M. (2006). Cloning of DOG1, a quantitative trait locus controlling seed dormancy in Arabidopsis. Proc Natl Acad Sci U S A **103,** 17042-17047.

Berr, A., Menard, R., Heitz, T., and Shen, W.H. (2012). Chromatin modification and remodelling: a regulatory landscape for the control of Arabidopsis defence responses upon pathogen attack. Cellular microbiology **14,** 829-839.

Beyer, A.L., and Osheim, Y.N. (1988). Splice site selection, rate of splicing, and alternative splicing on nascent transcripts. Genes Dev **2,** 754-765.

Bies-Etheve, N., Pontier, D., Lahmy, S., Picart, C., Vega, D., Cooke, R., and Lagrange, T. (2009). RNA-directed DNA methylation requires an AGO4-interacting member of the SPT5 elongation factor family. EMBO Rep **10,** 649-654.

Bird, G., Zorio, D.A., and Bentley, D.L. (2004). RNA polymerase II carboxy-terminal domain phosphorylation is required for cotranscriptional pre-mRNA splicing and 3'-end formation. Mol Cell Biol **24,** 8963-8969.

Birse, C.E., Minvielle-Sebastia, L., Lee, B.A., Keller, W., and Proudfoot, N.J. (1998). Coupling termination of transcription to messenger RNA maturation in yeast. Science **280,** 298-301.

Bolstad, B.M., Irizarry, R.A., Astrand, M., and Speed, T.P. (2003). A comparison of normalization methods for high density oligonucleotide array data based on variance and bias. Bioinformatics **19,** 185-193.

Bourgeois, C.F., Kim, Y.K., Churcher, M.J., West, M.J., and Karn, J. (2002). Spt5 cooperates with human immunodeficiency virus type 1 Tat by preventing premature RNA release at terminator sequences. Mol Cell Biol **22,** 1079-1093.

Boyes, D.C., Zayed, A.M., Ascenzi, R., McCaskill, A.J., Hoffman, N.E., Davis, K.R., and Gorlach, J. (2001). Growth stage-based phenotypic analysis of Arabidopsis: a model for high throughput functional genomics in plants. Plant Cell **13,** 1499-1510.

Brand, L., Horler, M., Nuesch, E., Vassalli, S., Barrell, P., Yang, W., Jefferson, R.A., Grossniklaus, U., and Curtis, M.D. (2006). A versatile and reliable two-component system for tissue-specific gene induction in Arabidopsis. Plant Physiol **141,** 1194-1204.

Brewster, N.K., Johnston, G.C., and Singer, R.A. (2001). A bipartite yeast SSRP1 analog comprised of Pob3 and Nhp6 proteins modulates transcription. Mol Cell Biol **21,** 3491-3502.

Buratowski, S. (2009). Progression through the RNA polymerase II CTD cycle. Mol Cell **36,** 541-546.

Burckin, T., Nagel, R., Mandel-Gutfreund, Y., Shiue, L., Clark, T.A., Chong, J.L., Chang, T.H., Squazzo, S., Hartzog, G., and Ares, M., Jr. (2005). Exploring functional relationships between components of the gene expression machinery. Nat Struct Mol Biol **12,** 175-182.

Bush, M.S., Hutchins, A.P., Jones, A.M., Naldrett, M.J., Jarmolowski, A., Lloyd, C.W., and Doonan, J.H. (2009). Selective recruitment of proteins to 5' cap complexes during the growth cycle in Arabidopsis. Plant J **59,** 400-412.

Bushnell, D.A., Westover, K.D., Davis, R.E., and Kornberg, R.D. (2004). Structural basis of transcription: an RNA polymerase II-TFIIB cocrystal at 4.5 Angstroms. Science **303,** 983-988.

Calvo, O., and Manley, J.L. (2003). Strange bedfellows: polyadenylation factors at the promoter. Genes Dev **17,** 1321-1327.

Cang, Y., Auble, D.T., and Prelich, G. (1999). A new regulatory domain on the TATA-binding protein. EMBO J **18,** 6662-6671.

Chapman, E.J., and Estelle, M. (2009). Mechanism of auxin-regulated gene expression in plants. Annu Rev Genet **43,** 265-285.

Chapman, R.D., Heidemann, M., Hintermair, C., and Eick, D. (2008). Molecular evolution of the RNA polymerase II CTD. Trends Genet **24,** 289-296.

Chen, Y., Yamaguchi, Y., Tsugeno, Y., Yamamoto, J., Yamada, T., Nakamura, M., Hisatake, K., and Handa, H. (2009). DSIF, the Paf1 complex, and Tat-SF1 have nonredundant, cooperative roles in RNA polymerase II elongation. Genes Dev **23,** 2765-2777.

Cheng, H., Dufu, K., Lee, C.S., Hsu, J.L., Dias, A., and Reed, R. (2006a). Human mRNA export machinery recruited to the 5' end of mRNA. Cell **127,** 1389-1400.

Cheng, Y., Dai, X., and Zhao, Y. (2006b). Auxin biosynthesis by the YUCCA flavin monooxygenases controls the formation of floral organs and vascular tissues in Arabidopsis. Genes Dev **20,** 1790-1799.

Cheng, Y., Dai, X., and Zhao, Y. (2007). Auxin synthesized by the YUCCA flavin monooxygenases is essential for embryogenesis and leaf formation in Arabidopsis. Plant Cell **19,** 2430-2439.

Cho, E.J., Takagi, T., Moore, C.R., and Buratowski, S. (1997). mRNA capping enzyme is recruited to the transcription complex by phosphorylation of the RNA polymerase II carboxy-terminal domain. Genes Dev **11,** 3319-3326.

Cho, E.J., Kobor, M.S., Kim, M., Greenblatt, J., and Buratowski, S. (2001). Opposing effects of Ctk1 kinase and Fcp1 phosphatase at Ser 2 of the RNA polymerase II C-terminal domain. Genes Dev **15,** 3319-3329.

Clapier, C.R., and Cairns, B.R. (2009). The biology of chromatin remodeling complexes. Annu Rev Biochem **78,** 273-304.

Clarke, J.D., Volko, S.M., Ledford, H., Ausubel, F.M., and Dong, X. (2000). Roles of salicylic acid, jasmonic acid, and ethylene in cpr-induced resistance in arabidopsis. Plant Cell **12,** 2175-2190.

Clough, S.J., and Bent, A.F. (1998). Floral dip: a simplified method for Agrobacterium-mediated transformation of Arabidopsis thaliana. Plant J **16,** 735-743.

Colon-Carmona, A., You, R., Haimovitch-Gal, T., and Doerner, P. (1999). Technical advance: spatio-temporal analysis of mitotic activity with a labile cyclin-GUS fusion protein. Plant J **20,** 503-508.

Conaway, J.W., and Conaway, R.C. (1999). Transcription elongation and human disease. Annu Rev Biochem **68,** 301-319.

Core, L.J., Waterfall, J.J., and Lis, J.T. (2008). Nascent RNA sequencing reveals widespread pausing and divergent initiation at human promoters. Science **322,** 1845-1848.

Cormack, B.P., and Struhl, K. (1992). The TATA-binding protein is required for transcription by all three nuclear RNA polymerases in yeast cells. Cell **69,** 685-696.

Cramer, P. (2004). RNA polymerase II structure: from core to functional complexes. Curr Opin Genet Dev **14,** 218-226.

Cui, Y., and Denis, C.L. (2003). In vivo evidence that defects in the transcriptional elongation factors RPB2, TFIIS, and SPT5 enhance upstream poly(A) site utilization. Mol Cell Biol **23,** 7887-7901.

Daneholt, B. (2001). Assembly and transport of a premessenger RNP particle. Proc Natl Acad Sci U S A **98,** 7012-7017.

Danko, C.G., Hah, N., Luo, X., Martins, A.L., Core, L., Lis, J.T., Siepel, A., and Kraus, W.L. (2013). Signaling pathways differentially affect RNA polymerase II initiation, pausing, and elongation rate in cells. Mol Cell **50,** 212-222.

Das, B., Butler, J.S., and Sherman, F. (2003). Degradation of normal mRNA in the nucleus of Saccharomyces cerevisiae. Mol Cell Biol **23,** 5502-5515.

Deuring, R., Fanti, L., Armstrong, J.A., Sarte, M., Papoulas, O., Prestel, M., Daubresse, G., Verardo, M., Moseley, S.L., Berloco, M., Tsukiyama, T., Wu, C., Pimpinelli, S., and Tamkun, J.W. (2000). The ISWI chromatin-remodeling protein is required for gene expression and the maintenance of higher order chromatin structure in vivo. Mol Cell **5,** 355-365.

Dharmasiri, N., Dharmasiri, S., and Estelle, M. (2005). The F-box protein TIR1 is an auxin receptor. Nature **435,** 441-445.

Dhawan, R., Luo, H., Foerster, A.M., Abuqamar, S., Du, H.N., Briggs, S.D., Mittelsten Scheid, O., and Mengiste, T. (2009). HISTONE MONOUBIQUITINATION1 interacts with a subunit of the mediator complex and regulates defense against necrotrophic fungal pathogens in Arabidopsis. Plant Cell **21,** 1000-1019.

Dieci, G., Fiorino, G., Castelnuovo, M., Teichmann, M., and Pagano, A. (2007). The expanding RNA polymerase III transcriptome. Trends Genet **23,** 614-622.

Ding, B., LeJeune, D., and Li, S. (2010). The C-terminal repeat domain of Spt5 plays an important role in suppression of Rad26-independent transcription coupled repair. J Biol Chem **285,** 5317-5326.

Ding, Y., Avramova, Z., and Fromm, M. (2011). Two distinct roles of ARABIDOPSIS HOMOLOG OF TRITHORAX1 (ATX1) at promoters and within transcribed regions of ATX1-regulated genes. Plant Cell **23,** 350-363.

Ding, Y., Fromm, M., and Avramova, Z. (2012). Multiple exposures to drought 'train' transcriptional responses in Arabidopsis. Nat Commun **3,** 740.

Dong, X. (2004). NPR1, all things considered. Curr Opin Plant Biol **7,** 547-552.

Duroux, M., Houben, A., Ruzicka, K., Friml, J., and Grasser, K.D. (2004). The chromatin remodelling complex FACT associates with actively transcribed regions of the Arabidopsis genome. Plant J **40,** 660-671.

Durrant, W.E., and Dong, X. (2004). Systemic acquired resistance. Annu Rev Phytopathol **42,** 185-209.

Dvir, A. (2002). Promoter escape by RNA polymerase II. Biochim Biophys Acta **1577,** 208-223.

Egloff, S., and Murphy, S. (2008). Cracking the RNA polymerase II CTD code. Trends Genet **24,** 280-288.

Egloff, S., O'Reilly, D., Chapman, R.D., Taylor, A., Tanzhaus, K., Pitts, L., Eick, D., and Murphy, S. (2007). Serine-7 of the RNA polymerase II CTD is specifically required for snRNA gene expression. Science **318,** 1777-1779.

Fish, R.N., and Kane, C.M. (2002). Promoting elongation with transcript cleavage stimulatory factors. Biochim Biophys Acta **1577,** 287-307.

Fleischmann, G., Pflugfelder, G., Steiner, E.K., Javaherian, K., Howard, G.C., Wang, J.C., and Elgin, S.C. (1984). Drosophila DNA topoisomerase I is associated with transcriptionally active regions of the genome. Proc Natl Acad Sci U S A **81,** 6958-6962.

Fleury, D., Himanen, K., Cnops, G., Nelissen, H., Boccardi, T.M., Maere, S., Beemster, G.T., Neyt, P., Anami, S., Robles, P., Micol, J.L., Inze, D., and Van Lijsebettens, M. (2007). The Arabidopsis thaliana homolog of yeast BRE1 has a function in cell cycle regulation during early leaf and root growth. Plant Cell **19,** 417-432.

Formosa, T. (2008). FACT and the reorganized nucleosome. Molecular bioSystems **4,** 1085-1093.

Friml, J., Vieten, A., Sauer, M., Weijers, D., Schwarz, H., Hamann, T., Offringa, R., and Jurgens, G. (2003). Efflux-dependent auxin gradients establish the apical-basal axis of Arabidopsis. Nature **426,** 147-153.

Fujita, T., Piuz, I., and Schlegel, W. (2009). The transcription elongation factors NELF, DSIF and P-TEFb control constitutive transcription in a gene-specific manner. FEBS Lett **583,** 2893-2898.

Fukaki, H., Taniguchi, N., and Tasaka, M. (2006). PICKLE is required for SOLITARY-ROOT/IAA14-mediated repression of ARF7 and ARF19 activity during Arabidopsis lateral root initiation. Plant J **48,** 380-389.

Giardina, C., Perez-Riba, M., and Lis, J.T. (1992). Promoter melting and TFIID complexes on Drosophila genes in vivo. Genes Dev **6,** 2190-2200.

Gilmour, D.S., and Lis, J.T. (1986). RNA polymerase II interacts with the promoter region of the noninduced hsp70 gene in Drosophila melanogaster cells. Mol Cell Biol **6,** 3984-3989.

Glover-Cutter, K., Kim, S., Espinosa, J., and Bentley, D.L. (2008). RNA polymerase II pauses and associates with pre-mRNA processing factors at both ends of genes. Nat Struct Mol Biol **15,** 71-78.

Gonzalez-Lamothe, R., El Oirdi, M., Brisson, N., and Bouarab, K. (2012). The conjugated auxin indole-3-acetic acid-aspartic acid promotes plant disease development. Plant Cell **24,** 762-777.

Grasser, K.D. (2005). Emerging role for transcript elongation in plant development. Trends Plant Sci **10,** 484-490.

Grasser, M., Lentz, A., Lichota, J., Merkle, T., and Grasser, K.D. (2006). The Arabidopsis genome encodes structurally and functionally diverse HMGB-type proteins. J Mol Biol **358,** 654-664.

Grasser, M., Kane, C.M., Merkle, T., Melzer, M., Emmersen, J., and Grasser, K.D. (2009). Transcript elongation factor TFIIS is involved in arabidopsis seed dormancy. J Mol Biol **386,** 598-611.

Greive, S.J., and von Hippel, P.H. (2005). Thinking quantitatively about transcriptional regulation. Nat Rev Mol Cell Biol **6,** 221-232.

Grieneisen, V.A., Xu, J., Maree, A.F., Hogeweg, P., and Scheres, B. (2007). Auxin transport is sufficient to generate a maximum and gradient guiding root growth. Nature **449,** 1008-1013.

Grohmann, D., Nagy, J., Chakraborty, A., Klose, D., Fielden, D., Ebright, R.H., Michaelis, J., and Werner, F. (2011). The initiation factor TFE and the elongation factor Spt4/5 compete for the RNAP clamp during transcription initiation and elongation. Mol Cell **43,** 263-274.

Gromak, N., West, S., and Proudfoot, N.J. (2006). Pause sites promote transcriptional termination of mammalian RNA polymerase II. Mol Cell Biol **26,** 3986-3996.

Grosso, A.R., de Almeida, S.F., Braga, J., and Carmo-Fonseca, M. (2012). Dynamic transitions in RNA polymerase II density profiles during transcription termination. Genome Res **22,** 1447-1456.

Grummt, I. (2003). Life on a planet of its own: regulation of RNA polymerase I transcription in the nucleolus. Genes Dev **17,** 1691-1702.

Gu, X.L., Wang, H., Huang, H., and Cui, X.F. (2012). SPT6L encoding a putative WG/GW-repeat protein regulates apical-basal polarity of embryo in Arabidopsis. Mol Plant **5,** 249-259.

Guilfoyle, T.J., and Hagen, G. (2012). Getting a grasp on domain III/IV responsible for Auxin Response Factor-IAA protein interactions. Plant science : an international journal of experimental plant biology **190,** 82-88.

Guo, M., Xu, F., Yamada, J., Egelhofer, T., Gao, Y., Hartzog, G.A., Teng, M., and Niu, L. (2008). Core structure of the yeast spt4-spt5 complex: a conserved module for regulation of transcription elongation. Structure **16,** 1649-1658.

Hagen, G., and Guilfoyle, T. (2002). Auxin-responsive gene expression: genes, promoters and regulatory factors. Plant Mol Biol **49,** 373-385.

Hajheidari, M., Koncz, C., and Eick, D. (2013). Emerging roles for RNA polymerase II CTD in Arabidopsis. Trends Plant Sci.

Hajheidari, M., Farrona, S., Huettel, B., Koncz, Z., and Koncz, C. (2012). CDKF;1 and CDKD protein kinases regulate phosphorylation of serine residues in the C-terminal domain of Arabidopsis RNA polymerase II. Plant Cell **24,** 1626-1642.

Harashima, H., Kato, K., Shinmyo, A., and Sekine, M. (2007). Auxin is required for the assembly of A-type cyclin-dependent kinase complexes in tobacco cell suspension culture. Journal of plant physiology **164,** 1103-1112.

Harris, J.K., Kelley, S.T., Spiegelman, G.B., and Pace, N.R. (2003). The genetic core of the universal ancestor. Genome Res **13,** 407-412.

Hartzog, G.A., and Fu, J. (2013). The Spt4-Spt5 complex: a multi-faceted regulator of transcription elongation. Biochim Biophys Acta **1829,** 105-115.

Hartzog, G.A., Wada, T., Handa, H., and Winston, F. (1998). Evidence that Spt4, Spt5, and Spt6 control transcription elongation by RNA polymerase II in Saccharomyces cerevisiae. Genes & Development **12,** 357-369.

Hartzog, G.A., Basrai, M.A., Ricupero-Hovasse, S.L., Hieter, P., and Winston, F. (1996). Identification and analysis of a functional human homolog of the SPT4 gene of Saccharomyces cerevisiae. Mol Cell Biol **16,** 2848-2856.

Hayashi, K. (2012). The interaction and integration of auxin signaling components. Plant Cell Physiol **53,** 965-975.

He, X.J., Hsu, Y.F., Zhu, S., Wierzbicki, A.T., Pontes, O., Pikaard, C.S., Liu, H.L., Wang, C.S., Jin, H., and Zhu, J.K. (2009). An effector of RNA-directed DNA methylation in arabidopsis is an ARGONAUTE 4- and RNA-binding protein. Cell **137,** 498-508.

Heidemann, M., Hintermair, C., Voss, K., and Eick, D. (2013). Dynamic phosphorylation patterns of RNA polymerase II CTD during transcription. Biochim Biophys Acta **1829,** 55-62.

Herr, A.J., Jensen, M.B., Dalmay, T., and Baulcombe, D.C. (2005). RNA polymerase IV directs silencing of endogenous DNA. Science **308,** 118-120.

Hieb, A.R., Baran, S., Goodrich, J.A., and Kugel, J.F. (2006). An 8 nt RNA triggers a rate-limiting shift of RNA polymerase II complexes into elongation. EMBO J **25,** 3100-3109.

Hirtreiter, A., Damsma, G.E., Cheung, A.C., Klose, D., Grohmann, D., Vojnic, E., Martin, A.C., Cramer, P., and Werner, F. (2010). Spt4/5 stimulates transcription elongation through the RNA polymerase clamp coiled-coil motif. Nucleic Acids Res **38,** 4040-4051.

Holstege, F.C., Fiedler, U., and Timmers, H.T. (1997). Three transitions in the RNA polymerase II transcription complex during initiation. EMBO J **16,** 7468-7480.

Huertas, P., and Aguilera, A. (2003). Cotranscriptionally formed DNA:RNA hybrids mediate transcription elongation impairment and transcription-associated recombination. Mol Cell **12,** 711-721.

Huh, W.K., Falvo, J.V., Gerke, L.C., Carroll, A.S., Howson, R.W., Weissman, J.S., and O'Shea, E.K. (2003). Global analysis of protein localization in budding yeast. Nature **425,** 686-691.

Iglesias, N., and Stutz, F. (2008). Regulation of mRNP dynamics along the export pathway. FEBS Lett **582,** 1987-1996.

Inoue, H., Nojima, H., and Okayama, H. (1990). High efficiency transformation of Escherichia coli with plasmids. Gene **96,** 23-28.

Ito, T., Arimitsu, N., Takeuchi, M., Kawamura, N., Nagata, M., Saso, K., Akimitsu, N., Hamamoto, H., Natori, S., Miyajima, A., and Sekimizu, K. (2006). Transcription elongation factor S-II is required for definitive hematopoiesis. Mol Cell Biol **26,** 3194-3203.

Izaurralde, E., Lewis, J., McGuigan, C., Jankowska, M., Darzynkiewicz, E., and Mattaj, I.W. (1994). A nuclear cap binding protein complex involved in pre-mRNA splicing. Cell **78,** 657-668.

Izban, M.G., and Luse, D.S. (1991). Transcription on nucleosomal templates by RNA polymerase II in vitro: inhibition of elongation with enhancement of sequence-specific pausing. Genes Dev **5,** 683-696.

Jager, K., Fabian, A., Tompa, G., Deak, C., Hohn, M., Olmedilla, A., Barnabas, B., and Papp, I. (2011). New phenotypes of the drought-tolerant cbp20 Arabidopsis thaliana mutant have changed epidermal morphology. Plant biology **13,** 78-84.

Jiang, Y., Yan, M., and Gralla, J.D. (1996). A three-step pathway of transcription initiation leading to promoter clearance at an activation RNA polymerase II promoter. Mol Cell Biol **16,** 1614-1621.

Jones, J.D., and Dangl, J.L. (2006). The plant immune system. Nature **444,** 323-329.

Juven-Gershon, T., Hsu, J.Y., Theisen, J.W., and Kadonaga, J.T. (2008). The RNA polymerase II core promoter - the gateway to transcription. Curr Opin Cell Biol **20,** 253-259.

Kaplan, C.D., Morris, J.R., Wu, C., and Winston, F. (2000). Spt5 and spt6 are associated with active transcription and have characteristics of general elongation factors in D. melanogaster. Genes Dev **14,** 2623-2634.

Kepinski, S., and Leyser, O. (2004). Auxin-induced SCFTIR1-Aux/IAA interaction involves stable modification of the SCFTIR1 complex. Proc Natl Acad Sci U S A **101,** 12381-12386.

Kettenberger, H., Armache, K.J., and Cramer, P. (2003). Architecture of the RNA polymerase II-TFIIS complex and implications for mRNA cleavage. Cell **114,** 347-357.

Kim, H.J., Jeong, S.H., Heo, J.H., Jeong, S.J., Kim, S.T., Youn, H.D., Han, J.W., Lee, H.W., and Cho, E.J. (2004). mRNA capping enzyme activity is coupled to an early transcription elongation. Mol Cell Biol **24,** 6184-6193.

Klein, B.J., Bose, D., Baker, K.J., Yusoff, Z.M., Zhang, X., and Murakami, K.S. (2011). RNA polymerase and transcription elongation factor Spt4/5 complex structure. Proc Natl Acad Sci U S A **108,** 546-550.

Komarnitsky, P., Cho, E.J., and Buratowski, S. (2000). Different phosphorylated forms of RNA polymerase II and associated mRNA processing factors during transcription. Genes Dev **14,** 2452-2460.

Komori, T., Inukai, N., Yamada, T., Yamaguchi, Y., and Handa, H. (2009). Role of human transcription elongation factor DSIF in the suppression of senescence and apoptosis. Genes Cells **14,** 343-354.

Konieczny, A., Voytas, D.F., Cummings, M.P., and Ausubel, F.M. (1991). A superfamily of Arabidopsis thaliana retrotransposons. Genetics **127,** 801-809.

Kostrewa, D., Zeller, M.E., Armache, K.J., Seizl, M., Leike, K., Thomm, M., and Cramer, P. (2009). RNA polymerase II-TFIIB structure and mechanism of transcription initiation. Nature **462,** 323-330.

Koutelou, E., Hirsch, C.L., and Dent, S.Y. (2010). Multiple faces of the SAGA complex. Curr Opin Cell Biol **22,** 374-382.

Kremer, S.B., Kim, S., Jeon, J.O., Moustafa, Y.W., Chen, A., Zhao, J., and Gross, D.S. (2012). Role of Mediator in regulating Pol II elongation and nucleosome displacement in Saccharomyces cerevisiae. Genetics **191,** 95-106.

Krishnamurthy, S., He, X., Reyes-Reyes, M., Moore, C., and Hampsey, M. (2004). Ssu72 Is an RNA polymerase II CTD phosphatase. Mol Cell **14,** 387-394.

Krishnan, K., Salomonis, N., and Guo, S. (2008). Identification of Spt5 target genes in zebrafish development reveals its dual activity in vivo. PLoS One **3,** e3621.

Krogan, N.J., Dover, J., Wood, A., Schneider, J., Heidt, J., Boateng, M.A., Dean, K., Ryan, O.W., Golshani, A., Johnston, M., Greenblatt, J.F., and Shilatifard, A. (2003). The Paf1 complex is required for histone H3 methylation by COMPASS and Dot1p: linking transcriptional elongation to histone methylation. Mol Cell **11,** 721-729.

Krogan, N.T., Ckurshumova, W., Marcos, D., Caragea, A.E., and Berleth, T. (2012). Deletion of MP/ARF5 domains III and IV reveals a requirement for Aux/IAA regulation in Arabidopsis leaf vascular patterning. New Phytol **194,** 391-401.

Kruk, J.A., Dutta, A., Fu, J., Gilmour, D.S., and Reese, J.C. (2011). The multifunctional Ccr4-Not complex directly promotes transcription elongation. Genes Dev **25,** 581-593.

Kuehner, J.N., Pearson, E.L., and Moore, C. (2011). Unravelling the means to an end: RNA polymerase II transcription termination. Nat Rev Mol Cell Biol **12,** 283-294.

Kuras, L., and Struhl, K. (1999). Binding of TBP to promoters in vivo is stimulated by activators and requires Pol II holoenzyme. Nature **399,** 609-613.

Laine, J.P., and Egly, J.M. (2006). When transcription and repair meet: a complex system. Trends Genet **22,** 430-436.

Laubinger, S., Sachsenberg, T., Zeller, G., Busch, W., Lohmann, J.U., Ratsch, G., and Weigel, D. (2008). Dual roles of the nuclear cap-binding complex and SERRATE in pre-mRNA splicing and microRNA processing in Arabidopsis thaliana. Proc Natl Acad Sci U S A **105,** 8795-8800.

Lee, K.A., Guertin, D., and Sonenberg, N. (1983). mRNA secondary structure as a determinant in cap recognition and initiation complex formation. ATP-Mg2+ independent cross-linking of cap binding proteins to m7I-capped inosine-substituted reovirus mRNA. J Biol Chem **258,** 707-710.

Lei, E.P., Krebber, H., and Silver, P.A. (2001). Messenger RNAs are recruited for nuclear export during transcription. Genes Dev **15,** 1771-1782.

Lenasi, T., and Barboric, M. (2010). P-TEFb stimulates transcription elongation and pre-mRNA splicing through multilateral mechanisms. Rna Biology **7,** 145-150.

Lenasi, T., and Barboric, M. (2013). Mutual relationships between transcription and pre-mRNA processing in the synthesis of mRNA. Wiley Interdiscip Rev RNA **4,** 139-154.

Lenasi, T., Peterlin, B.M., and Barboric, M. (2011). Cap-binding protein complex links pre-mRNA capping to transcription elongation and alternative splicing through positive transcription elongation factor b (P-TEFb). J Biol Chem **286,** 22758-22768.

Li, B., Carey, M., and Workman, J.L. (2007a). The role of chromatin during transcription. Cell **128,** 707-719.

Li, H., Zhang, Z., Wang, B., Zhang, J., Zhao, Y., and Jin, Y. (2007b). Wwp2-mediated ubiquitination of the RNA polymerase II large subunit in mouse embryonic pluripotent stem cells. Mol Cell Biol **27,** 5296-5305.

Li, Y., Zeng, S.X., Landais, I., and Lu, H. (2007c). Human SSRP1 has Spt16-dependent and -independent roles in gene transcription. J Biol Chem **282,** 6936-6945.

Liang, W., Li, C., Liu, F., Jiang, H., Li, S., Sun, J., Wu, X., and Li, C. (2009). The Arabidopsis homologs of CCR4-associated factor 1 show mRNA deadenylation activity and play a role in plant defence responses. Cell Res **19,** 307-316.

Licatalosi, D.D., Geiger, G., Minet, M., Schroeder, S., Cilli, K., McNeil, J.B., and Bentley, D.L. (2002). Functional interaction of yeast pre-mRNA 3' end processing factors with RNA polymerase II. Mol Cell **9,** 1101-1111.

Lindstrom, D.L., and Hartzog, G.A. (2001). Genetic interactions of Spt4-Spt5 and TFIIS with the RNA polymerase II CTD and CTD modifying enzymes in Saccharomyces cerevisiae. Genetics **159,** 487-497.

Lindstrom, D.L., Squazzo, S.L., Muster, N., Burckin, T.A., Wachter, K.C., Emigh, C.A., McCleery, J.A., Yates, J.R., 3rd, and Hartzog, G.A. (2003). Dual roles for Spt5 in pre-mRNA processing and transcription elongation revealed by identification of Spt5-associated proteins. Mol Cell Biol **23,** 1368-1378.

Lis, J. (1998). Promoter-associated pausing in promoter architecture and postinitiation transcriptional regulation. Cold Spring Harbor symposia on quantitative biology **63,** 347-356.

Littlefield, O., Korkhin, Y., and Sigler, P.B. (1999). The structural basis for the oriented assembly of a TBP/TFB/promoter complex. Proc Natl Acad Sci U S A **96,** 13668-13673.

Liu, P., Kenney, J.M., Stiller, J.W., and Greenleaf, A.L. (2010). Genetic organization, length conservation, and evolution of RNA polymerase II carboxyl-terminal domain. Molecular biology and evolution **27,** 2628-2641.

Liu, X., Bushnell, D.A., and Kornberg, R.D. (2013). RNA polymerase II transcription: structure and mechanism. Biochim Biophys Acta **1829,** 2-8.

Liu, Y., Kung, C., Fishburn, J., Ansari, A.Z., Shokat, K.M., and Hahn, S. (2004). Two cyclin-dependent kinases promote RNA polymerase II transcription and formation of the scaffold complex. Mol Cell Biol **24,** 1721-1735.

Liu, Y., Warfield, L., Zhang, C., Luo, J., Allen, J., Lang, W.H., Ranish, J., Shokat, K.M., and Hahn, S. (2009). Phosphorylation of the transcription elongation factor Spt5 by yeast Bur1 kinase stimulates recruitment of the PAF complex. Mol Cell Biol **29,** 4852-4863.

Logemann, J., Schell, J., and Willmitzer, L. (1987). Improved method for the isolation of RNA from plant tissues. Analytical biochemistry **163,** 16-20.

Lolas, I.B. (2009). Characterization of Arabidopsis plants harboring mutations in the genes encoding the chromatin associated FACT complex. In Department of Life Sciences (Aalborg University), pp. 168.

Lolas, I.B., Himanen, K., Gronlund, J.T., Lynggaard, C., Houben, A., Melzer, M., Van Lijsebettens, M., and Grasser, K.D. (2010). The transcript elongation factor FACT affects Arabidopsis vegetative and reproductive development and genetically interacts with HUB1/2. Plant J **61,** 686-697.

Luerssen, H., Kirik, V., Herrmann, P., and Misera, S. (1998). FUSCA3 encodes a protein with a conserved VP1/AB13-like B3 domain which is of functional importance for the regulation of seed maturation in Arabidopsis thaliana. Plant J **15,** 755-764.

MacKellar, A.L., and Greenleaf, A.L. (2011). Cotranscriptional association of mRNA export factor Yra1 with C-terminal domain of RNA polymerase II. J Biol Chem **286,** 36385-36395.

Maere, S., Heymans, K., and Kuiper, M. (2005). BiNGO: a Cytoscape plugin to assess overrepresentation of gene ontology categories in biological networks. Bioinformatics **21,** 3448-3449.

Malagon, F., Tong, A.H., Shafer, B.K., and Strathern, J.N. (2004). Genetic interactions of DST1 in Saccharomyces cerevisiae suggest a role of TFIIS in the initiation-elongation transition. Genetics **166,** 1215-1227.

Malone, E.A., Fassler, J.S., and Winston, F. (1993). Molecular and genetic characterization of SPT4, a gene important for transcription initiation in Saccharomyces cerevisiae. Molecular & general genetics : MGG **237,** 449-459.

Mandal, S.S., Chu, C., Wada, T., Handa, H., Shatkin, A.J., and Reinberg, D. (2004). Functional interactions of RNA-capping enzyme with factors that positively and negatively regulate promoter escape by RNA polymerase II. Proc Natl Acad Sci U S A **101,** 7572-7577.

Mandel, C.R., Bai, Y., and Tong, L. (2008). Protein factors in pre-mRNA 3'-end processing. Cell Mol Life Sci **65,** 1099-1122.

March-Diaz, R., Garcia-Dominguez, M., Lozano-Juste, J., Leon, J., Florencio, F.J., and Reyes, J.C. (2008). Histone H2A.Z and homologues of components of the SWR1 complex are required to control immunity in Arabidopsis. Plant J **53,** 475-487.

Martinez-Rucobo, F.W., and Cramer, P. (2013). Structural basis of transcription elongation. Biochim Biophys Acta **1829,** 9-19.

Martinez-Rucobo, F.W., Sainsbury, S., Cheung, A.C., and Cramer, P. (2011). Architecture of the RNA polymerase-Spt4/5 complex and basis of universal transcription processivity. EMBO J **30,** 1302-1310.

Mason, P.B., and Struhl, K. (2003). The FACT complex travels with elongating RNA polymerase II and is important for the fidelity of transcriptional initiation in vivo. Mol Cell Biol **23,** 8323-8333.

Mason, P.B., and Struhl, K. (2005). Distinction and relationship between elongation rate and processivity of RNA polymerase II in vivo. Mol Cell **17,** 831-840.

Mathis, D.J., and Chambon, P. (1981). The SV40 early region TATA box is required for accurate in vitro initiation of transcription. Nature **290,** 310-315.

Mavrich, T.N., Jiang, C., Ioshikhes, I.P., Li, X., Venters, B.J., Zanton, S.J., Tomsho, L.P., Qi, J., Glaser, R.L., Schuster, S.C., Gilmour, D.S., Albert, I., and Pugh, B.F. (2008). Nucleosome organization in the Drosophila genome. Nature **453,** 358-362.

Mayer, A., Lidschreiber, M., Siebert, M., Leike, K., Soding, J., and Cramer, P. (2010). Uniform transitions of the general RNA polymerase II transcription complex. Nat Struct Mol Biol **17,** 1272-1278.

Mehrnia, M., Balazadeh, S., Zanor, M.I., and Mueller-Roeber, B. (2013). EBE, an AP2/ERF transcription factor highly expressed in proliferating cells, affects shoot architecture in Arabidopsis. Plant Physiol **162,** 842-857.

Mischo, H.E., and Proudfoot, N.J. (2013). Disengaging polymerase: terminating RNA polymerase II transcription in budding yeast. Biochim Biophys Acta **1829,** 174-185.

Missra, A., and Gilmour, D.S. (2010). Interactions between DSIF (DRB sensitivity inducing factor), NELF (negative elongation factor), and the Drosophila RNA polymerase II transcription elongation complex. Proc Natl Acad Sci U S A **107,** 11301-11306.

Moore, M.J., and Proudfoot, N.J. (2009). Pre-mRNA processing reaches back to transcription and ahead to translation. Cell **136,** 688-700.

Morris, D.P., and Greenleaf, A.L. (2000). The splicing factor, Prp40, binds the phosphorylated carboxyl-terminal domain of RNA polymerase II. J Biol Chem **275,** 39935-39943.

Mosley, A.L., Pattenden, S.G., Carey, M., Venkatesh, S., Gilmore, J.M., Florens, L., Workman, J.L., and Washburn, M.P. (2009). Rtr1 is a CTD phosphatase that regulates RNA polymerase II during the transition from serine 5 to serine 2 phosphorylation. Mol Cell **34,** 168-178.

Muse, G.W., Gilchrist, D.A., Nechaev, S., Shah, R., Parker, J.S., Grissom, S.F., Zeitlinger, J., and Adelman, K. (2007). RNA polymerase is poised for activation across the genome. Nature genetics **39,** 1507-1511.

Myers, L.C., Gustafsson, C.M., Bushnell, D.A., Lui, M., Erdjument-Bromage, H., Tempst, P., and Kornberg, R.D. (1998). The Med proteins of yeast and their function through the RNA polymerase II carboxy-terminal domain. Genes Dev **12,** 45-54.

Narita, T., Yamaguchi, Y., Yano, K., Sugimoto, S., Chanarat, S., Wada, T., Kim, D.K., Hasegawa, J., Omori, M., Inukai, N., Endoh, M., Yamada, T., and Handa, H. (2003). Human transcription elongation factor NELF: identification of novel subunits and reconstitution of the functionally active complex. Mol Cell Biol **23,** 1863-1873.

Nelissen, H., Fleury, D., Bruno, L., Robles, P., De Veylder, L., Traas, J., Micol, J.L., Van Montagu, M., Inze, D., and Van Lijsebettens, M. (2005). The elongata mutants identify a functional Elongator complex in plants with a role in cell proliferation during organ growth. Proc Natl Acad Sci U S A **102,** 7754-7759.

Nelissen, H., De Groeve, S., Fleury, D., Neyt, P., Bruno, L., Bitonti, M.B., Vandenbussche, F., Van der Straeten, D., Yamaguchi, T., Tsukaya, H., Witters, E., De Jaeger, G., Houben, A., and Van Lijsebettens, M. (2010). Plant Elongator regulates auxin-related genes during RNA polymerase II transcription elongation. Proc Natl Acad Sci U S A **107,** 1678-1683.

O'Brien, T., Hardin, S., Greenleaf, A., and Lis, J.T. (1994). Phosphorylation of RNA polymerase II C-terminal domain and transcriptional elongation. Nature **370,** 75-77.

Onodera, Y., Haag, J.R., Ream, T., Costa Nunes, P., Pontes, O., and Pikaard, C.S. (2005). Plant nuclear RNA polymerase IV mediates siRNA and DNA methylation-dependent heterochromatin formation. Cell **120,** 613-622.

Otero, G., Fellows, J., Li, Y., de Bizemont, T., Dirac, A.M., Gustafsson, C.M., Erdjument-Bromage, H., Tempst, P., and Svejstrup, J.Q. (1999). Elongator, a multisubunit component of a novel RNA polymerase II holoenzyme for transcriptional elongation. Mol Cell **3,** 109-118.

Ouyang, J., Shao, X., and Li, J. (2000). Indole-3-glycerol phosphate, a branchpoint of indole-3-acetic acid biosynthesis from the tryptophan biosynthetic pathway in Arabidopsis thaliana. Plant J **24,** 327-333.

Overvoorde, P.J., Okushima, Y., Alonso, J.M., Chan, A., Chang, C., Ecker, J.R., Hughes, B., Liu, A., Onodera, C., Quach, H., Smith, A., Yu, G., and Theologis, A. (2005). Functional genomic analysis of the AUXIN/INDOLE-3-ACETIC ACID gene family members in Arabidopsis thaliana. Plant Cell **17,** 3282-3300.

Pal, M., and Luse, D.S. (2003). The initiation-elongation transition: lateral mobility of RNA in RNA polymerase II complexes is greatly reduced at +8/+9 and absent by +23. Proc Natl Acad Sci U S A **100,** 5700-5705.

Palangat, M., and Larson, D.R. (2012). Complexity of RNA polymerase II elongation dynamics. Biochim Biophys Acta **1819,** 667-672.

Pandit, S., Wang, D., and Fu, X.D. (2008). Functional integration of transcriptional and RNA processing machineries. Curr Opin Cell Biol **20,** 260-265.

Pandya-Jones, A., and Black, D.L. (2009). Co-transcriptional splicing of constitutive and alternative exons. Rna **15,** 1896-1908.

Paponov, I.A., Teale, W.D., Trebar, M., Blilou, I., and Palme, K. (2005). The PIN auxin efflux facilitators: evolutionary and functional perspectives. Trends Plant Sci **10,** 170-177.

Paponov, I.A., Paponov, M., Teale, W., Menges, M., Chakrabortee, S., Murray, J.A., and Palme, K. (2008). Comprehensive transcriptome analysis of auxin responses in Arabidopsis. Mol Plant **1,** 321-337.

Papp, I., Mur, L.A., Dalmadi, A., Dulai, S., and Koncz, C. (2004). A mutation in the Cap Binding Protein 20 gene confers drought tolerance to Arabidopsis. Plant Mol Biol **55,** 679-686.

Pauwels, L., Barbero, G.F., Geerinck, J., Tilleman, S., Grunewald, W., Perez, A.C., Chico, J.M., Bossche, R.V., Sewell, J., Gil, E., Garcia-Casado, G., Witters, E., Inze, D., Long, J.A., De Jaeger, G., Solano, R., and Goossens, A. (2010). NINJA connects the co-repressor TOPLESS to jasmonate signalling. Nature **464,** 788-791.

Pavri, R., Zhu, B., Li, G., Trojer, P., Mandal, S., Shilatifard, A., and Reinberg, D. (2006). Histone H2B monoubiquitination functions cooperatively with FACT to regulate elongation by RNA polymerase II. Cell **125,** 703-717.

Pei, Y., and Shuman, S. (2002). Interactions between fission yeast mRNA capping enzymes and elongation factor Spt5. J Biol Chem **277,** 19639-19648.

Pei, Y., Schwer, B., and Shuman, S. (2003). Interactions between fission yeast Cdk9, its cyclin partner Pch1, and mRNA capping enzyme Pct1 suggest an elongation checkpoint for mRNA quality control. J Biol Chem **278,** 7180-7188.

Perales, R., and Bentley, D. (2009). "Cotranscriptionality": the transcription elongation complex as a nexus for nuclear transactions. Mol Cell **36,** 178-191.

Peret, B., De Rybel, B., Casimiro, I., Benkova, E., Swarup, R., Laplaze, L., Beeckman, T., and Bennett, M.J. (2009). Arabidopsis lateral root development: an emerging story. Trends Plant Sci **14,** 399-408.

Peret, B., Swarup, K., Ferguson, A., Seth, M., Yang, Y., Dhondt, S., James, N., Casimiro, I., Perry, P., Syed, A., Yang, H., Reemmer, J., Venison, E., Howells, C., Perez-Amador, M.A., Yun, J., Alonso, J., Beemster, G.T.,

Laplaze, L., Murphy, A., Bennett, M.J., Nielsen, E., and Swarup, R. (2012). AUX/LAX genes encode a family of auxin influx transporters that perform distinct functions during Arabidopsis development. Plant Cell **24,** 2874-2885.

Pérez-Pérez, J.M., Candela, H., and Micol, J.L. (2009). Understanding synergy in genetic interactions. Trends in genetics : TIG **25,** 368-376.

Perrot-Rechenmann, C. (2010). Cellular responses to auxin: division versus expansion. Cold Spring Harb Perspect Biol **2,** a001446.

Petersson, S.V., Johansson, A.I., Kowalczyk, M., Makoveychuk, A., Wang, J.Y., Moritz, T., Grebe, M., Benfey, P.N., Sandberg, G., and Ljung, K. (2009). An auxin gradient and maximum in the Arabidopsis root apex shown by high-resolution cell-specific analysis of IAA distribution and synthesis. Plant Cell **21,** 1659-1668.

Pokholok, D.K., Hannett, N.M., and Young, R.A. (2002). Exchange of RNA polymerase II initiation and elongation factors during gene expression in vivo. Mol Cell **9,** 799-809.

Pontier, D., Yahubyan, G., Vega, D., Bulski, A., Saez-Vasquez, J., Hakimi, M.A., Lerbs-Mache, S., Colot, V., and Lagrange, T. (2005). Reinforcement of silencing at transposons and highly repeated sequences requires the concerted action of two distinct RNA polymerases IV in Arabidopsis. Genes Dev **19,** 2030-2040.

Ponting, C.P. (2002). Novel domains and orthologues of eukaryotic transcription elongation factors. Nucleic Acids Res **30,** 3643-3652.

Price, D.H. (2000). P-TEFb, a cyclin-dependent kinase controlling elongation by RNA polymerase II. Mol Cell Biol **20,** 2629-2634.

Proudfoot, N.J. (2011). Ending the message: poly(A) signals then and now. Genes Dev **25,** 1770-1782.

Proudfoot, N.J., and Brownlee, G.G. (1976). 3' non-coding region sequences in eukaryotic messenger RNA. Nature **263,** 211-214.

Proudfoot, N.J., Furger, A., and Dye, M.J. (2002). Integrating mRNA processing with transcription. Cell **108,** 501-512.

Przemeck, G.K., Mattsson, J., Hardtke, C.S., Sung, Z.R., and Berleth, T. (1996). Studies on the role of the Arabidopsis gene MONOPTEROS in vascular development and plant cell axialization. Planta **200,** 229-237.

Quan, T.K., and Hartzog, G.A. (2010). Histone H3K4 and K36 methylation, Chd1 and Rpd3S oppose the functions of Saccharomyces cerevisiae Spt4-Spt5 in transcription. Genetics **184,** 321-334.

Raczynska, K.D., Simpson, C.G., Ciesiolka, A., Szewc, L., Lewandowska, D., McNicol, J., Szweykowska-Kulinska, Z., Brown, J.W., and Jarmolowski, A. (2010). Involvement of the nuclear cap-binding protein complex in alternative splicing in Arabidopsis thaliana. Nucleic Acids Res **38,** 265-278.

Rahman, A., Bannigan, A., Sulaman, W., Pechter, P., Blancaflor, E.B., and Baskin, T.I. (2007). Auxin, actin and growth of the Arabidopsis thaliana primary root. Plant J **50,** 514-528.

Redig, P., Shaul, O., Inze, D., Van Montagu, M., and Van Onckelen, H. (1996). Levels of endogenous cytokinins, indole-3-acetic acid and abscisic acid during the cell cycle of synchronized tobacco BY-2 cells. FEBS Lett **391,** 175-180.

Reichert, V.L., Le Hir, H., Jurica, M.S., and Moore, M.J. (2002). 5' exon interactions within the human spliceosome establish a framework for exon junction complex structure and assembly. Genes Dev **16,** 2778-2791.

Reinberg, D., and Sims, R.J., 3rd. (2006). de FACTo nucleosome dynamics. J Biol Chem **281,** 23297-23301.

Reines, D., Chamberlin, M.J., and Kane, C.M. (1989). Transcription elongation factor SII (TFIIS) enables RNA polymerase II to elongate through a block to transcription in a human gene in vitro. J Biol Chem **264,** 10799-10809.

Reinhardt, D., Pesce, E.R., Stieger, P., Mandel, T., Baltensperger, K., Bennett, M., Traas, J., Friml, J., and Kuhlemeier, C. (2003). Regulation of phyllotaxis by polar auxin transport. Nature **426,** 255-260.

Rodriguez, C.R., Cho, E.J., Keogh, M.C., Moore, C.L., Greenleaf, A.L., and Buratowski, S. (2000). Kin28, the TFIIH-associated carboxy-terminal domain kinase, facilitates the recruitment of mRNA processing machinery to RNA polymerase II. Mol Cell Biol **20,** 104-112.

Rolland-Lagan, A.G. (2008). Vein patterning in growing leaves: axes and polarities. Curr Opin Genet Dev **18,** 348-353.

Rougvie, A.E., and Lis, J.T. (1988). The RNA polymerase II molecule at the 5' end of the uninduced hsp70 gene of D. melanogaster is transcriptionally engaged. Cell **54,** 795-804.

Rowley, M.J., Avrutsky, M.I., Sifuentes, C.J., Pereira, L., and Wierzbicki, A.T. (2011). Independent chromatin binding of ARGONAUTE4 and SPT5L/KTF1 mediates transcriptional gene silencing. PLoS Genet **7,** e1002120.

Rubery, P.H., and Sheldrake, A.R. (1973). Effect of pH and surface charge on cell uptake of auxin. Nature: New biology **244,** 285-288.

Sabatini, S., Beis, D., Wolkenfelt, H., Murfett, J., Guilfoyle, T., Malamy, J., Benfey, P., Leyser, O., Bechtold, N., Weisbeek, P., and Scheres, B. (1999). An auxin-dependent distal organizer of pattern and polarity in the Arabidopsis root. Cell **99,** 463-472.

Sambrook, J., Fritsch, E.F., and Maniatis, T. (1989). Molecular cloning : a laboratory manual. (Cold Spring Harbor: Cold Spring Harbor Laboratory Press).

Saunders, A., Core, L.J., and Lis, J.T. (2006). Breaking barriers to transcription elongation. Nat Rev Mol Cell Biol **7,** 557-567.

Sawchuk, M.G., Edgar, A., and Scarpella, E. (2013). Patterning of leaf vein networks by convergent auxin transport pathways. PLoS Genet **9,** e1003294.

Scarpella, E., Barkoulas, M., and Tsiantis, M. (2010). Control of leaf and vein development by auxin. Cold Spring Harb Perspect Biol **2,** a001511.

Schmid, M., and Jensen, T.H. (2008). Quality control of mRNP in the nucleus. Chromosoma **117,** 419-429.

Schneider, D.A., French, S.L., Osheim, Y.N., Bailey, A.O., Vu, L., Dodd, J., Yates, J.R., Beyer, A.L., and Nomura, M. (2006). RNA polymerase II elongation factors Spt4p and Spt5p play roles in transcription elongation by RNA polymerase I and rRNA processing. Proc Natl Acad Sci U S A **103,** 12707-12712.

Schneider, S., Pei, Y., Shuman, S., and Schwer, B. (2010). Separable functions of the fission yeast Spt5 carboxyl-terminal domain (CTD) in capping enzyme binding and transcription elongation overlap with those of the RNA polymerase II CTD. Mol Cell Biol **30,** 2353-2364.

Schwer, B., and Shuman, S. (2011). Deciphering the RNA polymerase II CTD code in fission yeast. Mol Cell **43,** 311-318.

Sehgal, P.B., Darnell, J.E., Jr., and Tamm, I. (1976). The inhibition by DRB (5,6-dichloro-1-beta-D-ribofuranosylbenzimidazole) of hnRNA and mRNA production in HeLa cells. Cell **9,** 473-480.

Serizawa, H., Conaway, J.W., and Conaway, R.C. (1993). Phosphorylation of C-terminal domain of RNA polymerase II is not required in basal transcription. Nature **363,** 371-374.

Shandilya, J., and Roberts, S.G. (2012). The transcription cycle in eukaryotes: from productive initiation to RNA polymerase II recycling. Biochim Biophys Acta **1819,** 391-400.

Shannon, P., Markiel, A., Ozier, O., Baliga, N.S., Wang, J.T., Ramage, D., Amin, N., Schwikowski, B., and Ideker, T. (2003). Cytoscape: a software environment for integrated models of biomolecular interaction networks. Genome Res **13,** 2498-2504.

Sheldon, C.C., Burn, J.E., Perez, P.P., Metzger, J., Edwards, J.A., Peacock, W.J., and Dennis, E.S. (1999). The FLF MADS box gene: a repressor of flowering in Arabidopsis regulated by vernalization and methylation. Plant Cell **11,** 445-458.

Shilatifard, A., Conaway, R.C., and Conaway, J.W. (2003). The RNA polymerase II elongation complex. Annu Rev Biochem **72,** 693-715.

Shuman, S. (2001). Structure, mechanism, and evolution of the mRNA capping apparatus. Progress in nucleic acid research and molecular biology **66,** 1-40.

Simic, R., Lindstrom, D.L., Tran, H.G., Roinick, K.L., Costa, P.J., Johnson, A.D., Hartzog, G.A., and Arndt, K.M. (2003). Chromatin remodeling protein Chd1 interacts with transcription elongation factors and localizes to transcribed genes. EMBO J **22,** 1846-1856.

Sims, R.J., 3rd, Belotserkovskaya, R., and Reinberg, D. (2004). Elongation by RNA polymerase II: the short and long of it. Genes Dev **18,** 2437-2468.

Sims, R.J., 3rd, Rojas, L.A., Beck, D., Bonasio, R., Schuller, R., Drury, W.J., 3rd, Eick, D., and Reinberg, D. (2011). The C-terminal domain of RNA polymerase II is modified by site-specific methylation. Science **332,** 99-103.

Singh, B.N., and Hampsey, M. (2007). A transcription-independent role for TFIIB in gene looping. Mol Cell **27,** 806-816.

Sogaard, T.M., and Svejstrup, J.Q. (2007). Hyperphosphorylation of the C-terminal repeat domain of RNA polymerase II facilitates dissociation of its complex with mediator. J Biol Chem **282,** 14113-14120.

Squazzo, S.L., Costa, P.J., Lindstrom, D.L., Kumer, K.E., Simic, R., Jennings, J.L., Link, A.J., Arndt, K.M., and Hartzog, G.A. (2002). The Paf1 complex physically and functionally associates with transcription elongation factors in vivo. EMBO J **21,** 1764-1774.

Stanlie, A., Begum, N.A., Akiyama, H., and Honjo, T. (2012). The DSIF subunits Spt4 and Spt5 have distinct roles at various phases of immunoglobulin class switch recombination. PLoS Genet **8,** e1002675.

Strasser, K., and Hurt, E. (2001). Splicing factor Sub2p is required for nuclear mRNA export through its interaction with Yra1p. Nature **413,** 648-652.

Suh, M.H., Meyer, P.A., Gu, M., Ye, P., Zhang, M., Kaplan, C.D., Lima, C.D., and Fu, J. (2010). A dual interface determines the recognition of RNA polymerase II by RNA capping enzyme. J Biol Chem **285,** 34027-34038.

Svejstrup, J.Q. (2002). Chromatin elongation factors. Curr Opin Genet Dev **12,** 156-161.

Svejstrup, J.Q. (2003). Rescue of arrested RNA polymerase II complexes. Journal of cell science **116,** 447-451.

Svejstrup, J.Q. (2004). The RNA polymerase II transcription cycle: cycling through chromatin. Biochim Biophys Acta **1677,** 64-73.

Swarup, K., Benkova, E., Swarup, R., Casimiro, I., Peret, B., Yang, Y., Parry, G., Nielsen, E., De Smet, I., Vanneste, S., Levesque, M.P., Carrier, D., James, N., Calvo, V., Ljung, K., Kramer, E., Roberts, R., Graham, N., Marillonnet, S., Patel, K., Jones, J.D., Taylor, C.G., Schachtman, D.P., May, S., Sandberg, G., Benfey, P., Friml, J., Kerr, I., Beeckman, T., Laplaze, L., and Bennett, M.J. (2008). The auxin influx carrier LAX3 promotes lateral root emergence. Nat Cell Biol **10,** 946-954.

Swarup, R., Kramer, E.M., Perry, P., Knox, K., Leyser, H.M., Haseloff, J., Beemster, G.T., Bhalerao, R., and Bennett, M.J. (2005). Root gravitropism requires lateral root cap and epidermal cells for transport and response to a mobile auxin signal. Nat Cell Biol **7,** 1057-1065.

Takada, S., Takada, N., and Yoshida, A. (2013). ATML1 promotes epidermal cell differentiation in Arabidopsis shoots. Development **140,** 1919-1923.

Tan, X., Calderon-Villalobos, L.I., Sharon, M., Zheng, C., Robinson, C.V., Estelle, M., and Zheng, N. (2007). Mechanism of auxin perception by the TIR1 ubiquitin ligase. Nature **446,** 640-645.

Tardiff, D.F., Abruzzi, K.C., and Rosbash, M. (2007). Protein characterization of Saccharomyces cerevisiae RNA polymerase II after in vivo cross-linking. Proc Natl Acad Sci U S A **104,** 19948-19953.

Teale, W.D., Paponov, I.A., and Palme, K. (2006). Auxin in action: signalling, transport and the control of plant growth and development. Nat Rev Mol Cell Biol **7,** 847-859.

Thoma, F. (1991). Structural changes in nucleosomes during transcription: strip, split or flip? Trends Genet **7,** 175-177.

Thomas, M.C., and Chiang, C.M. (2006). The general transcription machinery and general cofactors. Crit Rev Biochem Mol Biol **41,** 105-178.

Ubeda-Tomas, S., Federici, F., Casimiro, I., Beemster, G.T., Bhalerao, R., Swarup, R., Doerner, P., Haseloff, J., and Bennett, M.J. (2009). Gibberellin signaling in the endodermis controls Arabidopsis root meristem size. Curr Biol **19,** 1194-1199.

Ulmasov, T., Hagen, G., and Guilfoyle, T.J. (1997a). ARF1, a transcription factor that binds to auxin response elements. Science **276,** 1865-1868.

Ulmasov, T., Murfett, J., Hagen, G., and Guilfoyle, T.J. (1997b). Aux/IAA proteins repress expression of reporter genes containing natural and highly active synthetic auxin response elements. Plant Cell **9,** 1963-1971.

Van Leene, J., Witters, E., Inze, D., and De Jaeger, G. (2008). Boosting tandem affinity purification of plant protein complexes. DNA Res **13,** 517-520.

Van Leene, J., Eeckhout, D., Persiau, G., Van De Slijke, E., Geerinck, J., Van Isterdael, G., Witters, E., and De Jaeger, G. (2011). Plant Transcription Factors **754,** 195-218.

van Loon, L.C., Rep, M., and Pieterse, C.M. (2006). Significance of inducible defense-related proteins in infected plants. Annu Rev Phytopathol **44,** 135-162.

Vanneste, S., and Friml, J. (2009). Auxin: a trigger for change in plant development. Cell **136,** 1005-1016.

Vannini, A., and Cramer, P. (2012). Conservation between the RNA polymerase I, II, and III transcription initiation machineries. Mol Cell **45,** 439-446.

Vasiljeva, L., and Buratowski, S. (2006). Nrd1 interacts with the nuclear exosome for 3' processing of RNA polymerase II transcripts. Mol Cell **21,** 239-248.

Verhage, A., van Wees, S.C., and Pieterse, C.M. (2010). Plant immunity: it's the hormones talking, but what do they say? Plant Physiol **154,** 536-540.

Wada, T., Orphanides, G., Hasegawa, J., Kim, D.K., Shima, D., Yamaguchi, Y., Fukuda, A., Hisatake, K., Oh, S., Reinberg, D., and Handa, H. (2000). FACT relieves DSIF/NELF-mediated inhibition of transcriptional elongation and reveals functional differences between P-TEFb and TFIIH. Molecular Cell **5,** 1067-1072.

Wada, T., Takagi, T., Yamaguchi, Y., Ferdous, A., Imai, T., Hirose, S., Sugimoto, S., Yano, K., Hartzog, G.A., Winston, F., Buratowski, S., and Handa, H. (1998). DSIF, a novel transcription elongation factor that regulates RNA polymerase II processivity, is composed of human Spt4 and Spt5 homologs. Genes & Development **12,** 343-356.

Walley, J.W., Rowe, H.C., Xiao, Y., Chehab, E.W., Kliebenstein, D.J., Wagner, D., and Dehesh, K. (2008). The chromatin remodeler SPLAYED regulates specific stress signaling pathways. PLoS pathogens **4,** e1000237.

Wang, C., Gao, F., Wu, J., Dai, J., Wei, C., and Li, Y. (2010). Arabidopsis putative deacetylase AtSRT2 regulates basal defense by suppressing PAD4, EDS5 and SID2 expression. Plant Cell Physiol **51,** 1291-1299.

Wang, Y., An, C., Zhang, X., Yao, J., Zhang, Y., Sun, Y., Yu, F., Amador, D.M., and Mou, Z. (2013). The Arabidopsis elongator complex subunit2 epigenetically regulates plant immune responses. Plant Cell **25,** 762-776.

Weijers, D., Benkova, E., Jager, K.E., Schlereth, A., Hamann, T., Kientz, M., Wilmoth, J.C., Reed, J.W., and Jurgens, G. (2005). Developmental specificity of auxin response by pairs of ARF and Aux/IAA transcriptional regulators. EMBO J **24,** 1874-1885.

Wen, Y., and Shatkin, A.J. (1999). Transcription elongation factor hSPT5 stimulates mRNA capping service Transcription elongation factor hSPT5 stimulates mRNA capping**,** 1774-1779.

Wenzel, C.L., Schuetz, M., Yu, Q., and Mattsson, J. (2007). Dynamics of MONOPTEROS and PIN-FORMED1 expression during leaf vein pattern formation in Arabidopsis thaliana. Plant J **49,** 387-398.

West, M.L., and Corden, J.L. (1995). Construction and analysis of yeast RNA polymerase II CTD deletion and substitution mutations. Genetics **140,** 1223-1233.

Winston, F., Chaleff, D.T., Valent, B., and Fink, G.R. (1984). Mutations affecting Ty-mediated expression of the HIS4 gene of Saccharomyces cerevisiae. Genetics **107,** 179-197.

Wittschieben, B.O., Otero, G., de Bizemont, T., Fellows, J., Erdjument-Bromage, H., Ohba, R., Li, Y., Allis, C.D., Tempst, P., and Svejstrup, J.Q. (1999). A novel histone acetyltransferase is an integral subunit of elongating RNA polymerase II holoenzyme. Mol Cell **4,** 123-128.

Woodward, A.W., and Bartel, B. (2005). Auxin: regulation, action, and interaction. Annals of botany **95,** 707-735.

Worch, R., Niedzwiecka, A., Stepinski, J., Mazza, C., Jankowska-Anyszka, M., Darzynkiewicz, E., Cusack, S., and Stolarski, R. (2005). Specificity of recognition of mRNA 5' cap by human nuclear cap-binding complex. Rna **11,** 1355-1363.

Wu, C.H., Lee, C., Fan, R., Smith, M.J., Yamaguchi, Y., Handa, H., and Gilmour, D.S. (2005). Molecular characterization of Drosophila NELF. Nucleic Acids Res **33,** 1269-1279.

Xiao, Y., Yang, Y.H., Burckin, T.A., Shiue, L., Hartzog, G.A., and Segal, M.R. (2005). Analysis of a splice array experiment elucidates roles of chromatin elongation factor Spt4-5 in splicing. PLoS Comput Biol **1,** e39.

Yamada, T., Yamaguchi, Y., Inukai, N., Okamoto, S., Mura, T., and Handa, H. (2006). P-TEFb-mediated phosphorylation of hSpt5 C-terminal repeats is critical for processive transcription elongation. Mol Cell **21,** 227-237.

Yamaguchi, Y., Shibata, H., and Handa, H. (2013). Transcription elongation factors DSIF and NELF: promoter-proximal pausing and beyond. Biochim Biophys Acta **1829,** 98-104.

Yamaguchi, Y., Wada, T., Watanabe, D., Takagi, T., Hasegawa, J., and Handa, H. (1999a). Structure and function of the human transcription elongation factor DSIF. J Biol Chem **274,** 8085-8092.

Yamaguchi, Y., Takagi, T., Wada, T., Yano, K., Furuya, A., Sugimoto, S., Hasegawa, J., and Handa, H. (1999b). NELF, a multisubunit complex containing RD, cooperates with DSIF to repress RNA polymerase II elongation. Cell **97,** 41-51.

Yan, Q., Moreland, R.J., Conaway, J.W., and Conaway, R.C. (1999). Dual roles for transcription factor IIF in promoter escape by RNA polymerase II. J Biol Chem **274,** 35668-35675.

Yao, X., Feng, H., Yu, Y., Dong, A., and Shen, W.H. (2013). SDG2-mediated H3K4 methylation is required for proper Arabidopsis root growth and development. PLoS One **8,** e56537.

Yoh, S.M., Cho, H., Pickle, L., Evans, R.M., and Jones, K.A. (2007). The Spt6 SH2 domain binds Ser2-P RNAPII to direct Iws1-dependent mRNA splicing and export. Genes Dev **21,** 160-174.

Zawel, L., Kumar, K.P., and Reinberg, D. (1995). Recycling of the general transcription factors during RNA polymerase II transcription. Genes Dev **9,** 1479-1490.

Zazimalova, E., and Napier, R.M. (2003). Points of regulation for auxin action. Plant Cell Rep **21,** 625-634.

Zeevaart, J.A. (2008). Leaf-produced floral signals. Curr Opin Plant Biol **11,** 541-547.

Zhao, Y., Hull, A.K., Gupta, N.R., Goss, K.A., Alonso, J., Ecker, J.R., Normanly, J., Chory, J., and Celenza, J.L. (2002). Trp-dependent auxin biosynthesis in Arabidopsis: involvement of cytochrome P450s CYP79B2 and CYP79B3. Genes Dev **16,** 3100-3112.

Zhou, X., Li, Q., Chen, X., Liu, J., Zhang, Q., Liu, Y., Liu, K., and Xu, J. (2011). The Arabidopsis RETARDED ROOT GROWTH gene encodes a mitochondria-localized protein that is required for cell division in the root meristem. Plant Physiol **157,** 1793-1804.

Zhu, W., Wada, T., Okabe, S., Taneda, T., Yamaguchi, Y., and Handa, H. (2007). DSIF contributes to transcriptional activation by DNA-binding activators by preventing pausing during transcription elongation. Nucleic Acids Res **35,** 4064-4075.

Zuo, J., Niu, Q.W., and Chua, N.H. (2000). Technical advance: An estrogen receptor-based transactivator XVE mediates highly inducible gene expression in transgenic plants. Plant J **24,** 265-273.

7. Appendix

7.1 Microarray results

Table 6. Auxin-related genes differentially expressed in *SPT4-R3* relative to Col-0.

Probe set ID	Sig log ratio	Fold[a] change	p-value	AGI[b]	Gene, description[b]
249719_at	2.48	**5.56**	**0.00008**	At5g35735	auxin-responsive family protein
253253_at	1.81	**3.50**	**0.00002**	At4g34750	response to auxin stimulus
249606_at	1.81	**3.50**	**0.00006**	At5g37260	RVE2 (REVEILLE 2); DNA binding / transcription factor
266839_at	1.61	**3.05**	**0.00000**	At2g25930	ELF3 (EARLY FLOWERING 3); protein C-terminus binding / transcription factor
247643_at	1.60	**3.03**	**0.00003**	At5g60450	ARF4 (AUXIN RESPONSE FACTOR 4); transcription factor
246133_at	1.31	**2.47**	**0.00008**	At5g20960	AAO1 (ARABIDOPSIS ALDEHYDE OXIDASE 1); aldehyde oxidase/ indole-3-acetaldehyde oxidase
255479_at	1.30	**2.46**	**0.00000**	At4g02380	SAG21 (SENESCENCE-ASSOCIATED GENE 21)
256829_at	1.14	**2.20**	**0.00001**	At3g22850	similar to auxin down-regulated protein ARG10
247013_at	1.12	**2.17**	**0.00104**	At5g67480	BT4 (BTB AND TAZ DOMAIN PROTEIN 4); protein binding / transcription regulator
251436_at	-1.00	**-2.01**	**0.00009**	At3g59900	ARGOS (AUXIN-REGULATED GENE INVOLVED IN ORGAN SIZE)
247979_at	-1.03	**-2.04**	**0.00025**	At5g56750	auxin transport
250972_at	-1.04	**-2.06**	**0.00009**	At5g02840	LCL1 (LHY/CCA1-like 1); DNA binding / transcription factor
254758_at	-1.05	**-2.07**	**0.00041**	At4g13260	YUC2 (YUCCA2); FAD binding / NADP or NADPH binding / flavin-containing monooxygenase/ oxidoreductase
264598_at	-1.08	**-2.11**	**0.00038**	At1g04610	auxin biosynthetic process
247726_at	-1.12	**-2.17**	**0.00008**	At5g59430	TRP1 (TELOMERIC REPEAT BINDING PROTEIN 1); DNA binding / double-stranded telomeric DNA binding
258402_at	-1.13	**-2.18**	**0.00000**	At3g15450	similar to auxin down-regulated protein ARG10
254926_at	-1.13	**-2.19**	**0.00029**	At4g11280	ACS6 (1-AMINOCYCLOPROPANE-1-CARBOXYLIC ACID (ACC) SYNTHASE 6); 1-aminocyclopropane-1-carboxylate synthase
267092_at	-1.14	**-2.21**	**0.00008**	At2g38120	AUX1 (AUXIN RESISTANT 1); amino acid transmembrane transporter/ auxin binding / auxin influx transmembrane transporter/ transporter
245244_at	-1.15	**-2.22**	**0.00005**	At1g44350	ILL6; IAA-amino acid conjugate hydrolase/ metallopeptidase
264025_at	-1.15	**-2.22**	**0.00002**	At2g21050	auxin mediated signaling pathway
258797_at	-1.21	**-2.31**	**0.00005**	At3g04730	IAA16; transcription factor
245947_at	-1.27	**-2.41**	**0.00059**	At5g19530	ACL5 (ACAULIS 5); spermine synthase/ thermospermine synthase
254746_at	-1.27	**-2.42**	**0.00003**	At4g12980	auxin-responsive protein, putative
262951_at	-1.29	**-2.44**	**0.00026**	At1g75500	secondary cell wall biogenesis, positive regulation of auxin metabolic process
264323_at	-1.32	**-2.50**	**0.00014**	At1g04180	auxin biosynthetic process
263890_at	-1.35	**-2.55**	**0.00006**	At2g37030	response to auxin stimulus
263656_at	-1.41	**-2.66**	**0.00080**	At1g04240	SHY2 (SHORT HYPOCOTYL 2); transcription factor; IAA3
265454_at	-1.48	**-2.79**	**0.00002**	At2g46530	ARF11 (AUXIN RESPONSE FACTOR 11); transcription factor
253061_at	-1.56	**-2.95**	**0.00001**	At4g37610	BT5 (BTB AND TAZ DOMAIN PROTEIN 5); protein binding / transcription regulator

249109_at	-1.62	**-3.08**	**0.00027**	At5g43700	ATAUX2-11 (AUXIN INDUCIBLE 2-11); DNA binding / transcription factor; IAA4
265806_at	-1.62	**-3.08**	**0.00003**	At2g18010	response to auxin stimulus
267461_at	-1.63	**-3.09**	**0.00000**	At2g33830	dormancy/auxin associated family protein
253103_at	-1.63	**-3.10**	**0.00034**	At4g36110	response to auxin stimulus
263433_at	-1.67	**-3.18**	**0.00001**	At2g22240	MIPS2 (MYO-INOSITOL-1-PHOSTPATE SYNTHASE 2); binding / catalytic/ inositol-3-phosphate synthase
253908_at	-1.69	**-3.23**	**0.00005**	At4g27260	WES1; indole-3-acetic acid amido synthetase
261766_at	-1.77	**-3.41**	**0.00010**	At1g15580	IAA5 (INDOLE-3-ACETIC ACID INDUCIBLE 5); transcription factor
248163_at	-1.84	**-3.58**	**0.00278**	At5g54510	DFL1 (DWARF IN LIGHT 1); indole-3-acetic acid amido synthetase
266830_at	-1.86	**-3.64**	**0.00012**	At2g22810	ACS4 (1-AMINOCYCLOPROPANE-1-CARBOXYLATE SYNTHASE 4); 1-aminocyclopropane-1-carboxylate synthase
252965_at	-2.19	**-4.55**	**0.00000**	At4g38860	response to auxin stimulus
245593_at	-2.23	**-4.69**	**0.00000**	At4g14550	IAA14 (INDOLE-3-ACETIC ACID INDUCIBLE 14); protein binding / transcription factor/ transcription repressor
253794_at	-2.31	**-4.95**	**0.00001**	At4g28720	auxin biosynthetic process
257766_at	-2.36	**-5.14**	**0.00001**	At3g23030	IAA2 (INDOLE-3-ACETIC ACID INDUCIBLE 2); transcription factor
247925_at	-2.50	**-5.65**	**0.00000**	At5g57560	TCH4 (Touch 4); hydrolase, acting on glycosyl bonds / xyloglucan:xyloglucosyl transferase
259790_s_at	-2.50	**-5.68**	**0.00001**	At1g29430	response to auxin stimulus
259332_at	-2.63	**-6.20**	**0.00009**	At3g03830	response to auxin stimulus
259783_at	-2.66	**-6.33**	**0.00001**	At1g29510	SAUR68 (SMALL AUXIN UPREGULATED 68)
260152_at	-2.73	**-6.63**	**0.00000**	At1g52830	IAA6 (INDOLE-3-ACETIC ACID 6); transcription factor
245276_at	-2.77	**-6.81**	**0.00001**	At4g16780	ATHB-2 (ARABIDOPSIS THALIANA HOMEOBOX PROTEIN 2); DNA binding / protein homodimerization/ sequence-specific DNA binding / transcription factor
258399_at	-2.80	**-6.97**	**0.00000**	At3g15540	IAA19 (INDOLE-3-ACETIC ACID INDUCIBLE 19); transcription factor
257506_at	-2.81	**-7.03**	**0.00000**	At1g29440	response to auxin stimulus
245397_at	-3.07	**-8.42**	**0.00001**	At4g14560	IAA1 (INDOLE-3-ACETIC ACID INDUCIBLE); protein binding / transcription factor
259784_at	-3.17	**-9.01**	**0.00000**	At1g29450	response to auxin stimulus
259787_at	-3.21	**-9.28**	**0.00001**	At1g29460	response to auxin stimulus
248801_at	-3.41	**-10.61**	**0.00000**	At5g47370	HAT2; DNA binding / transcription factor/ transcription repressor
259331_at	-3.45	**-10.89**	**0.00001**	At3g03840	response to auxin stimulus
259773_at	-3.46	**-11.02**	**0.00000**	At1g29500	response to auxin stimulus
250012_x_at	-4.48	**-22.35**	**0.00000**	At5g18060	response to auxin stimulus
253423_at	-4.62	**-24.61**	**0.00000**	At4g32280	IAA29 (INDOLE-3-ACETIC ACID INDUCIBLE 29); transcription factor

[a]only genes are shown, whose transcript levels were ≥2-fold up- or down-regulated (highlighted in pink and blue, respectively) in SPT4-R3 relative to Col-0.

[b]*Aux/IAA* genes are highlighted in green.

7.2 Up- and down-regulated genes upon auxin treatment

Table 7. Auxin induced genes (Overvoorde et al., 2005).

AGI	Fold change[a]	Gene, description
Auxin related		
At4g14560	**-8.42**	IAA1 (INDOLE-3-ACETIC ACID INDUCIBLE)
At3g23030	**-5.14**	IAA2 (INDOLE-3-ACETIC ACID INDUCIBLE 2)
At5g43700	**-3.08**	ATAUX2-11 (AUXIN INDUCIBLE 2-11)
At1g15580	**-3.41**	IAA5 (INDOLE-3-ACETIC ACID INDUCIBLE 5)
At1g52830	**-6.63**	IAA6 (INDOLE-3-ACETIC ACID 6)
At4g26640	**-1.30**	WRKY20; transcription factor
At2g33310	**-1.51**	IAA13; transcription factor
At3g15540	**-6.97**	IAA19 (INDOLE-3-ACETIC ACID INDUCIBLE 19)
At4g32280	**-24.61**	IAA29 (INDOLE-3-ACETIC ACID INDUCIBLE 29)
At2g14960	**-1.29**	GH3.1
At1g59500	**-1.38**	GH3.4; indole-3-acetic acid amido synthetase
At4g27260	**-3.23**	WES1; indole-3-acetic acid amido synthetase
At5g54510	**-3.58**	DFL1 (DWARF IN LIGHT 1)
At4g34770	**-1.38**	putative protein small auxin up-regulated RNA
At4g36110	**-3.10**	putative auxin-induced protein high similarity to auxin-induced protein 15A
At4g38850	**-1.72**	SAUR15 (SMALL AUXIN UPREGULATED 15)
At5g18060	**-22.35**	auxin-induced protein-like
At4g22620	**-1.47**	putative protein auxin-induced protein 10A
At1g29450	**-9.01**	auxin-induced protein
At1g29500	**-11.02**	auxin-induced protein
At1g29510	**-6.33**	SAUR68 (SMALL AUXIN UPREGULATED 68)
At5g20820	**-1.07**	putative protein predicted proteins
At3g25290	**1.65**	unknown protein
At2g21050	**-2.22**	AUX1-like amino acid permease
At1g77690	**-1.78**	LAX3 (LIKE AUX1 3)
At1g70940	**-1.67**	PIN3 (PIN-FORMED 3)
At2g34650	**1.31**	PID (PINOID)
At4g15550	**-1.15**	IAGLU (INDOLE-3-ACETATE BETA-D-GLUCOSYLTRANSFERASE)
At4g30080	**-1.16**	ARF16 (AUXIN RESPONSE FACTOR 16)
At1g19220	**-1.13**	ARF19 (AUXIN RESPONSE FACTOR 19)
Ethylene related		
At2g22810	**-3.64**	ACS4 (1-AMINOCYCLOPROPANE-1-CARBOXYLATE SYNTHASE 4)
At4g11280	**-2.19**	ACS6 (1-AMINOCYCLOPROPANE-1-CARBOXYLIC ACID (ACC) SYNTHASE 6)
At4g37770	**-7.96**	ACS8; 1-aminocyclopropane-1-carboxylate synthase
At1g04310	**1.02**	ERS2 (ETHYLENE RESPONSE SENSOR 2)
At3g23150	**-1.01**	ETR2 (ethylene response 2)
At1g28370	**1.12**	ERF11 (ERF DOMAIN PROTEIN 11)
At5g44210	**-1.01**	ERF9 (ERF DOMAIN PROTEIN 9)
At5g25190	**-4.47**	ethylene-responsive element
At5g67430	**-1.15**	N-acetyltransferase hookless1-like protein
Other phytohormone related		
At3g63440	**-2.06**	CKX6 (CYTOKININ OXIDASE/DEHYDROGENASE 6)
At1g02400	**-1.11**	GA2OX6 (GIBBERELLIN 2-OXIDASE 6)
At2g26710	**-7.38**	BAS1 (PHYB ACTIVATION TAGGED SUPPRESSOR 1)
At4g26080	**1.45**	ABI1 (ABA INSENSITIVE 1)
At4g24960	**-1.06**	ATHVA22D
Cell wall		
At4g30280	**-1.28**	XTH18 (XYLOGLUCAN ENDOTRANSGLUCOSYLASE/HYDROLASE 18)
At1g22880	**-1.17**	CEL5 (CELLULASE 5)
At2g39700	**-1.84**	ATEXPA4 (ARABIDOPSIS THALIANA EXPANSIN A4)
At4g22470	**1.33**	extensin - like protein hybrid proline-rich protein
At4g00080	**-1.27**	UNE11 (unfertilized embryo sac 11)
At1g62770	**1.05**	unknown protein
At2g47550	**1.16**	putative pectinesterase

At3g10720	**-1.19**	putative pectinesterase
At4g30140	**1.28**	putative protein proline-rich protein APG C-terminus
Metabolism		
At5g14130	**1.30**	peroxidase ATP20a
At5g39580	**1.01**	peroxidase ATP24a
At5g09970	**-1.60**	CYP78A7
At2g23180	**1.09**	CYP96A1
At2g47130	**-1.13**	putative alcohol dehydrogenase
At3g26760	**-1.22**	putative short chain alcohol dehydrogenase
At4g13180	**-1.65**	short-chain alcohol dehydrogenase like protein
At2g47140	**1.04**	putative alcohol dehydrogenase
At1g22440	**1.31**	alcohol dehydrogenase ADH
At1g30760	**1.08**	putative reticuline oxidase-like protein
At2g39980	**1.33**	putative anthocyanin 5-aromatic acyltransferase
At2g45400	**-2.65**	BEN1
At5g07010	**-1.37**	ST2A (SULFOTRANSFERASE 2A)
At5g64250	**-1.17**	steroid sulfotransferase-like protein
At5g55050	**-1.46**	GDSL-motif lipase/hydrolase-like protein
At1g67750	**1.20**	F12A21.12 similar to pectate lyase like protein
At2g46740	**-1.15**	unknown protein
At3g13790	**1.27**	ATBFRUCT1
At2g29440	**1.44**	ATGSTU6 (ARABIDOPSIS THALIANA GLUTATHIONE S-TRANSFERASE TAU 6)
At3g10870	**-1.21**	MES17 (METHYL ESTERASE 17)
At1g23730	**-1.82**	BCA3 (BETA CARBONIC ANHYDRASE 4)
Development		
At2g42430	**-1.12**	LBD16 (LATERAL ORGAN BOUNDARIES-DOMAIN 16)
At2g45420	**1.00**	LBD18 (LOB DOMAIN-CONTAINING PROTEIN 18)
At3g58190	**-1.00**	LBD29 (LATERAL ORGAN BOUNDARIES-DOMAIN 29)
Stress/defence		
At2g19990	**-1.26**	PR-1-LIKE (PATHOGENESIS-RELATED PROTEIN-1-LIKE)
At2g19970	**-1.11**	putative pathogenesis-related protein
At5g53290	**1.12**	CRF3 (CYTOKININ RESPONSE FACTOR 3)
At5g06860	**-1.24**	PGIP1 (POLYGALACTURONASE INHIBITING PROTEIN 1)
At1g33790	**1.35**	myrosinase binding protein
At4g38410	**1.17**	putative cold-regulated protein cold-regulated protein cor47
At5g44910	**1.82**	putative protein contains similarity to disease resistance protein
At2g40000	**-2.00**	HSPRO2 (ARABIDOPSIS ORTHOLOG OF SUGAR BEET HS1 PRO-1 2)
Signalling		
At5g13330	**3.26**	Rap2.6L (related to AP2 6L)
At3g25730	**1.29**	AP2 domain transcription factor
At1g44830	**1.09**	transcription factor, putative contains AP2 domain
At5g47370	**-10.61**	HAT2
At5g61010	**-1.09**	ATEXO70E2 (EXOCYST SUBUNIT EXO70 FAMILY PROTEIN E2)
At5g40590	**-1.03**	putative protein predicted protein
At5g57520	**-1.27**	ZFP2 (ZINC FINGER PROTEIN 2)
At5g44260	**-3.25**	putative protein similar to unknown protein (gb AAD10689.1)
At1g34670	**-1.05**	AtMYB93 (myb domain protein 93)
At4g29190	**-1.73**	putative protein zinc finger transcription factor
At3g09760	**1.03**	unknown protein
At5g41400	**-1.22**	RING zinc finger protein-like
At2g34140	**1.03**	putative DOF zinc finger protein
At2g47260	**1.13**	WRKY23; transcription factor
At3g60530	**-1.29**	GATA transcription factor 4
At1g21910	**1.09**	TINY-like protein similar to TINY
At1g34110	**1.12**	hypothetical protein
At3g13380	**1.25**	BRL3 (BRI1-LIKE 3)
At1g77280	**1.04**	hypothetical protein
At1g33260	**-1.29**	protein kinase
At5g05160	**1.01**	receptor-like protein kinase
At3g20830	**-1.34**	unknown protein

At2g26290	**-1.03**	ARSK1 (root-specific kinase 1)
At2g30040	**-1.14**	MAPKKK14
At5g18470	**1.36**	putative protein S-receptor kinase PK3 precursor
At5g67060	**-1.27**	HEC1 (HECATE 1)
At5g65320	**1.32**	putative protein contains similarity to bHLH DNA-binding protein
At1g34750	**1.02**	protein phosphatase type 2C
At5g02760	**-8.09**	protein phosphatase
At5g54490	**-1.34**	PBP1 (PINOID-BINDING PROTEIN 1)
At2g41100	**-1.88**	TCH3 (TOUCH 3)
At3g63240	**-1.51**	inositol-1,4,5-trisphosphate 5-Phosphatase
Transport/channel		
At2g40540	**-1.61**	KT2 (POTASSIUM TRANSPORTER 2)
At3g06370	**-1.55**	NHX4 (SODIUM HYDROGEN EXCHANGER 4)
At1g59740	**1.07**	oligopeptide transporter
At1g72230	**-1.75**	blue copper protein
At5g50300	**-1.06**	transmembrane transport protein-like
Others		
At3g07390	**-1.44**	AIR12; extracellular matrix structural constituent
At3g04570	**-1.10**	hypothetical protein similar to putative DNA-binding proteins
At4g37890	**1.08**	EDA40 (embryo sac development arrest 40)
At4g36880	**-1.02**	CP1 (CYSTEINE PROTEINASE1)
At1g78100	**-1.32**	unknown protein
At4g22780	**-1.62**	ACR7
At3g60640	**1.11**	ATG8G (AUTOPHAGY 8G)
At1g74440	**1.52**	hypothetical protein
At4g01870	**-1.18**	predicted protein of unknown function
At5g54500	**1.34**	FQR1 (FLAVODOXIN-LIKE QUINONE REDUCTASE 1)
At2g03730	**-2.46**	ACR5
At2g41380	**-1.28**	putative embryo-abundant protein
At4g30420	**1.07**	nodulin-like protein MtN21 gene product
At5g57920	**1.03**	phytocyanin/early nodulin-like protein

[a]genes, whose transcript levels were ≥2-fold up- or down-regulated are highlighted in pink and blue, respectively in SPT4-R3 relative to Col-0.

Table 8. Auxin repressed genes (Overvoorde et al., 2005).

AGI	Fold change[a]	Gene, description
Auxin related		
At4g31320	**1.02**	auxin induced like-protein auxin-induced protein 15A
At4g39950	**1.47**	CYP79B2
At2g22330	**-2.37**	CYP79B3
At5g60890	**-2.04**	MYB34 (MYB DOMAIN PROTEIN 34)
Cell Wall		
At5g65730	**-2.56**	xyloglucan endo-transglycosylase-like protein
At5g53250	**-1.22**	AGP22 (ARABINOGALACTAN PROTEIN 22)
At4g25250	**1.13**	putative protein Group I Pectinesterase
At4g15290	**1.18**	ATCSLB05
Metabolism		
At3g01190	**-1.07**	putative peroxidase very similar to peroxidase
At4g30170	**1.71**	peroxidase ATP8a
At1g67110	**1.09**	CYP735A2
At5g42600	**-1.19**	MRN1 (MARNERAL SYNTHASE)
At1g13420	**1.25**	ST4B (SULFOTRANSFERASE 4B)
At3g01260	**1.02**	steroid sulfotransferase
At4g20460	**1.26**	UDP-glucose 4-epimerase
At1g15380	**-1.47**	hypothetical protein
At1g17190	**1.69**	ATGSTU26 (ARABIDOPSIS THALIANA GLUTATHIONE S-TRANSFERASE TAU 26)
At5g23220	**1.02**	NIC3 (NICOTINAMIDASE 3)
At2g01890	**1.17**	PAP8 (PURPLE ACID PHOSPHATASE 8)

At1g53680	**1.55**	ATGSTU28 (GLUTATHIONE S-TRANSFERASE TAU 28)
At1g80050	**1.66**	APT2 (ADENINE PHOSPHORIBOSYL TRANSFERASE 2)
Development		
At4g18510	**1.08**	CLE2 (CLAVATA3/ESR-RELATED)
Stress/defence		
At4g11210	**1.69**	putative disease resistance response protein
At5g62360	**1.51**	DC1.2 homologue
Signaling		
At3g16800	**-6.50**	protein phosphatase
At1g72200	**-1.13**	RING-H2 zinc finger protein ATL3
At1g49230	**1.21**	RING-H2 finger protein RHA3a
At3g13760	**1.90**	hypothetical protein
At5g65210	**1.10**	TGA1
At1g74840	**-1.67**	myb-related transcription activator
At5g61420	**-1.14**	MYB28 (myb domain protein 28)
At5g57150	**1.12**	putative protein
Transport/channel		
At5g60660	**-1.08**	PIP2;4 (PLASMA MEMBRANE INTRINSIC PROTEIN 2;4)
At5g47450	**-1.43**	AtTIP2;3
At2g16980	**-1.10**	putative tetracycline transporter protein
At1g15210	**1.06**	PDR7 (PLEIOTROPIC DRUG RESISTANCE 7)
At5g27350	**-1.04**	SFP1
Others		
At4g12510	**-1.31**	pEARLI 1-like protein
At4g19030	**1.03**	NLM1
At5g46900	**-1.46**	extA (emb CAA47807.1)
At4g35060	**-1.43**	putative protein
At5g60520	**-1.06**	like late embryonic abundant protein EMB7
At3g61060	**-3.99**	AtPP2-A13 (Arabidopsis thaliana phloem protein 2-A13)
At3g54770	**-1.02**	RNA binding protein - like SEB4 protein
At2g38760	**1.10**	ANNAT3 (ANNEXIN ARABIDOPSIS 3)
At4g08300	**-3.48**	nodulin-like protein
At1g76260	**1.47**	unknown protein
At2g28410	**1.05**	unknown protein

[a]genes, whose transcript levels were ≥2-fold up- or down-regulated are highlighted in pink and blue, respectively in SPT4-R3 relative to Col-0.

7.3 Mass spectrometry results

Table 9. Mass spectrometry results of the SPT4-GS affinity purification.

AGI	#IPs[1]	mass [kDa]	Mascot mean score	Description[2]
At4g08350	5	115.3	2115.30	SPT5-2
At5g04290	5	157.9	1103.76	SPT5L
At5g63670	5	13.4	330.78	SPT4-2
At5g08565	5	13.4	223.97	SPT4-1
At5g13680	5	146.5	176.90	ELO2
At1g02080	4	269.7	712.05	CCR4-NOT subunit 1
At4g19210	3	68.3	319.52	ABC transporter E family member 2
At2g42520	3	67.6	297.93	DEAD-box ATP-dependent RNA helicase 37
At5g50320	3	63.1	222.10	ELO3
At3g62530	3	38.1	127.45	armadillo/beta-catenin-like repeat-containing protein
At1g53165	2	76.5	461.20	map 4 kinase alpha1

At4g35800	2	204.9	393.60	NRPB1
At1g32380	2	43.3	318.15	ribose-phosphate pyrophosphokinase 2
At5g27970	2	180.4	259.06	armadillo/beta-catenin-like repeat-containing protein
At5g43780	2	52.1	251.81	sulfate adenylyltransferase
At2g02740	2	29.7	140.00	ssDNA-binding transcriptional regulator
At1g79530	2	44.8	122.45	glyceraldehyde 3-phosphate dehydrogenase
At5g53460	1	242.7	2953.00	NADH-dependent glutamate synthase
At3g46740	1	89.1	760.84	protein TOC75-3
At4g21710	1	134.9	667.08	NRPB2
At4g11820	1	51.1	604.11	hydroxymethylglutaryl-CoA synthase
At3g21140	1	42.8	528.56	Pyridoxamine 5'-phosphate oxidase family protein
At1g80070	1	275.3	501.99	Pre-mRNA-processing-splicing factor
At5g60790	1	66.8	428.71	ABC transporter F family member 1
At1g36160	1	251.6	412.81	acetyl-CoA carboxylase 1
At3g15220	1	76.3	389.84	putative protein kinase
At4g31490	1	106	350.33	coatomer subunit beta-2
At2g27040	1	102.8	329.86	argonaute 4
At1g33410	1	169.3	245.44	suppressor of auxin resistance1 protein (SAR1)
At3g09840	1	89.3	237.59	cell division control protein 48-A
At3g05680	1	226.8	220.79	embryo defective 2016
At1g72560	1	111.4	202.00	protein PAUSED (mediates nuclear export of tRNAs)
At2g41040	1	28.9	197.31	S-adenosyl-L-methionine-dependent methyltransferases
At3g48860	1	54.1	188.57	uncharacterized protein
At1g05460	1	113.3	188.41	RNA helicase SDE3
At5g03540	1	72.3	188.07	exocyst subunit exo70 family protein A1
At1g14850	1	159.9	178.50	nucleoporin 155
At3g05040	1	133.1	175.07	HASTY
At1g69220	1	124.5	169.50	putative serine/threonine kinase
At1g27595	1	104.9	165.16	symplekin
At5g36230	1	49.3	158.10	armadillo/beta-catenin-like repeat-containing protein
At4g38600	1	82.6	157.17	E3 ubiquitin-protein ligase UPL3
At2g41220	1	177.6	144.76	ferredoxin-dependent glutamate synthase precursor
At2g18960	1	104.2	141.64	H(+)-ATPase 1
At1g78900	1	68.8	138.58	V-type proton ATPase catalytic subunit A
At2g46280	1	36.3	133.01	eukaryotic translation initiation factor 3 delta subunit
At2g07698	1	85.9	130.15	F-type H+-transporting ATPase subunit alpha
At5g64270	1	141.4	127.50	putative splicing factor
At1g50360	1	129.9	127.36	P-loop containing nucleoside triphosphate hydrolase-like protein
At1g53500	1	75.2	119.68	UDP-glucose 4,6-dehydratase
At1g45000	1	44.7	117.48	AAA-type ATPase family protein
At1g21170	1	122.6	115.96	Exocyst complex component SEC5
At2g02560	1	134.8	108.73	cullin-associated NEDD8-dissociated protein 1
At5g26830	1	80.9	107.43	threonyl-tRNA synthetase
At4g00800	1	211.9	103.21	transducin family protein / WD-40 repeat family protein

[1]numbers indicate in how many out of a total of 5 experiments the respective protein was identified.

[2]proteins discussed in this report are highlighted in grey.

7.4 Plasmids

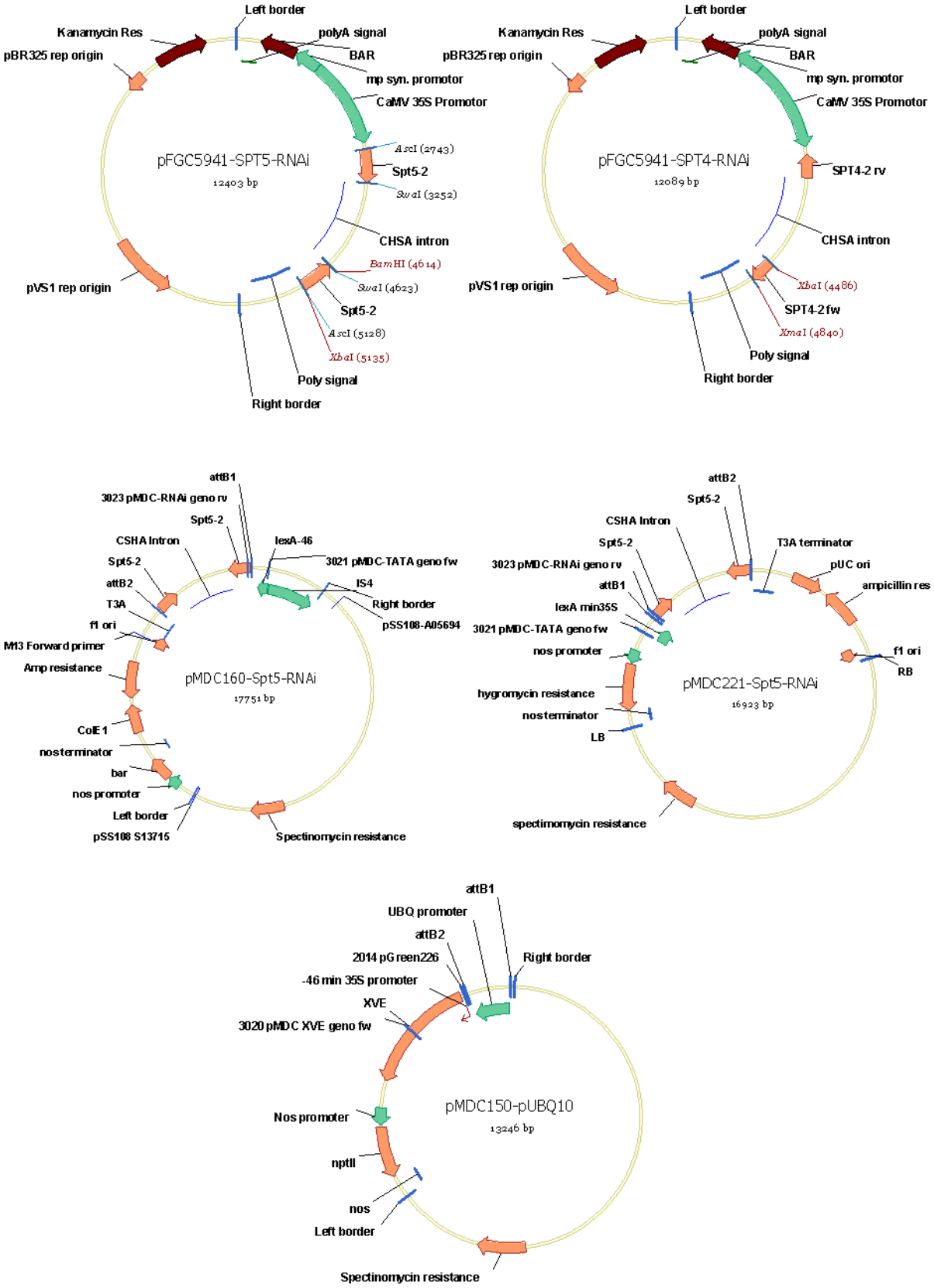

Figure 78. Vectors for *SPT4*-RNAi and (inducible) *SPT5*-RNAi.

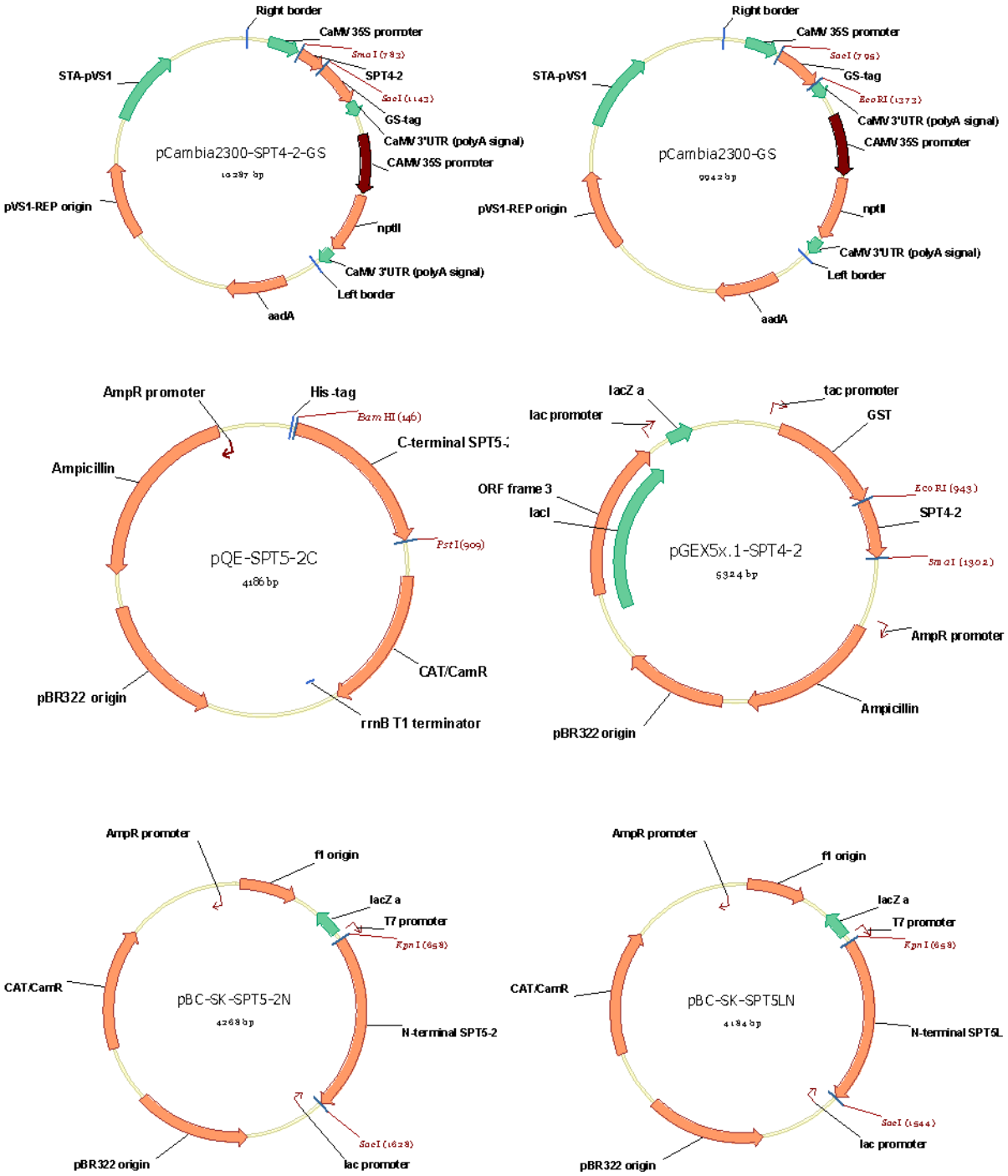

Figure 79. Vectors for stable cell culture transformation, antibody production and *in vitro* GST pull-down.

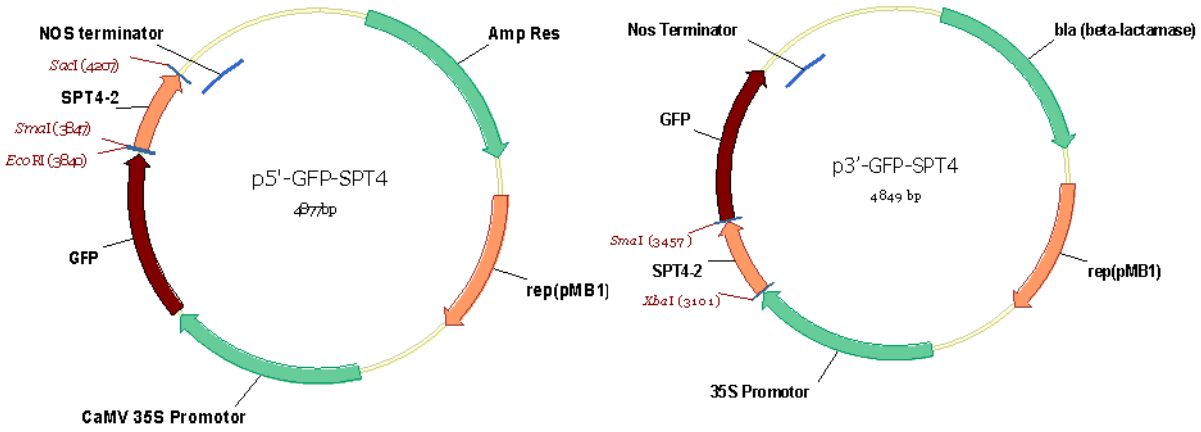

Figure 80. Vectors for sub-cellular localisation of SPT4.

Table 10. Oligonucleotide primers used in this study and construction of plasmids.

#	sequence	description	plasmid	restriction site
P1	ATGGGAGAAGCGCCTGCC	Expression of *SPT4-1* (At5g08565)		
P2	ACTTCCATTCATAACCTCCATC	Expression of *SPT4-1* (At5g08565)		
P3	ATGGGAAGCGCACCAGCT	Expression of *SPT4-2* (At5g63670)		
P4	CATCGACCATTCCACAAGATT	Expression of *SPT4-2* (At5g63670)		
P5	AACTTCCTACTTACCTACCACACCCG	Expression of *SPT5-1* (At2g34210)		
P6	GGCTCACTTTGTTCTGTGTCGCTC	Expression of *SPT5-1* (At2g34210)		
P7	CAGATAATGTTGCGACAACACCGTTTAG	Expression of *SPT5-2* (At4g08350)		
P8	CTGATATTGAGGACTCGTTCCCC	Expression of *SPT5-2* (At4g08350)		
P9	TGCTGGTCGTGACCTTACTGATTACC	Expression of *Actin8* (At1g49240)		
P10	TCTCCATCTCTTGCTCGTAGTCGACA	Expression of *Actin8* (At1g49240)		
P11	GCCTTTTCAGAAATGGATAAATAGCCTTGCTTCC	Genotyping, T-DNA insertion SAIL LB		
P12	TCACATGCGTTTCGGCAGAA	Expression of *SPT4-2* (At5g63670)		
P13	CAGCAAGTGTGTAGCAACCAGGAGC	Expression of *SPT4-2* (At5g63670)		
P14	GAAGGCGAAGATCCAAGACAAGGAA	Expression of *UBQ5* (At3g62250)		
P15	GGAGGACGAGATGAAGCGTCGA	Expression of *UBQ5* (At3g62250)		
P16	GGGAACCCGGGATCATGGGGA	Genotyping, T-DNA insertion *spt5-1* (At2g34210)		
P17	TGGGGTCACTCATGAACTAACTTGGC	Genotyping, T-DNA insertion *spt5-1* (At2g34210)		
P18	GTTCATAGGCGAAGCATCATGA	Genotyping, T-DNA insertion *spt5-2-1* (At4g08350)		
P19	GGTGACTTCTGAGAACCAATCT	Genotyping, T-DNA insertion *spt5-2-1* (At4g08350)		
P20	TGCATTCTTCACTGGTCTGCTGCAC	Genotyping, T-DNA insertion *spt5-2-2* (At4g08350)		
P21	ACCTCCAGAGTCCCGCATTGGA	Genotyping, T-DNA insertion *spt5-2-2* (At4g08350)		
P22	CTTGGCTAAGGCCAGGTC	Genotyping, T-DNA insertion *spt5-2-3* (At4g08350)		
P23	TTGTGTTGCACTTGTTCCCAG	Genotyping, T-DNA insertion *spt5-2-3* (At4g08350)		
P24	AGGAAATCAAGCCAAACCATG	Genotyping, T-DNA insertion *spt5-2-4* (At4g08350)		
P25	TGGTGGTAGTTACTCGGATGC	Genotyping, T-DNA insertion *spt5-2-4* (At4g08350)		
P26	ATTTTGCCGATTTCGGAAC	Genotyping, T-DNA insertion SALK LBb1.3 (*spt5-2-1, 2, 3*)		
P27	AATTTCTAGAGGCGCGCCTATATGTTGAAGCAGACAAGG	Insertion of *SPT5-2* (At4g08350) CDS in pFGC5941	pFGC5941-SPT5-RNAi	XbaI, AscI
P28	AATTGGATCCATTTAAATGTTGGTGTAACATTCTGAACAG	Insertion of *SPT5-2* (At4g08350) CDS in pFGC5941	pFGC5941-SPT5-RNAi	BamHI, SwaI
P29	CACCGGCGCGCCGAGCTCGGTACCCGACGAG	Insertion of UBQ10-Promotor (At4g05320) in pMDC150	pMDC150-UBQP	Gateway® cloning
P30	GGCGCGCCCTGTTAATCAGAAAAACTCAG	Insertion of UBQ10-Promotor (At4g05320) in pMDC150	pMDC150-UBQP	Gateway® cloning
P31	CACCTACATTTACAATTACCATGG	Insertion of SPT5-RNAi in pMDC160 or pMDC221	pMDC160/221-SPT5-RNAi	Gateway® cloning
P32	GTCTTAATTAACTCTCTAGA	Insertion of SPT5-RNAi in pMDC160 or pMDC221	pMDC160/221-SPT5-RNAi	Gateway® cloning
P33	TGGGCTGCAGGTCGAGGCTA	Genotyping, T-DNA insertion SPT5RNAi activator unit		
P34	CGCAAGACCCTTCCTCTATA	Genotyping, T-DNA insertion SPT5RNAi activator unit		

P35	TGGGCTGCAGGTCGAGGCTA	Genotyping, T-DNA insertion SPT5RNAi responder unit		
P36	TCCTCATGCCCTTGATTGCCTCTT	Genotyping, T-DNA insertion SPT5RNAi responder unit		
P37	AACCCGGGTCACATGCGTTTCGGCAGAA	Insertion of *SPT4-2* (At5g63670) CDS in pFGC5941	pFGC5941-SPT4-RNAi	XbaI, SwaI
P38	AATCTAGAATGGGAAGCGCACCAGCT	Insertion of *SPT4-2* (At5g63670) CDS in pFGC5941	pFGC5941-SPT4-RNAi	XmaI, SwaI
P39	TCACATGCGTTTCGGCAGAA	Genotyping, T-DNA insertion SPT4RNAi MCS1		
P40	GAAGAGCCAATTAAGATAAAACGTTGAATGTA	Genotyping, T-DNA insertion SPT4RNAi MCS1		
P41	ATGGGAAGCGCACCAGCT	Genotyping, T-DNA insertion SPT4RNAi MCS2		
P42	TCGCATATCTCATTAAAGCAGGACTCTAGG	Genotyping, T-DNA insertion SPT4RNAi MCS2		
P43	CCAGACTTCCCATGAAACTACAGGT	qRT-PCR, *PR3* (At3g12500)		
P44	ACGTGGCGCTCGGTTCACA	qRT-PCR, *PR3* (At3g12500)		
P45	TCTTCCTCGTGTTCATCAC	qRT-PCR, *PR5* (At1g75040)		
P46	TCTTCCTCGTGTTCATCAC	qRT-PCR, *PR5* (At1g75040)		
P47	AGAGCAAAGTTCCGGTGGTTACG	qRT-PCR, *GH3.2* (At4g37390)		
P48	CAGCAGATGTTCCTGAGCTTGTGA	qRT-PCR, *GH3.2* (At4g37390)		
P49	TCGTTTGGGATTACCCGGAGCA	qRT-PCR, *IAA1* (At4g14560)		
P50	TTGTGTTTTTGCAGGAGGAGGA	qRT-PCR, *IAA1* (At4g14560)		
P51	CCTCCTACCAAAACTCAAATCGTTGG	qRT-PCR, *IAA2* (At3g23030)		
P52	GAGATCGATCTTGCGAAGGTAAGGA	qRT-PCR, *IAA2* (At3g23030)		
P53	TCTCTGTGGGAGAGTACTTTGAGAGA	qRT-PCR, *SHY2/IAA3* (At1g04240)		
P54	GCACGTACATATGAACATCTCCCATG	qRT-PCR, *SHY2/IAA3* (At1g04240)		
P55	CCAGGGACAGAAGAAACTGTTTCTTG	qRT-PCR, *IAA4* (At5g43700)		
P56	CCAACAATCTGAGCCTTTGGAGGA	qRT-PCR, *IAA4* (At5g43700)		
P57	GGATGCTTGCTGGAGATGTTCCTT	qRT-PCR, *IAA5* (At1g15580)		
P58	CTGTAAGGCTCACTCACATTCACATG	qRT-PCR, *IAA5* (At1g15580)		
P59	AGTCACGGTTCTTGAGAATCTCTTCG	qRT-PCR, *IAA6* (At1g52830)		
P60	AGGTACATCTCCGACGAGCATCC	qRT-PCR, *IAA6* (At1g52830)		
P61	ATCTACGACTCATGACGTCGTGACT	qRT-PCR, *IAA17* (At1g04250)		
P62	ATCACGTTCTTCCGGTATGATCTCAC	qRT-PCR, *IAA17* (At1g04250)		
P63	CCTCCTACCAAAACTCAAATCGTTGG	qRT-PCR, *IAA19* (At3g15540)		
P64	GAGATCGATCTTGCGAAGGTAAGGA	qRT-PCR, *IAA19* (At3g15540)		
P65	GGGGATGTTACATGGAAGATCTTTGC	qRT-PCR, *IAA29* (At4g32280)		
P66	GGTCCGATTTGAACGCCTATCCTT	qRT-PCR, *IAA29* (At4g32280)		
P67	TGCTGGTCGTGACCTTACTGATTACC	qRT-PCR, *Actin8* (At1g49240)		
P68	TCTCCATCTCTTGCTCGTAGTCGACA	qRT-PCR, *Actin8* (At1g49240)		
P69	CTCACATTTTCGTAGCCGCAAGAC	qRT-PCR, *EF1α* (At5g60390)		
P70	GATCAAGTGACCAGTTGTGGTCGAT	qRT-PCR, *EF1α* (At5g60390)		

P71	CTTAGCCATTGCCTCCATCATCCA	qRT-PCR, *AUX1* (At2g38120)		
P72	GTAACCGCGTGACCTCCAAAGG	qRT-PCR, *AUX1* (At2g38120)		
P73	CTGGGCTTTCGGCGACCAAC	qRT-PCR, *LAX1* (At5g01240)		
P74	GTGTACACGCAAACCCGAACGT	qRT-PCR, *LAX1* (At5g01240)		
P75	CAGGGGCCACAAACATTCTTTACAC	qRT-PCR, *LAX2* (At2g21050)		
P76	GCGTTAGCGTCAGCACGTAGAG	qRT-PCR, *LAX2* (At2g21050)		
P77	CATGGCCAGGCTGAGGATGTG	qRT-PCR, *LAX3* (At1g77690)		
P78	CACATAGCGTGCATTATCTCCACTG	qRT-PCR, *LAX3* (At1g77690)		
P79	AATTGGATCCACTCCAATGCGGGACTCTGGAGC	Insertion of *SPT5-2* (At4g08350) C-terminal CDS in pQE9	pQE-SPT5-2C	BamHI
P8	AATTCTGCAGTCACGGTTGCACAAACTTGGCTAATAAGG	Insertion of *SPT5-2* (At4g08350) C-terminal CDS in pQE9	pQE-SPT5-2C	PstI
P81	TTGGGCCCAACAATGGGAAGCGCACCAGCTCAGATTC	Insertion of *SPT4-2* (At5g63670) CDS in pCambia2300-GS	pCambia2300-SPT4-2-GS	SmaI
P82	TTGAGCTCTCACATGCGTTTCGGCAGAACAT	Insertion of *SPT4-2* (At5g63670) CDS in pCambia2300-GS	pCambia2300-SPT4-2-GS	SacI
P83	AATTGAATTCAATGGGAAGCGCACCAGCTCAGATTC	Insertion of *SPT4-2* (At5g63670) CDS in pGEX5x.1	pGEX5X-1-SPT4-2	EcoRI
P84	AATTCCCGGGTCACATGCGTTTCGGCAGAACATATTGTAC	Insertion of *SPT4-2* (At5g63670) CDS in pGEX5x.1	pGEX5X-1-SPT4-2	SmaI
P85	AATTGGTACCATGCCGCGAAGCAGAGACGAAG	Insertion of *SPT5-2* (At4g08350) N-terminal CDS in pBC-SK	pBC-SK-SPT5-2N	KpnI
P86	AATGAGCTCCCAGCTTACTGGCTAGTGCC	Insertion of *SPT5-2* (At4g08350) N-terminal CDS in pBC-SK	pBC-SK-SPT5-2N	SacI
P87	AATTGGTACCATGGATCGCAAGGGAAAGGG	Insertion of *SPT5-L* (At5g04290) N-terminal CDS in pBC-SK	pBC-SK-SPT5LN	KpnI
P88	AATTGAGCTCGGACAGTAACTCCCCCACCAT	Insertion of *SPT5-L* (At5g04290) N-terminal CDS in pBC-SK	pBC-SK-SPT5LN	SacI
P89	AATTCCCGGGAATGGGAAGCGCACCAGCTCAGATTC	Insertion of *SPT4-2* (At5g63670) CDS in 5'-GFP	p5'-GFP-SPT4	SmaI
P90	AATTGAGCTCTCACATGCGTTTCGGCAGAACATATTGTAC	Insertion of *SPT4-2* (At5g63670) CDS in 5'-GFP	p5'-GFP-SPT4	SacI
P91	AATTTCTAGAAATGGGAAGCGCACCAGCTCAGATTC	Insertion of *SPT4-2* (At5g63670) CDS in 3'-GFP	p3'-GFP-SPT4	XbaI
P92	AATTCCCGGGCATGCGTTTCGGCAGAACATATTGTACAC	Insertion of *SPT4-2* (At5g63670) CDS in 3'-GFP	p3'-GFP-SPT4	SmaI
P93	TGGAATCTCAGGGTCAAGG	ChIP qPCR, *TA3*		
P94	CCTTCTGAGGTGAGGGACA	ChIP qPCR, *TA3*		
P95	TGCTGGTCGTGACCTTACTGATTACC	ChIP qPCR, *Actin8* (At1g49240)		
P96	TCTCCATCTCTTGCTCGTAGTCGACA	ChIP qPCR, *Actin8* (At1g49240)		
P97	TTGGGAAATACTGTAATAAGCTTCCT	ChIP qPCR, At3g02260-1		
P98	TCCATGTGTTATTCTAATGATGTGCT	ChIP qPCR, At3g02260-1		
P99	ACCGCCTTTCCCTCTTTGTCGT	ChIP qPCR, At3g02260-2		
P100	GTCTCAAAGCGTAGCTTGCCAGA	ChIP qPCR, At3g02260-2		
P101	AGATGGTTTCGGGGAGGAAAATCAC	ChIP qPCR, At3g02260-3		
P102	GCTTCTCTTTCGACAGGCCAGAG	ChIP qPCR, At3g02260-3		

P103	CAGGCGTTATCTCTTGAACCATTGC	ChIP qPCR, At3g02260-4		
P104	TACTTGCTGTAGCCACACTCGTTG	ChIP qPCR, At3g02260-4		
P105	CAAACCCAAGAAACCGGTCCACA	ChIP qPCR, At3g02260-5		
P106	GAGTTGATTTCGTCGAGCCACGA	ChIP qPCR, At3g02260-5		
P107	CCAACACATTTACGTTCACACAAACC	ChIP qPCR, At3g02260-6		
P108	TTAATTCAAACGCGACGAGTTTAACCAT	ChIP qPCR, At3g02260-6		
P109	CTCGTTTATGCTTTGTGTGGGTCA	ChIP qPCR, *DOG-1* ()		
P110	TCTTGCTCGCTGGGAAAAAGCTT	ChIP qPCR, *DOG-1* ()		
P111	GTGTATTAGCTGTTAGGTTTGCACA	ChIP qPCR, At1g48090-1		
P112	CTCGGTTCTCATGATACAAACATCCT	ChIP qPCR, At1g48090-1		
P113	GTTCGATGTTGTGATTCTGGGTGA	ChIP qPCR, At1g48090-2		
P114	CTTCTCCAGTAACAGCTACCATTGCT	ChIP qPCR, At1g48090-2		
P115	CTCTCTCGAGTCTCTTGCTTCTTCTC	ChIP qPCR, At1g48090-3		
P116	GATCCGAGAAACGAACCGATTCAAC	ChIP qPCR, At1g48090-3		
P117	GCAGCAGTCAGGAAGTGCTCAG	ChIP qPCR, At1g48090-4		
P118	CTCTGGTAAAGCATCTGTGTAGGCAT	ChIP qPCR, At1g48090-4		
P119	GCTTCTCCCTGACACTTCTAGATGG	ChIP qPCR, At1g48090-5		
P120	GACAGTTGTGTCAAAGAGAGGAGTCA	ChIP qPCR, At1g48090-5		
P121	ACCATGGAACTGAGTGACGGGAA	ChIP qPCR, At1g48090-6		
P122	AACATCAAAGGCCTGCTTGCTGT	ChIP qPCR, At1g48090-6		
P123	ATGGGCTTAACCTTAAGGACACAGAG	ChIP qPCR, *IAA1-5'* (At4g14560)		
P124	GAGCAGATTCTTCTGTTGAGTCGTTG	ChIP qPCR, *IAA1-5'* (At4g14560)		
P125	GGATGTTGGTCGGTGATGTTCCA	ChIP qPCR, *IAA1-3'* (At4g14560)		
P126	GTTTTTGCCTCGACCAAAAGGTGT	ChIP qPCR, *IAA1-3'* (At4g14560)		
P127	GGGAGAGATGTGGCAGAGAAGATG	ChIP qPCR, *IAA19-5'* (At3g15540)		
P128	CCTTCTCAGCGTCACCACCAGA	ChIP qPCR, *IAA19-5'* (At3g15540)		
P129	CATATTTGTGCAGGTGTGGCCTTG	ChIP qPCR, *IAA19-3'* (At3g15540)		
P130	TAGAACATACCCCCAAGGTACATCAC	ChIP qPCR, *IAA19-3'* (At3g15540)		
P131	GACGAAGCTGCCTTAGAAATGGAGT	ChIP qPCR, *IAA29-5'* (At4g32280)		
P132	GGTACCCAAACAAGACGCAGCA	ChIP qPCR, *IAA29-5'* (At4g32280)		
P133	TAGAGATCGACCGTGTGCATATACAAG	ChIP qPCR, *IAA29-3'* (At4g32280)		
P134	TAGAAGAATAGAGGAAAAAGATCGAGTGGA	ChIP qPCR, *IAA29-3'* (At4g32280)		
P135	ATCCTCTGGAATGTTGATAGT	Genotyping, T-DNA insertion *tflls-1* (At2g38560)		
P136	TTTCCTCTTGTCACTTGCCAT	Genotyping, T-DNA insertion *tflls-1* (At2g38560)		
P137	CCCTCATCTTACGCGTATCAGA	Genotyping, T-DNA insertion *ssrp1-2* (At3g28730)		
P138	AACCGGATCCGTAGTCATCCATTTGCTTC	Genotyping, T-DNA insertion *ssrp1-2* (At3g28730)		

P139	CTATCTCTGCATTGCCTCTTAGC	Genotyping, T-DNA insertion *spt16-1* (At4g10710)			
P140	TACTTGTCTAACGCAGCGAAATC	Genotyping, T-DNA insertion *spt16-1* (At4g10710)			
P141	GGCCATGAAACCGGATACTCG	Genotyping, T-DNA insertion *cbp20* (At5g44200)			
P142	GCATCTTCAGTATCCTCTCTAGAG	Genotyping, T-DNA insertion *cbp20* (At5g44200)			
P143	GGTAAAGCTCATCAGCGTGGTCG	Genotyping, T-DNA insertion *cbp20* (At5g44200) LB			
P144	TAATTTAGGCTCTTCCGGGTG	Genotyping, T-DNA insertion *cbp80* (At2g13540)			
P145	AATACTTGGCCATATCGCTCC	Genotyping, T-DNA insertion *cbp80* (At2g13540)			

Danksagung

Zunächst möchte ich mich ganz herzlich bei meinem Doktorvater Prof. Dr. Klaus D. Grasser bedanken, der es mir ermöglicht hat an diesem Projekt zu arbeiten und in seiner Arbeitsgruppe zu promovieren. Danke für die Begutachtung meiner Doktorarbeit und die Unterstützung durch Ratschläge und Diskussionen.

Dr. Andreas Houben möchte ich für die Betreuung als externen Mentor, die Zweitbegutachtung meiner Arbeit, sowie für die Bereitschaft zweimal den weiten Weg nach Regensburg auf sich zu nehmen, danken.

Bei Dr. Joachim Griesenbeck und Prof. Dr. Thomas Dresselhaus möchte ich mich, für die Bereitschaft als Drittprüfer beziehungsweise als Prüfungsvorsitzender zu fungieren, bedanken.

Bei allen aktuellen und ehemaligen Mitgliedern der AG Grasser bedanke ich mich für die freundschaftliche und entspannte Atmosphäre. Im Besonderen möchte ich mich bei Brian für seine Bereitschaft mir zu jeder Zeit mit Rat und Tat zur Seite zu stehen und für das Korrekturlesen meiner Arbeit bedanken.

Allen Mitarbeitern des Lehrstuhls, auf deren Hilfestellung und Tipps ich mich immer verlassen konnte, möchte ich ebenfalls herzlich danken besonders bei Astrid, Alex, Birgit, Tine, Philipp A. und D., Susanne, Maren, Svenja, Lisa und allen anderen die ich vergessen haben sollte.

Ein besonderer Dank gilt Joe und Andrea für die mir stets entgegengebrachte Unterstützung und für ihre Freundschaft. Nicht zu vergessen sind auch Alina und Nadine.

Meiner Freundin Marie möchte ich für die andauernde Unterstützung in jeglicher Situation und vor allem in den letzten Wochen bedanken.

Schlussendlich möchte ich mich besonders bei meinen Eltern für die Unterstützungen in den letzten Jahren bedanken, da ohne sie das alles nicht möglich gewesen wäre. Danke, dass ich mich immer auf euch verlassen kann und für die aufmunternden Pakete in den letzten Monaten.

Eidesstattliche Erklärung

Ich erkläre hiermit an Eides statt, dass ich die vorliegende Arbeit ohne unzulässige Hilfe Dritter und ohne Benutzung anderer als der angegebenen Hilfsmittel angefertigt habe.

Die aus anderen Quellen direkt oder indirekt übernommenen Daten und Konzepte sind unter Angabe des Literaturzitats gekennzeichnet.

Julius Dürr

Regensburg, den 08.10.2013